Norwegian University of Life Sciences
Faculty of Chemistry, Biotechnology and Food Science

Philosophiae Doctor (PhD)
Thesis 2019:14

Applied and fundamental perspectives on brown-rot fungal decay mechanisms

Anvende og fundamentale perspektiver på nedbrytningsmekanismer hos brunråtesopp

Olav Aaseth Hegnar

Applied and fundamental perspectives on brown-rot fungal decay mechanisms

Anvendte og fundamentale perspektiver på nedbrytningsmekanismer hos brunråtesopp

Philosophiae Doctor (PhD) Thesis

Olav Aaseth Hegnar

Norwegian University of Life Sciences

Faculty of Chemistry, Biotechnology and Food Science

Ås (2018)

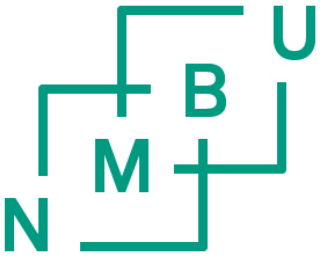

Thesis number: 2019:14

ISSN: 1894-6402

ISBN: 978-82-575-1579-9

Nobody ever figures out what life is all about, and it doesn't matter. Explore the world. Nearly everything is really interesting if you go into it deeply enough.

-Richard Feynman

Table of contents

Acknowledgements ..... **I**

Summary ..... **III**

Sammendrag ..... **V**

List of papers ..... **VII**

1 Introduction **1**

1.1 The wood cell wall **1**

1.1.1 Cellulose 3

1.1.2 Hemicellulose 5

1.1.3 Lignin 8

1.2 Lignocellulose-active enzymes in fungi **9**

1.2.1 Glycoside hydrolases (GHs) 10

1.2.2 Auxiliary activity enzymes 12

1.2.3 Carbohydrate-binding modules 15

1.2.4 Carbohydrate esterases 15

1.2.5 Expansins 15

1.3 Lytic polysaccharide monooxygenases **17**

1.3.1 Phylogeny, specificity and three dimensional structure of LPMOs 18

1.3.2 Catalytic mechanism(s) of LPMOs 20

1.3.3 LPMO reduction and the source of H_2O_2 – *in vitro* and *in vivo* 24

1.4 Brown-rot fungi **27**

1.4.1 Phylogeny and evolution of brown-rot fungi 27

1.4.2 Lignocellulose-active enzymes in brown-rot fungi 30

1.4.3 Chelator mediated Fenton (CMF) 31

1.4.4 Expression of decay associated genes 34

1.5 Pretreatment of lignocellulosic biomass **38**

1.6 Wood modification **42**

1.6.1 Acetylation 42

2 Outline and aim of thesis **45**

3 Main results and discussion **47**

Paper I: Challenges and opportunities in mimicking non-enzymatic brown-rot decay mechanisms for pretreatment of Norway spruce **47**

Paper II: Acetylation of *Pinus radiata* delays hydrolytic depolymerization by the brown-rot fungus *Rhondonia placenta* **52**

Paper III: Characterization of a lytic polysaccharide monooxygenase from *Gloeophyllum trabeum* shows a pH-dependent relationship between catalytic activity and hydrogen peroxide production **58**

4 Conclusions and future perspectives **65**

5 References **69**

Papers ..... **I-III**

Acknowledgements

This thesis is submitted in the fulfillment of the requirements for the degree of Philosophiae Doctor (PhD) at the Norwegian University of Life Sciences (NMBU), Faculty of Chemistry, Biotechnology and Food Science. The work was financed by the Norwegian Institute for Bioeconomy Research (NIBIO) and conducted at NIBIO and NMBU. I am very grateful for both NMBU and NIBIO for giving me this opportunity.

First and foremost I would like to thank all my supervisors for all the guidance and support I have received over the past three and a half years. **Gry**, thank you for being the most badass supervisor one could hope for, endlessly optimistic and knowledgeable, with your door always open for discussions both on and of topic. **Vincent**, thank you for letting me make a mess in your lab and making me feel welcome with the PEP group, and thank you for your invaluable insight and enthusiasm. I am truly humbled. **Aniko**, thank you for always being available for my endless questions and for taking more time than you probably should have to help me with the editing of my manuscripts and figures. **Barry** and **Carl Gunnar,** thank you for all the highly illuminating conversations, scientific or otherwise**.**

Thank you to all my colleagues at NIBIO, especially **Eva**, **Sigrun**, **Monica** and **Inger** for helping out with lab work and technical expertise when work piled up. Dere er best! Thank you to **Erik** the boss man for making everyone feel at home at the department. Also, thank you to **Greeley** and **Kärt** for being such awesome office mates, and for becoming such close friends, love ya.

Thank you to everyone at the PEP group for making me feel included. Particularly, a gigantic thank you **Dejan** for giving me the best crash course in LPMO biochemistry one could hope for, making me feel comfortable with the topics in a matter of weeks. **Bastien**, a huge thank you for some of the most valuable scientific conversations of my entire PhD, on topics that would have been too complicated for my feeble brain to handle by itself. Thank you **John**, guardian of instruments and knower of all things. Also, a special thank you to **Piotr** for many invaluable and illuminating conversations.

Thanks to all my brilliant BioMim-collaborators **Lars, Inger, Niki, Makoto, Zarah, Stig, Gudbrand** and **Claus,** for 3 ½ years of fruitful collaboration. The conversations, both scientific and non-scientific in nature, and meetings have been a true highlight.

Last but not least, a massive thank you to all my friends and family for all the support over the past 3 ½ years, especially **Erlend** and **Kjersti** for listening to all my science babble, and to **Anette** for keeping me sane through the final hours of this ordeal.

Summary

Woody biomass is an important material for the growing bioeconomy, and has gained significant attention as a feedstock for second-generation biorefineries. Wood has traditionally been used as a building material for millennia, but due to its biogenic nature is susceptible to degradation by wood decaying fungi. The biochemistry used by these fungi to degrade wood is of interest, both from a wood protection perspective, and as potential bioprocessing tools. In Nature, wood-degrading basidiomycetes, which can be grouped as white- or brown-rot fungi, are the only organism known to fully degrade the polysaccharides of lignified woody biomass. Brown-rot fungi are unique, in that they successfully remove holocellulose without the mineralization of lignin, unlike white-rot fungi, which degrade both holocellulose and lignin. The objective of this thesis is the study of fundamental brown-rot fungal decay mechanisms for applied utilization.

This thesis describes studies on brown-rot decay from three perspectives; 1) the oxidative non-enzymatic early decay mechanisms as potential pretreatment of wood, 2) the expression of brown-rot decay associated genes on modified wood and 3) the interplay of cellulose-oxidizing lytic polysaccharide monooxygenases with hydrogen peroxide and reductants.

In **Paper I** the early decay mechanisms of brown-rot fungi was studied as a potential pretreatment for Norway spruce wood. We show that Norway spruce pretreated with two species of brown-rot fungi yielded more than 250% increases in glucose release when subsequently treated with a commercial enzyme cocktail. A series of experiments were performed that aimed at mimicking the brown-rot pretreatment, using a modified version of the Fenton reaction. After pretreatment, where the aim was to generate reactive oxygen species within the wood cell wall matrix, a small increase in digestibility was observed, Further experiments were performed to assess the possibility of performing pretreatment and saccharification in a single system to avoid loss of solubilized sugars, but the results indicated the need for a complete separation of oxidative pretreatment and saccharification. We conclude that a biomimicking approach to pretreatment of softwoods using brown-rot fungal mechanisms is possible, but that there are additional factors of the system that need to be known and optimized before serious advances can be made to compete with already existing pretreatment methods.

In **Paper II**, the aim was to determine the effect of acetylation of *Pinus radiata* wood (a type of wood modification), on the expression of genes involved in wood decay by brown-rot

fungus *Rhodonia placenta.* The initiation of decay was delayed as a result the degree of acetylation, and gene expression analysis using qRT-PCR captured incipient to advanced decay stages. Once decay was established, the rate of degradation in acetylated samples was similar to that of unmodified wood. This suggests a delay in decay, rather than an absolute protection threshold at higher acetylation levels. In accordance with previous studies, the oxidative system of *R. placenta* was more active in wood with higher degrees of acetylation and expression of hydrolytic enzymes was delayed in acetylated samples compared to untreated samples. Enzymes involved in hemicellulose and pectin degradation have previously not been the focus of studies on degradation of acetylated wood. Interestingly, we observed that a CE16 carbohydrate esterase assumed to be involved in deacetylation of carbohydrates was expressed significantly higher in untreated samples compared to highly acetylated samples. We hypothesize that this enzyme might be regulated through a negative feedback system, where acetic acid suppresses the expression. The up-regulation of two expansin genes in acetylated samples suggests that their function, to loosen the cell wall, is needed more in acetylated wood due the physical bulking of the cell wall. In this study, we demonstrate that acetylation affects the expression of specific target genes not previously reported, resulting in delayed initiation of decay.

In **Paper III** we purified and characterized a recombinant family AA9 lytic polysaccharide monooxygenase from *Gloeophyllum trabeum*, *Gt*LPMO9B, which is active on both cellulose and xyloglucan. Activity of the enzyme was tested in the presence of three different reductants: ascorbic acid, gallic acid and 2,3-dihydroxybenzoic acid (2,3-DHBA). When using standard aerobic conditions typically used in LPMO experiments, the former two reductants could drive LPMO catalysis whereas 2,3-DHBA could not. In agreement with the recent discovery that H_2O_2 can drive LPMO catalysis, we show that gradual addition of H_2O_2 allowed LPMO activity at very low, sub-stoichiometric (relative to products formed) reductant concentrations. Most importantly, we found that while 2,3-DHBA is not capable of driving the LPMO reaction under standard aerobic conditions, it can do so in the presence of externally added H_2O_2. At alkaline pH, 2,3-DHBA is able to drive the LPMO reaction without externally added H_2O_2 and this ability overlaps entirely with endogenous generation of H_2O_2 by *Gt*LPMO9B-catalyzed oxidation of 2,3-DHBA. These findings support the notion that H_2O_2 is a co-substrate of LPMOs, and provide insight into how LPMO reactions depend on, and may be controlled by, the choice of pH and reductant.

Sammendrag

Biomasse fra tre er et viktig materiale for den gryende bioøkonomien, og har tiltrukket seg betydelig oppmerksomhet som et råstoff for 2. generasjons bioraffinerier. Tre har tradisjonelt blitt brukt som byggemateriale i årtusener, men er på grunn av sitt biologiske opphav utsatt for angrep av vednedbrytende sopp. Biokjemien benyttet av disse soppene til å bryte ned tre er av interesse, både fra et trebeskyttelsesperspektiv, og som potensielle bioprosesseringsverktøy. I naturen er basidiomycete brun- og hvitråtesopp de eneste som bryter ned alle polysakkaridene i lignifisert plantemateriale. Brunråtesoppene er unike i at de fjerner holocellulose uten å mineralisere lignin, mens hvitråtesoppene bryter ned både lignin og holocellulose. Målet ved denne avhandlingen er å studere fundamentale brunråtesoppmekanismer for anvendte øyemed.

Denne avhandlingen beskriver brunråtenedbrytning fra tre perspektiver: 1) oksidative ikke-enzymatiske nedbrytningsmekanismer som forbehandling av tremasse, 2) genuttrykk av nedbrytningsassosierte gener under vekst på modifisert tre, og 3) samspillet mellom celluloseoksiderende lytisk polysakkaridmonooksygenaser, hydrogenperoksid og reduktanter.

I **Paper I** var de tidlig nedbrytningstrinn hos brunråtesopp studert som en potensiell forbehandling for gran (*Picea abies*). Vi viser at ved å forbehandle gran med to brunråtesopparter, kan enzymatisk hydrolyse med en kommersiell enzymcocktail forbedres, og fikk en over 250% økning i glukosefrigivelse. Vi utførte deretter en rekke eksperimenter, hvor målet var å mimikere brunråteforhåndsbehandlingen, ved bruk av en modifisert Fenton reaksjon. Her fikk vi en marginal økning i fornøyelighet etter forhåndsbehandling, hvor hensikten var å generere reaktive oksygenarter inne i treets cellevegg. Videre eksperimenter ble utført for å undersøke mulighetene for å gjøre forhåndsbehandling og sakkarifisering i ett og samme system, og resultatene her indikerer et behov for komplett seperasjon av forhåndsbehandling og sakkarifisering, da kjemikaliene i forhåndsbehandlingen viste seg å være skadelige for enzymene. Vi konkluderer med at en biomimetisk tilnærming til forhåndsbehandling av gran er teoretisk mulig, men at systemet trenger optimalisering før videre arbeid kan gjøres.

I **Paper II** var målet å bestemme hvordan acetylering (trebeskyttelse) av *Pinus radiata* påvirket uttrykk av nedbrytningsgener hos brunråtesoppen *Rhodonia placenta*. Genuttrykk

ble analysert ved bruk av qRT-PCR og fanget både tidlige og sene nedbrytningstrinn. Initieringen av nedbrytning ble forsinket som et resultat av acetylering. Når nedbrytningen først var etablert i acetylert tre var raten sammenlignbar med umodifisert tre, noe som indikerer en hemning av nedbrytning og ikke en total beskyttelse. I samsvar med tidligere studier var det oksidative nedbrytningssystemet hos *R. placenta* mer aktivt i tre med høy grad av acetylering, og uttrykk av hydrolytiske gener var forsinket sammenlignet med umodifisert tre. Vi studerte uttrykk av gener involvert i hemicellulose og pektin nedbrytning som ikke tidligere er beskrevet i studier på nedbrytning av acetylert tre. Vi observerte at en karbohydratesterase (CE16) som er antatt å være involvert i deacetylering av hemicellulose var nedregulert i acetylert tre, og fremsetter en hypotese om at dette genet er regulert via en negativ feedback mekanisme. Oppreguleringen av to expansin-gener i acetylert tre indikerer at denne modifiseringen øker behovet for å løsne cellevegginteraksjoner som en konsekvens av økte massetettheten. I denne studien demonstrerer vi at acetylering påvirker uttrykk av en rekke gener ikke tidligere studert under disse forholdene, og resulterer i forsinket nedbrytning.

I **Paper III** har vi renset og karakterisert en rekombinant familie AA9 lytisk polysakkaridmonooksygenase (LPMO, *Gt*LPMO9B) fra brunråtesoppen *Gloeophyllum trabeum*, som er aktiv på både cellulose og xyloglucan. Enzymaktivitet ble testet med tre forsjellige reduktanter: ascorbic acid (AscA), gallic acid (GA) og 2,3-dihydroxybenzoic acid (2,3-DHBA). Under reaksjonsforhold vanligvis brukt i LPMO reaksjoner, var enzymet katalytisk aktivt med AscA og GA, man var det ikke med 2,3-DHBA. I samsvar med den nylige oppdagelsen at LPMO-katalyse kan drives av H_2O_2, viser vi at gradvis tilføring av H_2O_2 tillater LPMO aktivitet ved svært lave, sub-støkiometriske (relativt til produkt) reduktantkonsentrasjoner. Viktigst, så vi viser at, mens 2,3-DHBA ikke kunne drive LPMO reaksjonen under standard aerobe forhold, så kan den det i nærvær av tilført H_2O_2. Ved alkalisk pH (8.0-9.0), ble aktivitet med *Gt*LPMO9B observert med 2,3-DHBA (uten ekstern tilførsel av H_2O_2), noe som overlappet 100% med endogen H_2O_2 produksjon via *Gt*LPMO9B-katalysert oksidering av 2,3-DHBA. Disse funnen støtter teorien om at H_2O_2 er et kosubstrat for LPMOer, og tilfører ny kunnskap om hvorledes LPMO reaksjoner er avhengige, og potensielt kan kontrolleres med bruk av forskjellige reduktanter.

List of papers

Paper I

Challenges and opportunities in mimicking non-enzymatic brown-rot decay mechanisms for pretreatment of Norway spruce

Olav A. Hegnar, Barry Goodell, Claus Felby, Lars Johansson, Nicole Labbé, Keonhee Kim, Vincent G. H. Eijsink, Gry Alfredsen, Anikó Várnai (2018). Manuscript accepted for publication in *Wood Science and Technology.*

Paper II

Acetylation of *Pinus radiata* delays hydrolytic depolymerisation by the brown-rot fungus *Rhondonia placenta*

Greeley Beck, Olav A. Hegnar, Carl Gunnar Fossdal, Gry Alfredsen (2018) *International Biodeterioration & Biodegradation*, 135, 39-52.

Paper III

Characterization of a lytic polysaccharide monooxygenase from *Gloeophyllum trabeum* shows a pH-dependent relationship between catalytic activity and hydrogen peroxide production

Olav A. Hegnar, Dejan M. Petrovic, Bastien Bissaro, Gry Alfredsen, Anikó Várnai, Vincent G.H. Eijsink (2018). Revised manuscript submitted to *Applied and Environmental Microbiology*

Other publications by the author

Wood modification by furfuryl alcohol causes delayed decomposition response in *Rhodonia (Postia) placenta*

Inger Skrede, Monica Hongrø Solbakken, Jaqueline Hess, Carl Gunnar Fossdal, Olav A. Hegnar, Gry Alfredsen (2018*).* Manuscript

Structure of the essential peptidoglycan amidotransferase MurT/GatD complex from Streptococcus pneumoniae

Cécile Morlot, Daniel Straume, Katharina Peters, Olav A. Hegnar, Nolwenn Simon, Anne-Marie Villard, Carlos Contreras-Martel, Francisco Leisico, Eefjan Breukink, Christine Gravier-Pelletier, Laurent Le Corre, Waldemar Vollmer, Nicolas Pietrancosta, Leiv Sigve Håvarstein & André Zapun (2018). *Nature Communications* 9: 3180

1 Introduction

An estimated three trillion standing trees make lignocellulosic biomass an abundant and attractive renewable feedstock for the production of biofuels, chemicals, food and other products. The high recalcitrance of the lignocellulosic wood cell wall hampers its utilization, and significant pretreatment is needed in order to access the valued polysaccharides within. In Nature, the decay and breakdown of woody biomass is a key part of the global carbon cycle, ultimately resulting in the release of CO_2 that re-enters the atmosphere. The organisms responsible for this decay are found in all three domains of life, and include fungi, bacteria, archaea, nematodes, insects and even marine organisms. Of these groups, the only able to fully degrade lignified woody plant matter is fungi. There is evidence indicating that the first forests appeared approximately 370 million years ago (Labandeira, 2007) and that more than 80 million years passed before the evolution of wood decay fungi able to degrade lignin (Floudas et al., 2012). Today, these fungi are found within Basidiomycota, one of the two major divisions of the subkingdom Dikarya, along with Ascomycota. Wood decaying basidiomycetes are traditionally divided into two polyphyletic groups, characterized by the visual appearance of the decaying material, as either white-rot or brown-rot. The biochemistry these fungi use to degrade wood is of high interest in applied settings, as it has the potential of solving the lignocellulose recalcitrance bottleneck.

In addition to its potential as a biorefinary feedstock, wood has traditionally been used as construction material. Due to its natural susceptibility to biodegradation by fungi, protection of wood to extend its service life is of high interest. Expanding knowledge on wood decay mechanisms could allow development of new and better methods to protect wood. This thesis deals with the mechanisms of wood decay by brown-rot fungi, addressing both applied and fundamental perspectives, and discussing how knowledge of these mechanisms may be used to both break down wood and protect it.

1.1 The wood cell wall

The wood cell wall has evolved to give structural support and to provide the basis for transport of water and nutrients in higher plants (Tracheophytes). Some trees reach as high as 100 meters above the ground, and thus, robustness is needed in order to withstand the large

physical forces at play. The composition of the wood cell wall varies depending on organism and tissue type. It is composed of a complex network of polysaccharides (cellulose, hemicelluloses and pectin) and lignin that is interspersed with proteins, waxes, fatty acids, resins, terpenes and various inorganic compounds (Figure 1).

The wood cell wall generally has three layers that differ in structure and chemical composition: the middle lamella, the primary cell wall and the secondary cell wall. The middle lamella is responsible for connecting adjacent plant cells and is mainly composed of pectin. This pectin usually becomes lignified as the plant grows, reinforcing the structure. The primary cell wall is a thin layer that is formed during the formation of new plant cells and is composed of a network of crystalline cellulose that is embedded in a matrix of hemicelluloses, pectin, protein and lignin (Cosgrove, 2005). The much thicker secondary cell wall is formed after the primary cell wall, when the cell is fully grown, and is the main provider of structural support. The secondary cell wall is highly organized, with layered sheaths of parallel cellulose microfibrils that are interlinked with lignin and hemicelluloses. The secondary cell wall may be divided into three layers based on the orientation of the cellulose fibers (S1, S2 and S3) (Fujita and Harada, 2000) (Figure 1). The S2 layer is the largest, with a thickness of 1-5 μm, and contains most of the lignin in the cell wall. In certain tree species (softwoods and some hardwoods), there is a fourth layer, which is referred to as the warty layer. This layer is composed of lignin and hemicelluloses that are in excess after formation of the S3 layer of the secondary cell wall (Fujita and Harada, 2000). The relative amount of cellulose, hemicellulose and lignin in the wood cell wall varies within the wood cell wall itself and between wood species, typically within the range of 40-50% cellulose, 25-35% hemicellulose and 15-20% lignin (Alonso et al., 2010).

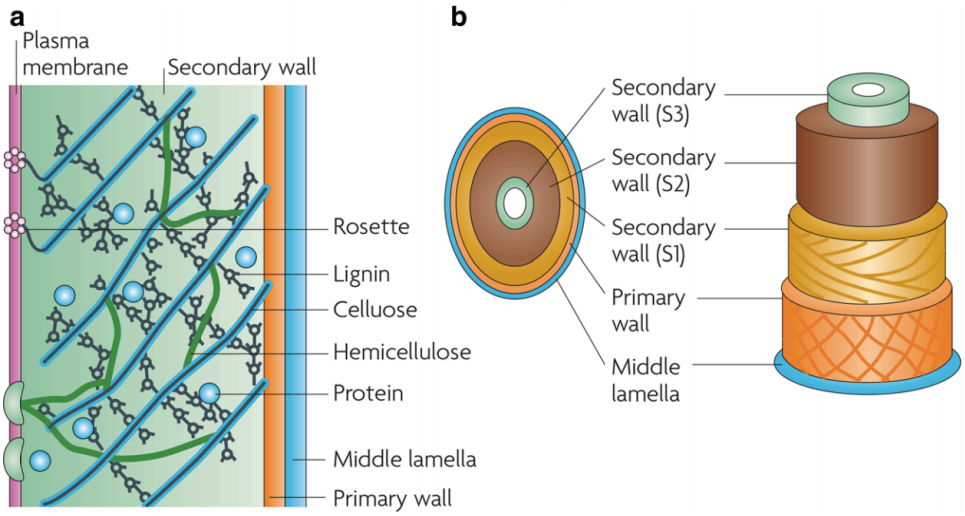

Figure 1. Wood cell wall structure. Panel a shows a cross-section showing the three main layers: the middle lamella, the primary cell wall and the secondary cell wall. Panel b provides another view of the wood cell wall, showing orientation of fibers. This figure was taken from Mathews et al. (2015).

1.1.1 Cellulose

Cellulose is the main component of the wood cell wall and is the most abundant biopolymer on earth. It is found within plant cell walls as well as in certain bacteria and algae. Cellulose is built up of β-(1,4) linked glucose units that are rotated every other unit at 180 degrees, which makes the repeating unit cellobiose (Glc2). These repeating cellobiose units form linear polysaccharides that are anywhere from hundreds to several thousand units in length. The length of the cellulose chain is referred to as degree of polymerization (DP). In native cellulose the individual chains are bundled together in sheaths via 3→5 and 2→6 intramolecular and 3→6 intermolecular hydrogen bonding, while van der Waals bonds between the sheaths lead to formation of insoluble, crystalline cellulose microfibrils (Figure 2).

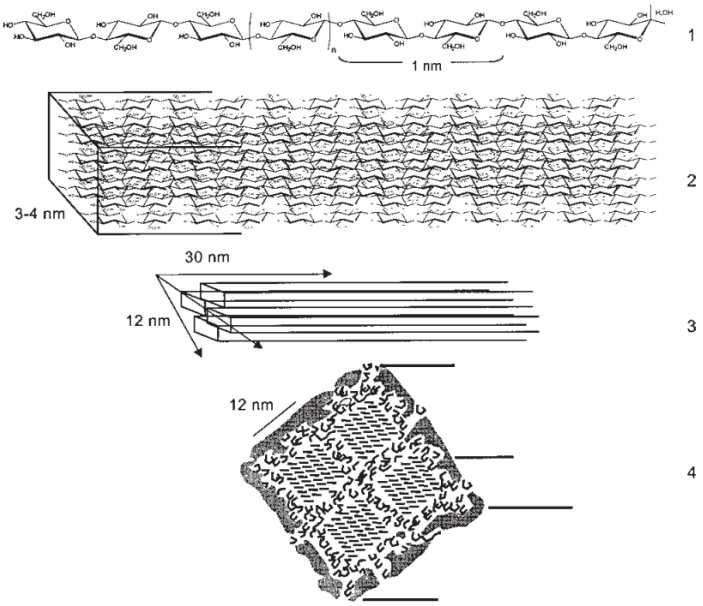

Figure 2. Cellulose structure, from single strand to microfibril. **1)** The β-1,4-linked glucose units in cellulose are rotated 180 degrees relative to each other, making the repeating unit cellobiose. **2)** Cellulose single strands bundle together in elementary fibrils, **3)** which in turn form crystalline fibers (microfibrils). **4)** Cross section of a microfibril. Figure taken from Ramos (2003).

In Nature, crystalline cellulose is encountered in two allomorphs, referred to as either Iα or Iβ (Wang et al., 2016). Iα is the dominant form found in bacteria and algae, while the more thermostable Iβ form dominates in higher plants. The major difference between the two forms is the way in which inter chain hydrogen bonding is arranged between the parallel glucan chains (Fernandes et al., 2011). Along the cellulose microfibrils, there are both crystalline and amorphous regions. The amorphous regions are important in enzymatic depolymerization, as they serve as the main point of attack by hydrolytic cellulases (Bertran and Dale, 1985). In addition to the natural I allomorphs, cellulose can be encountered in five other polymorphs (II, III_I, III_{II}, IV_I and IV_{II}), which may be obtained by pretreating lignocellulosic material and which can be differentiated by x-ray diffraction (Isogai et al., 1989). Cellulose II is formed via alkali pretreatment or dissolution of cellulose I followed by repolymerization, and its formation is irreversible (Beckham et al., 2011). In cellulose II the glucan chains are arranged in an antiparallel manner, which is more thermodynamically favorable. Furthermore the hydrogen bonding pattern of cellulose II is different, being dominated by 2→6 intermolecular bonding. Cellulose III_I and III_{II} are formed upon

pretreatment of cellulose I or II with liquid ammonia or diamine, respectively, and its formation is reversible. Further heat treatment of cellulose III leads to the formation of cellulose IV. Of the four types of cellulose, I is the stiffer and stronger compound, and also shows a much greater resistance to enzymatic depolymerization than the other three man-made polymorphs (Wada et al., 2010, Nishino et al., 1995).

1.1.2 Hemicellulose

Unlike cellulose, which is well defined and is composed of *only* linear glucan chains, hemicellulose is a heterogeneous collective term for a wide variety of amorphous linear and branched polysaccharides that are present in the plant cell wall. Hemicelluloses include xylans, mannans, xyloglucans, glucomannans and glucans (β-(1,3) and β-(1-4)). The structure, composition and localization of hemicelluloses vary depending on plant species and tissue type (Scheller and Ulvskov, 2010). The most important role of hemicelluloses is in strengthening the plant cell via interactions with cellulose and lignin, although the exact organization and interactions are still not perfectly understood (Busse-Wicher et al., 2016). An overview of the most common hemicelluloses is shown in Figure 3. In hardwoods (angiosperm dicot trees), the primary cell wall usually contains xyloglucan (20-25%), glucomannan (5%) and glucoronoarabinoxylan (3-5%), while glucoronoxylan (20-30%) is most prevalent in the secondary cell wall, in addition to glucomannan (2-5%) and galactoglucomannan (0-3%). In softwoods (gymnosperm trees) xyloglucan (10%) and glucoronoarabinoxylan (2%) are the main hemicelluloses of the primary cell wall, whereas galactoglucomannan (10-30%) dominates the secondary cell wall along with glucoronoarabinoxylan (5-15%) (Scheller and Ulvskov, 2010).

1.1.2.1 Xyloglucan

Xyloglucan is found in the primary cell wall of both softwood and hardwood trees, and is composed of a β-(1,4) glucan backbone that is substituted with α-(1,6) linked xylose residues that may be O-2 substituted with galactose or arabinose. In addition, substitutions with galacturonic acid and fucose occur (Pauly and Keegstra, 2016). Xyloglucans are made of repetitive units of these substitutions, where the pattern is dependent on the plant species (Fry et al., 1993). Further modifications in the form of acetylation of terminal galactose or arabinose units, as well as of unsubstituted glucose units, may occur. To date, 24 different side chain modifications are known to occur (Pauly and Keegstra, 2016). The degree of branching and substitution is correlated with solubility (higher branching→higher solubility)

(Peña et al., 2008). In the cell wall, xyloglucan interacts and is intertwined with cellulose through hydrogen bonding, thus contributing to non-covalent cross-linking of cellulose microfibrils (Somerville et al., 2004). The interaction of xyloglucan with cellulose has been suggested to prevent excessive microfibril hydrogen bonding, thus avoiding aggregation of cellulose and ensuring sufficient flexibility during cell wall growth (Park and Cosgrove, 2012). In addition, xyloglucan has been suggested to act as a natural protectant against pathogens, as it may protect cellulose from the action of traditional hydrolytic cellulases (Vincken et al., 1994).

1.1.2.2 Xylans

Xylans consist of a variety of polysaccharides, where the common feature is a backbone made up of β-(1,4) linked xylose residues (Scheller and Ulvskov, 2010). They are dominant in the secondary cell wall of hardwoods (as glucoronoxylan) and make up a part of the secondary cell wall of softwoods (as glucoronoarabinoxylan). Common substitutions include α-(1,2) linked glucoronosyl, 4-O-methyl glucoronosyl residues and arabinose. Acetylations occur frequently at the O-2 or O-3 positions of the xylose residues. It is common for one side of the xylose backbone to be free of substitutions, allowing hydrophobic interactions with cellulose, coating the microfibril in a helical fashion (Grantham et al., 2017, Busse-Wicher et al., 2014).

1.1.2.3 Mannans and glucomannans

Mannans and glucomannans have a backbone of β-(1,4) linked mannose or mannose and glucose, respectively. In glucomannans, glucose units are interspersed in the backbone in a non-repeating pattern. Mannans are usually substituted with α-(1-6) linked galactose, yielding either galactomannan or galactoglucomannan, and acetylations often occur (Capek et al., 2002). In softwoods, galactoglucomannans make up the largest portion of hemicellulose in the secondary cell wall, providing and play a key role in maintaining cell wall integrity through interactions with cellulose (Moreira, 2008).

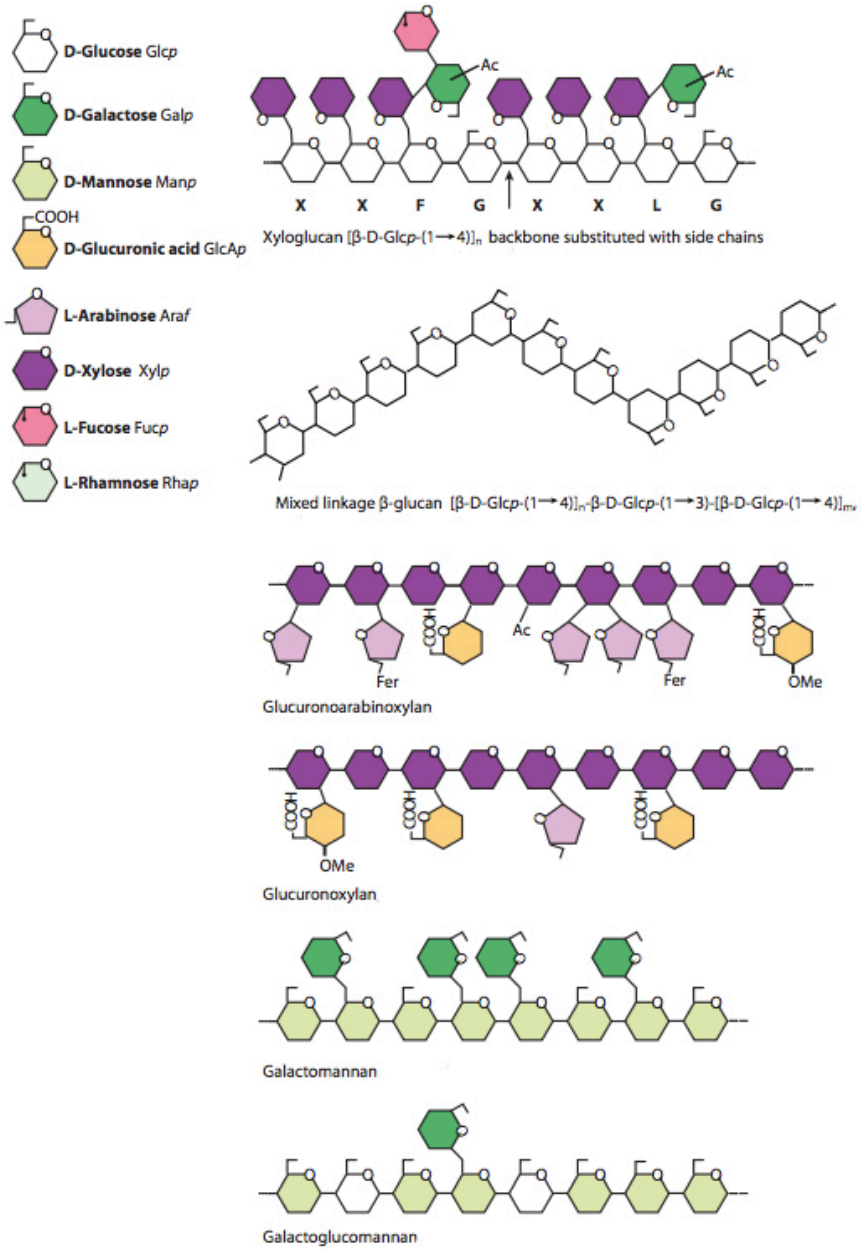

Figure 3. Hemicellulose structures. Hemicelluloses are built up of a variety of monosaccharides and shows varying patterns of branching, substitution and modification. In softwoods, galactoglucomannan is most prevalent, while xylans are most common in hardwoods. The figure is adapted from Scheller and Ulvskov (2010).

1.1.3 Lignin

The third major component of the wood cell wall is lignin. It is a complex amorphous polyphenolic polymer that does not have a defined primary structure, and its composition varies depending on the plant species. Depending on tissue and cell wall compartment, the lignin content can vary between 15-35% by weight (Mosier et al., 2005). Lignin is composed of three different monolignols: coumaryl alcohol, sinapyl alcohol and coniferyl alcohol (Figure 4a), where the former is more prevalent in hardwoods while the latter is more prevalent in softwoods. The monolignols can be polymerized via β-O-4, β-β-(γ-O-α), 5-5 or 5-O-4 linkages (Figure 4b) (Wang et al., 2015), and the polymer molecule can have a mass of more than 10 kDa.

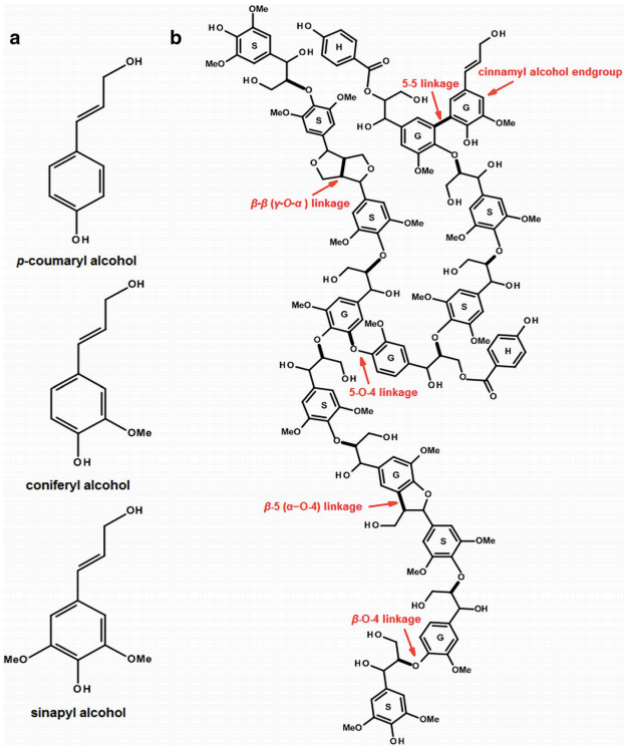

Figure 4. Lignin. **a**) The structure of the tree lignin precursors p-coumaryl alcohol, coniferyl alcohol and sinapyl alcohol. **b**) Model of a lignin polymer, illustrating the different bonds that are formed between the monolignols. This figure was taken from Wang et al. (2015).

Lignin fills the cell walls of vascular plants between the polysaccharides and provides rigidity and structural support. It may be covalently bound to hemicellulose. Being more hydrophobic

in nature than cellulose and hemicellulose, it is considered important for water transport in the lumen, as it limits water uptake in the wood cell (Boerjan et al., 2003). Higher amounts of lignin (Cragg et al., 2015) normally confer a stiffer, less flexible cell wall. The presence of lignin is a major challenge in industrial depolymerization of lignocellulosic materials, as it significantly contributes to the high recalcitrance of these materials. In Nature, fungi have evolved powerful enzymatic systems to depolymerize the wood cell wall, which includes depolymerization of lignin, or leaves the lignin seemingly untouched, as in white- and brown-rot fungi, respectively (Hatakka, 1994).

1.2 Lignocellulose-active enzymes in fungi

The abundance and dominance of lignified plants in terrestrial environments have provided ample opportunity for the evolution of a wide variety of lignocellulose-degrading organisms. Organisms able to fully or partially degrade lignocellulose occur in all three domains of life (Archaea, Bacteria and Eukarya), in soils, water sediments, compost, ruminant intestinal tracts and insect guts (Cragg et al., 2015). These organisms include, but are not limited to, basidiomycetous and ascomycetous fungi, bacteria, archaea, insects, nematodes and marine molluscs (Cragg et al., 2015). The enzymes employed by these organisms attack the different cell wall components, depolymerize them and make their constituents, primarily carbohydrates accessible for metabolization. Lignocellulose-active enzymes usually appear in concert with auxiliary activity enzymes that are secreted by the microbe, with synergistic modes of action and activities that collectively attack the plant cell wall components.

When it comes to degrading woody biomass, the unquestionably most successful microorganisms are the fungi, in particular white- and brown-rot fungi in the Basidiomycota (Blanchette, 1991). Brown rot is typically characterized by the selective removal of cell wall polysaccharides, without the removal of lignin. The lignin that remains is what gives the brown color of the leftover residues. Brown-rot fungi are believed to utilize a Fenton-like (non-enzymatic) system to aid in depolymerization of cell wall polysaccharides, as described in section 1.5. White-rot fungi on the other hand degrade all wood cell wall components simultaneously, including lignin. Common for fungal decay, which occurs aerobically, is the simultaneous secretion of cellulose-, hemicellulose- and lignin-active enzymes to the local environment or attachment of these enzymes to the outward facing cell membrane (Wood and Garcia-Campayo, 1990).

The Carbohydrate Active enZyme (CAZy) database was launched in 1999 and has become the standard in classification of enzymes active on carbohydrates, including those that are active on lignocellulose (Cantarel et al., 2008, Levasseur et al., 2013, Lombard et al., 2013). Enzymes are manually added and curated, and classified into families based on amino acid sequence, catalytic mechanism and three-dimensional structure (Cantarel et al., 2008). Consequently enzymes with the same types of activity and substrate specificity, as defined by the Enzyme Comission (EC), can occur in multiple families (Lombard et al., 2013). At the time of writing (autumn 2018), CAZy contained 402 families, which are all based on experimentally characterized proteins. These families comprise six classes: Glycoside Hydrolases (GH), Glycosyl Transferases (GT), Polysaccharide Lyases (PL), Carbohydrate Esterases (CE), Auxilliary Activities (AA) and Carbohydrate Binding Modules (CBMs). Several CAZymes are multimodular, and can have domains belonging to different families (e.g. GHs attached to CMBs). Figure 5 shows an overview of some of the enzyme types (potentially) involved in the depolymerization of lignocellulose. Further descriptions of some of these enzymes appear in the section on LPMOs (section 1.3).

1.2.1 Glycoside hydrolases (GHs)

Within the CAZy database, the largest class is the GH class with 153 families (autumn 2018). These enzymes catalyze the cleavage of glycosidic bond in carbohydrates via general acid catalysis, requiring an amino acid residue to act as proton donor and another to act as nucleophile/base. Two major mechanisms are utilized, resulting in either the inversion or retention of the anomeric configuration (Davies and Henrissat, 1995). GHs are among the most common enzymes in nature, and are key players in the depolymerization of polysaccharides such as cellulose and hemicellulose.

Cellulose-active GHs can be either exo- or endo-acting, meaning that they attack either at one of the chain ends or within the polymer. Exo-acting cellulose-active GHs that processively degrade their substrate from either reducing or non-reducing chian are called cellobiohydrolases (CBH) and and produce cellobiose. Fungal CBHs are typically found in GH families 6 and 7, and also, less frequently, in families 5 and 9. They are normally multi-modular enzymes where the catalytic GH domain domain is attached to a carbohydrate-binding module (CBM) (Ståhlberg et al., 1991). The active site topology normally has the

shape of as deep groove or tunnel that fits a single cellulose strand (Divne et al., 1994). Cellobiose released by CBHs is further hydrolyzed to glucose by β-glucosidases.

Endo-acting cellulases (endoglucanases, EGs) are generally non-processive (although there are exceptions, see (Cohen et al., 2005, Zhang et al., 2010)) and catalyze bond cleavage in amorphous regions of the cellulose microfibril, generating free chain ends for the CBHs to act upon. The active site architecture in these enzymes is typically more open compared to CBHs, with shallow grooves that bind several sugar units within the cellulose chain (Davies and Henrissat, 1995). Both mono-modular and multi-modular EGs are known. In basidiomycetous fungi, EGs are typically found in GH families 5 and 12 (Floudas et al., 2012).

In the plant cell wall cellulose is closely associated with hemicellulose and lignin, and removal of hemicellulose is often needed to facilitate cellulose depolymerization. The genomes of wood-degrading organisms usually contain up to several dozens of different genes associated with hemicellulose depolymerization (Riley et al., 2014). Hemicellulases can be found in several different GH families, and can be both endo- and exo-acting on the main chain or hydrolyze the side chains. To date more than 25 hemicellulase activities are known, and it is common for several different enzymes to be required in concert to break down complex hemicelluloses such as glucoronoarabinoxylan (Brigham et al., 2018). Endo-acting enzymes mainly include xylanases and mannanases, whereas exo-acting hemicellulases include arabinases, glucoronidases, galactosidases, arabinofurosidases, mannosidases and xylosidases, several of which act on substitutions. Furthermore, O-acetyl modifications on hemicelluloses are handled by carbohydrate esterases (CEs).

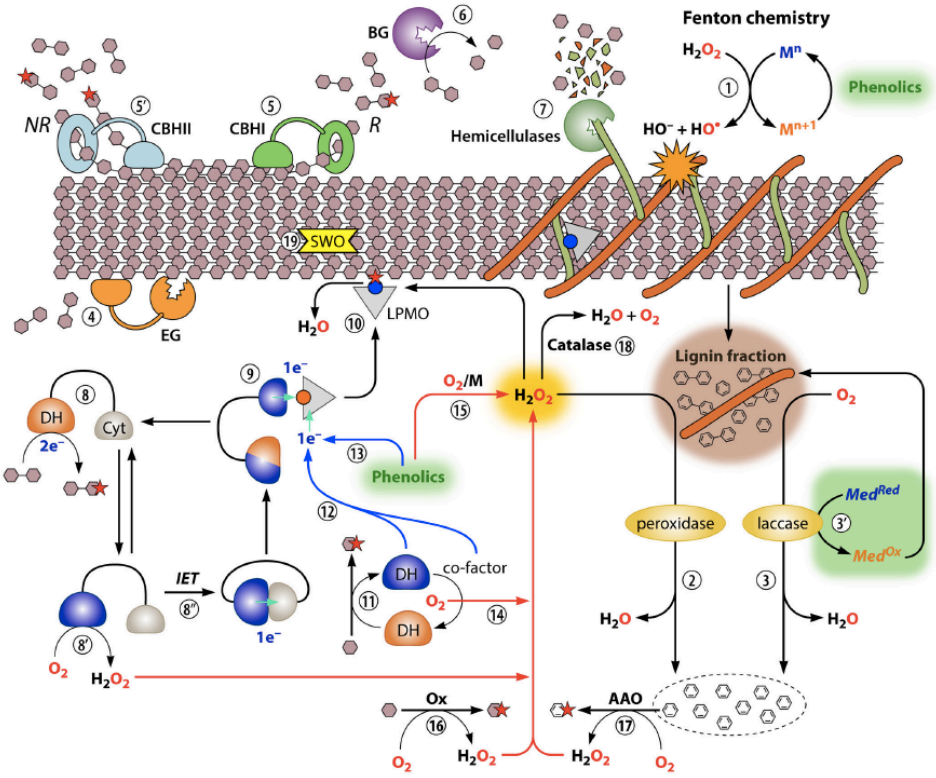

Figure 5. Enzymatic and non-enzymatic systems involved in lignocellulose depolymerization by fungi. In Nature decay fungi use a large number of GH and AA family enzymes to depolymerize wood cell wall components. (1) Non-enzymatic Fenton reactions oxidize lignin and polysaccharides; (2,3) laccases and peroxidases oxidize lignin; (4,5) endo- and exo-acting GHs hydrolyze cellulose; (6) beta-glucosidases hydrolyse cellobiose; (7) hemicellulases attack hemicellulose. Cellobiose dehydrogenase (CDH, an AA3) (8) oxidizes cellobiose and delivers electrons to LPMOs (9), which then oxidize cellulose (10). CDH (8') also has the ability to generate H_2O_2 via reduction of O_2. LPMOs can also be activated by other (single-domain) dehydrogenases (11, 12) or reduced phenolic compounds (13). H_2O_2 can also be generated by these single-domain dehydrogenases (14), reduced phenolics in the presence of transition metals (15), oxidases (16) and aryl-alcohol oxidases (17). Catalases regulate H_2O_2 levels (18). Swollenins (19) may aid in substrate disruption. This figure and most of the legend were taken from Bissaro et al. (2018).

1.2.2 Auxiliary activity enzymes

In addition to the GHs described in the previous section, the genomes of wood degrading fungi encode a large suite of auxiliary activity redox enzymes that are or may be involved in lignocellulose depolymerization, either through direct action on the biopolymer or via the

generation of non-enzymatic secondary metabolites (phenolics) and enzyme co-substrates (H_2O_2) (Levasseur et al., 2013, Floudas et al., 2012, Riley et al., 2014) (Fig. 5). At the time of writing there were 15 AA families described in CAZy (Table 1). Only the AA families most relevant to this thesis are discussed in this section.

Table 1. *Auxiliary activity families in the CAZy database.*

AA family	Class	Activity/function
1	Laccases	Lignin oxidation
2	Class II peroxidases	Lignin oxidation
3	GMC Oxidoreductases	Dehydrogenases and oxidases acting on various substrates; H_2O_2 generation, detoxification of lignin degradation products and reduction of LPMOs
4	Vanilyl-alcohol oxidases	Detoxification of lignin degradation products, H_2O_2 production
5	Copper radical oxidases	Oxidize alcohols and sugars, H_2O_2 generation
6	Benzoquinone reductases	Production of iron chelators, detoxification of lignin degradation products
7	Glucooligosaccharide oxidases	Oxidize the reducing end of oligosaccharides
8	Cytochromes and iron reductases	Iron transfer and iron reduction
9	LPMO	Fungal; cellulose and hemicellulose oxidation
10	LPMO	Bacterial; chitin and cellulose oxidation
11	LPMO	Fungal; chitin oxidation
12	PQQ oxidoreductases	Oxidize various sugars; Redox partner for LPMO
13	LPMO	Fungal; starch active
14	LPMO	Fungal; xylan active
15	LPMO	Insects; chitin active

Enzymatic lignin mineralization only occurs in white-rot fungi and involves the action enzymes in AA families 1 and 2, while brown-rot fungi use a non-enzymatic Fenton-like system that is discussed in section 1.5. AA1 family enzymes are laccases, which are multi-copper oxidases that perform one-electron oxidizations of phenolic compounds. In wood-degrading organisms they are involved in lignin depolymerization (Cohen et al., 2002). Family AA2 consists of lignin modifying class II peroxidases that contain a heme cofactor

(Hiner et al., 2002). These enzymes utilize H_2O_2 as an electron acceptor to oxidize the active site transition metal (iron or manganese), which in turn oxidizes lignin.

The GMC oxidoreductases (family AA3) are flavoenzymes that oxidize various sugars and alcohols with the concomitant reduction of either O_2 (to H_2O_2) or phenolic compounds (Cavener, 1992). Cellobiose dehydrogenases (EC 1.1.98.18) (CDHs) oxidize cellobiose with concomitant reduction of enzymatic electron acceptors or O_2. Multi-modular CDHs often have a cytochrome domain (AA8), which is used to transfer electrons to an acceptor, such as lytic polysaccharide monooxygenases (LPMOs) (Kracher et al., 2016). Aryl alcohol oxidases (EC 1.1.3.7) and alcohol oxidases (1.1.3.13) oxidize aromatic primary alcohols and primary aliphatic alcohols, respectively, reducing O_2 resulting in the production of H_2O_2 (Hernández-Ortega et al., 2012, Ledeboer et al., 1985). The roles of these enzymes in wood decay are likely multifunctional, as they generate the H_2O_2 needed as a co-substrate for several other enzymes, and protect the fungus from toxicity of degradation products. Glucose 1-oxidases (EC 1.1.3.4) and pyranose oxidases (EC 1.1.3.10) oxidize glucose to D-glucono-1,5-lactone or 2-dehydro-D-glucose respectively, also resulting in the production of H_2O_2 via the reduction of O_2 (Albrecht and Lengauer, 2003, Kiess et al., 1998).

Family AA5 enzymes are copper radical oxidases, a class of enzymes that is known to be highly expressed during wood decay by both white- and brown-rot fungi (Kersten and Cullen, 2014). These enzymes are believed to be key in extracellular H_2O_2 production, and include alcohol oxidases (EC 1.1.3.13), galactose oxidases (EC 1.1.3.9) and glyoxal oxidases (EC 1.2.3.15).

Benzoquinone reductases (EC 1.6.5.6, family AA6) are intracellular enzymes that have several suggested roles in wood decay (Jensen Jr et al., 2002, Brock et al., 1995, Cohen et al., 2004). They are hypothesized to be involved in the synthesis and regeneration of low molecular weight secondary metabolites involved in non-enzymatic decay mechanisms, such as 2,5-dimethoxyhydroquinone in *Gloeophyllum trabeum* (Paszczynski et al., 1999), as well as be important for detoxification and protection against reactive quinone compounds (Spain and Gibson, 1991). Expression of enzymes in AA families 3, 5, 6 and 9 during brown-rot decay on native and modified wood was studied in paper II in this thesis.

Lytic polysaccharide monooxygenases (LPMOs) are placed in AA families 9, 10, 11, 13, 14 and 15, and oxidize crystalline or amorphous polysaccharides. They are discussed in detail in section 1.3.

1.2.3 Carbohydrate-binding modules

CMBs are non-catalytic domains that often occur in multi-modular cellulases and hemicellulases (Boraston et al., 2004). These CMBs are thought to promote association of GH domains with the often difficult to access polysaccharide substrate and to prolong enzyme association with the substrate. Interestingly, CBMs that bind one particular polysaccharide are sometimes observed in association with GH domains that hydrolyze another class of polysaccharide, which can be explained by a proximity effect: due to the co-polymeric nature of the wood cell wall, proximity to the substrate of the catalytic domain (e.g. cellulose) may be achieved by binding to an associated polysaccharide (e.g. xylan) (Hervé et al., 2010).

The linker connecting CBMs to GHs vary in length and degree of post-translational modifications (e.g. glycosylation). Whether these linkers serve any biological function other than connecting the domains remains unresolved, although there is some evidence indicating that the linkers contribute to substrate-binding (Payne et al., 2013).

1.2.4 Carbohydrate esterases

Esterifications like O- and N-acetylations and ferulation occur frequently in wood cell wall polysaccharides and may need to be removed by CEs, to allow efficient depolymerization by GHs (Biely, 2012). Hemicellulose-active CEs include acetyl-xylan estereases (EC 3.1.1.72, CE families 1-7, 12, 15 and 16), which hydrolyze acetyl substitutions on xylose residues, broad specificity acetyl-mannan esterases in family CE2 (Montanier et al., 2009), and ferulic acid esterases (EC 3.1.1.73, CE family CE1), which hydrolyze ferrulic acid substitutions on arabinose residues. Ferulic acid modifications are known to be involved in covalently connecting xylan to lignin (Shallom and Shoham, 2003).

1.2.5 Expansins

Expansins are a class of proteins that enable and regulate the extension of the growing plant cell wall during synthesis (Rose and Bennett, 1999). They have also been implicated in wood cell wall depolymerization, as genes encoding expansins are found in several organisms that degrade lignocellulosic materials, such as wood decay fungi. Although expansins have no known catalytic activity, they have been shown to improve the enzymatic depolymerization

of wood cell wall components through a unknown molecular mechanism (Baker et al., 2000). Expansins are currently not described in the CAZy database. Of note, the expression profiles of expansin-encoding genes during wood decay by *Rhodonia placenta* are described in Paper II of this thesis.

1.3 Lytic polysaccharide monooxygenases

Hydrolytic cellulases and hemicellulases (see section 1.3.1) have been known for over 100 years to be involved in depolymerization of lignocellulosic materials, but were also known to only or primarily attack the amorphous regions of these highly recalcitrant materials (Pringsheim, 1912). Since the majority of the wood cell wall cellulose is crystalline in nature, the question how various wood degrading microorganisms are able to efficiently access and degrade this cellulose remained an unsolved problem for years. In 1950, Reese and colleagues hypothesized that organisms that grow on cellulose utilize two enzymatic systems, which they called C_1 and C_x. In this model, the C_1 system would convert the crystalline cellulose into a more easily accessible substrate for the C_x system, which would release soluble oligosaccharides (Reese et al., 1950). The molecular nature of cellulose degradation was unknown at that time, but it was suggested that the C_x system included endoglucanase activity.

In the 1970s, it was suggested that an oxidative enzyme mechanism was involved in cellulose depolymerization. Eriksson et al. (Eriksson et al., 1974) observed a two-fold enhancement of cellulose depolymerization by culture supernatants of *Sporotrichulum pulverulentum* in the presence of oxygen compared to under anaerobic conditions. In 1992 a novel enzyme was cloned from *Agaricus bisporus* (CelI) that was described as a potential cellulose-degrading enzyme, although no activity was found (Raguz et al., 1992). In subsequent years, several new proteins were described and classified as family GH61 endoglucanases, although the activity of these enzymes was very low compared to other well-known cellulases (Beeson et al., 2015). These GH61 proteins were later shown to boost the conversion of cellulose by traditional cellulases (Merino and Cherry, 2007). Today we know that these GH61 proteins are Lytic Polysaccharide Monooxygenases or LPMOs.

The catalytic activity of LPMOs was first described in 2010, when it was shown that the chitin-binding protein CBP21 from *Serratia marcescens* catalyzes oxidative cleavage of chitin (Vaaje-Kolstad et al., 2010). Five years earlier, it had been shown that this protein, which is member of a large family of similar “chitin-binding” proteins first described in the 1990s, enhances the depolymerization of chitin when incubated with chitinases, and was at time incorrectly identified as “non-catalytic” (Vaaje-Kolstad et al., 2005a). The crystal structure of Cel61B from *Hypocrea jecornia* (Karkehabadi et al., 2008) showed a striking resemblance to that of CBP21 (Vaaje-Kolstad et al., 2005b), possibly linking the boosting

effects observed for GH61s and CBP21. In 2011, the first cellulose-active bacterial LPMO (CBM33) was characterized and oxidative cleavage of cellulose was demonstrated (Forsberg et al., 2011). That same year, several fungal GH61s were shown to cause oxidative cleavage of cellulose (Langston et al., 2011, Quinlan et al., 2011, Phillips et al., 2011, Westereng et al., 2011). Following these discoveries, the two enzyme families were collectively named lytic polysaccharide monooxygenases (Horn et al., 2012), and in 2013 the auxiliary activity (AA) families classification was created in CAZy to accommodate the growing number of non-hydrolytic enzymes involved in lignocellulose depolymerization (Levasseur et al., 2013).

1.3.1 Phylogeny, specificity and three dimensional structure of LPMOs

LPMOs are found in CAZy families AA 9, 10, 11, 13, 14 and 15, are ubiquitous in wood degrading organisms, and are found within all three domains of life. Fungal cellulose- (and hemicellulose-) active LPMOs are placed in family AA9, while bacterial cellulose- and chitin- active LPMOs are found in family AA10. Family AA11 is composed of fungal chitin-active LPMOs, while family AA13 LPMOs are from fungi and active on starch. The recently discovered family AA14 is composed of LPMOs that attack the xylan chains that coat cellulose microfibrils (Couturier et al., 2018). Family AA15, the most recent addition to the CAZY AA families at the time of writing (fall 2018), contains cellulose- and chitin-active LPMOs encoded by the genomes of termites and other insects (Sabbadin et al., 2018).

Fungal genomes can have anywhere from a few to more than 30 genes encoding LPMOs (Bissaro et al., 2018), and in some organisms the number of LPMOs is higher than that of hydrolytic cellulases (Lenfant et al., 2017). The numbers of LPMO-encoding genes are generally higher in white-rot than in brown-rot fungi (Floudas et al., 2012). *Gloeophyllum trabeum* (Paper I and III) and *Rhodonia placenta* (Paper I and II) carry six (4 AA9s, 2 AA14s) and four (2 AA9s and 2 AA14s) LPMO genes respectively. Growth on different types of biomass will affect the expression of different LPMOs, which may indicate different substrate specificities present REF) (Rytioja et al., 2014). Fungal LPMOs may display several substrate specificities, including activity on cellulose, soluble cellulose oligosaccharides, xyloglucan, glucomannan and xylan, or combinations thereof (Beeson et al., 2015, Agger et al., 2014, Courtade et al., 2018). The characterization of cellulose- and xyloglucan-active *Gt*LPMO9B is described in Paper III.

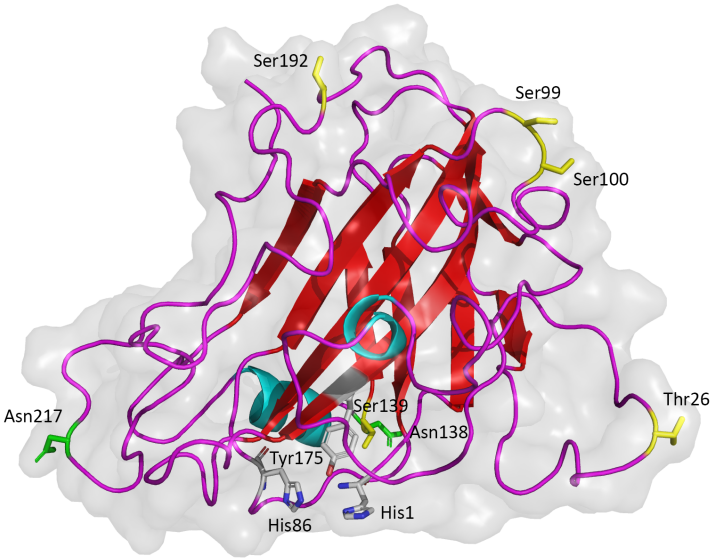

Figure 6. Structural model of *Gt*LPMO9B. The model was built with PHYRE2, using the crystal structure of *Nc*LPMO9M (PDB: 4EIS) as template and is presented in the supplementary material of Paper III. Typical features of AA9 LPMOs are highlighted. Beta-strands, helices and loops are coloured red, blue and magenta, respectively**.** The side chains of the copper coordinating histidines (His1 and His86) and of Tyr175 in the proximal axial copper coordination sphere are shown as sticks, with grey carbons. The side chains of potentially glycosylated residues are shown as green (N-glycosilation) and yellow (O-glycosilation) sticks.

The overall fold of LPMOs (Figure 6) is highly conserved, despite low sequence similarities within and between the various LPMO families. The core structure is a β-sandwhich module consisting of seven to nine anti-parallel β-strands that are connected by loops that vary in length (Vaaje-Kolstad et al., 2017). Some of these loops can contain shorter helices. The length and positioning of the loops on the catalytic surface have been implicated in determining substrate specificity (Vaaje-Kolstad et al., 2017, Wu et al., 2013). The substrate-facing surface of the enzyme has a flat topography with a solvent-exposed type II copper center (Quinlan et al., 2011). This copper is coordinated by two histidines (one of which is always N-terminal) that form a histidine brace providing three equatorial coordination positions. The distal axial coordination is exposed to the solvent, while the proximal axial position is shaped by a highly conserved tyrosine residue (Tyr175 in Fig. 6). In fungi the N-terminal histidine residue is Nε-methylated. It has recently been shown that this methylation leaves most LPMO properties unchanged but may help protecting the enzyme from auto-

inactivation caused by peroxidase side activities (see 1.3.3) (Petrovic et al., 2018). Fungal LPMOs are often post-translationally modified by *O*- and *N*-glycosylations, which sometimes leads to more than a doubling the molecular weight of the enzyme. In some fungal LPMOs the C-terminus of the catalytic domain is covalently attached to one or more CBMs via a flexible linker, whereas a few multi-modular enzymes containing an LPMO and a GH domain also occur (Vaaje-Kolstad et al., 2017).

LPMOs can act on both the C_1 the C_4 carbon of the scissile glycosidic bond. Some LPMOs are strictly C_1 or C_4 oxidizing, whereas others can oxidize at either position (Isaksen et al., 2014, Vu et al., 2014). It may seem that this variation in regioselectivity is caused by minor variation in how the substrate is positioned in the enzyme-substrate complex (Forsberg et al., 2018, Danneels et al., 2018). Using a mechanism that is discussed in detail below, LPMOs hydroxylate a carbon in the scissile glycosidic bond, which results in spontaneous bond cleavage (Beeson et al., 2012). Several fungal cellulose-active AA9 LPMOs also oxidize certain hemicelluloses. This can be exemplified by two characterized AA9s from *G. trabeum* (*Gt*LPMO9A-2 and *Gt*LPMO9B; Kojima et al. 2016 and Paper III, respectively) that both display C_1/C_4 oxidization of cellulose and also oxidize xyloglucan. *Gt*LPMO9A-2 seemingly has the widest substrate specificity since it oxidizes xyloglucan regardless of the substitution pattern of the glucan backbone.

1.3.2 Catalytic mechanism(s) of LPMOs

Several LPMO mechanisms have been proposed by different authors (Phillips et al., 2011, Beeson et al., 2015, Walton and Davies, 2016, Bissaro et al., 2017). Initially, it was thought that LMPOs use molecular oxygen, and are thus monooxygenases but recent discoveries by Bissaro et al. (2016a, 2017) have challenged the monooxygenase paradigm by proposing a peroxygenase mechanism that is dependent on H_2O_2. The role of H_2O_2 as a co-substrate for LPMOs is a major subject of Paper III.

1.3.2.1 The O_2 reaction mechanism: oxidase and monooxygenase activities

Subsequent to their identification as proteins with catalytic activity (Vaaje-Kolstad et al., 2010), LPMOs were classified as monooxygenases due to the observation that O_2, in addition to a reducing agent (commonly ascorbic acid, AscA), was needed to perform oxidative cleavage of the substrate. The incorporation of radiolabelled $^{18}O_2$ into the C_1 position of chitin oxidized by CBP21 (or *Sm*LPMO10A), and an observed dependency on dissolved O_2

(anaerobically performed experiments yielded no products) provided strong indications towards a monooxygenase-like mechanism. Product analysis by mass spectrometry and chromatography showed that the primary products of LPMOs are aldonic acids (Vaaje-Kolstad et al., 2010) or gem-diols (Phillips et al., 2011), which are generated through spontaneous hydration of a lactone or ketoaldose, respectively (Isaksen et al., 2014).

The suggested monooxygenase mechanism involves a one-electron reduction of the copper site from Cu(II) to Cu(I), followed by the binding and reduction of O_2, to form a superoxide intermediate (Cu(II)-O-O●) (Kjaergaard et al., 2014). A second electron and two protons are then required to complete the catalytic cycle, via different possible routes (Beeson et al., 2015, Walton and Davies, 2016), leading to incorporation of a hydroxyl group at the C_1 or C_4 in the scissile glycosidic bond, which is followed by spontaneous bond cleavage (Beeson et al., 2012) (Figure 7a).

The monooxygenase paradigm has been widely accepted by the scientific community. However, it is important to note that in reducing environments, O_2-derived intermediates such as superoxide and H_2O_2 will be generated. It is unequivocally accepted that reduced LPMOs can act as oxidases in the absence of substrate, meaning that they reduce O_2 to generate H_2O_2 (Isaksen et al., 2014, Kittl et al., 2012). Whether this H_2O_2 is generated through the disproportionation, in solution, of superoxide generated by the LPMO via a single-electron reduction of O_2 or whether H_2O_2 is generated by a two-electron reduction of O_2 to H_2O_2 in the active site of the enzyme, is currently under investigation. There are indications that the latter scenario is the most probable: (Span et al., 2017) demonstrated that addition of superoxide dismutase (SOD) to LPMO reactions did not inhibit the production of H_2O_2, suggesting that H_2O_2 formation occurs in the active site and that superoxide is not released from the enzyme.

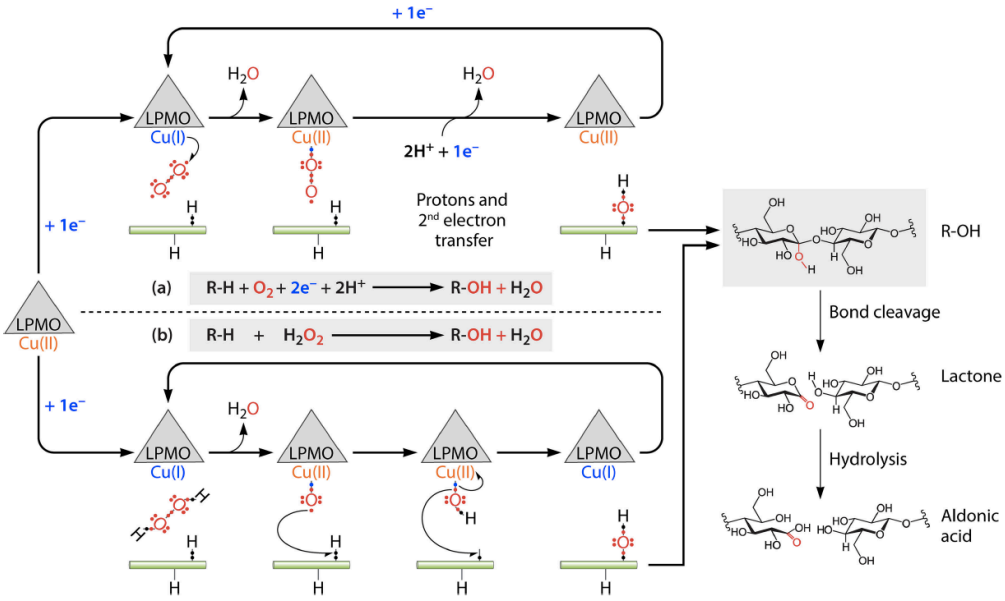

Figure 7. Proposed LPMO cleavage mechanisms. Both pathways require an initial one-electron reduction of the active site copper center, from Cu(II) to Cu(I), and both pathways result in the incorporation of an hydroxyl group in the scissile glycosidic bond which results in spontaneous bond cleavage (right hand side of the figure). The upper part (**a**) of the figure shows an O_2-dependent monooxygenase mechanism where a total of two electron and two protons is needed to complete one catalytic cycle. Panel (**b**) shows a possible H_2O_2-dependent mechanism. Here, only H_2O_2 is needed after the initial reduction of the active site to complete a catalytic cycle. Note that the nature of the reactive copper-oxygen species is not known and that multiple possible scenarios exist, of which only one is shown here. This figure was taken from Bissaro et al. (2018).

The O_2-mechanism poses an unresolved challenge in regards to the delivery of the second electron (and the two protons), since it requires the electron to reach the active site while the enzyme is bound to the substrate. Whereas the first electron can be "stored" on the reduced Cu(I), the second electron needs to be delivered while catalysis is ongoing. This challenge could be solved either through electron storage elsewhere on the enzyme (aromatic residues in proximity to the active site have been suggested) (Solomon et al., 2014) or via an electron transport chain or channel in the enzyme (Walton and Davies, 2016, Beeson et al., 2015). Neither of these options is supported by solid experimental data. Structural studies show that substrate binding by AA9 LPMOs shields the copper ion from the solvent and that the catalytic oxygen species must bind in the equatorial position, which is secluded from the solvent in the enzyme-substrate complex (Frandsen et al., 2016). The somewhat enigmatic delivery of the second electron is not relevant in a mechanism where H_2O_2 is the co-substrate,

since, in that case, only a single electron "priming" reduction of the copper is needed for catalysis.

1.3.2.2 The H_2O_2 reaction mechanism: peroxygenase and peroxidase activities

The monooxygenase mechanism (R-H + O_2 + $2e^-$ + 2H → R-OH + H_2O) has recently been challenged by Bissaro et al. (2016a, 2017), who demonstrated through extensive experimental work that H_2O_2 could drive LPMO reactions. It was observed that the addition of H_2O_2 to LPMO reaction mixtures could significantly boost reaction rates, and that performing reactions anaerobically with supplied H_2O_2 yields oxidized LPMO-generated products. Competition experiments with molecular oxygen and labeled H_2O_2 showed that the LPMO uses the latter. Importantly, it was also shown that (H_2O_2-consuming) horseradish peroxidase (HRP) inhibits LPMO activity. Bissaro et al concluded that the previously observed O_2-dependency of LPMO action can be attributed to O_2 serving as a precursor for generation of the true co-substrate, H_2O_2. These data combined suggest that LPMOs should be reclassified as peroxygenases (R-H + H_2O_2 → R-OH + H_2O). These groundbreaking results have since been supported by other researchers in both experimental (Hangasky et al., 2018, Petrovic et al., 2018, Kuusk et al., 2018), and computational studies (Wang et al., 2018, Hedegård and Ryde, 2018).

The H_2O_2 mechanism entails an initial one-electron "priming" reduction of the active site copper from Cu(II) to Cu(I) which is followed by a reaction with H_2O_2, resulting in proton abstraction and hydroxylation of the substrate with the concomitant release of water (Figure 7b). Importantly, this leads to regeneration of the LPMO-Cu(I) state, allowing for further catalytic cycles without an additional reduction of the active site copper. This scenario is supported by the supra-stoichiometric release of oxidized products in LPMO reactions with sub-stoichiometric amounts of reductant in combination with supplied H_2O_2 (Bissaro et al., 2017, Paper III) It has been shown that LPMO affinity for H_2O_2 is significantly higher than the affinity for O_2, which mirrors the properties of well-known peroxygenases (Kuusk et al., 2018). Computational quantum mechanical studies have shown that the peroxygenase reaction is plausible, with low overall energy barriers involving a Cu(O^+) intermediate as oxidant (Wang et al., 2018, Hedegård and Ryde, 2018). Furthermore, studies support a 1:1 stoichiometric ratio between the amount of supplied H_2O_2 and the amount of generated oxidized product in reactions with both AA9 and AA10 LPMOs (Hangasky et al., 2018, Kuusk et al., 2018, Müller et al., 2018).

The exact molecular mechanism of H_2O_2-dependent LPMO action has not yet been elucidated, and whether LPMOs can utilize both O_2 and H_2O_2 as co-substrate remains unclear. It is worth noting that the H_2O_2-based mechanism solves the problem of the second electron delivery described in the previous section, since H_2O_2 carries both the protons and the reducing equivalents required for catalysis. Of note, it is well known that H_2O_2 generating enzymes are ubiquitous in the secretomes of wood degrading organisms (see 1.3.4 and the following section). Finally, it is now clearly demonstrated that LPMOs react much more efficiently with H_2O_2 than with O_2 (Bissaro et al., 2017, Hangasky et al., 2018, Paper III).

1.3.3 LPMO reduction and the source of H_2O_2 – *in vitro* and *in vivo*

LPMOs require reduction of the active site copper to be catalytically activity. The source of reducing power in natural systems is not well known, but it is well established that LPMOs are promiscuous when it comes to reducing agents *in vitro*. The open and flat topology of the LPMO active site exposes the Cu-center directly to the solvent, and most components with a more negative redox potential than the copper have the potential of performing the LPMO reduction (Kracher et al., 2016). While the redox potential of Cu(II)/Cu(I) in solution is +160 mV at neutral pH, it is considerably more positive when complexed in the active site of the enzyme. Most reported LPMO-Cu(II)/LPMO-Cu(I) redox potentials are in the range of +240 to +326 mV (Garajova et al., 2016). Kracher et al (2016) have shown a clear correlation between the redox potential of the reducing agent and the rate of LPMO reduction (Kracher et al., 2016). Although not often addressed in published studies, the performance of the reductant-LPMO system may be strongly pH-dependent, due, at least in part to the pH-dependency of redox potentials (Frommhagen et al., 2018a, Paper III). Interestingly, reported catalytic rates, usually in the per-minute range, are much lower that reported reduction rates, which are in the per-second range (Bissaro et al., 2018). If the O_2-based mechanism is assumed correct, this rate discrepancy may indicate that the transfer of the second electron is rate limiting and can be affected by the reductant type. However, in the H_2O_2-based mechanism, the priming reduction cannot be rate limiting, suggesting that the catalytic rate of the LPMO in reactions without added H_2O_2 is governed by the ability of the reductant-LPMO system to generate and/or accumulate H_2O_2.

Literature shows that several reducing systems can drive LPMO activity, both enzymatic and non-enzymatic. The most commonly used reducing agent is ascorbic acid (AscA) (Bissaro et al., 2018), but a wide range of phenolic compounds can also drive LPMO reactions (Kracher

et al., 2016, Frommhagen et al., 2018b), in addition to lignin-derived compounds (Westereng et al., 2015). For phenolic compounds, there is a clear relationship between the degree of hydroxylation and the catalytic rates observed with LPMOs, with tri-hydroxy compounds being the most efficient, followed by di-hydroxy compounds and finally mono-hydroxy compounds, which are the least efficient (Frommhagen et al., 2018b). Of note, it is known that H_2O_2 generation (via auto-oxidation) by tri-hydroxy phenols like pyrogallol and 1,2,4-benezenetriol is significantly higher than with di-hydroxy compounds like catechol and hydroquinone under physiological conditions (pH 7.4, 37°C) (Akagawa et al., 2003).

The best understood enzymatic systems for driving LPMO reactions are GMC oxidoreductases in family AA3 (Kracher et al., 2016) (Fig. 5). These extracellular enzymes include well-known multi-modular cellobiose dehydrogenases (CDHs), where the catalytic domain is often linked to a cytochrome domain that is able to deliver electrons to the LPMO (Phillips et al., 2011, Langston et al., 2011), as well as single-domain aryl alcohol oxidases (Garajova et al., 2016). AA3 enzymes can couple the oxidization of a wide variety of substrates (sugars, aromatic alcohols and aliphatic alcohols) to the reduction of quinones to their hydroquinone state, which can subsequently reduce the LPMO (Kracher et al., 2016). In addition, AA3 enzymes are known to generate H_2O_2 via the reduction of dissolved O_2 (Cavener, 1992), an activity that has been implicated in wood decay for decades (Floudas et al., 2012, Westermark and Eriksson, 1975). In Nature, organisms that degrade woody biomass can have more than 50 genes encoding AA3 family enzymes (Riley et al., 2014). Another recently discovered enzyme that can drive LPMO reactions is a family AA12 pyrroloquinoline-dependent pyranose dehydrogenase (Várnai et al., 2018).

In 2016, a study reported that the light sensitive pigment chlorophyllin, in combination with AscA, was able to fuel LPMO reactions when exposed to visible light (Cannella et al., 2016). The authors reported reaction rates that were 10-100 fold higher compared to standard conditions (reductant+O_2), and it was hypothesized that the observed enhanced rates were due to high redox potential electrons generated by the photo-excited pigment. This suggestion is difficult to reconcile with the notion that single-electron reduction of LPMOs is orders of magnitude higher than the catalytic rate, which implies that reduction cannot be the rate-limiting factor unless it is the delivery of the a second electron. An alternative explanation has been proposed by (Bissaro et al., 2016a), who hypothesized that these observations could be a result of the generation of H_2O_2 by the pigment-reductant system. It is known that under aerobic conditions, excited pigments like chlorophyllin can perform single-electron reduction

of O_2, yielding superoxide, which may be converted to H_2O_2 by spontaneous disproportionation or reactions with AscA. A subsequent study dismissed the claim by Bissaro et al. (2016b) that the light-chlorophyllin system drives the LPMO reaction through H_2O_2 formation by showing that incubation of the LPMO-Chlorophyllin system with catalase ($2H_2O_2 \rightarrow 2H_2O + O2$) did not inhibit activity (Möllers et al., 2017). The nature of the chlorophyllin-light system remains controversial. Of note, it has been claimed that the difference in H_2O_2 affinity between catalase (typically in the mM range, (Switala and Loewen, 2002)) and peroxidases and LPMOs (µM range, (Singh et al., 2008)) will cause the LPMO to outcompete the catalase, which could explain why catalase does not inhibit (H_2O_2–driven) LPMO activity (Bissaro et al., 2018). Fungi, including the brown-rot fungus *Rhodonia placenta* secrete catalases, which are believed to regulate extracellular H_2O_2 levels (Zhang et al., 2016). The comparatively low K_m of these catalases likely keeps H_2O_2 at a level high enough do drive LPMO, peroxygenases and the Fenton system (see next section), and low enough to avoid damage to the energetically costly secreted enzymatic machinery.

1.4 Brown-rot fungi

In Nature, fungi play a key part in the carbon cycle, as they are the main decomposers of dead lignified plant matter (Floudas et al., 2012). Wood-decay fungi have traditionally been classified according to the physical appearance of the material they are degrading, as either soft-, white- or brown-rot. Soft-rot fungi are found Ascomycota and to not have the enzymatic apparatus for complete removal of all cell wall components in lignified wood, but only partially degrade wood, usually under high moisture content (Goodell et al., 2008). White- and brown-rot fungi are found in Basidiomycota and are the only organisms able to fully degrade and access the polysaccharides within the wood cell wall. White-rot fungi are able to fully degrade all wood cell wall polymers, including lignin, resulting in the white appearance of the decaying material. Brown-rot fungi on the other hand do not depolymerize lignin, although they have been shown to extensively modify it (Filley et al., 2002, Yelle et al., 2008), and only remove the polysaccharides.

1.4.1 Phylogeny and evolution of brown-rot fungi

The evolution of lignocellulose-degrading fungi must be considered one of the most ecologically important events of the last 300 million years, but the exact evolutionary origins of these fungi remain an area of research with several unknowns. Of the two major divisions of dikaryotic fungi, only Basidiomycota contain true wood-degrading species (Floudas et al., 2012). The evolution of lignin decomposition is estimated to have occurred approximately 290 million years ago, coinciding with the first appearance of Agaricomycetes (Floudas et al., 2012). Brown-rot fungi are thought to have evolved from ancestral saprotrophic white-rot ancestors, with an subsequent reduction in key lignin and cellulose degrading enzymes over time (Arantes et al., 2012). Well-studied brown-rot fungi include *Rhodonia placenta* (previously *Postia placenta*), *Gloeophyllum trabeum, Fomitopsis pinicola*, *Serpula lacrymans* and *Coniophora puteana*. These fungi are distantly related to each other, and as such brown-rot is believed to be a convergently evolved trait without a shared common ancestor, which make brown-rot fungi a polyphyletic group. It has been suggested that a strict white/brown-rot dichotomy should not be applied, as each group displays major genetic differences and varying decay mechanisms, and that one should rather consider a continuum (Riley et al., 2014). Riley et al. (2014) came to this suggestion after comparing 33 basidiomycetous genomes. Previous studies grouped white- and brown-rot according to the

presence or absence of class II peroxidases (PODs), respectively. The authors sequenced the genomes of two fungi that cause a little characterized type of brown-rot (*Botryobasidium botryosum* and *Jaapia argillacea*) that lack PODs but have a significant number of enzymes active on crystalline cellulose normally only seen in white-rot fungi. These two fungi, which due to the absence of PODs may look like brown rots, grouped closely with the white-rot fungus *Phanerochaete chrysosporium* in the genetic analysis.

This picture was complicated by Nagy et al. (2015), who demonstrated that a genetically distant clade believed to have diverged before the appearance of Agaricomyctes, the Dacrymycetes, have members that cause brown-rot (Figure 8). They claimed that PODs evolved later in Agaricomycetes, and show that early divergent clades Cantharellales, Sebacinales, Auriculariales, and Trechisporales do not contain POD genes. This points to white-rot fungi evolving after the divergence of these primitive fungi. As such, generalizations concerning the decay mechanisms of brown-rot fungi should be done with caution, as brown-rot decay apparently occurs in very distantly related species. However it remains a general trend that fungi that cause this type of rot have significantly reduced numbers of genes encoding cellulose- and lignin-active enzymes.

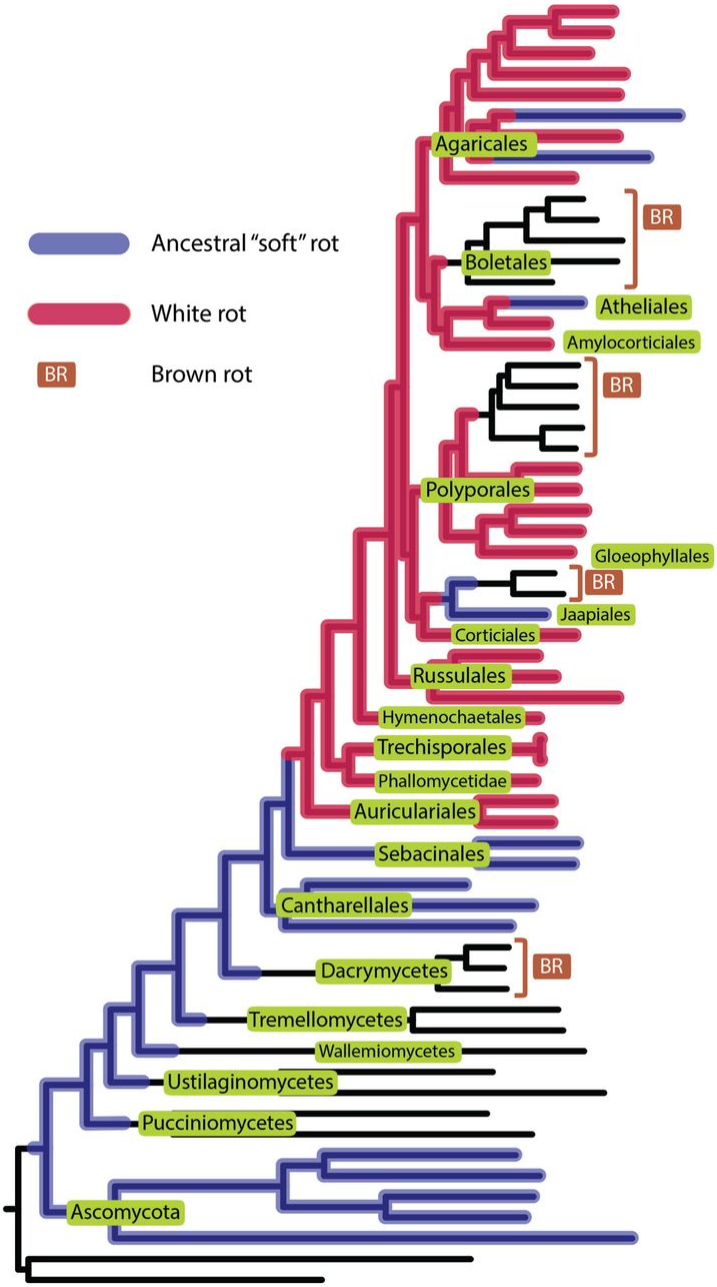

Figure 8. Phylogenetic tree of wood decay fungi. Organisms that causes brown-rot ("BR") are found in distantly related clades, indicating that brown-rot is a convergent trait. The most primitive organisms to cause brown-rot are jelly fungi in the Dacrymycetes. Until recently, it was believed that brown-rot fungi had all evolved from white-rot ancestors, which has recently been challenged. Figure taken from Nagy et al. (2015).

1.4.2 Lignocellulose-active enzymes in brown-rot fungi

The advent of next-generation sequencing has enabled comparative studies of a large number of fungal genomes, which has resulted in several key publications in recent years (Floudas et al., 2012, Nagy et al., 2015, Riley et al., 2014, Eastwood et al., 2011). These studies have shed light on the genetic similarities and differences in brown-rot fungi and have revealed one aspect in particular: compared to white-rot fungi, brown-rot fungi are significantly reduced in their number of lignocellulose-active enzymes (Figure 9).

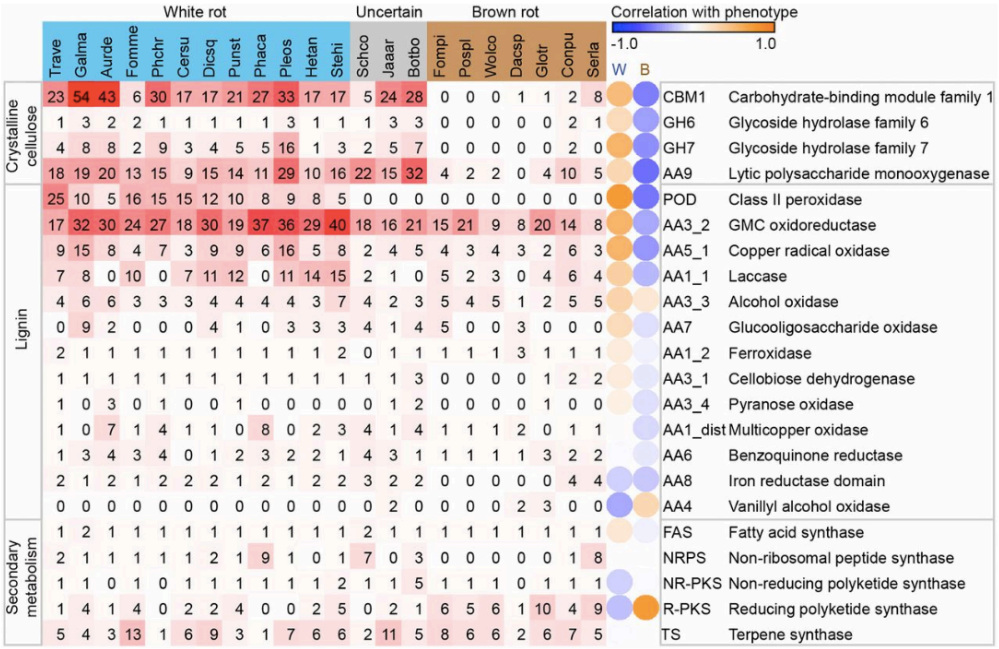

Figure 9. Selected lignocellulose-active enzymes in white- and brown-rot fungi. The cellulolytic apparatus of brown-rot fungi is severely reduced in comparison to white-rot fungi. Brown rot fungi contain few or no GH6 and GH7 cellobiohydrolases, a lower number of LPMOs (AA9) and few or no lignin-active enzymes. Note that GH5 and GH12 family cellulases are not shown in the figure. Figure taken from Riley et al. (2014).

The main classes of enzymes that act upon cellulose in basidiomycetous fungi are endoglucanases in families GH5 and GH12, cellobiohydrolases in families GH6 and GH7 and LPMOs in family AA9 (Floudas et al., 2012, Lombard et al., 2013). Hemicellulases are also a major constituent of the enzymatic repertoire of these fungi, with some species

carrying several dozens of genes encoding a suite of mannanases, xylanases, arabinases and glucuronidases. LPMOs may act on both cellulose and certain hemicelluloses (Kojima et al., 2016, Agger et al., 2014) (Couturier et al., 2018). Several brown-rot species, such as *Fomitopsis pinicola* and *R. placenta* completely lack genes encoding cellobiohydrolases, and CBMs (like CBM1) and only retain a few endoglucanases (GH5 and GH12) and AA9s. Most brown-rot fungi also lack CDH (with few exceptions, see (Hyde and Wood, 1997)). Interestingly, the number of hemicellulose-active enzymes does not appear to be equally reduced, with both *R. placenta* and *G. trabeum* having retained a wide suite of enzymes active on hemicellulose (Martinez et al., 2009, Floudas et al., 2012). The numbers of genes encoding lignin-active enzymes are also severely reduced in the genomes of brown-rot fungi. Class II peroxidase genes are completely absent, whereas laccase genes are either completely missing (*G. trabeum*, see Floudas et al., 2012) or very limited in number (*R. placenta,* see Wei et al., 2010, Martinez et al., 2009).

It has been suggested that the porosity of the wood cell wall is too low for traditional cellulases and hemicellulases to penetrate (at least during the initial phase of decay), as they are generally larger than 50 Å in size, which is an order of magnitude larger than pores observed in wood (Flournoy et al., 1991, Cowling, 1961). There are cytochemical experiments that have shown that endocellulases are present in the S2 layer of the wood cell wall during decay by *R. placenta* (Murmanis et al., 1987), but the role of these enzymes during initial decay remains controversial as they are believed to be incapable of initiating depolymerization (Arantes et al., 2012, Goodell et al., 2017, Zhang et al., 2016).

This apparent paradox in brown-rot fungi, namely the ability to degrade wood, despite the low number of lignocellulose-active enzymes of brown-rot fungal genomes and the low porosity of sound wood, is believed to be circumvented by the generation of highly reactive oxygen species within the wood cell wall by a non-enzymatic Fenton-like system, commonly referred to as the chelator mediated Fenton-system (CMF) (Arantes and Goodell, 2014).

1.4.3 Chelator mediated Fenton (CMF)

It has been known for more than 50 years that in wood attacked by brown-rot fungi, an initial decrease in plant-cell wall crystallinity and strength precedes any detectable mass-loss (i.e. removal of polysaccharides) (Cowling, 1961, Richards, 1954, Toole, 1971). The observation that the depolymerization of cellulose and hemicellulose within the wood cell wall occurs at a

faster rate than the rate of removal led to the hypothesis that non-enzymatic small diffusible oxidative agents were responsible (Cowling and Brown, 1969).

There is now strong evidence that brown-rot fungi utilize a non-enzymatic "pretreatment" mechanism (CMF) to gain access to the polysaccharides within the highly recalcitrant wood cell wall. The mechanism leads to selective removal of polysaccharides and reorganization of the lignin (Arantes and Goodell, 2014), although the details of the mechanisms are under debate (Goodell et al., 2017, Zhang et al., 2016). The core of the CMF mechanism is the solubilization and reduction of iron in close proximity to wood cell wall components, where it can react with H_2O_2 to generate hydroxyl radicals, in what is called the Fenton reaction ($Fe^{2+} + H_2O_2 \rightarrow Fe^{3+} + {}^{-}OH + \bullet OH$) (Figure 10). Hydroxyl radicals are among the most potent oxidizing agents in nature with a half-life in the nanosecond range. It is thus important to generate these radicals close to their intended substrate and away from the fungal hyphae.

The fungus chelates and solubilizes iron from the environment by secreting oxalic acid, at the same time lowering the pH of the area immediately surrounding the hyphae to around 2.0 (Espejo and Agosin, 1991). Iron is not freely available as Fe^{3+}, but is found as iron-oxide complexes and it has been shown that oxalic acid is able to chelate this iron (Zhu et al., 2016, Arantes et al., 2009). Oxalic acid is produced by the incomplete oxidation of glucose via the tricarboxylic acid (TCA) cycle (Munir et al., 2001). Dilute acid hydrolysis by oxalic acid may increase the accessibility of wood cell wall polysaccharides (Lee et al., 2011, Zhang et al., 2013), and it is likely that this is an additional function in natural brown-rot systems (Green et al., 1991).

Iron-oxalate complexes can occur as either mono-, bi- or tridentate, depending on oxalic acid:iron concentration ratios (Arantes et al., 2009). These iron-oxalate complexes will diffuse away from the fungal hyphae and into the wood cell wall (which has a pH of approximately 4.5), as a result of concentration and pH differences. Simultaneously, the fungus secretes catecholate and hydroquinone compounds (from here called "chelator-reductants"), which also diffuse into the wood cell wall (Kerem et al., 1999, Jensen et al., 2001, Korripally et al., 2013). At high oxalic acid concentrations (i.e. in the lumen, surrounding the hyphae), iron remains inaccessible to these chelator-reductants due to tridentate coordination of the oxalate-iron complexes (Arantes et al., 2009). However, once within the wood cell wall, the higher pH and the lower oxalate concentrations permit the chelation and reduction of Fe^{3+} to Fe^{2+} by these chelator-reductants. Once reduced within the

wood cell wall, iron can react with H_2O_2 in a Fenton-like reaction. It is well-known that at pH 4.5, Fe^{3+} will bind to wood cell wall components, and it has been hypothesized that, once within the wood cell wall, iron can undergo several oxidation-reduction cycles without leaching out (Arantes et al., 2009).

As described in sections 1.3.2 and 1.4.4, the fungi secrete several enzymes that generate H_2O_2, the main culprits in brown-rot fungi being AA3 aryl alcohol oxidases and alcohol oxidases, and AA5 copper radical oxidases. Several AA3 alcohol oxidases are thought to be bifunctional since they act as a source of extracellular H_2O_2 by oxidizing toxic methanol (Daniel et al., 2007) that is generated via oxidation of lignin (Yelle et al., 2008, Filley et al., 2002). Thus, they may fuel Fenton reaction while detoxifying the environment. H_2O_2-producing AA5 copper radical oxidases, which are ubiquitous in wood decay fungi, often making up a large percentage of the secreted enzymes (Kersten and Cullen, 2014). Intracellular family AA6 benzoquinone reductases have been implicated in oxidative brown-rot depolymerization (Jensen Jr et al., 2002), and are upregulated in early decay stages (Zhang et al., 2016, Martinez et al., 2009). They may be important in synthesis and regeneration of reductant-chelators such as 2,5-dimethoxyhydroquinone in *G. trabeum* (Paszczynski et al., 1999, Arantes et al., 2012), as well as in the detoxification of decay byproducts (Cohen et al., 2004).

There is some current scientific debate concerning whether the increase in substrate porosity caused by oxygen radicals generated via the CMF mechanism increase access for cellulases and hemicellulases, or whether the main effect is to make soluble oligosaccharides diffuse out of the wood cell wall where they are further depolymerized by cellulases. Goodell et al. (2017) claimed that there is no increase in porosity in early-stage (low mass loss) decayed wood and neither when using a biomimetic approach based on simulating CMF in the laboratory. However, it has been shown that pretreatment of wood with brown-rot fungi leads to significantly increased saccharifiability (Ray et al., 2010, Paper I). Recent developments in high throughput gene expression studies have shed further light on the mechanisms involved in brown-rot decay (next section).

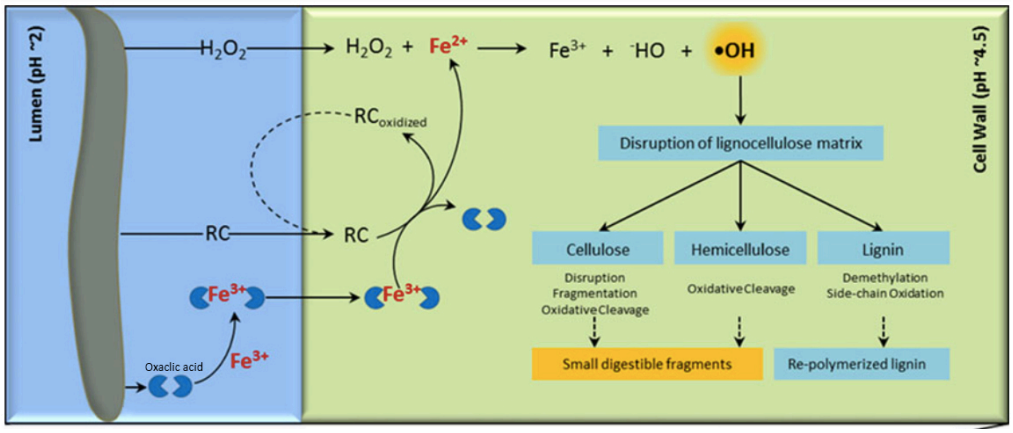

Figure 10. The chelator mediated Fenton mechanism. Oxalate is secreted by the fungus, which solubilizes iron from the environment and acts as phase transfer agent, moving iron into the wood cell wall. Within the wood cell wall, because of lower oxalate concentrations and higher pH, iron is reduced by chelator-reductants secreted by the fungus and released from the oxalate. Once reduced, Fe^{2+} reacts with H_2O_2 via the Fenton reaction, generating •OH radicals that disrupt the lignocellulose matrix. Figure adapted from Arantes et al. (2012).

1.4.4 Expression of decay associated genes

Initial studies trying to elucidate the decay mechanisms of brown-rot fungi were based on microscopy, enzyme immunolabeling, chemical characterization of the substrate and isolation and identification of secreted compounds (Green III and Highley, 1997, Jellison et al., 1991, Goodell et al., 1997, Fekete et al., 1989). In addition, several fundamental studies on the chemistry believed to be involved in non-enzymatic oxidative attack by brown-rot fungi have been performed *in vitro* (Arantes et al., 2009, Paszczynski et al., 1999, Goodell et al., 2006, Qian et al., 2002). While genome sequencing is comparatively straightforward nowadays, performing gene expression studies on brown-rot fungi requires some careful considerations. Because the proposed decay mechanism involves a potentially highly damaging oxidative "pretreatment" followed by enzymatic saccharification, it is essential for the fungus to obtain sufficient separation of these two non-compatible systems, either temporally or spatially.

Two landmark studies published in the Proceedings of the National Academy of Sciences USA by Martinez et al. (2009) and Zhang et al. (2016) have shed new light on the decay mechanisms of *R. placenta* (previously *Postia placenta*). In the former publication, the genome of *R. placenta* MAD 698-R was sequenced and annotated. Then, both transcriptome and proteome analyses were performed,. This study demonstrated that growth on cellulose led to overexpression of hemicellulases and a single GH5 endocellulase (compared to growth

on glucose). Other upregulated enzymes included iron reductases, quinone reductases and a suite of AA3 and AA5 oxidases. Since then, several other studies of gene expression in *R. placenta* have appeared, based on whole transcriptome analysis (Wymelenberg et al., 2010), proteomics (San Ryu et al., 2011) or analysis of selected genes using qRT-PCR (Alfredsen and Fossdal, 2010, Ringman et al., 2014b, Paper II). These studies all support the theory of a temporal separation of an oxidative and a hydrolytic decay stage: genes related to oxidative depolymerization tend to be upregulated in the early stages of decay, whereas upregulation of hemicellulase and cellulase genes appears later.

In Zhang et al. 2016, the authors described a novel method for cultivating brown-rot fungi that allowed for spatiotemporal separation of gene expression during different stages of decay (Figure 11). This was achieved by growing *R. placenta* vertically on thin wooden wafers, and then cutting the wafers into separate sections along the growth axis of the fungal hyphae. Whole-transcriptome analyses of three different sections were performed, from the hyphal tip to old hyphae, and further along the growth axis. By using wood as growth medium (as opposed to cellulose, Martinez et al. 2009), Zhang et al. were able to capture a more accurate picture of what appears to be a very well regulated separation of the two-step decay mechanism. They showed that at the foraging hyphal tip, a vast number of genes related to oxidative depolymerization were significantly upregulated. These included genes involved in oxalate synthesis (Glyoxylate dehydrogenase and Oxaloacetate acetylhydrolase), several genes possibly involved in Fenton chemistry (alcohol oxidases, glyoxal oxidase, amino acid/amine oxidases, iron reductases, Fe^{2+} transporters) and genes involved in the biosynthesis of aromatic secondary metabolites (benzoquinone reductases, phenylalanine ammonia lyase and aromatic ring monooxygenases). Upregulated proteins in the hyphal tip included 31 cytochrome P450s, which are involved in hydroxylation of aromatics, which is useful both for detoxification and, possibly, for the synthesis of reductant-chelators. Other upregulated proteins included a single GH28 pectinase as well as several expansins.

Interestingly, at least 21 oxidoreductases were significantly upregulated in the older sections of hyphae, seven of which were believed to be involved in oxidative depolymerization, signifying that some oxidative activity likely occurs at later stages of decay. However, overexpressed genes in the older hyphae, away from the tip, were dominated by 70 GHs, 15 carbohydrate esterases and 3 carbohydrate-binding module family genes, 50 of which were predicted to have activity on lignocellulose (82% of which were GHs). Interestingly, the expression of hemicellulose-active GHs was higher in the middle 15-20 mm sections than the

oldest 30-35 mm sections, which is in accordance with previous observations that hemicelluloses are preferentially removed prior to cellulose degradation in wood undergoing brown-rot attack (Pandey and Pitman, 2003, Curling et al., 2001, Curling et al., 2002).

The study by Zhang et al. (2016) resolved two long-standing questions by showing (1) that CMF and enzymatic hydrolysis are spatially separated, explaining how hydrolytic enzymes avoid being destroyed by the powerful oxidative reactions of initial decay, and (2) that at later stages of decay, hydrolysis by CAZymes is crucial for continued consumption of the wood-cell wall. The latter implies that the CAZymes are not merely acting on what is being solubilized by the CMF system, since very little oxidative gene expression is observed in older hyphae where high expression of GHs correspond with significant removal of polysaccharides. These data are supported by a follow-up study where the authors looked at the secretome, observing similar trends (Presley et al., 2018). All in all, expression studies support a scenario in which CMF and oxidative mechanisms act as a pretreatment, and where enzyme catalyze removal of polysaccharides from the “pre-treated” wood cell wall.

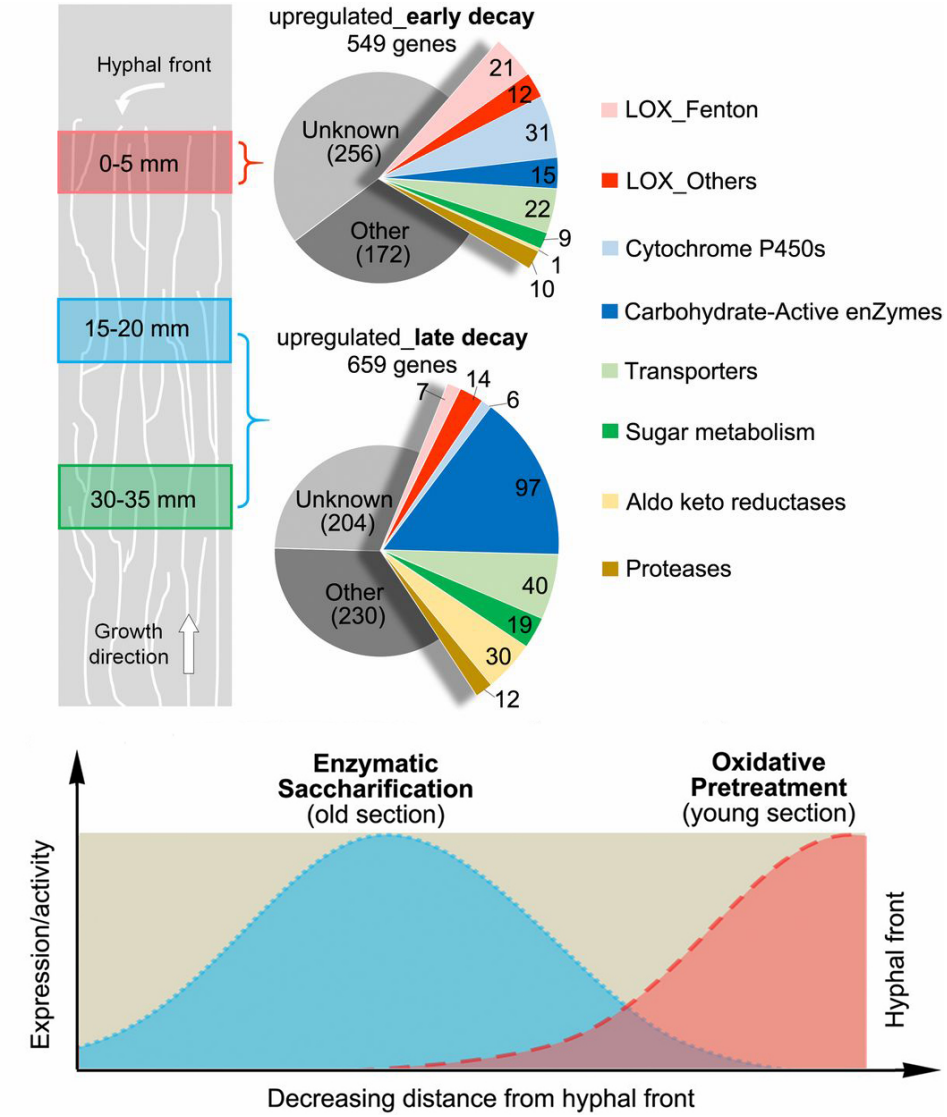

Figure 11. Spatiotemporal gene expression of decay associated genes in *R. placenta*. Genes related to lignocellulose oxidation (LOX) and cytochrome P450s are highly upregulated at the hyphal front, whereas CAZymes are overrepresented in older hyphae, supporting the theory of two differentially expressed systems during brown-rot decay. Figure adapted from Zhang et al. (2016).

1.5 Pretreatment of lignocellulosic biomass

Lignocellulosic biomass has attracted massive attention in recent years as a potential source of biofuels, food, feed and fiber, but its inherent recalcitrance to enzymatic hydrolysis is a major bottleneck for cost-efficient utilization (Himmel et al., 2007, Pedersen and Meyer, 2010, Zhao et al., 2012). In order to access the cellulose embedded in the wood cell-wall matrix with enzymes, a pretreatment step is needed, which usually leads to depolymerization and solubilization of hemicelluloses and modification of lignin (Figure 12). Recalcitrance is multifactorial, relating to the degree of lignification, the complexity and structural heterogeneity of the substrate, the insolubility of the substrate and the presence of natural enzyme inhibitors (Himmel et al., 2007).

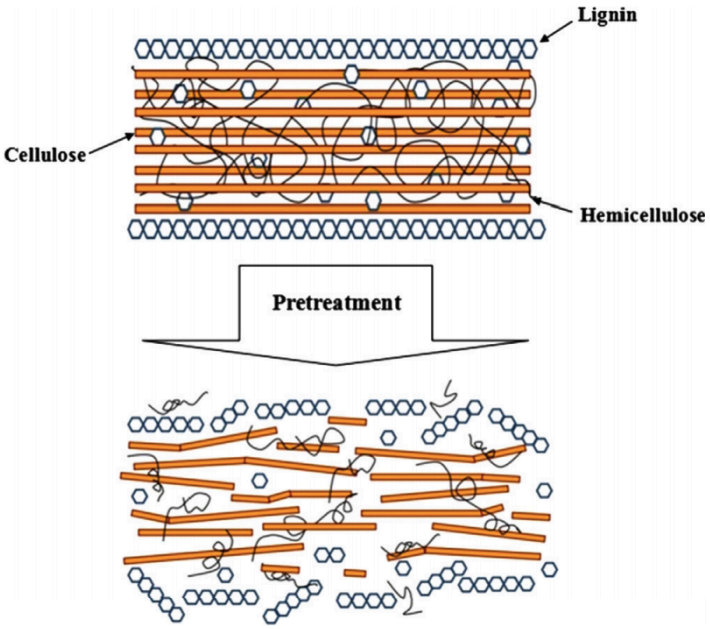

Figure 12. Pretreatment of lignocellulosic biomass. The aim of the pretreatment is disruption of the lignocellulose matrix in order to increase enzyme access to the cellulose within. Figure taken from Mood et al. (2013).

Pretreatment can be divided into (1) physical methods, such as milling, grinding, chipping, freezing and exposure to high temperatures, (2) chemical methods, such as using acidic or alkaline conditions, ionic liquids and organic solvents, (3) physio-chemical pretreatments, such as steam explosion, ammonia fiber explosion (AFEX), CO_2 explosion, hot water

extraction and wet oxidation or (4) biological pretreatment, such as pretreatment with fungi (Mood et al., 2013). It is common for different pretreatment methods to be combined before enzymatic saccharification, e.g. milling and grinding before acid treatment. For a pretreatment strategy to be considered viable it needs to be energetically cost efficient and environmentally friendly, and this is in fact one of the larger challenges in the development of so-called 2nd generation biorefineries that are based on the use of (non-food) lignocellulosic biomass, such as wood and agricultural waste streams.

The first step of pretreatment usually involves some form of size reduction to increase the relative surface area of the substrate. Depending on what type of physical pretreatment is used, particle size is normally in the range of 0.2-30 mm, with chipping and grinding giving larger particle sizes than milling (Sun and Cheng, 2002). It is well-known that the choice of physical pretreatment can have a significant effect on conversion yields of both the glucans and the xylans in the biomass (Hideno et al., 2009, da Silva et al., 2010).

One of the most commonly used chemical pretreatments is acid pretreatment, where the primary aim is to hydrolyze hemicelluloses, thereby increasing enzymatic accessibility to cellulose (Mood et al., 2013). Acid pretreatment is usually performed using high temperatures and low acid concentrations or low temperatures and high acid concentrations. While using high acid concentrations (and low temperature) is considered the more economically viable approach, it also presents several challenges. These include corrosion of equipment, degradation of monosaccharides like glucose, and the production of fermentation inhibitors like 2-furfuraldehyde and 5-hydroxy methyl furfural (HMF) (Almeida et al., 2007). When performing acid hydrolysis at low concentrations and high temperatures these inhibitors can be further transformed into formic and levulinic acid (Larsson et al., 1999). Sugar conversion yields upon enzymatic hydrolysis of acid-pretreated straw typically range from 60-80%, but can be considerably lower for softwoods and hardwoods (Mood et al., 2013).

Alkaline pretreatment is employed to remove lignin, acetyl groups and uronic acid substitutions (Li et al., 2010), and it solubilizes less of the polysaccharides compared to acid treatment (Carvalheiro et al., 2008). The method causes chemical swelling of fibrous cellulose and disruption of xylan-lignin cross-linkages, thus increasing porosity (Sun and Cheng, 2002). This type of pretreatment is performed at comparatively low temperatures, but

requires long reaction times (hours to days), and neutralization of the pretreated slurry is needed.

Ionic liquid (IL) pretreatments aim at dissolving both cellulose and lignin components, and are comparatively new methods. Ionic liquids are composed of organic salts (cations and anions) that have a melting point of <100°C and have attracted attention due to their remarkable ability to dissolve cellulose (Mood et al., 2013). The structure of the biomass usually changes considerably when using ILs, whereas the relative composition remains fairly intact (Tan et al., 2011). The recovered cellulose becomes amorphous and porous making it susceptible to enzymatic depolymerization (Dadi et al., 2006). The advantages of IL pretreatment over the two previously described methods include the use of less dangerous processing conditions and chemicals, lower temperature requirements, "greener" reagents as a consequence of lower vapor pressure, high thermal and chemical stability, and that ILs are recyclable (Mood et al., 2013). However, ILs are costly (and so is recycling them), and they are relatively viscous which makes them difficult to handle.

Steam-explosion is a physiochemical pretreatment that involves steam-heating, shearing and auto-hydrolysis of glycosidic bonds, and is one of the most extensively investigated pretreatment methods (Mood et al., 2013). Using pressurized steam (20-50 bar and 160-270°C), biomass particles are heated for seconds to several minutes before a rapid pressure drop to atmospheric conditions is used to provoke instant evaporation of the condensed moisture, causing disruption of the lignocellulose matrix. Steam explosion causes hydrolysis of hemicellulose and lignin remodeling (Mabee et al., 2006). Acetic acid produced by the hydrolysis of acetylated hemicellulose contributes to hemicellulose hydrolysis during steam-pretreatment, and may also promote degradation of sugars and formation of inhibitors like HMF (García-Aparicio et al., 2006). For steam-explosion of certain types of biomass, such as softwoods, an acid catalyst such as H_2SO_4 may be needed to create the acidity that is otherwise provided by acetate, which also leads to increased production of inhibitory compounds (Mood et al., 2013). This means that washing of the pretreated material is often required to avoid complications in the downstream processes of enzymatic hydrolysis and fermentation (Mackie et al., 1985).

Fenton chemistry has also been used to pretreat lignocellulosic materials, but research on this topic remains limited (He et al., 2015, Kato et al., 2014, Michalska et al., 2012). Previous studies, which were largely performed with grasses and agricultural wastes, all showed a

positive impact of Fenton reagents (H_2O_2 + Fe) on improving enzymatic saccharification yields. Fenton chemistry has been applied either as the sole pretreatment step (Kato et al., 2014, Michalska et al., 2012) or with sequential Fenton treatment and dilute NaOH extraction (He et al., 2015). Michalska et al. (2012) showed delignification as a result of Fenton pretreatment on biomass from *Mischantus giganteus, Sorgum sp.* and *Sida hermaphrodita*, with values ranging from 30-60% depending on feedstock. As of time of writing, limited positive effect of Fenton-chemistry pretreatment has been reported on softwoods or hardwoods,

In general terms, Fenton chemistry seems an attractive pretreatment method since 1) it can be performed without extensive heat requirements, 2) the cost of H_2O_2 and iron is comparatively low to other reagents, and 3) it has the potential to limit the production of fermentation inhibitors. An identified challenge with using Fenton chemistry is the extremely short-lived nature of the hydroxyl radicals generated (10^{-9} seconds) and the consequent need to generate these radicals in close proximity to the wood cell-wall polysaccharides and lignin (Arantes et al., 2012). This implies that gravity (w/v %) of biomass needs to be very high to avoid generation of radicals in solution (and away from the material). Alternatively, one needs to develop a system that ensures accurate delivery of the powerful oxidative radicals to the right locations in the substrate. The latter scenario is the topic of Paper I.

1.6 Wood modification

Wood is a renewable building material and as such an important medium for storage of carbon, effectively removing CO_2 from the carbon cycle. Among the challenges of using wood is its natural susceptibility to fungal decay organisms. In northern latitudes, brown-rot is the main type of decay found both in natural systems and in wood used as construction material. In order to extend the service life and quality of the wood, the use of protective agents is widespread. Wood protection can broadly be divided into wood preservatives and wood modification. Whereas traditional wood preservation involves the impregnation of the wood matrix with various chemical agents that inhibit fungal growth via toxic biocidal action, wood modification aims at physically and/or chemically changing the wood. One challenge with traditional wood protection methods such as application of copper- or borate-based preservatives is the tendency of these preservatives to leach out as they are not covalently bound to the wood cell wall matrix, causing environmental concerns as potential pollutants.

Hill (2011) defines wood modification as "*a generic term describing the application of chemical, physical or biological methods to alter the properties of the material. The aim is to get better performance from the wood, resulting in improvements in dimensional stability, decay resistance, weathering resistance, etc. It is essential that the modified wood is non-toxic in service life and that disposal at the end of life does not result in the generation of any toxic residues*". Wood modification approaches can be classified as chemical processing (acetylation, furfurylation, resin impregnation etc), thermo-hydro processing (thermal treatment) and thermo-hydro-mechanical processing (surface densification) (Sandberg et al., 2017). The effect of wood acetylation on gene expression of core oxidative and hydrolytic enzymes during decay by *R. placenta* is the topic of Paper II.

1.6.1 Acetylation

Acetylation is among the most widely studied and commercially used chemical wood modification approaches (Rowell, 2006), and was first demonstrated to protect against fungal decay by Tarkow (1945), who used acetylated balsa wood. In the acetylation reaction, acetic anhydride is made to react with free exposed hydroxyl groups in cellulose and hemicellulose in an esterification reaction, releasing acetic acid as a byproduct (Rowell, 2012). Acetylation physically bulks the wood cell wall because of the larger size of the substituted acetyl ester moieties (59 Da, versus 17 Da for a hydroxyl). Weight percent gains (WPG) of 17-21% are

normally achieved industrially, and acetylation has proven very efficient in protecting against brown-rot fungal attack. Acetylated samples inoculated with brown-rot fungi usually display mass losses reaching no more than 1-2% after 12 weeks, whereas the unmodified control boards reach >60% mass loss in the same timeframe (Rowell, 2006).

Three mechanisms have been suggested to explain why acetylation hampers fungal decay of wood: 1) the fungal enzymatic apparatus cannot recognize nor act on the chemically changed substrate, 2) physical expulsion of fungal metabolites as a consequence of the higher density of the cell wall and 3) inhibited diffusion because of lower water activity.

In acetylated wood, water exclusion has been demonstrated to be the result of fewer sorption sites caused by the replacement of OH groups by acetyl groups, and by steric hindrance of unmodified OH groups by the bulkier acetyl groups (Papadopoulos and Hill, 2003, Popescu et al., 2014, Beck et al., 2017). The possibility that the fungal enzymes do not recognize the modified substrate has been debated in a review by Ringman et al. (2014a), but was considered unlikely, because this scenario would not explain why the initial non-enzymatic oxidative mechanisms would not be able to depolymerize the wood cell wall components. The CMF mechanism does not rely on the same substrate recognition as with enzymatic depolymerization, and would thus not be affected. The inhibition of gene expression can also be ruled out, as it is shown that oxidative genes are over expressed in early decay on acetylated wood (Alfredsen et al., 2016, Paper II).

It is now well known that brown-rot fungi possess a large number of carbohydrate esterase genes, where several are likely to deacetylate polysaccharides (Eastwood et al., 2011, Riley et al., 2014, Martinez et al., 2009). Indeed, significant deacetylation of acetylated *Pinus radiata* has been shown to occur in wood samples inoculated with *R. placenta* (Beck et al., 2018). Since the deacetylation observed by Beck et al. (2018) occurred during the early stages of brown-rot decay, it is not known whether it is caused by oxidative mechanisms or enzymatically, but the authors claimed that once deacetylation had occurred, decay proceeded at a similar rate to the unmodified controls. Using solute exclusion, Hill et al. (2005) demonstrated that with acetylated wood, probe molecules up to 4 nm were able to penetrate the wood cell wall, and so physical exclusion of CMF metabolites seems an unlikely scenario. This leaves the third scenario the most likely explanation; with water exclusion and lower water activity being responsible for the delay or inhibition of decay, although a multifactorial mode of action cannot be completely ruled out. Water activity is well known to

affect fungal growth (Ayerst, 1969, Beuchat, 1981, Magan and Lacey, 1984), and the lower water content of acetylated wood likely affects diffusion of metabolites as well as enzyme action. It has been demonstrated that soluble cellobiose is the primary signaling molecule when *R. placenta* switches on gene expression from oxidative to cellulolytic (Zhang and Schilling, 2017), and it is possible that acetylation hinders diffusion, or even generation, of soluble oligosaccharides that act both as a carbon source and as a signaling molecules. Furthermore, the diffusion of CMF metabolites into the wood cell wall is likely to be affected.

2 Outline and aim of thesis

Brown-rot fungi are among the most important organisms on earth as they are key players in the global carbon cycle, degrading woody biomass and releasing carbon back to ecosystems and the atmosphere. Understanding the wood degradation mechanisms utilized by these fungi will not only improve our understanding of fundamental processes in Nature, but also be of major applied interest. On the one hand brown-rot-inspired tools may be used for lignocellulose processing, whereas on the other hand knowledge of the brown-rot process may direct development of better methods to preserve wood that is used as building material.

The present thesis deals with the decay mechanisms of brown-rot fungi, in particular those of the two distantly related species, *Gloeophyllum trabeum* and *Postia placenta*. The overall goal of the research was to gain a further understanding of brown-rot decay mechanisms, using different approaches and with primarily an applied perspective.

Paper I describes novel approaches to oxidative pretreatment of Norway spruce (*Picea abies*), based on the chelator-mediated Fenton mechanism employed by brown-rot fungi. As a proof-of concept, biological pretreatment of spruce wood was performed using *Gloeophyllum trabeum* and *Rhodonia placenta*. Saccharification experiments were then performed on the pretreated material, using the commercial cellulase cocktail Cellic CTec2 from Novozymes. In addition, the effect of *in vitro* pretreatments with modified Fenton reagents on the efficiency of subsequent enzymatic saccharification was explored.

Paper II describes an investigation of the effects of acetylation (wood modification) on the expression of core decay genes in *Rhodonia placenta* using quantitative real-time PCR. The experiments targeted the expression of genes involved in early oxidative decay (oxidoreductases, oxalic acid synthesis) and in later cellulolytic decay (cellulases, hemicellulases, oxalic acid degradation) during growth on unmodified *Pinus radiata* wood as well as wood with three different levels of acetylation.

Paper III describes the characterization of a previously uncharacterized lytic polysaccharide monooxygenase (*Gt*LPMO9B) from *Gloeophyllum trabeum*. Substrate specificities and oxidative regioselectivity were determined by product analysis using chromatography. The larger part of the paper concerns the effect of different reductants on the activity of *Gt*LPMO9B, with particular focus on how endogenous H_2O_2 generation in the system is connected to LPMO activity. Based on the newly proposed H_2O_2-dependent LPMO

mechanism, the use of H_2O_2 as a co-substrate was studied with different reducing agents, among them one (2,3-dihydroxybenzoic acid) that allowed LPMO activity only in the presence of added or endogenous H_2O_2 generation.

3 Main results and discussion

Paper I: Challenges and opportunities in mimicking non-enzymatic brown-rot decay mechanisms for pretreatment of Norway spruce

Pretreatment of recalcitrant lignocellulosic biomass is essential to ensure subsequent cost-efficient and sufficient conversion of cellulose and hemicellulose to soluble sugars (Mood et al., 2013). Most pretreatment methods used today rely on extreme conditions such as high temperature, extreme pHs and high pressures, and consequently are costly and generate fermentation inhibitors. In an attempt to find a more environmentally benign, cost-efficient and low severity pretreatment method, we looked to the chemistry used by brown-rot fungi in early stages of decay as a potential pretreatment method. The substrate chosen for this study was Norway spruce (*Picea abies*). While softwoods such as Norway spruce is notoriously difficult to work with as a feedstock for biorefineries (Jönsson and Martín, 2016, Zhu et al., 2010, Várnai et al., 2010), its abundance as the dominating European softwood makes it an attractive potential feedstock.

Boards derived from a single Norway spruce tree were hammer milled with liquid nitrogen and sieved to a size of 0.4-0.5 mm. These size parameters were chosen because we wanted particles that could be handled in small volumes in a test tube, but that were large enough to still maintain intact wood cell wall structures. As a proof-of-concept, this material was pretreated with two brown-rot strains (*Rhodonia placenta* FPRL 280 or *Gloeophyllum trabeum* BAM Ebw. 109). Note: *Rhodonia placenta* was until recently known as *Postia placenta*. The milled Norway spruce was inoculated with the two fungi and incubated for 18, 35 or 46 days, before the fungi were killed by boiling for 15 minutes. This gave mass losses in the range of 3.7-14.5% (Figure 1, Paper I). Upon subsequent saccharification with Cellic CTec 2 for 120 hours, almost all glucose was released during the first 24 hours (Figure 2A, Paper I) and there was a clear relationship between mass loss during pretreatment and glucan conversion yields (released glucose as % of the pre-decay cellulose amount, with the highest yield (13.7% solubilization with *G. trabeum*) achieved at the highest mass loss. Figure 13 shows a close to linear correlation between mass loss and cellulose conversion yields for both fungi (*G. trabeum* R^2=0.83, *R. placenta* R^2=0.96). The lowest mass loss of 3.7% was obtained with *R. placenta* after 18 days, which gave only 6.8% glucan conversion, whereas in

the control (i.e. 0 days) 5.9% glucan conversion was observed. Thus, while the data clearly indicate a positive effect of the brown-rot pretreatment on cellulose conversion yields, it appears that significant mass loss is needed to obtain major effects.

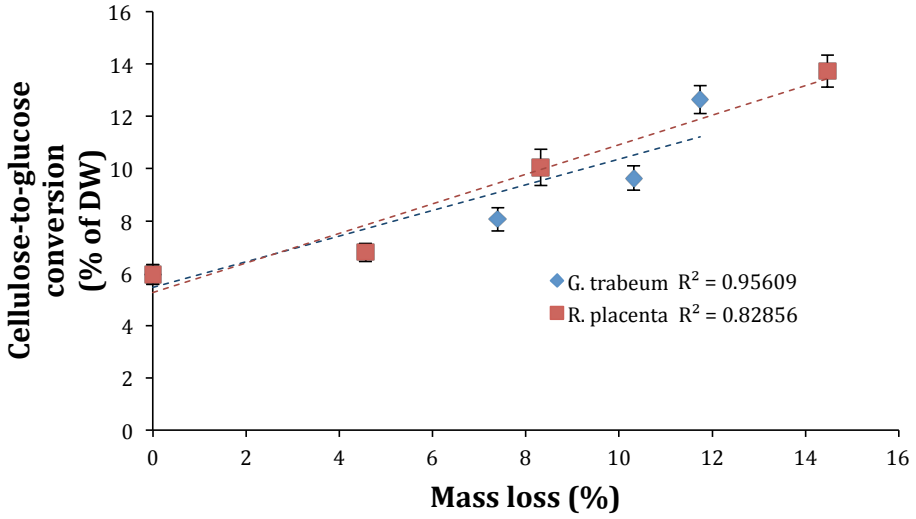

Figure 13. Brown-rot pretreatment of Norway spruce. Milled spruce wood was inoculated with either *R. placenta* or *G. trabeum* for up to 45 days and mass loss of the samples was monitored. Samples where then saccharified with Cellic CTec2, and a close to linear relationship between mass loss and glucose release was established. The term "DW" on the y-axis refers to the dry weight. Cellulose-to-glucose conversion calculated on the basis on w% before pretreatment. Figure adapted from Figure 2B in Paper I.

The current hypothesis is that initial oxidative decay mechanisms allow a limited number of hydrolytic enzymes access to the polysaccharides within the wood cell wall (Zhang et al., 2016), and that during initial decay very little mass is lost despite significant depolymerization of cellulose (Curling et al., 2002). We observed close to no increase in conversion when mass loss was low, and needed higher mass loss to see benefits of the pretreatment. This may be taken to indicate that significant depolymerization of hemicellulose (and cellulose), which could have led to higher efficiency of the subsequent enzymatic hydrolysis, did not occur at low mass loss. It is well known that hemicelluloses are removed prior to cellulose during brown-rot decay (Curling et al., 2001, Curling et al., 2002, Pandey and Pitman, 2003), which we also observed for our pretreated material. The substrate was rich in galactoclucomannan (GGM) (approx. 18%), and mannose was preferentially removed, along with some glucan, which is assumed to also be from GGM (Figure 10, Paper

I). The genomes of both *R. placenta* (Martinez et al., 2009) and *G. trabeum* (Floudas et al., 2012) encode several hemicellulose-active hydrolases and LPMOs, and it is possible that the initial oxidative decay primarily leads to removal of hemicelluloses and/or improved substrate access for hemicellulases. It is well known that a major effect of certain pretreatment methods, such as acid pretreatment, is the hydrolysis and solubilization of hemicelluloses, which leads to disrupted cell wall interactions and improved enzyme accessibility (Mood et al. 2013).

After this initial proof-of-concept study we then attempted to pretreat the wood with a CMF-like system. We hypothesized that for a CMF-mimicking system (called modified Fenton, MF in Paper I) to be successful, radicals needed to be generated with nano-scale accuracy within the wood cell wall. Hydroxyl radicals have a half-life in the nanoseconds range, and so any hydroxyl radical occurring in solution will likely only react at the surface of the wood or not react with the wood at all (i.e. consumed in other reactions). The MF system was designed to saturate the wood fibers with Fe^{3+} (using $FeCl_3$) without leaving any iron in solution, followed by reducing this iron to Fe^{2+} with the biomimetic chelator-reductant 2,3-dihydroxybenzoic acid (2,3-DHBA). Only Fe^{3+} (and not Fe^{2+}) will bind to the wood cell wall (Arantes et al., 2009), and so *in situ* reduction was considered a requirement (rather then just adding Fe^{2+}). 2,3-DHBA is well known as a chelator of transition metals (Graziano et al., 1974), and will reduce both iron (Xu and Jordan, 1988) and copper (Liu et al., 2005). Immediately following reduction, H_2O_2 was added, which will then react with 2,3-DHBA-Fe^{2+} via a Fenton-like reaction, theoretically generating OH radicals within the wood cell wall.

The iron-binding capacity of our milled Norway spruce was determined by incubating it with $FeCl_3$ at four different pH values (2.0, 3.6, 4.5 and 5.5) after which remaining soluble iron was quantified using inductively coupled plasma mass spectrometry (Figure 3, Paper I). For MF reactions, a pH of 4.0 was chosen, since for Fenton reactions hydroxyl radical generation is faster under acidic conditions (Zepp et al., 1992, Hug and Leupin, 2003). For MF pretreatment, milled wood was incubated in a solution with $FeCl_3$ under conditions where no free Fe^{3+} was expected to remain in solution, followed by reduction with equimolar amounts of 2,3-DHBA and immediately followed by the addition of H_2O_2 (at ten times the $FeCl_3$/2,3-DHBA concentration). Saccharification of the MF pretreated material after washing only yielded a marginal increase in glucan conversion (Figure 4, Paper I) when working at wood-iron saturation levels (7.3% to 9.6% (Student's t-test p=0.0305) (0.5 mM $FeCl_3$, 5% w/v

wood), whereas there were no positive effects when going above saturation levels (1 mM $FeCl_3$, 5% w/v wood).

The above observations led to the hypothesis that the poor improvements in saccharification efficiency could be caused by solubilized polysaccharides getting removed by the washing procedure that was being applied after pretreatment. Thus an experiment similar to the above was performed using both crystalline cellulose (Avicel) (Figure 5, Paper I) and milled wood (Figure 6, Paper I), but without the washing step after the MF pretreatment. A pH of 4.5 was chosen for these experiments, as a compromise between the presumably optimal pH for MF treatment (4.0) and the optimal pH for Cellic CTec2 (pH 5.0). This approach had a negative impact on conversion yields both for Avicel (cellulose) and milled wood, and the biggest negative impact was observed for cellulose. In order to determine what factors of the MF system were responsible for these negative effects, the components (i.e. $FeCl_3$, 2,3-DHBA and H_2O_2) were incubated alone or in pairs (e.g. $FeCl_3$+H_2O_2) with Avicel at pH 4.5 (Figure 7, Paper I) and 5.0 (Figure 8, Paper I). Subsequent saccharification with CTec2 revealed that the combination of $FeCl_3$+H_2O_2 had the largest negative impact on saccharification, while the single compound with the largest negative impact was $FeCl_3$. These findings reveal serious complications associated with the use of MF reagents for pretreatment, since significant washing of the material would be needed to reduce iron concentrations to levels that are not inhibiting to saccharification enzymes.

Since the MF pretreatment at wood-iron saturation levels (with washing) only yielded a marginal increase in saccharification efficiency, a more severe pretreatment protocol was also tested, working with iron concentrations well above saturation levels. We suspended our milled wood (5% w/v) in 10 mM $FeCl_3$ with an equimolar concentration of 2,3-DHBA and with H_2O_2 concentrations of 200 or 300 mM (1:1:20 or 1:1:30 reagent ratios). The samples were then incubated at room temperature for 3, 4 or 7 days before being washed thoroughly to remove any MF reagents. Despite the higher reagent concentrations and the longer incubations times, this pretreatment had only minor effect on cellulose saccharification yields (Figure 9, Paper I). For the 1:1:20 reactions no effect was observed, and only a minor improvement in saccharification efficiency was seen for the 1:1:30 reactions. Two important observations were made in these experiments; 1) mass losses were below 1% w/w, and 2) the amount of soluble sugars in the wash liquid was below detection levels. Thus, the apparent failure of this rough pretreatment really seems to be due to the fact that it does not improve accessibility for the enzymes in Cellic CTec2. Brown-rot pretreatment of Norway spruce was

successful and resulted in more than a doubling of conversion yields for wood pretreated for 45 days with *G. trabeum*, compared to wood that had not been pretreated. Whereas previous studies have reported positive effects of Fenton pretreatment of lignocellulosic materials (Jung et al., 2015, Kato et al., 2014), no such effect was observed in our experiments. It is important to note that these previous studies concerned saccharification of grasses and other non-woody substrates, whereas, to the best of our knowledge, there are no peer reviewed studies on the use of Fenton chemistry for pretreatment of Norway spruce (or other softwoods). Spruce wood is naturally more resistant to enzymatic hydrolysis, with cellulose conversion yields of approximately 5-6% percent with our untreated milled wood, whereas in untreated corn stover the cellulose conversion of untreated materials is >20% (Kaar and Holtzapple, 2000). Since we avoided having iron in solution, iron concentrations may in fact have been too low for efficient disruption of the wood cell wall components. In Nature, brown-rot fungi are able to utilize the same iron for several cycles of oxidation and reduction by secretion of chelator-reductants in a timely manner, whereas in our system, Fe^{2+} that is oxidized in the Fenton reaction will remain in the Fe^{3+} state unless it undergoes a second reduction.

Development of gradual, controlled feeding of reagents (thus possibly creating multiple redox cycles) could perhaps improve the results. Another aspect to consider is the chelating effect of the reductant. As 2,3-DHBA complexes with iron, it is possible that iron (as an iron-DHBA complex) will diffuse out of the wood and into solution, thus losing its potential to act on the wood. In Nature, brown-rot fungi use several enzymatic systems to generate H_2O_2 (Bissaro et al., 2018), potentially in close proximity to wood cell wall components, whereas in our system H_2O_2 exists freely in solution. This difference, relating to the delivery of H_2O_2 with high spatial accuracy, could be another explanation for the limited success of the MF treatment described in Paper I.

Paper II: Acetylation of *Pinus radiata* delays hydrolytic depolymerization by the brown-rot fungus *Rhondonia placenta*

Wood is a renewable building material that has major potential for storage of atmospheric carbon, but is naturally susceptible to fungal decay. To extend the service life of wood used for outdoor constructions, several wood protection methods have been developed over the years. One of the most common commercially applied wood modification methods today is acetylation, which significantly inhibits decay. The exact mechanisms that confer decay resistance against brown-rot fungi are not perfectly understood. In the study described in Paper II, the aim was to analyze gene expression of a set of decay-associated genes in *R. placenta* using qRT-PCR, with emphasis on genes that are assumed to be involved in early oxidative decay or later stage hydrolytic decay.

R. placenta FPRL 280 was inoculated on small *Pinus radiata* wood plugs (1 cm height, 0.6 cm diameter) that were acetylated to 12.5% (Ac13), 17.1% (Ac17) or 21.4% (Ac21) weight percent gain (WPG). Non-acetylated control samples were included. Samples were harvested at different time points to capture both incipient and later stages of decay. Based on mass loss, samples for further analysis were selected as follows: control samples were harvested at weeks 1–4, Ac13 at weeks 2, 4 and 6, Ac17 at weeks 4, 6 and 10 and Ac21 at weeks 10, 16, 24 and 28 (Figure 14).

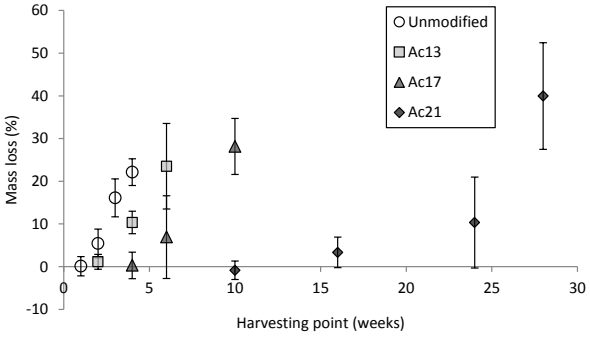

Figure 14. Mass loss during incubation of unmodified and acetylated *Pinus radiata* wood with *Rhodonia placenta*. Samples were acetylated to 12.5% (Ac13), 17.1% (Ac17) or 21.4% (Ac21) weight percent gain (WPG) and inoculated with *R. placenta*. Samples harvested to achieve approximately identical mass losses across treatment levels. The figure is identical to Figure 1 in Paper II.

We observed significant delay of decay as a result of acetylation, but once decay was initiated it proceeded at a rate comparable to the control. For the control, significant mass loss was detected after two weeks, for Ac13 after four weeks, for Ac17 after six weeks and for Ac21 after 16 weeks. The high mass losses in the acetylated samples are noteworthy, since acetylation to around 20% WPG has been claimed to give complete resistance to fungal degradation (Goldstein, 1961, Kumar and Agarwal, 1983, Takahashi et al., 1989, Papadopoulos and Hill, 2002, Hill et al., 2006). However, it has been suggested that this apparent protection threshold may simply be due to the length of the decay trials, which normally do not extend over 16 weeks (EN 113), whereas longer incubation times may be needed, as shown here (Hill, 2006). Our results indicate that acetylation delays but does not entirely inhibit fungal decay. Of note, the small sample sizes (10 mm height, 6 mm diameter) used here increase the surface to volume ratio compared to standard wood block trials (EN113, 50x25x15 mm) possibly allowing for greater diffusion of water into the samples, which will promote fungal decay. Acetylation reduces the water capacity of the wood cell wall (Papadopoulos and Hill, 2003), and lower moisture content in decayed acetylated samples were observed in our study when compared to the control.

We selected a total of 22 genes for qRT-PCR analysis and grouped them into five groups (Table 1, Paper II): 1) oxalic acid metabolism, 2) oxidative decay enzymes, 3) cellulose degradation, 4) hemicellulose degradation and 5) expansins. For all qRT-PCR analyses a housekeeping gene for β-tubulin was used as baseline. The relative gene expressions of these five groups (minus oxalate decarboxylase from the oxalic acid synthesis group) were compared within each harvesting point for all treatment (WPG) levels (Figure 15). For the unmodified wood control, this analysis revealed upregulation of oxalic acid synthesis in week 1, as well as a significant expression of oxidative decay enzymes, hemicellulases and expansins, while cellulase expression remained low. The high expression of hemicellulase genes at week one indicates that the fungus is in the process of switching from oxidative to hydrolytic depolymerization. The high expression of hemicellulases prior to cellulases is in agreement with previous studies (Zhang et al., 2016). Data for Ac13 suggest that, at the first harvest point, the fungus was already in the stage of hydrolytic attack, since we observed significant cellulase expression next to expression of oxidative decay enzyme-encoding genes. For Ac17 and Ac21 the first harvest point is dominated by expression of oxidative decay genes and high expression of expansins (Figure 15).

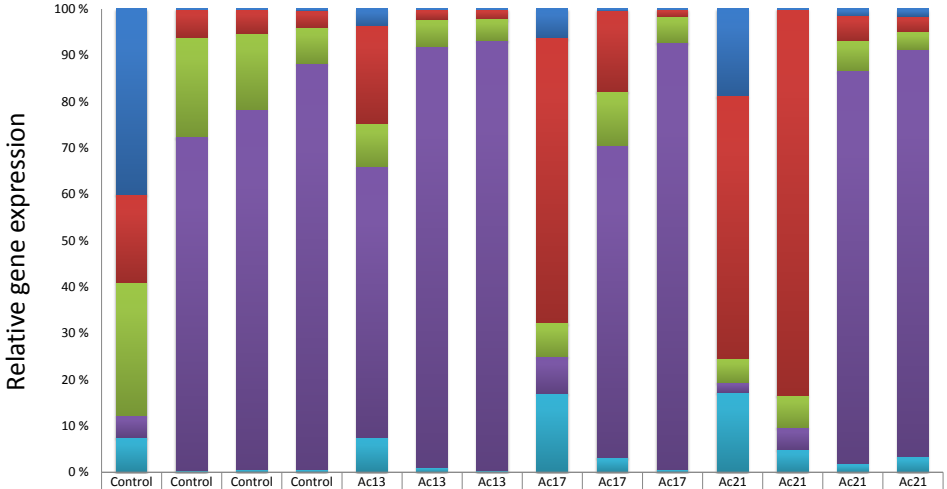

	Control week 1	Control week 2	Control week 3	Control week 4	Ac13 week2	Ac13 week 4	Ac13 week 6	Ac17 week4	Ac17 week6	Ac17 week10	Ac21 week 10	Ac21 week 16	Ac21 week 24	Ac21 week 28
Oxalate synthesis	12904	283	711	2088	8211	1828	1953	5336	1414	582	8067	278	5813	5777
Oxidative	6148	26524	31552	25405	48208	23136	33559	52467	65676	17568	24357	290476	20403	12939
Hemicellulolytic	9259	92267	101997	53603	21045	65948	77126	6159	44178	58905	2173	24286	25537	14324
Cellulolytic	1511	310489	479679	606412	133266	1028376	1535878	6824	253281	983356	975	16648	328117	331314
Expansins	2437	1898	4131	3677	16974	11953	6635	14502	12313	6507	7399	17185	7154	12846

Figure 15. Relative expression of 22 *R. placenta* genes during decay of unmodified and acetylated (13, 17 and 21% WPG) *Pinus radiata* wood. The units given are arbitrary gene expression units, relative to the constitutively expressed beta-tubulin gene with the expression level given as 10^4. Note that the sum total expression level varies between harvesting points and treatment levels. The figure is the same as Figure 2 in Paper II.

For all treatment levels, the trend after the first harvest point was the downregulation of oxidative genes and the upregulation of cellulases. In the most heavily acetylated samples (Ac21), oxidative genes were also highly upregulated at the second harvest point after 16 weeks (i.e. 6 weeks after the first harvest point at 10 weeks). It is important to note that these analyses only show the relative expression between the groups, and that actual expression levels can be high although they appear low in comparison to another group. Group expression levels are therefore also included in Figure 15 for clarity.

Expression levels of all genes from the five groups were analyzed in all samples, and are shown in Figures 3-7 in Paper II, which also provides a detailed discussion for all genes. **Group 1** contained two genes involved in oxalic acid synthesis (Glyoxylate dehydrogenase and oxaloacetate acetylhydrolase) and one involved in oxalic acid decomposition (oxalate decarboxylase). **Group 2** contained six genes believed to be associated with oxidative decay mechanisms, encoding three GMC oxidoreductases, two copper radical oxidases, and one

benzoquinone reductase. **Group 3** contained two GH5 endocellulases, a GH12 endocellulase, a GH3 beta-glucosidase and an AA9 LPMO. **Group 4** contained one GH5 endomannanase, two GH10 endoxylanases, a GH3 beta-xylosidase, a CE16 carbohydrate esterase and a GH28 polygalacturonidase. Finally, **Group 5** contained two expansins.

Change in gene expression was compared within each WPG treatment level over time (e.g. Ac21) and between WPG treatment levels (e.g. Ac21 vs. control). For the oxalic acid synthesis genes, no statistical trends were observed. Oxalic acid is believed to be a phase transfer agent and chelator of iron (Arantes and Goodell, 2014). The genes selected here have previously been shown to be expressed during the first 48 hours of decay by (Zhang et al., 2016). It is possible that our experimental setup did not allow for the capture of this crucial initial decay stage, since the first sample in the control experiment was taken after 1 week, which perhaps was too late. Expression of one of the AA3 GMC oxidoreductase genes (AOx3) was significantly affected by acetylation, and was upregulated in both Ac17 and Ac21 samples compared to the control. AOx3 shows high sequence similarity to known methanol oxidases (Waterham et al., 1997), and was the most highly expressed oxidative gene at week 16 in Ac21 (93% of expression in the oxidative group). We hypothesize that acetylation leads to an increased need for oxidative depolymerization, which again leads to more severe demethoxylation of lignin and generation of methanol. AOx3 would then oxidize and detoxify the methanol, generating H_2O_2 as a by-product (Filley et al., 2002, Niemenmaa et al., 2008). Another AA3 GMC oxidoreductase (AOx2 – Likely an aryl alcohol oxidase based on sequence analysis) was upregulated at later decay stages in the control, and was, interestingly, significantly upregulated at the first harvest point for all acetylated samples when compared to the control. There appeared to be no co-regulation of the GMC oxidoreductases selected in this study, indicating that the various enzymes have different roles during decay. The later expression of AOx2 suggests it could be involved in detoxification of lignin-derived compounds, as previously described with another aryl alcohol oxidase from *Pleurotus ostreatus* (Feldman et al., 2015). In addition, expression of one copper radical oxidase (Cro1) was significantly upregulated at the first harvest point for Ac21, compared to all other samples.

As to the cellulose-active genes, all three cellulases and the beta-glucosidase showed a pattern of delayed expression, with upregulation at later harvest points. Interestingly, the overall expression levels were lower in all acetylated samples. It has been shown that diffusible oligosaccharides like cellobiose regulate the expression of cellulases in *R. placenta*

(Zhang and Schilling, 2017), and inhibited diffusion of molecules that trigger this expression could be an effect of the acetylation. Furthermore, it is possible that partially acetylated oligosaccharides do not trigger cellulase expression because the signaling pathway does not recognize them. Crucially, the expression of the three core cellulases (the two GH5s and the GH12) was significantly delayed by acetylation, with little to no expression detected until week 24 in the Ac21 samples. *R. placenta* has two AA9 LPMO genes, but we were only able do detect expression of one of these. There were no significant differences in expression of this LPMO between treatment levels, but it was upregulated in tandem with the cellulases.

For the hemicellulase genes, the pattern was similar to that of the cellulases, displaying delayed expression for all WPG treatment levels and the control. Interestingly, upregulation of the GH5 endomannanase and the two GH10 endoxylanases in the Ac21 samples occurred at week 16, before the cellulase upregulation observed at week 24. No major differences were found as an effect of acetylation other than the observed delayed expression. The GH28 polygalacturonase (Gal28a) was upregulated at the first harvest point for the control, and showed an overall downregulation in the acetylated samples when compared to the control. Polygalacturonases degrade pectin, and it is likely that pectin is removed during the acetylation procedure, rendering this enzyme less important during early decay. The overall expression level of a carbohydrate esterase (CE16a) that we suspected to be involved in hemicellulose deacetylation was higher in the controls than in the Ac21 samples. This CE16 was show by Zhang et al. (2016) to be co-upregulated with hemicellulases in later stages of decay. The downregulation of CE16a in the acetylated samples was surprising, since with higher acetylation levels one might expect up-regulation of enzymes capable of deacetylating wood polysaccharides. Deacetylation is necessary for cellulases and hemicellulases to function most efficiently, and a negative impact of cellulose acetylation has been reported (Pan et al., 2006). However, Ringman et al. (2015) showed that cellulases are still capable of depolymerizing acetylated substrates, and it has even been suggested that under certain conditions acetylation will actually improve saccharification (Olaru et al., 2011). It is known that deacetylation does occur in acetylated wood (Beck et al., 2018), but this may happen during initial oxidative degradation. Perhaps, CE16a is regulated via a negative feedback system, where acetic acid, produced via deacetylation during oxidative degradation, suppresses expression.

Of the two expansins studied, Exp2 was more highly expressed in all acetylated samples. We interpret this as a direct effect of the acetylation, since it is conceivable that the increase

density of the material somehow is perceived by the fungus as an increased need for loosening and opening up the of the wood cell wall structure to cope with lower cell wall nano-porosity.

In conclusion, oxidative genes in *R. placenta* were upregulated in highly acetylated wood and the expression of genes encoding cellulose-active enzymes was delayed for acetylated samples compared to untreated samples. The delay observed for cellulose-active enzymes could be explained by slower diffusion rates of signaling metabolites such as cellobiose in acetylated wood, or by assuming that acetylated cellobiose is less effective in triggering expression of core cellulases. Importantly, the gene expression analysis revealed differential expression of selected genes that had not been reported previously, as outlined in Paper II. This opens up for new future studies and, eventually, a deeper understanding, of wood decay. In particular, the detected upregulation of expansins is of major interest.

Paper III: Characterization of a lytic polysaccharide monooxygenase from Gloeophyllum trabeum shows a pH-dependent relationship between catalytic activity and hydrogen peroxide production

LPMOs are ubiquitously found in wood-degrading organisms, where they perform oxidative cleavage of crystalline cellulose (AA9s) and certain hemicelluloses (AA9s, AA14s) (Beeson et al., 2015, Couturier et al., 2018). This cleavage improves substrate accessibility and saccharification of the substrate by hydrolytic cellulases (Eibinger et al., 2014). Paper III describes the expression and characterization of a previously uncharacterized AA9 LPMO from *G. trabeum* called *Gt*LPMO9B.

Enzyme activity was tested on a wide range of substrates, including phosphoric acid swollen cellulose (PASC), soluble cello-oligosaccharides (Glc_5 and Glc_6), konjac glucomannan, lichenan from Iceland moss, birchwood xylan, galactomannan, wheat arabinoxylan, barley beta-glucan, ivory nut mannan, and xyloglucan from tamarind seed, using ascorbic acid (AscA) as reducing agent. Analysis with HPAEC-PAD revealed activity on PASC with oxidization of both C_1 and C_4 positions, as well as activity on tamarind xyloglucan (Figure 2, Paper III). The genome of *G. trabeum* encodes four AA9 LPMOs, and the previously characterized *Gt*LPMO9A-2 showed similar substrate specificity for both cellulose and xyloglucan (Kojima et al., 2016).

Analysis of product formation after incubating *Gt*LPMO9B with PASC in the presence of various reducing agents at pH 6.5 showed product levels similar to those obtained with AscA for gallic acid, pyrogallol, caffeic acid, catechol and hydroquinone, all of which are di-hydroxy or tri-hydroxy aromatic compounds. Monohydroxy coniferyl alcohol, a natural lignin precursor, gave lower product yields, with peak intensities being >15 times lower than with AscA, whereas no product formation was observed in reactions with 2,3-dihydroxybenzoic acid, 3,5-dihydroxybenzoic acid, vanillic acid, guaiacol, veratryl alcohol, 2,4-hexadien-1-ol and 4-hydroxybenzoic acid under standard conditions (1 µM LPMO, 1 mM reductant, pH 6.5, 45°C).

In accordance with the recent discovery that LPMO activity can be modulated by H_2O_2 (Bissaro et al., 2017, Bissaro et al., 2016a), experiments were designed to investigate whether this applied to *Gt*LPMO9B. In these experiments, product formation was monitored over

time, so that both enzyme activity and enzyme inactivation could be observed. In addition, different reductant concentrations (1 and 5 mM) were tested in standard assays.

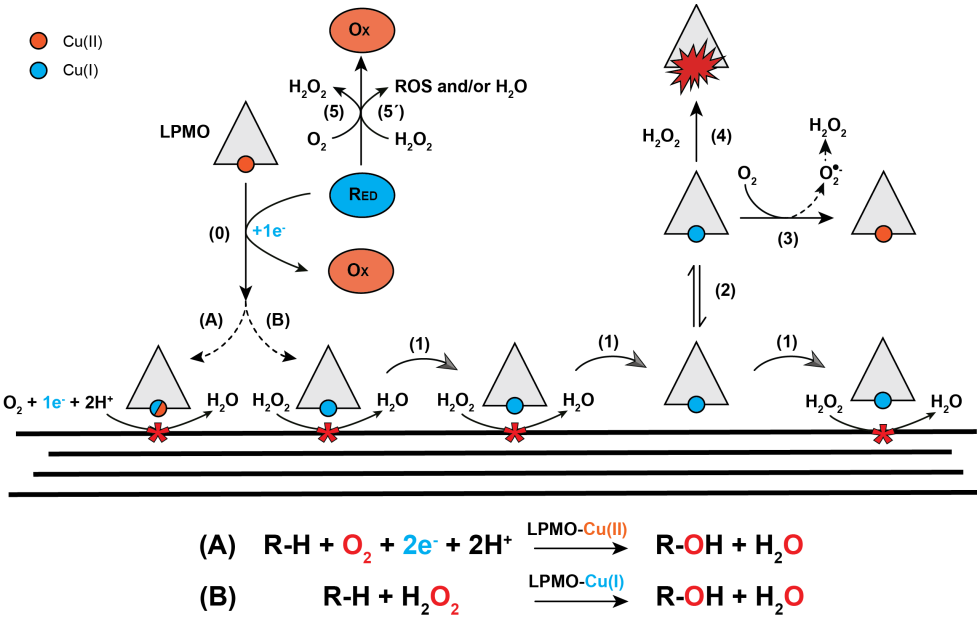

Figure 16: Overview of LPMO reactions. (0) Cu(II) in the LPMO is reduced to Cu(I) by the reductant (e.g. AscA or 2,3-DHBA) via a single-electron reduction. Reduced LPMO then performs oxidative cleavage of the cellulose substrate through one of two suggested mechanisms: **(A)** the reduced LPMO uses O_2 directly and requires two protons and a second electron to complete the hydroxylation of a carbon in the scissile glycosidic bond, or **(B)**, the reduced LPMO uses H_2O_2. Several scenarios have been proposed for reaction **A**, including scenarios where the copper stays reduced in between reactions (this uncertainty is indicated by the mixed blue/red colour of the copper); in any case, each catalytic cycle requires two externally delivered electrons as shown in the reaction scheme below the drawing. For reaction **B** the copper stays in the Cu(I) state and the enzyme will go through multiple catalytic cycles without a need for additional delivery of electrons. **(2,3)** Non-substrate-bound, reduced LPMO will generate H_2O_2 through reduction of O_2, via superoxide formed by the reaction of the reduced copper with O_2. H_2O_2 production may occur through the release of superoxide from the LPMO, followed by reduction or dismutation in solution, or via delivery of a second electron and two protons to the LPMO-superoxide complex, with subsequent release of H_2O_2. **(4)** Reaction of a reduced LPMO with H_2O_2 in solution, i.e. in the absence of substrate, will lead to formation of reactive oxygen species that can damage and inactivate the LPMO. **(5)** Reductants can reduce O_2 to H_2O_2, and **(5')** may also be oxidized by H_2O_2, generating reactive oxygen species (ROS) and/or water. The processes denoted by 5 and 5' may be affected by the presence of transition metals in the solution. See the main text for references and further details. This figure and legend is identical to Figure 1 in Paper III.

When using AscA, the most widely used reductant in LPMO experiments under standard conditions, activity was observed for 120 minutes when 1 mM was used to initiate the reaction. It is important to note that LPMO performance will depend on both the catalytic rate and the rate of autocatalytic inactivation (Bissaro et al., 2017). The latter is likely due to too high levels of H_2O_2; if a reduced LPMO in solution, i.e. not bound to substrate, meets H_2O_2 it runs the risk of carrying out a non-productive reaction that leads to inactivation. This scenario, along with other activities thought to occur in LPMO reactions are shown in Figure 16. When the AscA concentration was increased to 5 mM, the initial reaction rate was slightly higher, but severe auto-inactivation was observed after 60 minutes (Figure 3A, Paper III). This inactivation is thought to be a result of too high levels of endogenous H_2O_2 generation by the LPMO-reductant system (Petrovic et al., 2018, Kittl et al., 2012), and *Gt*LPMO9B was indeed shown to generate H_2O_2 with AscA in the absence of substrate (Figure 3C, Paper III). By gradually supplying the reaction with H_2O_2 and low concentrations of AscA (50 µM and 15 µM respectively) every 15 minutes for 240 minutes, we were able to achieve rates similar to those observed with 1 mM AscA (Figure 3B, Paper III). When replacing H_2O_2 with water, activity was observed but with much lower rate and final product level. This shows that the LPMO reaction can be driven by endogenously generated H_2O_2, at the expense of high reductant concentrations, or by exogenously added H_2O_2, at much lower reductant concentrations.

Of the other tested reductants, gallic acid (GA) was selected because of observations in trial experiments that suggested improved enzyme stability, and experiments similar to those described above with AscA were performed. When using either 1 or 5 mM GA to initiate LPMO reactions with PASC, activity was maintained for 24 hours giving final product yields that where more than two-fold higher than those obtained with AscA (Figure 4A, Paper III). In contrast to experiments with AscA, increasing the concentration of GA (from 1 to 5 mM) increased both rate and final yield. Two observations were made that could explain these results. Firstly, H_2O_2 accumulation by the LPMO+GA system (Figure 4C, Paper III) was much slower compared to LPMO+AscA. Secondly, GA was shown to be a significantly more efficient H_2O_2 scavenger, removing 94% H_2O_2 when incubate at a 1:1 ratio for 1 hour at pH 6.5, whereas AscA removed only 54% (Figure S2, Paper III). This latter result highlights an important challenge when measuring H_2O_2 production by LPMOs in the presence of reductant (Kittl et al., 2012). Since reductants react with H_2O_2, the measured levels reflect H_2O_2 accumulation rather than H_2O_2 production. Taken together, these results showcase the

importance of the choice of reductant and its impact on enzyme stability in LPMO reactions. It would seem that, when using GA and no exogenous H_2O_2, the lower rate and the higher stability are due to lower H_2O_2 levels. Experiments with gradual addition of H_2O_2 and GA showed higher rates (Figure 4B, Paper III). Final yields similar to those obtained after 24 hours with 5 mM GA were obtained in only 3 hours. This observation confirms that the lower reaction rate observed in reactions with only GA and no added H_2O_2 is due to lack of H_2O_2 rather than insufficient reduction of the LPMO.

Considering the observation that GA was equally effective as AscA in reactions with added H_2O_2, we then tested whether something similar might apply to the reductants that were not able to drive LPMO reactions under standard (aerobic, no added H_2O_2) conditions. Of these, 2,3-dihydroxybenzoic acid (2,3-DHBA) led to the formation of oxidized cellulose products when H_2O_2 was externally supplied at pH 6.5 (Figure 17). In the absence of 2,3-DHBA the addition of H_2O_2 did not lead to generation of oxidized products.

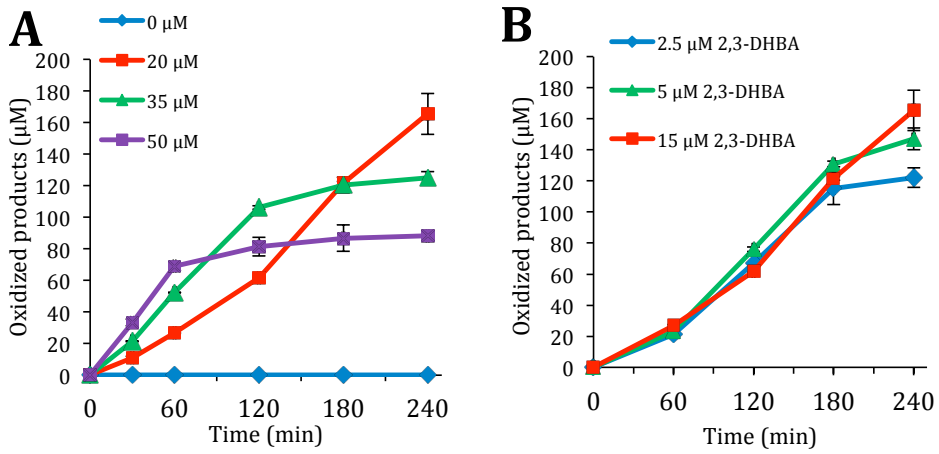

Figure 17. Activity of *Gt*LPMO9B with gradual addition of 2,3-dihydroxybenzoic acid (2,3-DHBA) and H_2O_2. The reaction mixtures were incubated at 45°C, 1000 rpm and contained 1 µM enzyme, 50 mM BisTris buffer pH 6.5, 0.5% (w/v) PASC, and were subjected to repetitive additions, every 15 minutes, starting at time zero of **(A)** 15 µM 2,3-DHBA and either 0, 20, 35 or 50 µM H_2O_2 (indicated in the figure) or **(B)** 20 µM H_2O_2 and either 2.5, 5 or 15 µM 2,3-DHBA. Error bars show standard deviations (n=3, independent experiments). Note that only soluble products were quantified; a fraction of the reaction products will remain associated with the insoluble substrate, as discussed in Paper III. Adapted from Figure 5 in Paper III.

These results suggest that, at pH 6.5, 2,3-DHBA is able to reduce the *Gt*LPMO9B, but unable to drive LPMO activity without added H_2O_2. Figure 17A shows that the initial rate, as well as the onset of enzyme inactivation correlates with the concentration of H_2O_2. The lowest tested H_2O_2 concentration (20 μM) gave the most stable reaction kinetics, whereas there was no product formation in the absence of added H_2O_2. Figure 17B shows that the reductant concentration could be lowered to 2.5 μM per 15 minutes, without a major decrease in the LPMO catalytic rate. The latter experiment proves that there is a non-stoichiometric relationship between the amount of reductant supplied and product formation. In this case, the product-to-reductant ratio was 3.1 and may be underestimated by a factor of approximately two because only soluble products were quantified.

The redox potential of 2,3-DHBA is known to be strongly affected by pH (Liu et al., 2005). Therefore, we tested the activity of *Gt*LPMO9B with AscA and 2,3-DHBA at pH 6.0, 6.5, 7.0, 8.0 and 9.0, using "standard" reductant concentrations of 1 mM. Activity was detected with AscA at pH 6.0-9.0, and, while 2,3-DHBA was not able to drive LPMO reactions at pH 6.0-7.0, it was able to do so at pH 8.0 and 9.0 (Figure 18A).

Figure 18 shows that the LPMO activity at alkaline pH in reactions with 2,3-DHBA overlaps with endogenous H_2O_2 production by the LPMO. Whereas no H_2O_2 accumulation was detected in reactions with the LPMO and 2,3-DHBA at pH 6.0 or 7.0, there was such accumulation at pH 8.0 and 9.0 (Figure 18B) and this is reflected in the generation of oxidized products in reactions with substrate. The redox potential of 2,3-DHBA becomes more negative with increasing pH (Liu et al., 2005), which could explain the ability to generate H_2O_2 and consequently also drive LPMO reactions at pH 8.0 and 9.0.

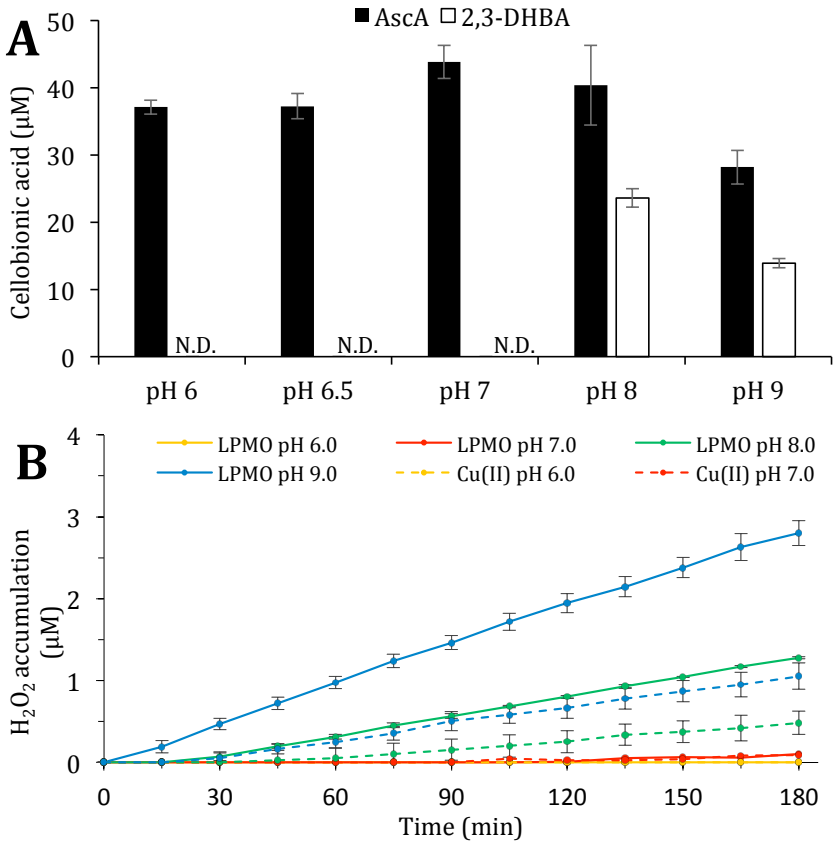

Figure 18. pH dependency of LPMO activity. (A) Product formation in reaction mixtures containing 1 µM *Gt*LPMO9B, 0.5% (w/v) PASC and 1 mM AscA or 2,3-DHBA, at pH 6.0-9.0, after incubation for 24 h at 45 °C. N.D. = "not detected". **(B)** H_2O_2 accumulation in reaction mixtures containing 1 µM *Gt*LPMO9B and 30 µM 2,3-DHBA at pH 6.0-9.0, and in control reactions containing 1 µM Cu(II) ($CuSO_4$) instead of the LPMO. Error bars show standard deviations (n=3, independent experiments). Adapted from Figure 6 in Paper III.

The mechanism by which LPMO-reductant systems produce H_2O_2 is debated (see, 1.3.2 and 1.3.3). One scenario entails that a single electron reduction of O_2 in the active site of the reduced LPMO is followed by release and subsequent dismutation of superoxide to H_2O_2. Another scenario entails that the two-electron reduction of O_2 to H_2O_2 is completed on the enzyme. The results described in Paper III support the latter hypothesis, as it is unlikely that 2,3-DHBA would not reduce released superoxide to H_2O_2, since the redox potential of superoxide ($O_2^- \rightarrow H_2O_2$, 890 mV at pH 7.0 (Wood, 1988) is more positive than that of 2,3-

DHBA (approx. 500 mV at pH 7, (Liu et al., 2005). This could imply that, while 2,3-DHBA is likely able to perform a single-electron reduction of the LPMO as is evident by the activity observed when supplying H_2O_2 externally, it is unable to generate ROS like H_2O_2 endogenously in the system that can drive the reaction at pH 6.5. It is conceivable that the superoxide-Cu(II) in the active site is rather stable, which will reduce its redox potential, making reduction less probable. In other words, the redox potential of the superoxide-Cu(II) may be too close to that of 2,3-DHBA for oxidation of 2,3-DHBA to occur. Paper III provides the first example of H_2O_2-dependent LPMO catalysis under aerobic conditions, but without endogenous H_2O_2 generation. This results strongly supports claims that H_2O_2 is an important, and perhaps the only, natural co-substrate of LPMOs. Next to providing fundamental insight into LPMO catalysis, Paper III provides a new and useful tool that enables control of LPMO activity in future LPMO studies, by allowing reduction of the LPMO without creating conditions that lead to enzyme inactivation in aerobic conditions.

4 Conclusions and future perspectives

The mechanisms underlying fungal decay are of high scientific interest, from both a fundamental and an applied perspective. The breakdown of lignocellulosic biomass and, ultimately, the release of carbon back to the environment are key processes in Nature, and, as such, fungal decay represents an essential ecosystem service. There is increasing public interest in the use of lignocellulosic materials for food and fuel, but the recalcitrant nature of the plant cell wall makes utilization a challenge. The decay mechanisms of fungi have the potential of solving the recalcitrance bottleneck, if properly understood and applied in an industrial setting.

Brown-rot fungi are highly successful in degrading wood, using a mechanism that gives them access to the polysaccharides within the wood cell wall without significantly mineralizing lignin. This unique mode of attack has potential as a pretreatment method, but has yet to be mimicked successfully. For the use of wood as construction material, brown-rot decay poses a particularly high threat, as significant strength can be lost without any detectable mass loss during early stages of decay. Better understanding of brown-rot decay mechanisms is therefore also needed for the development and improvement of wood protection strategies. The research in this thesis covers three aspects of wood decay by the brown-rot fungi *G. trabeum* and *R. placenta.*

Paper I describes attempts to improve saccharification of cellulose in *P. abies* wood by brown-rot inspired non-enzymatic pretreatments. This strategy was based on the idea that incipient oxidative decay would open up the wood cell wall, thus increasing access to the polysaccharides. Biological pretreatment with *R. placenta* and *G. trabeum* was successful, with the best performing pretreatment giving an improvement of 230% in glucose release over the control. However, the pretreatments giving the highest conversion yields were also the ones with the longest incubation time (45 days), and thus the highest mass losses, which amounted to 11.7% for *G. trabeum* and 14.5% for *R. placenta*. These mass losses are beyond the few percent of mass loss that are normally classified as incipient decay, and our compositional analyses showed that considerable amounts of galactoglucomannan had been removed. The results thus point to a synergistic effect of oxidative early decay and removal of hemicellulose on (subsequent) cellulose depolymerization. Neither of the *in vitro* pretreatment strategies tested, either working at wood-iron saturation levels or at significantly higher iron concentrations, proved successful. The mass losses obtained remained low (<1%).

Testing of the effects of MF reagents on downstream saccharification showed the need for elimination of H_2O_2 and iron to avoid enzyme inhibition.

It remains to be seen if the potential of brown-rot inspired pretreatments can be materialized in an industrially feasible process. One potential future development could entail gradual feeding of reagents over several reduction-oxidation cycles, if it is possible to ensure close association of reduced iron and the wood cell wall matrix. Clearly, chelation and leakage of iron out into solution should be avoided, and this does not seem straightforward. Another possible strategy would be to use H_2O_2 generating enzymes like AA3 GMC oxidoreductases or AA5 copper radical oxidases with CBMs that bring them in close association with the substrate. Such enzymes could be capable of spatially (close to the substrate) and temporally (i.e. only when a proper substrate is provided) controlled delivery of H_2O_2. Potentially also including iron reductases, and/or hemicellulases or pectinases.

In Paper II, the expression of 22 genes assumed to be involved in wood decay by *R. placenta* was studied during growth on unmodified and acetylated wood. Reporting for the first time higher mass losses than previously shown for acetylated wood, we discovered that acetylation causes delayed but not inhibited expression of hemicellulose- and cellulose- active enzymes. Expression of genes involved in incipient oxidative attack was detected after 16 weeks in the most highly acetylated samples, while these genes were downregulated after 2 weeks in the control. This implies that the switch from oxidative decay to hydrolytic decay is inhibited by acetylation, possibly because of lower diffusion or modification of signaling molecules like cellobiose. Interestingly, expansins were upregulated in acetylated wood, which could be a response to the densification of the wood cell wall caused by acetylation. We also detected a possible negative feedback mechanism for a CE16 carbohydrate esterase. Although limited in scope, with only 22 genes tested, the study described in Paper II provides novel insight into how acetylation affects gene expression of *R. placenta*. In future studies, whole transcriptome and secretome analyses could provide more high-resolution datasets. In addition, chemical characterization of the decaying acetylated wood, with direct comparison to gene expression and/or proteomics could serve to generate higher resolution data to deepen our understanding of the decay mechanisms, and at what potential threshold the fungus is able to access the wood cell wall polysaccharides.

Paper III deals with fundamental aspects of cellulose depolymerization and describes the characterization of *Gt*LPMO9B. LPMOs are potentially connected to the processes described

in Papers I and II since they can both produce and consume H_2O_2 and since they need to interact with reductants, which could be the same as those used in Fenton chemistry (e.g. 2,3-DHBA, which was used in both the LPMO study and the CMF study of Paper I). The functional analysis of *Gt*LPMO9B showed that it acts on both cellulose and xyloglucan and shows promiscuity for reducing agents.

The main focus of Paper III is on the role of H_2O_2 as a co-substrate for LPMOs. H_2O_2-producing enzymes are ubiquitous in brown-rot fungi (Floudas et al., 2012, Riley et al., 2014). These enzymes have previously been implicated in the non-enzymatic depolymerization of wood cell wall components, in particular by Fenton-type processes. We show here that under certain conditions H_2O_2 is needed for LPMO activity. The results show that the reductant 2,3-DHBA is capable of reducing *Gt*LPMO9B, but is not able to drive the LPMO reaction without externally provided H_2O_2 at pH 6.5. Endogenous H_2O_2 generation by the LPMO – 2,3-DHBA system was not observed at the pH values at which 2,3-DHBA alone could not drive the LPMO reaction. We hypothesize that a single-electron reduction of the LPMO occurs with 2,3-DHBA, but that activity is not observed due to the lack of endogenously generated H_2O_2. The author has done preliminary work with the well-characterized C_4-oxidizing *Nc*LPMO9C in combination with 2,3-DHBA and H_2O_2, which show similar trends (Figure S3, Paper III). Broad generalizations should be avoided until even more LPMOs have been tested, preferably including LPMOs from other AA families, but the results appear promising. Furthermore, copper reduction by 2,3-DHBA was not proven directly, despite several attempts using fluorescence spectroscopy (unpublished results; not in paper III). Reduction the copper site in the chitin oxidizing CBP21 (an AA10 LPMO) has previously been demonstrated using AscA as a reductant (Bissaro et al. 2016b), but preliminary work using fluorescence spectroscopy to study 2,3-DHBA as reductant with CBP21 and *Nc*LPMO9C have been inconclusive, since we have observed that 2,3-DHBA quenches the fluorescent signal. Measuring the oxidation of 2,3-DHBA by LPMOs with UV-VIS is an alternative, but has unfortunately not been performed due to insufficient enzyme stocks. Finally, redox potential measurements of all components in the system could contribute to supporting some of the claims made in paper III. Nevertheless, we would argue that Paper III supports claims that H_2O_2 is the preferred, if not the only, co-substrate for LPMOs.

In conclusion, this thesis highlights the importance of studying a fundamental mechanism in Nature, namely the decay of woody biomass by brown-rot fungi. The utilization of the

knowledge on the biology and biochemistry of these fungi has the potential to be applied in both breaking down and protecting wood. There are challenges and unanswered questions, but still promising work can be done. Nature has found a way, and so it only remains to unlock its full potential.

5 References

AGGER, J. W., ISAKSEN, T., VÁRNAI, A., VIDAL-MELGOSA, S., WILLATS, W. G., LUDWIG, R., HORN, S. J., EIJSINK, V. G. & WESTERENG, B. 2014. Discovery of LPMO activity on hemicelluloses shows the importance of oxidative processes in plant cell wall degradation. *Proceedings of the national academy of sciences USA*, 111(17):87-92

AKAGAWA, M., SHIGEMITSU, T. & SUYAMA, K. 2003. Production of hydrogen peroxide by polyphenols and polyphenol-rich beverages under quasi-physiological conditions. *Bioscience, biotechnology, and biochemistry,* 67, 2632-2640.

ALBRECHT, M. & LENGAUER, T. 2003. Pyranose oxidase identified as a member of the GMC oxidoreductase family. *Bioinformatics,* 19, 1216-1220.

ALFREDSEN, G. & FOSSDAL, C. G. *Postia placenta* gene expression during growth in furfurylated wood. 41st Annual Meeting of the International Research Group on Wood Protection, Biarritz, France, 9-13 May 2010, 2010. IRG Secretariat.

ALFREDSEN, G., PILGÅRD, A. & FOSSDAL, C. G. 2016. Characterisation of *Postia placenta* colonisation during 36 weeks in acetylated southern yellow pine sapwood at three acetylation levels including genomic DNA and gene expression quantification of the fungus. *Holzforschung,* 70, 1055-1065.

ALMEIDA, J. R., MODIG, T., PETERSSON, A., HÄHN-HÄGERDAL, B., LIDÉN, G. & GORWA-GRAUSLUND, M. F. 2007. Increased tolerance and conversion of inhibitors in lignocellulosic hydrolysates by *Saccharomyces cerevisiae*. *Journal of chemical technology & biotechnology: international research in process, Eenvironmental & clean technology,* 82, 340-349.

ALONSO, D. M., BOND, J. Q. & DUMESIC, J. A. 2010. Catalytic conversion of biomass to biofuels. *Green chemistry,* 12, 1493-1513.

ARANTES, V. & GOODELL, B. 2014. Current understanding of brown-rot fungal biodegradation mechanisms: a review. *Deterioration and protection of sustainable biomaterials,* 1158, 3-21.

ARANTES, V., JELLISON, J. & GOODELL, B. 2012. Peculiarities of brown-rot fungi and biochemical Fenton reaction with regard to their potential as a model for bioprocessing biomass. *Applied microbiology and biotechnology,* 94, 323-338.

ARANTES, V., QIAN, Y., MILAGRES, A. M., JELLISON, J. & GOODELL, B. 2009. Effect of pH and oxalic acid on the reduction of Fe^{3+} by a biomimetic chelator and on Fe^{3+} desorption/adsorption onto wood: Implications for brown-rot decay. *International biodeterioration & biodegradation,* 63, 478-483.

AYERST, G. 1969. The effects of moisture and temperature on growth and spore germination in some fungi. *Journal of stored products research,* 5, 127-141.

BAKER, J. O., KING, M. R., ADNEY, W. S., DECKER, S. R., VINZANT, T. B., LANTZ, S. E., NIEVES, R. E., THOMAS, S. R., LI, L.-C. & COSGROVE, D. J. 2000. Investigation of the cell-wall loosening protein expansin as a possible additive in the enzymatic saccharification of lignocellulosic biomass. Twenty-First Symposium on Biotechnology for Fuels and Chemicals. Springer, 84-86:217-223.

BECK, G., STROHBUSCH, S., LARNØY, E., MILITZ, H. & HILL, C. 2017. Accessibility of hydroxyl groups in anhydride modified wood as measured by deuterium exchange and saponification. *Holzforschung,* 72, 17-23.

BECK, G., THYBRING, E. E. & THYGESEN, L. G. 2018. Brown-rot fungal degradation and de-acetylation of acetylated wood. *International biodeterioration & biodegradation,* 135, 62-70.

BECKHAM, G. T., MATTHEWS, J. F., PETERS, B., BOMBLE, Y. J., HIMMEL, M. E. & CROWLEY, M. F. 2011. Molecular-level origins of biomass recalcitrance: decrystallization free energies for four common cellulose polymorphs. *The journal of physical chemistry B,* 115, 4118-4127.

BEESON, W. T., PHILLIPS, C. M., CATE, J. H. & MARLETTA, M. A. 2012. Oxidative cleavage of cellulose by fungal copper-dependent polysaccharide monooxygenases. *Journal of the American chemical society,* 134, 890-892.

BEESON, W. T., VU, V. V., SPAN, E. A., PHILLIPS, C. M. & MARLETTA, M. A. 2015. Cellulose degradation by polysaccharide monooxygenases. *Annual review of biochemistry,* 84, 923-946.

BERTRAN, M. S. & DALE, B. E. 1985. Enzymatic hydrolysis and recrystallization behavior of initially amorphous cellulose. *Biotechnology and bioengineering,* 27**,** 177-181.

BEUCHAT, L. R. 1981. Microbial stability as affected by water activity [Bacteria, fungi, spoilage]. *Cereal foods world (USA)*.

BIELY, P. 2012. Microbial carbohydrate esterases deacetylating plant polysaccharides. *Biotechnology advances,* 30**,** 1575-1588.

BISSARO, B., RØHR, A. K., SKAUGEN, M., FORSBERG, Z., HORN, S. J., VAAJE-KOLSTAD, G. & EIJSINK, V. 2016a. Fenton-type chemistry by a copper enzyme: molecular mechanism of polysaccharide oxidative cleavage. *bioRxiv***,** 097022.

BISSARO, B., FORSBERG, Z., NI, Y., HOLLMANN, F., VAAJE-KOLSTAD, G., & EIJSINK, V. G. 2016b. Fueling biomass-degrading oxidative enzymes by light-driven water oxidation. *Green chemistry*, 18(19), 5357-5366.

BISSARO, B., RØHR, Å. K., MÜLLER, G., CHYLENSKI, P., SKAUGEN, M., FORSBERG, Z., HORN, S. J., VAAJE-KOLSTAD, G. & EIJSINK, V. G. 2017. Oxidative cleavage of polysaccharides by monocopper enzymes depends on H_2O_2. *Nature chemical biology,* 13**,** 1123.

BISSARO, B., VÁRNAI, A., RØHR, Å. K. & EIJSINK, V. G. 2018. Oxidoreductases and Reactive Oxygen Species in Conversion of Lignocellulosic Biomass. *Microbiology and molecular biology reviews,* 82**,** e00029-18.

BLANCHETTE, R. A. 1991. Delignification by wood-decay fungi. *Annual review of phytopathology,* 29**,** 381-403.

BOERJAN, W., RALPH, J. & BAUCHER, M. 2003. Lignin biosynthesis. *Annual review of plant biology,* 54**,** 519-546.

BORASTON, A. B., BOLAM, D. N., GILBERT, H. J. & DAVIES, G. J. 2004. Carbohydrate-binding modules: fine-tuning polysaccharide recognition. *Biochemical journal,* 382**,** 769-781.

BRIGHAM, J. S., ADNEY, W. S. & HIMMEL, M. E. 2018. Hemicellulases: diversity and applications. *Handbook on bioethanol.* Routledge.

BROCK, B. J., RIEBLE, S. & GOLD, M. H. 1995. Purification and Characterization of a 1,4-Benzoquinone Reductase from the Basidiomycete *Phanerochaete chrysosporium*. *Applied and environmental microbiology,* 61**,** 3076-3081.

BUSSE-WICHER, M., LI, A., SILVEIRA, R. L., PEREIRA, C. S., TRYFONA, T., GOMES, T. C., SKAF, M. S. & DUPREE, P. 2016. Evolution of xylan substitution patterns in gymnosperms and angiosperms: implications for xylan interaction with cellulose. *Plant physiology***,** 1(4), 2418-2431

BUSSE-WICHER, M., GOMES, T. C., TRYFONA, T., NIKOLOVSKI, N., STOTT, K., GRANTHAM, N. J., BOLAM, D. N., SKAF, M. S. & DUPREE, P. 2014. The pattern of xylan acetylation suggests xylan may interact with cellulose microfibrils as a twofold helical screw in the secondary plant cell wall of Arabidopsis thaliana. *The Plant Journal,* 79**,** 492-506.

CANNELLA, D., MÖLLERS, K. B., FRIGAARD, N.-U., JENSEN, P. E., BJERRUM, M. J., JOHANSEN, K. S. & FELBY, C. 2016. Light-driven oxidation of polysaccharides by photosynthetic pigments and a metalloenzyme. *Nature communications,* 7**,** 11134.

CANTAREL, B. L., COUTINHO, P. M., RANCUREL, C., BERNARD, T., LOMBARD, V. & HENRISSAT, B. 2008. The Carbohydrate-Active EnZymes database (CAZy): an expert resource for glycogenomics. *Nucleic acids research,* 37**,** D233-D238.

CAPEK, P., ALFÖLDI, J. & LIŠKOVÁ, D. 2002. An acetylated galactoglucomannan from *Picea abies* L. Karst. *Carbohydrate research,* 337**,** 1033-1037.

CARVALHEIRO, F., DUARTE, L. C. & GÍRIO, F. M. 2008. Hemicellulose biorefineries: a review on biomass pretreatments. *Journal of Scientific & industrial research***,** 849-864.

CAVENER, D. R. 1992. GMC oxidoreductases: a newly defined family of homologous proteins with diverse catalytic activities. *Journal of molecular biology,* 223**,** 811-814.

COHEN, R., PERSKY, L. & HADAR, Y. 2002. Biotechnological applications and potential of wood-degrading mushrooms of the genus *Pleurotus*. *Applied microbiology and biotechnology,* 58**,** 582-594.

COHEN, R., SUZUKI, M. R. & HAMMEL, K. E. 2004. Differential stress-induced regulation of two quinone reductases in the brown rot basidiomycete *Gloeophyllum trabeum*. *Applied and environmental microbiology,* 70**,** 324-331.

COHEN, R., SUZUKI, M. R. & HAMMEL, K. E. 2005. Processive endoglucanase active in crystalline cellulose hydrolysis by the brown rot basidiomycete *Gloeophyllum trabeum*. *Applied and environmental microbiology,* 71**,** 2412-2417.

COSGROVE, D. J. 2005. Growth of the plant cell wall. *Nature reviews molecular cell biology,* 6(11)**,** 850-861.

COURTADE, G., FORSBERG, Z., HEGGSET, E. B., EIJSINK, V. G. & AACHMANN, F. L. 2018. The carbohydrate-binding module and linker of a modular lytic polysaccharide monooxygenase promote localized cellulose oxidation. *Journal of biological chemistry,* 293**,** 13006-13015.

COUTURIER, M., LADEVÈZE, S., SULZENBACHER, G., CIANO, L., FANUEL, M., MOREAU, C., VILLARES, A., CATHALA, B., CHASPOUL, F. & FRANDSEN, K. E. 2018. Lytic xylan oxidases from wood-decay fungi unlock biomass degradation. *Nature chemical biology,* 14(3)**,** 306-310.

COWLING, E. B. 1961. Comparative biochemistry of the decay of sweetgum sapwood by white-rot and brown-rot fungi, *US Dept. of Agriculture.*

COWLING, E. B. & BROWN, W. 1969. Structural features of cellulosic materials in relation to enzymatic hydrolysis. *Advances in chemistry,* 95**,** 152-187.

CRAGG, S. M., BECKHAM, G. T., BRUCE, N. C., BUGG, T. D., DISTEL, D. L., DUPREE, P., ETXABE, A. G., GOODELL, B. S., JELLISON, J. & MCGEEHAN, J. E. 2015. Lignocellulose degradation mechanisms across the Tree of Life. *Current opinion in chemical biology,* 29**,** 108-119.

CURLING, S., CLAUSEN, C. A. & WINANDY, J. E. 2001. The effect of hemicellulose degradation on the mechanical properties of wood during brown rot decay. International Research Group on Wood Preservation IRG/WP**,** 01-20219.

CURLING, S. F., CLAUSEN, C. A. & WINANDY, J. E. 2002. Relationships between mechanical properties, weight loss, and chemical composition of wood during incipient brownrot decay. *Forest products journal,* 52**,** 34-39.

DA SILVA, A. S. A., INOUE, H., ENDO, T., YANO, S. & BON, E. P. 2010. Milling pretreatment of sugarcane bagasse and straw for enzymatic hydrolysis and ethanol fermentation. *Bioresource technology,* 101**,** 7402-7409.

DADI, A. P., VARANASI, S. & SCHALL, C. A. 2006. Enhancement of cellulose saccharification kinetics using an ionic liquid pretreatment step. *Biotechnology and bioengineering,* 95**,** 904-910.

DANIEL, G., VOLC, J., FILONOVA, L., PLÍHAL, O., KUBÁTOVÁ, E. & HALADA, P. 2007. Characteristics of *Gloeophyllum trabeum* alcohol oxidase, an extracellular source of H_2O_2 in brown rot decay of wood. *Applied and environmental microbiology,* 73**,** 6241-6253.

DANNEELS, B., TANGHE, M. & DESMET, T. 2018. Structural Features on the Substrate-Binding Surface of Fungal Lytic Polysaccharide Monooxygenases Determine Their Oxidative Regioselectivity. *Biotechnology journal*. [Epub ahead of print]

DAVIES, G. & HENRISSAT, B. 1995. Structures and mechanisms of glycosyl hydrolases. *Structure,* 3**,** 853-859.

DIVNE, C., STAHLBERG, J., REINIKAINEN, T., RUOHONEN, L., PETTERSSON, G., KNOWLES, J., TEERI, T. T. & JONES, T. A. 1994. The three-dimensional crystal structure of the catalytic core of cellobiohydrolase I from *Trichoderma reesei*. *Science,* 265**,** 524-528.

EASTWOOD, D. C., FLOUDAS, D., BINDER, M., MAJCHERCZYK, A., SCHNEIDER, P., AERTS, A., ASIEGBU, F. O., BAKER, S. E., BARRY, K. & BENDIKSBY, M. 2011. The plant cell wall–decomposing machinery underlies the functional diversity of forest fungi. *Science,* 333**,** 762-765.

EIBINGER, M., GANNER, T., BUBNER, P., ROSKER, S., KRACHER, D., HALTRICH, D., LUDWIG, R., PLANK, H. & NIDETZKY, B. 2014. Cellulose surface degradation by a lytic polysaccharide monooxygenase and its effect on cellulase hydrolytic efficiency. *Journal of biological chemistry***,** 289, 35929-35938.

ERIKSSON, K.-E., PETTERSSON, B. & WESTERMARK, U. 1974. Oxidation: an important enzyme reaction in fungal degradation of cellulose. *FEBS letters,* 49**,** 282-285.

ESPEJO, E. & AGOSIN, E. 1991. Production and degradation of oxalic acid by brown rot fungi. *Applied and environmental microbiology,* 57**,** 1980-1986.

FEKETE, F. A., CHANDHOKE, V. & JELLISON, J. 1989. Iron-binding compounds produced by wood-decaying basidiomycetes. *Applied and environmental microbiology,* 55**,** 2720-2722.

FELDMAN, D., KOWBEL, D. J., GLASS, N. L., YARDEN, O. & HADAR, Y. 2015. Detoxification of 5-hydroxymethylfurfural by the *Pleurotus ostreatus* lignolytic enzymes aryl alcohol oxidase and dehydrogenase. *Biotechnology for biofuels,* 8**,** 63.

FERNANDES, A. N., THOMAS, L. H., ALTANER, C. M., CALLOW, P., FORSYTH, V. T., APPERLEY, D. C., KENNEDY, C. J. & JARVIS, M. C. 2011. Nanostructure of cellulose microfibrils in spruce wood. *Proceedings of the national academy of sciences USA*. 108(47):E1195-203.

FILLEY, T., CODY, G., GOODELL, B., JELLISON, J., NOSER, C. & OSTROFSKY, A. 2002. Lignin demethylation and polysaccharide decomposition in spruce sapwood degraded by brown rot fungi. *Organic geochemistry,* 33**,** 111-124.

FLOUDAS, D., BINDER, M., RILEY, R., BARRY, K., BLANCHETTE, R. A., HENRISSAT, B., MARTÍNEZ, A. T., OTILLAR, R., SPATAFORA, J. W. & YADAV, J. S. 2012. The Paleozoic origin of enzymatic lignin decomposition reconstructed from 31 fungal genomes. *Science,* 336**,** 1715-1719.

FLOURNOY, D. S., KIRK, T. K. & HIGHLEY, T. 1991. Wood decay by brown-rot fungi: changes in pore structure and cell wall volume. *Holzforschung-International Journal of the Biology, Chemistry, Physics and technology of wood,* 45**,** 383-388.

FORSBERG, Z., BISSARO, B., GULLESEN, J., DALHUS, B., VAAJE-KOLSTAD, G. & EIJSINK, V. G. 2018. Structural determinants of bacterial lytic polysaccharide monooxygenase functionality. *Journal of biological chemistry,* 293**,** 1397-1412.

FORSBERG, Z., VAAJE-KOLSTAD, G., WESTERENG, B., BUNÆS, A. C., STENSTRØM, Y., MACKENZIE, A., SØRLIE, M., HORN, S. J. & EIJSINK, V. G. 2011. Cleavage of cellulose by a CBM33 protein. *Protein science,* 20**,** 1479-1483.

FRANDSEN, K. E., SIMMONS, T. J., DUPREE, P., POULSEN, J.-C. N., HEMSWORTH, G. R., CIANO, L., JOHNSTON, E. M., TOVBORG, M., JOHANSEN, K. S. & VON FREIESLEBEN, P. 2016. The molecular basis of polysaccharide cleavage by lytic polysaccharide monooxygenases. *Nature chemical biology,* 12(4):298-303

FROMMHAGEN, M., WESTPHAL, A. H., HILGERS, R., KOETSIER, M. J., HINZ, S. W., VISSER, J., GRUPPEN, H., VAN BERKEL, W. J. & KABEL, M. A. 2018a. Quantification of the catalytic performance of C1-cellulose-specific lytic polysaccharide monooxygenases. *Applied microbiology and biotechnology,* 102**,** 1281-1295.

FROMMHAGEN, M., WESTPHAL, A. H., VAN BERKEL, W. J. & KABEL, M. A. 2018b. Distinct substrate specificities and electron-donating systems of fungal lytic polysaccharide monooxygenases. *Frontiers in microbiology,* 9:1080

FRY, S. C., YORK, W. S., ALBERSHEIM, P., DARVILL, A., HAYASHI, T., JOSELEAU, J. P., KATO, Y., LORENCES, E. P., MACLACHLAN, G. A. & MCNEIL, M. 1993. An unambiguous nomenclature for xyloglucan-derived oligosaccharides. *Physiologia plantarum,* 89**,** 1-3.

FUJITA, M. & HARADA, H. 2000. Ultrastructure and formation of wood cell wall. *Wood and cellulosic chemistry***,** 1-49. CRC Press

GARAJOVA, S., MATHIEU, Y., BECCIA, M. R., BENNATI-GRANIER, C., BIASO, F., FANUEL, M., ROPARTZ, D., GUIGLIARELLI, B., RECORD, E. & ROGNIAUX, H. 2016. Single-domain flavoenzymes trigger lytic polysaccharide monooxygenases for oxidative degradation of cellulose. *Scientific reports,* 6**,** 28276.

GARCÍA-APARICIO, M. P., BALLESTEROS, I., GONZÁLEZ, A., OLIVA, J. M., BALLESTEROS, M. & NEGRO, M. J. 2006. Effect of inhibitors released during steam-explosion pretreatment of barley straw on enzymatic hydrolysis. *Applied biochemistry and biotechnology,* 129**,** 278-288.

GOLDSTEIN, I. S. 1961. Acetylation of wood in lumber thickness. *Forest products journal,* 11**,** 363-370.

GOODELL, B., DANIEL, G., JELLISON, J. & QIAN, Y. 2006. Iron-reducing capacity of low-molecular-weight compounds produced in wood by fungi. *Holzforschung,* 60**,** 630-636.

GOODELL, B., JELLISON, J., LIU, J., DANIEL, G., PASZCZYNSKI, A., FEKETE, F., KRISHNAMURTHY, S., JUN, L. & XU, G. 1997. Low molecular weight chelators and phenolic compounds isolated from wood decay fungi and their role in the fungal biodegradation of wood. *Journal of biotechnology,* 53**,** 133-162.

GOODELL, B., YUHUI, Q. & JELLISON, J. Fungal decay of wood: Soft rot-brown rot-white rot. ACS symposium series, 2008. Oxford University Press, 9-31.

GOODELL, B., ZHU, Y., KIM, S., KAFLE, K., EASTWOOD, D., DANIEL, G., JELLISON, J., YOSHIDA, M., GROOM, L. & PINGALI, S. V. 2017. Modification of the nanostructure of lignocellulose cell walls via a non-enzymatic lignocellulose deconstruction system in brown rot wood-decay fungi. *Biotechnology for biofuels,* 10**,** 179.

GRANTHAM, N. J., WURMAN-RODRICH, J., TERRETT, O. M., LYCZAKOWSKI, J. J., STOTT, K., IUGA, D., SIMMONS, T. J., DURAND-TARDIF, M., BROWN, S. P. & DUPREE, R. 2017. An even pattern of xylan substitution is critical for interaction with cellulose in plant cell walls. *Nature plants,* 3**,** 859.

GRAZIANO, J., GRADY, R. & CERAMI, A. 1974. The identification of 2,3-dihydroxybenzoic acid as a potentially useful iron-chelating drug. *Journal of pharmacology and experimental therapeutics,* 190**,** 570-575.

GREEN, F., LARSEN, M. J., WINANDY, J. E. & HIGHLEY, T. L. 1991. Role of oxalic acid in incipient brown-rot decay. *Material und organismen,* 26**,** 191-213.

GREEN III, F. & HIGHLEY, T. L. 1997. Mechanism of brown-rot decay: paradigm or paradox. *International Biodeterioration & biodegradation,* 39**,** 113-124.

HANGASKY, J. A., IAVARONE, A. T. & MARLETTA, M. A. 2018. Reactivity of O_2 versus H_2O_2 with polysaccharide monooxygenases. *Proceedings of the national academy of sciences USA,* 115**,** 4915-4920.

HATAKKA, A. 1994. Lignin-modifying enzymes from selected white-rot fungi: production and role from in lignin degradation. *FEMS microbiology reviews,* 13**,** 125-135.

HE, Y.-C., DING, Y., XUE, Y.-F., YANG, B., LIU, F., WANG, C., ZHU, Z.-Z., QING, Q., WU, H. & ZHU, C. 2015. Enhancement of enzymatic saccharification of corn stover with sequential Fenton pretreatment and dilute NaOH extraction. *Bioresource technology,* 193**,** 324-330.

HEDEGÅRD, E. D. & RYDE, U. 2018. Molecular mechanism of lytic polysaccharide monooxygenases. *Chemical science,* 9**,** 3866-3880.

HERNÁNDEZ-ORTEGA, A., FERREIRA, P. & MARTÍNEZ, A. T. 2012. Fungal aryl-alcohol oxidase: a peroxide-producing flavoenzyme involved in lignin degradation. *Applied microbiology and biotechnology,* 93**,** 1395-1410.

HERVÉ, C., ROGOWSKI, A., BLAKE, A. W., MARCUS, S. E., GILBERT, H. J. & KNOX, J. P. 2010. Carbohydrate-binding modules promote the enzymatic deconstruction of intact plant cell walls by targeting and proximity effects. *Proceedings of the national academy of sciences USA,* 107**,** 15293-15298.

HIDENO, A., INOUE, H., TSUKAHARA, K., FUJIMOTO, S., MINOWA, T., INOUE, S., ENDO, T. & SAWAYAMA, S. 2009. Wet disk milling pretreatment without sulfuric acid for enzymatic hydrolysis of rice straw. *Bioresource technology,* 100**,** 2706-2711.

HILL, C., FORSTER, S., FARAHANI, M., HALE, M., ORMONDROYD, G. & WILLIAMS, G. 2005. An investigation of cell wall micropore blocking as a possible mechanism for the decay resistance of anhydride modified wood. *International biodeterioration & biodegradation,* 55**,** 69-76.

HILL, C. A. 2006. Wood modification: chemical, thermal and other processes, John Wiley & Sons.

HILL, C. A. 2011. Wood modification: An update. *BioResources,* 6**,** 918-919.

HILL, C. A., HALE, M. D., ORMONDROYD, G. A., KWON, J. H. & FORSTER, S. C. 2006. Decay resistance of anhydride-modified Corsican pine sapwood exposed to the brown rot fungus *Coniophora puteana*. *Holzforschung,* 60**,** 625-629.

HIMMEL, M. E., DING, S.-Y., JOHNSON, D. K., ADNEY, W. S., NIMLOS, M. R., BRADY, J. W. & FOUST, T. D. 2007. Biomass recalcitrance: engineering plants and enzymes for biofuels production. *Science,* 315**,** 804-807.

HINER, A. N., RUIZ, J. H., LÓPEZ, J. N. R. G., CÁNOVAS, F. G. A., BRISSET, N. C., SMITH, A. T., ARNAO, M. B. & ACOSTA, M. 2002. Reactions of the class II peroxidases, lignin peroxidase and *Arthromyces ramosus* peroxidase, with hydrogen peroxide catalase-like activity, compound III formation, and enzyme inactivation. *Journal of biological chemistry,* 277**,** 26879-26885.

HORN, S. J., VAAJE-KOLSTAD, G., WESTERENG, B. & EIJSINK, V. 2012. Novel enzymes for the degradation of cellulose. *Biotechnology for biofuels,* 5**,** 45.

HUG, S. J. & LEUPIN, O. 2003. Iron-catalyzed oxidation of arsenic (III) by oxygen and by hydrogen peroxide: pH-dependent formation of oxidants in the Fenton reaction. *Environmental science & technology,* 37**,** 2734-2742.

HYDE, S. M. & WOOD, P. M. 1997. A mechanism for production of hydroxyl radicals by the brown-rot fungus Coniophora puteana: Fe(III) reduction by cellobiose dehydrogenase and Fe(II) oxidation at a distance from the hyphae. *Microbiology,* 143**,** 259-266.

ISAKSEN, T., WESTERENG, B., AACHMANN, F. L., AGGER, J. W., KRACHER, D., KITTL, R., LUDWIG, R., HALTRICH, D., EIJSINK, V. G. & HORN, S. J. 2014. A C4-oxidizing lytic polysaccharide monooxygenase cleaving both cellulose and cello-oligosaccharides. *Journal of biological chemistry,* 289**,** 2632-2642.

ISOGAI, A., USUDA, M., KATO, T., URYU, T. & ATALLA, R. H. 1989. Solid-state CP/MAS carbon-13 NMR study of cellulose polymorphs. *Macromolecules,* 22**,** 3168-3172.

JELLISON, J., CHANDHOKE, V., GOODELL, B. & FEKETE, F. A. 1991. The isolation and immunolocalization of iron-binding compounds produced by *Gloeophyllum trabeum*. *Applied microbiology and biotechnology,* 35**,** 805-809.

JENSEN JR, K. A., RYAN, Z. C., WYMELENBERG, A. V., CULLEN, D. & HAMMEL, K. E. 2002. An NADH: quinone oxidoreductase active during biodegradation by the brown-rot basidiomycete *Gloeophyllum trabeum*. *Applied and environmental microbiology,* 68**,** 2699-2703.

JENSEN, K. A., HOUTMAN, C. J., RYAN, Z. C. & HAMMEL, K. E. 2001. Pathways for extracellular Fenton chemistry in the brown rot basidiomycete *Gloeophyllum trabeum*. *Applied and environmental microbiology,* 67**,** 2705-2711.

JUNG, Y. H., KIM, H. K., PARK, H. M., PARK, Y.-C., PARK, K., SEO, J.-H. & KIM, K. H. 2015. Mimicking the Fenton reaction-induced wood decay by fungi for pretreatment of lignocellulose. *Bioresource technology,* 179**,** 467-472.

JÖNSSON, L. J. & MARTÍN, C. 2016. Pretreatment of lignocellulose: formation of inhibitory by-products and strategies for minimizing their effects. *Bioresource technology,* 199**,** 103-112.

KARKEHABADI, S., HANSSON, H., KIM, S., PIENS, K., MITCHINSON, C. & SANDGREN, M. 2008. The first structure of a glycoside hydrolase family 61 member, Cel61B from *Hypocrea jecorina*, at 1.6 Å resolution. *Journal of molecular biology,* 383**,** 144-154.

KATO, D. M., ELÍA, N., FLYTHE, M. & LYNN, B. C. 2014. Pretreatment of lignocellulosic biomass using Fenton chemistry. *Bioresource technology,* 162**,** 273-278.

KEREM, Z., JENSEN, K. A. & HAMMEL, K. E. 1999. Biodegradative mechanism of the brown rot basidiomycete *Gloeophyllum trabeum*: evidence for an extracellular hydroquinone-driven fenton reaction. *FEBS letters,* 446**,** 49-54.

KERSTEN, P. & CULLEN, D. 2014. Copper radical oxidases and related extracellular oxidoreductases of wood-decay Agaricomycetes. *Fungal genetics and biology,* 72**,** 124-130.

KIESS, M., HECHT, H. J. & KALISZ, H. M. 1998. Glucose oxidase from *Penicillium amagasakiense*: Primary structure and comparison with other glucose-methanol-choline (GMC) oxidoreductases. *European journal of biochemistry,* 252**,** 90-99.

KITTL, R., KRACHER, D., BURGSTALLER, D., HALTRICH, D. & LUDWIG, R. 2012. Production of four *Neurospora crassa* lytic polysaccharide monooxygenases in *Pichia pastoris* monitored by a fluorimetric assay. *Biotechnology for biofuels,* 5**,** 79.

KJAERGAARD, C. H., QAYYUM, M. F., WONG, S. D., XU, F., HEMSWORTH, G. R., WALTON, D. J., YOUNG, N. A., DAVIES, G. J., WALTON, P. H. & JOHANSEN, K. S.

2014. Spectroscopic and computational insight into the activation of O_2 by the mononuclear Cu center in polysaccharide monooxygenases. *Proceedings of the national academy of sciences USA*, 111(24):797-802

KOJIMA, Y., VÁRNAI, A., ISHIDA, T., SUNAGAWA, N., PETROVIC, D. M., IGARASHI, K., JELLISON, J., GOODELL, B., ALFREDSEN, G. & WESTERENG, B. 2016. Characterization of an LPMO from the brown-rot fungus *Gloeophyllum trabeum* with broad xyloglucan specificity, and its action on cellulose-xyloglucan complexes. *Applied and environmental microbiology*, 82 (22) 6557-6572

KORRIPALLY, P., TIMOKHIN, V. I., HOUTMAN, C. J., MOZUCH, M. D. & HAMMEL, K. E. 2013. Evidence from *Serpula lacrymans* that 2, 5-dimethoxyhydroquinone is a lignocellulolytic agent of divergent brown-rot basidiomycetes. *Applied and environmental microbiology*, 79 (7) 2377-2383

KRACHER, D., SCHEIBLBRANDNER, S., FELICE, A. K., BRESLMAYR, E., PREIMS, M., LUDWICKA, K., HALTRICH, D., EIJSINK, V. G. & LUDWIG, R. 2016. Extracellular electron transfer systems fuel cellulose oxidative degradation. *Science,* 352, 1098-1101.

KUMAR, S. & AGARWAL, S. 1983. Biological degradation resistance of wood acetylated with thioacetic acid. International Research Group on Wood Preservation IRG/WP/3223.

KUUSK, S., BISSARO, B., KUUSK, P., FORSBERG, Z., EIJSINK, V. G., SØRLIE, M. & VÄLJAMÄE, P. 2018. Kinetics of H_2O_2-driven degradation of chitin by a bacterial lytic polysaccharide monooxygenase. *Journal of Biological Chemistry,* 293, 523-531.

KAAR, W. E. & HOLTZAPPLE, M. T. 2000. Using lime pretreatment to facilitate the enzymic hydrolysis of corn stover. *Biomass and bioenergy,* 18, 189-199.

LABANDEIRA, C. 2007. The origin of herbivory on land: initial patterns of plant tissue consumption by arthropods. *Insect science,* 14, 259-275.

LANGSTON, J. A., SHAGHASI, T., ABBATE, E., XU, F., VLASENKO, E. & SWEENEY, M. D. 2011. Oxidoreductive cellulose depolymerization by the enzymes cellobiose dehydrogenase and glycoside hydrolase 61. *Applied and environmental microbiology*, 77 (19) 7007-7015

LARSSON, S., PALMQVIST, E., HAHN-HÄGERDAL, B., TENGBORG, C., STENBERG, K., ZACCHI, G. & NILVEBRANT, N.-O. 1999. The generation of fermentation inhibitors during dilute acid hydrolysis of softwood. *Enzyme and microbial technology,* 24, 151-159.

LEDEBOER, A., EDENS, L., MAAT, J., VISSER, C., BOS, J., VERRIPS, C., JANOWICZ, Z., ECKART, M., ROGGENKAMP, R. & HOLLENBERG, C. 1985. Molecular cloning and characterization of a gene coding for methanol oxidase in *Hansenula polymorpha*. *Nucleic acids research,* 13, 3063-3082.

LEE, J.-W., HOUTMAN, C. J., KIM, H.-Y., CHOI, I.-G. & JEFFRIES, T. W. 2011. Scale-up study of oxalic acid pretreatment of agricultural lignocellulosic biomass for the production of bioethanol. *Bioresource technology,* 102, 7451-7456.

LENFANT, N., HAINAUT, M., TERRAPON, N., DRULA, E., LOMBARD, V. & HENRISSAT, B. 2017. A bioinformatics analysis of 3400 lytic polysaccharide oxidases from family AA9. *Carbohydrate research,* 448, 166-174.

LEVASSEUR, A., DRULA, E., LOMBARD, V., COUTINHO, P. M. & HENRISSAT, B. 2013. Expansion of the enzymatic repertoire of the CAZy database to integrate auxiliary redox enzymes. *Biotechnology for biofuels,* 6, 41.

LI, X., KIM, T. H. & NGHIEM, N. P. 2010. Bioethanol production from corn stover using aqueous ammonia pretreatment and two-phase simultaneous saccharification and fermentation (TPSSF). *Bioresource technology,* 101, 5910-5916.

LIU, R., GOODELL, B., JELLISON, J. & AMIRBAHMAN, A. 2005. Electrochemical study of 2,3-dihydroxybenzoic acid and its interaction with Cu(II) and H_2O_2 in aqueous solutions: implications for wood decay. *Environmental science & technology,* 39, 175-180.

LOMBARD, V., GOLACONDA RAMULU, H., DRULA, E., COUTINHO, P. M. & HENRISSAT, B. 2013. The carbohydrate-active enzymes database (CAZy) in 2013. *Nucleic acids research,* 42, D490-D495.

MABEE, W. E., GREGG, D. J., ARATO, C., BERLIN, A., BURA, R., GILKES, N., MIROCHNIK, O., PAN, X., PYE, E. K. & SADDLER, J. N. Updates on softwood-to-ethanol process

development. Twenty-Seventh Symposium on Biotechnology for Fuels and Chemicals, 2006. Springer, 55-70.

MACKIE, K., BROWNELL, H., WEST, K. & SADDLER, J. 1985. Effect of sulphur dioxide and sulphuric acid on steam explosion of aspenwood. *Journal of wood chemistry and technology,* 5**,** 405-425.

MAGAN, N. & LACEY, J. 1984. Effect of water activity, temperature and substrate on interactions between field and storage fungi. *Transactions of the british mycological society,* 82**,** 83-93.

MARTINEZ, D., CHALLACOMBE, J., MORGENSTERN, I., HIBBETT, D., SCHMOLL, M., KUBICEK, C. P., FERREIRA, P., RUIZ-DUENAS, F. J., MARTINEZ, A. T. & KERSTEN, P. 2009. Genome, transcriptome, and secretome analysis of wood decay fungus Postia placenta supports unique mechanisms of lignocellulose conversion. *Proceedings of the national academy of sciences USA,* 106**,** 1954-1959.

MATHEWS, S. L., PAWLAK, J. & GRUNDEN, A. M. 2015. Bacterial biodegradation and bioconversion of industrial lignocellulosic streams. *Applied microbiology and biotechnology,* 99**,** 2939-2954.

MERINO, S. T. & CHERRY, J. 2007. Progress and challenges in enzyme development for biomass utilization. *Biofuels*. Springer.

MICHALSKA, K., MIAZEK, K., KRZYSTEK, L. & LEDAKOWICZ, S. 2012. Influence of pretreatment with Fenton's reagent on biogas production and methane yield from lignocellulosic biomass. *Bioresource technology,* 119**,** 72-78.

MONTANIER, C., MONEY, V. A., PIRES, V. M., FLINT, J. E., PINHEIRO, B. A., GOYAL, A., PRATES, J. A., IZUMI, A., STÅLBRAND, H. & MORLAND, C. 2009. The active site of a carbohydrate esterase displays divergent catalytic and noncatalytic binding functions. *PLoS biology,* 7**,** e1000071.

MOOD, S. H., GOLFESHAN, A. H., TABATABAEI, M., JOUZANI, G. S., NAJAFI, G. H., GHOLAMI, M. & ARDJMAND, M. 2013. Lignocellulosic biomass to bioethanol, a comprehensive review with a focus on pretreatment. *Renewable and Sustainable Energy Reviews,* 27**,** 77-93.

MOREIRA, L. 2008. An overview of mannan structure and mannan-degrading enzyme systems. *Applied microbiology and biotechnology,* 79**,** 165.

MOSIER, N., WYMAN, C., DALE, B., ELANDER, R., LEE, Y., HOLTZAPPLE, M. & LADISCH, M. 2005. Features of promising technologies for pretreatment of lignocellulosic biomass. *Bioresource technology,* 96**,** 673-686.

MUNIR, E., YOON, J. J., TOKIMATSU, T., HATTORI, T. & SHIMADA, M. 2001. A physiological role for oxalic acid biosynthesis in the wood-rotting basidiomycete *Fomitopsis palustris*. *Proceedings of the National Academy of Sciences,* 98**,** 11126-11130.

MURMANIS, L., HIGHLEY, T. L. & PALMER, J. 1987. Cytochemical localization of cellulases in decayed and nondecayed wood. *Wood science and technology,* 21**,** 101-109.

MÜLLER, G., CHYLENSKI, P., BISSARO, B., EIJSINK, V. G. & HORN, S. J. 2018. The impact of hydrogen peroxide supply on LPMO activity and overall saccharification efficiency of a commercial cellulase cocktail. *Biotechnology for biofuels,* 11**,** 209.

MÖLLERS, K., MIKKELSEN, H., SIMONSEN, T., CANNELLA, D., JOHANSEN, K., BJERRUM, M. J. & FELBY, C. 2017. On the formation and role of reactive oxygen species in light-driven LPMO oxidation of phosphoric acid swollen cellulose. *Carbohydrate research,* 448**,** 182-186.

NAGY, L. G., RILEY, R., TRITT, A., ADAM, C., DAUM, C., FLOUDAS, D., SUN, H., YADAV, J. S., PANGILINAN, J. & LARSSON, K.-H. 2015. Comparative genomics of early-diverging mushroom-forming fungi provides insights into the origins of lignocellulose decay capabilities. *Molecular biology and evolution,* 33**,** 959-970.

NIEMENMAA, O., UUSI-RAUVA, A. & HATAKKA, A. 2008. Demethoxylation of [O14 CH3]-labelled lignin model compounds by the brown-rot fungi *Gloeophyllum trabeum* and *Poria (Postia) placenta*. *Biodegradation,* 19**,** 555.

NISHINO, T., TAKANO, K. & NAKAMAE, K. 1995. Elastic modulus of the crystalline regions of cellulose polymorphs. *Journal of Polymer Science Part B: Polymer Physics,* 33**,** 1647-1651.

OLARU, N., OLARU, L., VASILE, C. & ANDER, P. 2011. Surface modified cellulose obtained by acetylation without solvents of bleached and unbleached kraft pulps. *Polimery,* 56.

PAN, X., GILKES, N. & SADDLER, J. N. 2006. Effect of acetyl groups on enzymatic hydrolysis of cellulosic substrates. *Holzforschung,* 60**,** 398-401.

PANDEY, K. K. & PITMAN, A. 2003. FTIR studies of the changes in wood chemistry following decay by brown-rot and white-rot fungi. *International biodeterioration & biodegradation,* 52**,** 151-160.

PAPADOPOULOS, A. & HILL, C. 2003. The sorption of water vapour by anhydride modified softwood. *Wood Science and Technology,* 37**,** 221-231.

PAPADOPOULOS, A. N. & HILL, C. 2002. The biological effectiveness of wood modified with linear chain carboxylic acid anhydrides against *Coniophora puteana*. *Holz als roh-und werkstoff,* 60**,** 329-332.

PARK, Y. B. & COSGROVE, D. J. 2012. A revised architecture of primary cell walls based on biomechanical changes induced by substrate-specific endoglucanases. *Plant physiology***,** 158(4):1933-1943

PASZCZYNSKI, A., CRAWFORD, R., FUNK, D. & GOODELL, B. 1999. De Novo Synthesis of 4,5-Dimethoxycatechol and 2, 5-Dimethoxyhydroquinone by the Brown Rot Fungus *Gloeophyllum trabeum*. *Applied and environmental eicrobiology,* 65**,** 674-679.

PAULY, M. & KEEGSTRA, K. 2016. Biosynthesis of the plant cell wall matrix polysaccharide xyloglucan. *Annual review of plant biology,* 67**,** 235-259.

PAYNE, C. M., RESCH, M. G., CHEN, L., CROWLEY, M. F., HIMMEL, M. E., TAYLOR, L. E., SANDGREN, M., STÅHLBERG, J., STALS, I. & TAN, Z. 2013. Glycosylated linkers in multimodular lignocellulose-degrading enzymes dynamically bind to cellulose. *Proceedings of the national academy of sciences USA***,** 110(36):14646-14651

PEDERSEN, M. & MEYER, A. S. 2010. Lignocellulose pretreatment severity–relating pH to biomatrix opening. *New biotechnology,* 27**,** 739-750.

PEÑA, M. J., DARVILL, A. G., EBERHARD, S., YORK, W. S. & O'NEILL, M. A. 2008. Moss and liverwort xyloglucans contain galacturonic acid and are structurally distinct from the xyloglucans synthesized by hornworts and vascular plants. *Glycobiology,* 18**,** 891-904.

PETROVIC, D. M., BISSARO, B., CHYLENSKI, P., SKAUGEN, M., SØRLIE, M., JENSEN, M. S., AACHMANN, F. L., COURTADE, G., VÁRNAI, A. & EIJSINK, V. G. 2018. Methylation of the N-terminal histidine protects a lytic polysaccharide monooxygenase from auto-oxidative inactivation. *Protein science*. 27(9):1636-1650

PHILLIPS, C. M., BEESON IV, W. T., CATE, J. H. & MARLETTA, M. A. 2011. Cellobiose dehydrogenase and a copper-dependent polysaccharide monooxygenase potentiate cellulose degradation by *Neurospora crassa*. *ACS chemical biology,* 6**,** 1399-1406.

POPESCU, C.-M., HILL, C. A., CURLING, S., ORMONDROYD, G. & XIE, Y. 2014. The water vapour sorption behaviour of acetylated birch wood: how acetylation affects the sorption isotherm and accessible hydroxyl content. *Journal of materials science,* 49**,** 2362-2371.

PRESLEY, G. N., PANISKO, E., PURVINE, S. O. & SCHILLING, J. S. 2018. Coupling secretomics with enzyme activities to compare the temporal processes of wood metabolism among white and brown rot fungi. *Applied and environmental microbiology,* 84 (16) e00159-18

PRINGSHEIM, H. 1912. Über den fermentativen Abbau der Cellulose. *Hoppe-Seyler´ s zeitschrift für physiologische chemie,* 78**,** 266-291.

QIAN, Y., GOODELL, B. & FELIX, C. C. 2002. The effect of low molecular weight chelators on iron chelation and free radical generation as studied by ESR measurement. *Chemosphere,* 48**,** 21-28.

QUINLAN, R. J., SWEENEY, M. D., LEGGIO, L. L., OTTEN, H., POULSEN, J.-C. N., JOHANSEN, K. S., KROGH, K. B., JØRGENSEN, C. I., TOVBORG, M. & ANTHONSEN, A. 2011. Insights into the oxidative degradation of cellulose by a copper metalloenzyme that exploits biomass components. *Proceedings of the national academy of sciences USA,* 108**,** 15079-15084.

RAGUZ, S., YAGUEA, E., WOOD, D. & THURSTON, C. 1992. Isolation and characterization of a cellulose-growth-specific gene from *Agaricus bisporus*. *Gene,* 119**,** 183-190.

RAMOS, L. P. 2003. The chemistry involved in the steam treatment of lignocellulosic materials. *Química Nova,* 26**,** 863-871.

RAY, M. J., LEAK, D. J., SPANU, P. D. & MURPHY, R. J. 2010. Brown rot fungal early stage decay mechanism as a biological pretreatment for softwood biomass in biofuel production. *Biomass and bioenergy,* 34**,** 1257-1262.

REESE, E. T., SIU, R. G. & LEVINSON, H. S. 1950. The biological degradation of soluble cellulose derivatives and its relationship to the mechanism of cellulose hydrolysis. *Journal of bacteriology,* 59**,** 485.

RICHARDS, D. 1954. Physical changes in decaying wood. *Journal of Forestry,* 52**,** 260-265.

RILEY, R., SALAMOV, A. A., BROWN, D. W., NAGY, L. G., FLOUDAS, D., HELD, B. W., LEVASSEUR, A., LOMBARD, V., MORIN, E. & OTILLAR, R. 2014. Extensive sampling of basidiomycete genomes demonstrates inadequacy of the white-rot/brown-rot paradigm for wood decay fungi. *Proceedings of the national academy of sciences USA,* 111**,** 9923-9928.

RINGMAN, R., PILGÅRD, A., BRISCHKE, C. & RICHTER, K. 2014a. Mode of action of brown rot decay resistance in modified wood: a review. *Holzforschung,* 68**,** 239-246.

RINGMAN, R., PILGÅRD, A. & RICHTER, K. 2014b. Effect of wood modification on gene expression during incipient *Postia placenta* decay. *International biodeterioration & biodegradation,* 86**,** 86-91.

RINGMAN, R., PILGÅRD, A. & RICHTER, K. 2015. In vitro oxidative and enzymatic degradation of modified wood. *International wood products journal,* 6**,** 36-39.

ROSE, J. K. & BENNETT, A. B. 1999. Cooperative disassembly of the cellulose–xyloglucan network of plant cell walls: parallels between cell expansion and fruit ripening. *Trends in plant science,* 4**,** 176-183.

ROWELL, R. M. 2006. Chemical modification of wood: A short review. *Wood Material Science and Engineering,* 1**,** 29-33.

ROWELL, R. M. 2012. *Handbook of wood chemistry and wood composites*, CRC press.

RYTIOJA, J., HILDÉN, K., HATAKKA, A. & MÄKELÄ, M. R. 2014. Transcriptional analysis of selected cellulose-acting enzymes encoding genes of the white-rot fungus Dichomitus squalens on spruce wood and microcrystalline cellulose. *Fungal Genetics and Biology,* 72**,** 91-98.

SABBADIN, F., HEMSWORTH, G. R., CIANO, L., HENRISSAT, B., DUPREE, P., TRYFONA, T., MARQUES, R. D., SWEENEY, S. T., BESSER, K. & ELIAS, L. 2018. An ancient family of lytic polysaccharide monooxygenases with roles in arthropod development and biomass digestion. *Nature communications,* 9**,** 756.

SAN RYU, J., SHARY, S., HOUTMAN, C. J., PANISKO, E. A., KORRIPALLY, P., JOHN, F. J. S., CROOKS, C., SIIKA-AHO, M., MAGNUSON, J. K. & HAMMEL, K. E. 2011. Proteomic and functional analysis of the cellulase system expressed by *Postia placenta* during brown rot of solid wood. *Applied and environmental microbiology***,** 77(22): 7933–7941.

SANDBERG, D., KUTNAR, A. & MANTANIS, G. 2017. Wood modification technologies-a review. *iForest-Biogeosciences and Forestry,* 10**,** 895.

SCHELLER, H. V. & ULVSKOV, P. 2010. Hemicelluloses. *Annual review of plant biology,* 61:263-289

SHALLOM, D. & SHOHAM, Y. 2003. Microbial hemicellulases. *Current opinion in microbiology,* 6**,** 219-228.

SINGH, R., WISEMAN, B., DEEMAGARN, T., JHA, V., SWITALA, J. & LOEWEN, P. C. 2008. Comparative study of catalase-peroxidases (KatGs). *Archives of biochemistry and biophysics,* 471**,** 207-214.

SOLOMON, E. I., HEPPNER, D. E., JOHNSTON, E. M., GINSBACH, J. W., CIRERA, J., QAYYUM, M., KIEBER-EMMONS, M. T., KJAERGAARD, C. H., HADT, R. G. & TIAN, L. 2014. Copper active sites in biology. *Chemical reviews,* 114**,** 3659-3853.

SOMERVILLE, C., BAUER, S., BRININSTOOL, G., FACETTE, M., HAMANN, T., MILNE, J., OSBORNE, E., PAREDEZ, A., PERSSON, S. & RAAB, T. 2004. Toward a systems approach to understanding plant cell walls. *Science,* 306**,** 2206-2211.

SPAIN, J. C. & GIBSON, D. T. 1991. Pathway for biodegradation of p-nitrophenol in a *Moraxella* sp. *Applied and Environmental Microbiology,* 57**,** 812-819.

SPAN, E. A., SUESS, D. L., DELLER, M. C., BRITT, R. D. & MARLETTA, M. A. 2017. The role of the secondary coordination sphere in a fungal polysaccharide monooxygenase. *ACS chemical biology,* 12**,** 1095-1103.

STÅHLBERG, J., JOHANSSON, G. & PETTERSSON, G. 1991. A new model for enzymatic hydrolysis of cellulose based on the two-domain structure of cellobiohydrolase I. *Nature Biotechnology,* 9**,** 286-290

SUN, Y. & CHENG, J. 2002. Hydrolysis of lignocellulosic materials for ethanol production: a review. *Bioresource technology,* 83**,** 1-11.

SWITALA, J. & LOEWEN, P. C. 2002. Diversity of properties among catalases. *Archives of biochemistry and biophysics,* 401**,** 145-154.

TAKAHASHI, M., IMAMURA, Y. & TANAHASHI, M. Effect of acetylation on decay resistance of wood against brown rot, white rot and soft rot fungi. *International Congress of Pacific Basin Societies, Agrochemistry, Sub-Symposium on Chemical Modification of Lignocellulosic Materials–Chemical Reactions*, Hawaii, 1989.

TAN, H. T., LEE, K. T. & MOHAMED, A. R. 2011. Pretreatment of lignocellulosic palm biomass using a solvent-ionic liquid [BMIM] Cl for glucose recovery: An optimisation study using response surface methodology. *Carbohydrate polymers,* 83**,** 1862-1868.

TARKOW, H. 1945. Decay resistance of acetylated balsa. *USDA Forest service, forest products laboratory, Madison, WI.*

TOOLE, E. R. 1971. Reduction in crushing strength and weight associated with decay by rot fungi. *Wood science,* 3**,** 172-178.

VÁRNAI, A., SIIKA-AHO, M. & VIIKARI, L. 2010. Restriction of the enzymatic hydrolysis of steam-pretreated spruce by lignin and hemicellulose. *Enzyme and Microbial Technology,* 46**,** 185-193.

VÁRNAI, A., UMEZAWA, K., YOSHIDA, M. & EIJSINK, V. G. 2018. The pyrroloquinoline-quinone dependent pyranose dehydrogenase from *Coprinopsis cinerea* (CcPDH) drives lytic polysaccharide monooxygenase (LPMO) action. *Applied and environmental microbiology***,** 84 (11) e00156-18

VINCKEN, J.-P., BELDMAN, G. & VORAGEN, A. G. J. 1994. The effect of xyloglucans on the degradation of cell-wall-embedded cellulose by the combined action of cellobiohydrolase and endoglucanases from Trichoderma viride. *Plant physiology,* 104**,** 99-107.

VU, V. V., BEESON, W. T., PHILLIPS, C. M., CATE, J. H. & MARLETTA, M. A. 2014. Determinants of regioselective hydroxylation in the fungal polysaccharide monooxygenases. *Journal of the American chemical society,* 136**,** 562-565.

VAAJE-KOLSTAD, G., FORSBERG, Z., LOOSE, J. S., BISSARO, B. & EIJSINK, V. G. 2017. Structural diversity of lytic polysaccharide monooxygenases. *Current opinion in structural biology,* 44**,** 67-76.

VAAJE-KOLSTAD, G., HORN, S. J., VAN AALTEN, D. M., SYNSTAD, B. & EIJSINK, V. G. 2005a. The non-catalytic chitin-binding protein CBP21 from *Serratia marcescens* is essential for chitin degradation. *Journal of Biological Chemistry*. 280(31):28492-28497

VAAJE-KOLSTAD, G., HOUSTON, D. R., RIEMEN, A. H., EIJSINK, V. G. & VAN AALTEN, D. M. 2005b. Crystal structure and binding properties of the *Serratia marcescens* chitin-binding protein CBP21. *Journal of Biological Chemistry,* 280**,** 11313-11319.

VAAJE-KOLSTAD, G., WESTERENG, B., HORN, S. J., LIU, Z., ZHAI, H., SØRLIE, M. & EIJSINK, V. G. 2010. An oxidative enzyme boosting the enzymatic conversion of recalcitrant polysaccharides. *Science,* 330**,** 219-222.

WADA, M., IKE, M. & TOKUYASU, K. 2010. Enzymatic hydrolysis of cellulose I is greatly accelerated via its conversion to the cellulose II hydrate form. *Polymer Degradation and Stability,* 95**,** 543-548.

WALTON, P. H. & DAVIES, G. J. 2016. On the catalytic mechanisms of lytic polysaccharide monooxygenases. *Current opinion in chemical biology,* 31**,** 195-207.

WANG, B., JOHNSTON, E. M., LI, P., SHAIK, S., DAVIES, G. J., WALTON, P. H. & ROVIRA, C. 2018. QM/MM studies into the H_2O_2-dependent activity of lytic polysaccharide monooxygenases: Evidence for the formation of a caged hydroxyl radical intermediate. *ACS Catalysis,* 8**,** 1346-1351.

WANG, J., FENG, J., JIA, W., CHANG, S., LI, S. & LI, Y. 2015. Lignin engineering through laccase modification: a promising field for energy plant improvement. *Biotechnology for biofuels,* 8**,** 145.

WANG, T., YANG, H., KUBICKI, J. D. & HONG, M. 2016. Cellulose structural polymorphism in plant primary cell walls investigated by high-field 2D solid-state NMR spectroscopy and density functional theory calculations. *Biomacromolecules,* 17**,** 2210-2222.

WATERHAM, H. R., RUSSELL, K. A., DE VRIES, Y. & CREGG, J. M. 1997. Peroxisomal targeting, import, and assembly of alcohol oxidase in *Pichia pastoris*. *The Journal of cell biology,* 139**,** 1419-1431.

WEI, D., HOUTMAN, C. J., KAPICH, A. N., HUNT, C. G., CULLEN, D. & HAMMEL, K. E. 2010. Laccase and its role in production of extracellular reactive oxygen species during wood decay by the brown rot basidiomycete Postia placenta. *Applied and environmental microbiology,* 76**,** 2091-2097.

WESTERENG, B., CANNELLA, D., AGGER, J. W., JØRGENSEN, H., ANDERSEN, M. L., EIJSINK, V. G. & FELBY, C. 2015. Enzymatic cellulose oxidation is linked to lignin by long-range electron transfer. *Scientific reports,* 5**,** 18561.

WESTERENG, B., ISHIDA, T., VAAJE-KOLSTAD, G., WU, M., EIJSINK, V. G., IGARASHI, K., SAMEJIMA, M., STÅHLBERG, J., HORN, S. J. & SANDGREN, M. 2011. The putative endoglucanase PcGH61D from Phanerochaete chrysosporium is a metal-dependent oxidative enzyme that cleaves cellulose. *PloS one,* 6**,** e27807.

WESTERMARK, U. & ERIKSSON, K.-E. 1975. Purification anidul'roperties of Cellobiose: Quinone. *Acta Chemica Scandinavian B,* 29**,** 419-424.

WOOD, P. M. 1988. The potential diagram for oxygen at pH 7. *Biochemical journal,* 253**,** 287-289.

WOOD, T. M. & GARCIA-CAMPAYO, V. 1990. Enzymology of cellulose degradation. *Biodegradation,* 1**,** 147-161.

WU, M., BECKHAM, G. T., LARSSON, A. M., ISHIDA, T., KIM, S., PAYNE, C. M., HIMMEL, M. E., CROWLEY, M. F., HORN, S. J. & WESTERENG, B. 2013. Crystal structure and computational characterization of the lytic polysaccharide monooxygenase GH61D from the Basidiomycota fungus *Phanerochaete chrysosporium*. *Journal of biological chemistry***,** 288(18):12828-12839

WYMELENBERG, A. V., GASKELL, J., MOZUCH, M., SABAT, G., RALPH, J., SKYBA, O., MANSFIELD, S. D., BLANCHETTE, R. A., MARTINEZ, D. & GRIGORIEV, I. 2010. Comparative transcriptome and secretome analysis of wood decay fungi *Postia placenta* and Phanerochaete chrysosporium. *Applied and environmental microbiology,* 76**,** 3599-3610.

XU, J. & JORDAN, R. 1988. Kinetics and mechanism of the oxidation of 2,3-dihydroxybenzoic acid by iron(III). *Inorganic chemistry,* 27**,** 4563-4566.

YELLE, D. J., RALPH, J., LU, F. & HAMMEL, K. E. 2008. Evidence for cleavage of lignin by a brown rot basidiomycete. *Environmental microbiology,* 10**,** 1844-1849.

ZEPP, R. G., FAUST, B. C. & HOIGNE, J. 1992. Hydroxyl radical formation in aqueous reactions (pH 3-8) of iron (II) with hydrogen peroxide: the photo-Fenton reaction. *Environmental Science & Technology,* 26**,** 313-319.

ZHANG, J., PRESLEY, G. N., HAMMEL, K. E., RYU, J.-S., MENKE, J. R., FIGUEROA, M., HU, D., ORR, G. & SCHILLING, J. S. 2016. Localizing gene regulation reveals a staggered wood decay mechanism for the brown rot fungus *Postia placenta*. *Proceedings of the national academy of sciences USA,* 113**,** 10968-10973.

ZHANG, J. & SCHILLING, J. S. 2017. Role of carbon source in the shift from oxidative to hydrolytic wood decomposition by Postia placenta. *Fungal genetics and biology,* 106**,** 1-8.

ZHANG, T., KUMAR, R. & WYMAN, C. E. 2013. Sugar yields from dilute oxalic acid pretreatment of maple wood compared to those with other dilute acids and hot water. *Carbohydrate polymers,* 92**,** 334-344.

ZHANG, X.-Z., SATHITSUKSANOH, N. & ZHANG, Y.-H. 2010. Glycoside hydrolase family 9 processive endoglucanase from *Clostridium phytofermentans*: heterologous expression, characterization, and synergy with family 48 cellobiohydrolase. *Bioresource technology,* 101**,** 5534-5538.

ZHAO, X., ZHANG, L. & LIU, D. 2012. Biomass recalcitrance. Part I: the chemical compositions and physical structures affecting the enzymatic hydrolysis of lignocellulose. *Biofuels, bioproducts and biorefining,* 6**,** 465-482.

ZHU, J. Y., PAN, X. & ZALESNY, R. S. 2010. Pretreatment of woody biomass for biofuel production: energy efficiency, technologies, and recalcitrance. *Applied microbiology and biotechnology,* 87**,** 847-857.

ZHU, Y., ZHUANG, L., GOODELL, B., CAO, J. & MAHANEY, J. 2016. Iron sequestration in brown-rot fungi by oxalate and the production of reactive oxygen species (ROS). *International biodeterioration & biodegradation,* 109**,** 185-190.

Paper I

Challenges and opportunities in mimicking non-enzymatic brown-rot decay mechanisms for pretreatment of Norway spruce

Olav Aaseth Hegnar[1,2], Barry Goodell[3], Claus Felby[4], Lars Johansson[5], Nicole Labbé[6], Keonhee Kim[6], Vincent G. H. Eijsink[2], Gry Alfredsen[1], Anikó Várnai[2]

Norwegian Institute for Bioeconomy Research, Department of Wood Technology, PO Box 115, 1431 Ås, Norway. [1]

Faculty of Chemistry, Biotechnology and Food Science, Norwegian University of Life Sciences, Campus Ås, Chr. Magnus Falsensvei 1, 1432 Ås, Norway [2]

Microbiology, University of Massachusetts, 313 Stockbridge/220 Morrill 80 Campus Center Way/627 N Pleasant ST Ahmerst, MA 01003-9292, USA [3]

Department of Geosciences and Nature Resource Management, University of Copenhagen, Rolighedsvej 23, Fredriksberg, Denmark [4]

RISE PFI AS, Høgskoleringen 6B, 7034 Trondheim, Norway [5]

Center for Renewable Carbon, The University of Tennessee, 2506 Jacob Drive, Knoxville, TN 67996-4570, USA [6]

Correspondence: Phone: +47 472 39 162, email: olav.aaseth.hegnar@nibio.no

Abstract

The recalcitrance bottleneck of lignocellulosic materials presents a major challenge for biorefineries, including 2nd generation biofuel production. Because of their abundance in the Northern hemisphere, softwoods, such as Norway spruce, are of major interest as a potential feedstock for biorefineries. In nature, softwoods are primarily degraded by Basidiomycetous fungi causing brown-rot. These fungi employ a non-enzymatic oxidative system to depolymerize wood cell wall components prior to depolymerization by a limited set of hydrolytic and oxidative enzymes. Here we show that Norway spruce pretreated with two species of brown-rot fungi yielded more than 250% increases in glucose release when treated with a commercial enzyme cocktail, and that there is a good correlation between mass loss and the degree of digestibility. We performed a series of experiments that aimed at mimicking the brown-rot pretreatment, using a modified version of the Fenton reaction. We showed a small increase in digestibility after pretreatment where the aim was to generate reactive oxygen species within the wood cell wall matrix. Further experiments were performed to assess the possibility of performing pretreatment and saccharification in a single system, and the results indicated the need for a complete separation of oxidative pretreatment and saccharification. A more severe pretreatment was also completed, which interestingly did not yield a more digestible material. We conclude that a biomimicking approach to pretreatment of softwoods using brown-rot fungal mechanisms is possible, but that there are additional factors of the system that need to be known and optimized before serious advances can be made to compete with already existing pretreatment methods.

1 Introduction

The recalcitrance of lignocellulosic biomass presents a major challenge for modern biorefineries, which depend on efficient enzymatic conversion of cellulose to glucose (Himmel et al. 2007; Pedersen and Meyer 2010; Zhao et al. 2012). The major components of lignocellulosic materials (cellulose, hemicelluloses and lignin) are linked together in a complex network, making plant biomass highly resistant to enzymatic hydrolysis. Industrially, some form of pretreatment is thus necessary before efficient saccharification can be achieved. In nature, woody lignocellulosic biomass is mainly degraded by basidiomycetous fungi in two polyphyletic groups, generally characterized as white- or brown-rot fungi. White-rot fungi are able to fully degrade cellulose, hemicelluloses and lignin, using a battery of enzymes that act upon the polysaccharides (e.g. endo- and exo-acting cellulases and hemicellulases and lytic polysaccharide monooxygenases) and lignin (e.g. lignin peroxidases, manganese peroxidases and laccases). Brown-rot fungi remove the polysaccharides and extensively depolymerize and modify lignin before rapidly repolymerizing it (Filley et al. 2002, Yelle et al. 2008), however, compared to white-rot fungi only few enzymes are associated with this process (Eastwood et al. 2011; Riley et al. 2014).

The main classes of enzymes acting on cellulose in basidiomycetes are endoglucanases belonging to the GH5 and GH12 families, cellobiohydrolases belonging to families GH6 and GH7 and lytic polysaccharide monooxygenases (LPMOs) belonging to the family AA9 (as classified in the Carbohydrate-Active enZYmes database CAZy (Floudas et al. 2012; Lombard et al. 2013). Hemicellulose active enzymes also play an important role in the repertoire of these fungi; some species have several dozens of genes encoding mannanases, xylanases, arabinases, glucuronidases. Furthermore, some endoglucanases and AA9 LPMOs possess hemicellulolytic activity (Vlasenko et al. 2010, Agger et al. 2014), whereas xylanolytic AA14 LPMOs also occur (Couturier et al. 2018). These cellulases and hemicellulases can be either monomodular or multimodular enzymes and may include non-catalytic binding domains referred to as carbohydrate binding modules (CBMs) (Baldrian and Valášková 2008). Cellulases and hemicellulases, which are generally larger than 50 Å in diameter, are thought to be too large to penetrate the native wood cell wall, where porosity is low. In brown rot fungi, this problem is thought to be circumvented by the production of low molecular weight compounds that can penetrate the wood cell wall and generate highly reactive radical oxygen species (ROS), to depolymerize the polysaccharides and lignin therein, and increase porosity. ROS can be generated both enzymatically (e.g. peroxidases)

and non-enzymatically through Fenton-like reactions (Evans et al. 1991; Flournoy et al. 1991). While white-rot fungal genomes generally contain a large number of genes involved in the depolymerization of cellulose and lignin, brown-rot fungal genomes are surprisingly sparse in comparison (Floudas et al. 2012). Several brown-rot species, like the model species *Rhodonia placenta* and *Gloeophyllum trabeum*, completely lack GH6, GH7, CBM1 (a well-known cellulose-binding CBM) and peroxidase genes. Brown rot fungi have only retained a few GH5s, GH12s and AA9s, yet are perfectly capable of depolymerizing and degrading the polysaccharides of the wood cell wall (Eastwood et al. 2011; Floudas et al. 2012; Martinez et al. 2009; Riley et al. 2014).

The currently accepted paradigm behind the efficiency of wood decay by brown-rot fungi is that they employ a non-enzymatic system for wood cell wall depolymerization that uses iron, oxalic acid and iron-chelating/reducing secondary metabolites (Xu and Goodell 2001). This system is referred to as the chelator mediated Fenton (CMF) system. The CMF system entails that the fungus chelates iron from the environment and produces reducing compounds as well as hydrogen peroxide, eventually leading to the generation of hydroxyl radicals through the Fenton reaction mechanism ($Fe^{(II)}+H_2O_2 \rightarrow {}^{\bullet}OH+{}^{-}OH+Fe^{(III)}$) within the wood cell wall, away from the fungus. The fungus alters its local environment by secreting large amounts of oxalic acid, lowering the pH around the hyphae to around 2 while the natural pH of the wood cell wall is approximately 5-6. These high concentrations of oxalic acid are able to chelate iron (Fe^{3+}) from iron-oxide complexes and from the wood. As a consequence of the pH and concentration gradients generated by the high concentration of oxalic acid, the iron is not reduced in the immediate environment of the fungus. However, once the iron-oxalate complexes diffuse into the higher pH environment of the wood cell wall, iron-reducing compounds produced by the fungus such as 2,5-dimethoxyhydroquinone (2,5-DMHQ) will reduce and solubilize the iron (Arantes et al. 2009). Once reduced within the wood cell wall, the iron is able to react with hydrogen peroxide, thereby to generating ROS (Arantes et al. 2012).

There are several potential sources for hydrogen peroxide. The genomes of brown rot fungi suggest the presence of a number of auxiliary activity enzymes that are known to generate H_2O_2. Among these are AA3 GMC oxidoreductases, AA5 copper radical oxidases and AA7 gluco-oligosaccharide oxidases, all of which have been suggested to generate H_2O_2, necessary for Fenton reactions (Floudas et al. 2012; Levasseur et al. 2013). AA6 1,4-benzoquinone reductases are most likely involved in the regeneration/reduction of

catecholate and hydroquinone chelators, and are highly expressed during the early stages of brown-rot fungal decay (Floudas et al. 2012; Jensen Jr et al. 2002). Notably, catecholate compounds can generate hydrogen peroxide in the presence of transition metals, by reducing molecular oxygen. Brown-rot fungi produce several catecholate secondary metabolites, which can obviously penetrate the wood cell wall where they can participate in several of the steps needed for Fenton chemistry to take place (Paszczynski et al. 1999).

It is well established that H_2O_2-derived ROS are damaging to enzymes (Prousek 2007), thus the brown-rot fungi have evolved into a system to spatially segregate enzymatic saccharification from the CMF system (Arantes and Goodell 2014). Genes involved in oxidative deconstruction of the wood cell wall, including genes related to hydrogen peroxide production, oxalic acid production and secondary metabolite production, are expressed at the hyphal front, in the early stages of decay, while genes encoding lignocellulose-depolymerizing enzymes are expressed in later stages, in older hyphae (Presley and Schilling 2017; Zhang et al. 2016). It has been reported for more than 50 years that brown-rot fungi cause considerable loss in the mechanical strength of sound wood before any significant mass loss is detected and this is thought to be due to oxidative depolymerization of wood cell wall polysaccharides (Cowling 1961; Curling et al. 2002; Green and Highley 1997). Recent findings by Zhang et al. (2016) and Presley and Schilling (2017) agree well with a model where the fungus uses an oxidative system to prepare the wood for later action by depolymerizing enzymes.

The goal of the present study was to assess whether a modified Fenton-type pretreatment of wood could improve enzymatic digestibility. Norway spruce (*Picea* abies) was chosen as the substrate because it is abundant in northern Eurasia and the preferred substrate of brown-rot fungi. Furthermore, softwoods, such as Norway spruce, are generally considered the most recalcitrant type of lignocellulosic biomass. In commercial biorefineries, pretreatment of lignocellulosic material is necessary before saccharification to loosen up the structural framework of the plant cell wall, making the polysaccharides more accessible to the various cell wall degrading enzymes (Zhao et al. 2012). The most common pretreatment methods, including steam explosion, acid treatment and alkaline treatment rely on extreme conditions, such as high temperature, extreme pH and high pressures. As a consequence these methods are costly and generate byproducts that can act as inhibitors in the downstream saccharification and fermentation steps (Palmqvist and Hahn-Hägerdal 2000). Fenton chemistry has previously been shown to increase saccharification yields for less recalcitrant

biomasses such as grasses, but no work has so far been published for softwoods (He et al. 2015; Kato et al. 2014; Michalska et al. 2012). Previous studies have shown that pretreatment of wood with brown-rot fungi can increase saccharification yields, but to our knowledge no studies have been published on fungal pretreatment of Norway spruce performed in this manner (Lee et al. 2008; Ray et al. 2010).

The work presented here was set out to identify a mild, site-directed pretreatment for softwoods that is inspired by the biomass-degrading mechanism thought to be present in brown-rot fungi, the primarily degraders of softwoods in the northern hemisphere. We performed a mild, modified Fenton (MF) treatment, attempting to mimic the CMF system used by brown-rot fungi, to pretreat Norway spruce wood. The effect of the MF treatment on cellulose accessibility was assessed and quantified by monitoring saccharification yields upon incubation of the pretreated wood with a commercial enzyme cocktail. As a reference, Norway spruce at various stages of brown rot decay was subjected to saccharification using a commercially available enzyme cocktail under the same conditions.

2 Materials and methods

2.1 Preparation of wood material

Boards from a single Norway spruce (*Picea abies*) tree were used in all experiments. The composition of cellulose, hemicelluloses and lignin was determined according to NREL/TP-510-42618 (Sluiter et al. 2008), by RISE PFI, Trondheim. The wood was dried in room temperature and milled using a hammer mill (Shutte Buffalo W-6-H) operated at 4500 rpm and using a 2 mm screen outlet. The hammer mill was cooled with liquid nitrogen to avoid heating of the material during size reduction. After milling, the powdered wood was dry fractionated by particle size using a laboratory screen system and the fraction with a particle size of 0.4-0.5 mm was used for all experiments.

2.2 Fungal pretreatment

Brown-rot fungi *Rhodonia* (previously *Postia*) *placenta* MAD 698-R and *Gloeophyllum trabeum* BAM Ebw. 109 were pre-grown on malt agar plates (1.5 g/l) until hyphae covered the entire Petri dish (7 days). The hyphae from five plates were then removed by adding 15 ml distilled deionized water directly to the plate and carefully loosening the hyphae with a triangle glass spatula without disturbing the solid medium. The resulting suspension was decanted into a sterile glass flask, after which a cell suspension was generated by mixing using a pipette. 7.5 ml of this suspension was used to inoculate 1.5 g (dry weight) milled, autoclaved Norway spruce wood (0.4-0.5 mm) and incubated in a 50 ml Falcon tube. Initial dry weight was calculated by drying sub-samples of the same material at 103 °C for 24 h. For each fungus, six replicates were made for each harvesting time point (18, 35 and 46 days), meaning that there were 18 samples per fungus. The samples were incubated at 25 °C and 70% relative humidity. Three samples from each harvesting point were used to assess mass loss, while the remaining three were used for enzymatic digestion. At the harvesting point, the fungus was killed by incubating the samples in a water bath at 95 °C for 15 min, after which the samples were frozen at -30 °C until further processing. To determine total mass loss, the samples were dried at 103 °C for 24 h. To avoid drying the samples that were to be used for enzymatic digestion, a small sub sample was taken from each sample and dried at 103 °C for 24 h to assess moisture content. For saccharification, 250 mg (dry weight) wood at various stages of decay were suspended in 15 ml Na-acetate buffer (50 mM, pH 5.0). Sodium azide (final concentration 0.01%) was added to inhibit microbial growth. Cellic CTec2 (Novozymes A/S, Bagsværd, Denmark) was loaded to a final concentration of 3% (w/w)

enzyme solution per dry substrate, and the reaction mixtures were incubated in an Infors Minitron shaking incubator (Infors, Bottmingen, Switzerland) at 50 °C and 120 rpm for 120 h, with 50 µl aliquots being taken at 0, 3, 6, 24 and 120 h. The aliquots were incubated for 5 min in boiling water to terminate enzyme activity and then stored at -30 °C until further processing. For all experiments, wood powder (0.4-0.5 mm) that had not been subjected to fungal decay were used as control.

2.3 Iron binding capacity

The iron binding capacity of the milled spruce wood (0.4-0.5 mm) was determined by soaking 400 mg wood in 20 ml buffer solutions (2% w/v) containing 0.36 mM $FeCl_3 \cdot 6H_2O$ for 1 h at ambient temperature. Four different pHs were tested: 2.0, 3.6, 4.5 and 5.5. For pH 2.0, a 200 mM HCl-KCl buffer was used. For all other pH ranges, Na-acetate buffer was used with three different molarities: 10, 20 and 50 mM, respectively. Solutions without any wood added were used as control. Following the incubation, the samples were centrifuged at 3000 *g* for 15 min and 1.5 ml of liquid was removed for measuring the iron content using Inductively Coupled Plasma Mass Spectrometry (Ogner et al. 1999). The difference in iron concentration in the samples and the control (same conditions, but without wood) was used to calculate the iron bound to the wood. All experiments were done in triplicate.

2.4 Mild chelator-assisted Fenton (MF) treatment and saccharification with intermediate washing step

0.5 g milled Norway spruce wood was suspended in 10 ml 20 mM Na-acetate buffer pH 4.0 (5% w/v). Then $FeCl_3 \cdot 6H_2O$ was added to final concentrations of 0.25 mM, 0.5 mM or 1 mM (0.279, 0.558 and 1.116 mg Fe^{3+}/g wood), followed by incubation for 1 h at room temperature without mixing. Then, 2,3-dihydroxybenzoic acid (2,3-DHBA) was added to each reaction to the same final molar concentration as the originally added Fe^{3+}, to reduce the iron bound to the wood. Immediately afterwards, H_2O_2 was added to final concentrations of 2.5 mM, 5 mM and 10 mM respectively, bringing the final reagent molar ratio to 1:1:10 ($FeCl_3$:2,3-DHBA:H_2O_2). The reaction mixtures were incubated in an Infors Minitron shaking incubator at 25 °C for 24 h. The solid fractions were then washed free of the reagents in multiple rounds of centrifugation (at 3220 *g*, 20 min) using 50 ml 100 mM oxalic acid (2X) and 50 ml distilled water (4X). Subsequently, the MF treated wood (without drying) was suspended in 20 mM Na-acetate buffer (pH 5.0) to a 50 ml total volume. Saccharification reactions were carried out as described above in section 2.2 using Cellic CTec2 at a loading

of 60 mg enzyme solution per gram cellulose (6%, w/w) for 96 h. For the control, all MF reagents were replaced with buffer. All experiments were carried out in triplicate.

2.5 Fenton or MF treatment and saccharification with no washing

290 mg crystalline cellulose (Avicel, from Fluka Chemie GmbH, Buchs, Switzerland) or 750 mg milled Norway spruce (0.4-0.5 mm; corresponding to approx. 290 mg cellulose) were suspended in 12.5 ml 50 mM Na-acetate buffer (pH 4.5) and treated with either MF reagents ($FeCl_3$, 2,3-DHBA and H_2O_2) or Fenton reagents ($FeSO_4$ and H_2O_2). For MF treatment, the following concentrations were used: 0.54 mM $FeCl_3$, 0.54 mM 2,3-DHBA and 5.4 mM, 10.8 mM or 16.2 mM H_2O_2 (giving reagent ratios of 1:1:10, 1:1:20 and 1:1:30). For Fenton treatment, the following concentrations were used: 0.54 mM $FeSO_4$ and 5.4 mM, 10.8 mM or 16.2 mM H_2O_2 (giving reagent ratios of 1:10, 1:20 and 1:30). For both treatment types, the wood was incubated for 1 h with iron before the addition of the remaining reagents. All reactions were incubated in an Infors Minitron shaking incubator for 3 h at 50 °C. After 3 h, the hydrogen peroxide content was measured using Quantofix Peroxide 100 strips from Macherey-Nagels (Düren, Germany), confirming that H_2O_2 levels had dropped to below 30 µM in the 1:1.10 MF reaction. Before saccharification, reaction mixtures were diluted twofold, to a total of 25 ml, by adding 50 mM Na-acetate buffer (pH 4.5) and Cellic CTec2 (20 mg enzyme solution per g cellulose; 2%, w/w). The saccharification reactions were incubated in the shaking incubator at 50 °C for an additional 120 h; samples were taken at 0, 3, 6, 12, 24 and 120 h and treated as described above. All experiments were done in triplicate.

To investigate the inhibitory effect of MF reagents on the cellulase cocktail, the following control reactions were performed with cellulose. 200 mg crystalline cellulose (Avicel) were suspended in 10 ml Na-acetate buffer (50 mM, pH 4.5 or pH 5.0) containing various combinations of 0.54 mM $FeCl_3 \cdot 6H_2O$, 0.54 mM 2,3-DHBA and/or 5.4 mM H_2O_2, followed by incubation for 3 h at 50 °C and 120 rpm. Seven combinations of reagents were used, as follows: 1) $FeCl_3$+2,3-DHBA, 2) 2,3-DHBA+H_2O_2, 3) $FeCl_3$+H_2O_2, 4) $FeCl_3$, 5) 2,3-DHBA, 6) H_2O_2 and 7) no reagents, buffer only. After this incubation, Cellic CTec2 was added to the reaction mixtures to a final concentration of 0.5% enzyme solution per gram substrate. The reactions were then incubated under the same conditions as above, and samples were taken at 0, 3, 6, 24 and 120 h. Samples were boiled for 5 min to inactivate enzyme activity and then stored frozen at -30 °C until further processing. All experiments were carried out in triplicate.

2.6 Severe MF treatment

One gram of milled Norway spruce wood (0.4-0.5 mm) was suspended in 20 ml 1 M Na-acetate buffer pH 4.0 in a 50 ml Falcon tube. Then $FeCl_3 \cdot 6H_2O$ was added to a final concentration of 10 mM, followed by the addition of 2,3-DHBA to a final concentration of 10 mM. Finally, hydrogen peroxide was added to a final concentration of either 200 or 300 mM (reagent ratios of 1:1:20 and 1:1:30). The reaction mixtures were then incubated for 72, 96 and 168 h at room temperature without shaking. At harvesting, the wood material was washed using centrifugation at 3220 *g* for 15 min, once with 50 ml 100 mM oxalic acid and twice with 50 ml distilled H_2O before being stored at -30 °C until further processing. For saccharification, the material was suspended in 40 ml 50 mM Na-acetate buffer (pH 5.0), and Cellic CTec2 was added to a final concentration of 40 mg enzyme solution per g substrate (4%, w/w). The reactions were incubated in an Infors Minitron shaking incubator at 50 °C at 120 rpm. Samples were taken after 0, 6, 24 and 120 h and treated as described above. Untreated wood was used as control; this wood was subjected to the same procedure in which the CMF reagents were substituted with distilled H_2O. All experiments were carried out in triplicate.

2.7 Compositional analysis of wood samples

Boards from single Norway spruce tree were used as substrate for all experiments in this work. The polysaccharide, lignin and monosaccharide composition of the top and butt of the tree was performed according to NREL/TP-510-42618 (Tables 1 & 2). The monosaccharide composition of the milled wood decayed by brown-rot fungi was analyzed according to the NREL/TP-510-42618, "Determination of Structural Carbohydrates and Lignin in Biomass" procedure (Table 3). High Pressure Liquid Chromatography (HPLC) was employed to quantify structural monomeric forms of sugars after a two-step acid hydrolysis. The HPLC system was equipped with an Aminex HPX-87P column (BIORAD, 300 nm × 7.8 nm, 9 µm particle size) attached to a micro-guard Carbo-P guard column (BIORAD), and a refractive index detector (Perkin Elmer). The RI detector temperature was 50 °C and the oven temperature 85 °C. The injection volume was 30 µl with 0.25 ml/min of flow rate. Acetyl content was measured with an Aminex HPX-87H column (BIORAD, 300 nm × 7.8 nm, 9 µm particle size) with micro-guard cation H refill cartridges attached. The RI detector temperature was set at 50 °C and the oven 45 °C. Acid insoluble lignin was measured gravimetrically and acid soluble lignin was determined by UV/VIS spectrometry. Ash

content was quantified by combusting the samples (0.2 – 0.3 g) in a furnace at 575 °C for 24 h (Fisher Scientific Isotemp Programmable Muffle Furnace 750).

2.8 Evaluation of saccharification experiments

To determine saccharification yields, glucose content was analyzed with High Performance Liquid Chromatography (HPLC) using an Agilent 1100 Series instrument (Santa Clara, USA) equipped with an HP-X87H column (BioRad, Hercules, USA) and a Shimadzu Refractory Index detector (Kyoto, Japan). The mobile phase was 20 mM H_2SO_4, isocratic flow rate was 0.5 ml/min, temperature was 50 °C and the run time was 22 min per sample. The integrals of the peaks for a series of samples with known glucose concentration were used to generate a standard curve.

The cellulose-to-glucose conversion yield was calculated from the glucose concentrations as percentage according to the following method. First, the background glucose concentration (at time 0, after adding Cellic CTec2) was subtracted from the glucose concentration measured at each time point to correct for any background signal coming from the substrate or the enzyme cocktail. Then the conversion yield was calculated according to the following equation:

$Conversion(\%) = \frac{Corrected\ glucose(^g/_l)}{Cellulose(^g/_l)} \cdot 0.9 \cdot 100\%$, where 0.9 is the factor needed to correct for the hydrolytic gain.

3 Results and discussion

3.1 Fungal treatment

To generate a reference point resembling natural brown rot, we pretreated milled spruce wood with two brown-rot strains, *R. placenta* MAD 698-R and *G. trabeum* BAM Ebw. 109, before killing the fungus and saccharifying the wood with the commercial cellulase cocktail Cellic CTec2 from Novozymes. This engineered enzyme cocktail contains powerful cellulases, high levels of β-glucosidases and a number of hemicellulases and has been shown to be very successful in releasing sugars from pretreated lignocellulosic materials (Chen et al. 2013, Rodriguez et al. 2015, Ko et al. 2015). Treating milled wood with brown-rot fungi for 18, 35 and 46 days led to mass loss averages of 7.4%, 10.3% and 12.5% with *G. trabeum* and 3.7%, 8.3% and 14.5% with *R. placenta*, respectively (Figure 1). As it has been previously observed during brown-rot decay (Curling et al. 2002; Kirk and Highley 1973), there was a preferential removal of hemicelluloses (>50% of the initial amount of mannan and >20% of the initial amount of xylan removed after 45 days; Table 3 and Figure 10 in the supplement), while no lignin removal was observed. Our Norway spruce substrate was rich in galactoglucomannan (GGM) (Table 1 in the supplement), and therefore the modest removal of glucan observed during fungal decay could partially be accounted for removal of GGM.

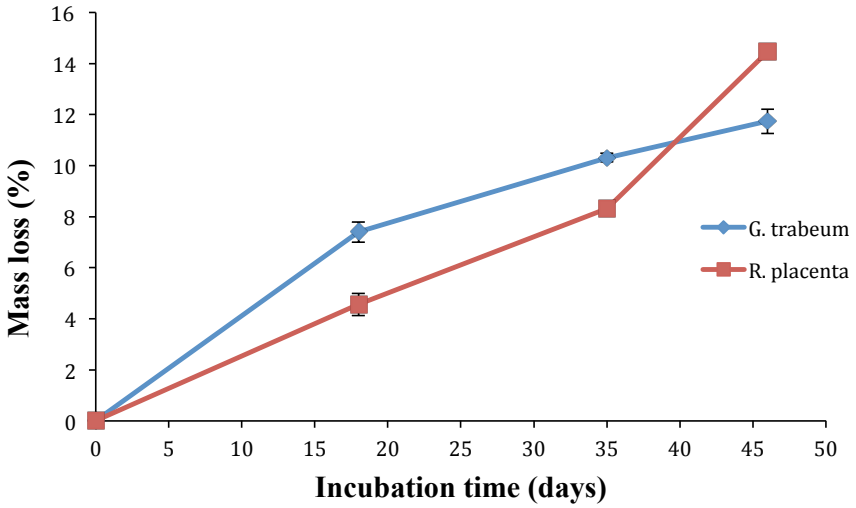

Fig. 1 Mass loss of milled Norway spruce during brown rot. Milled Norway spruce (0.4-0.5 mm) was decayed with brown rot species *Rhodonia placenta* and *Gloeophyllum trabeum*. Samples were incubated at 25 °C and 70% relative humidity. Experiments were carried out in triplicate; the error bars represent standard deviations.

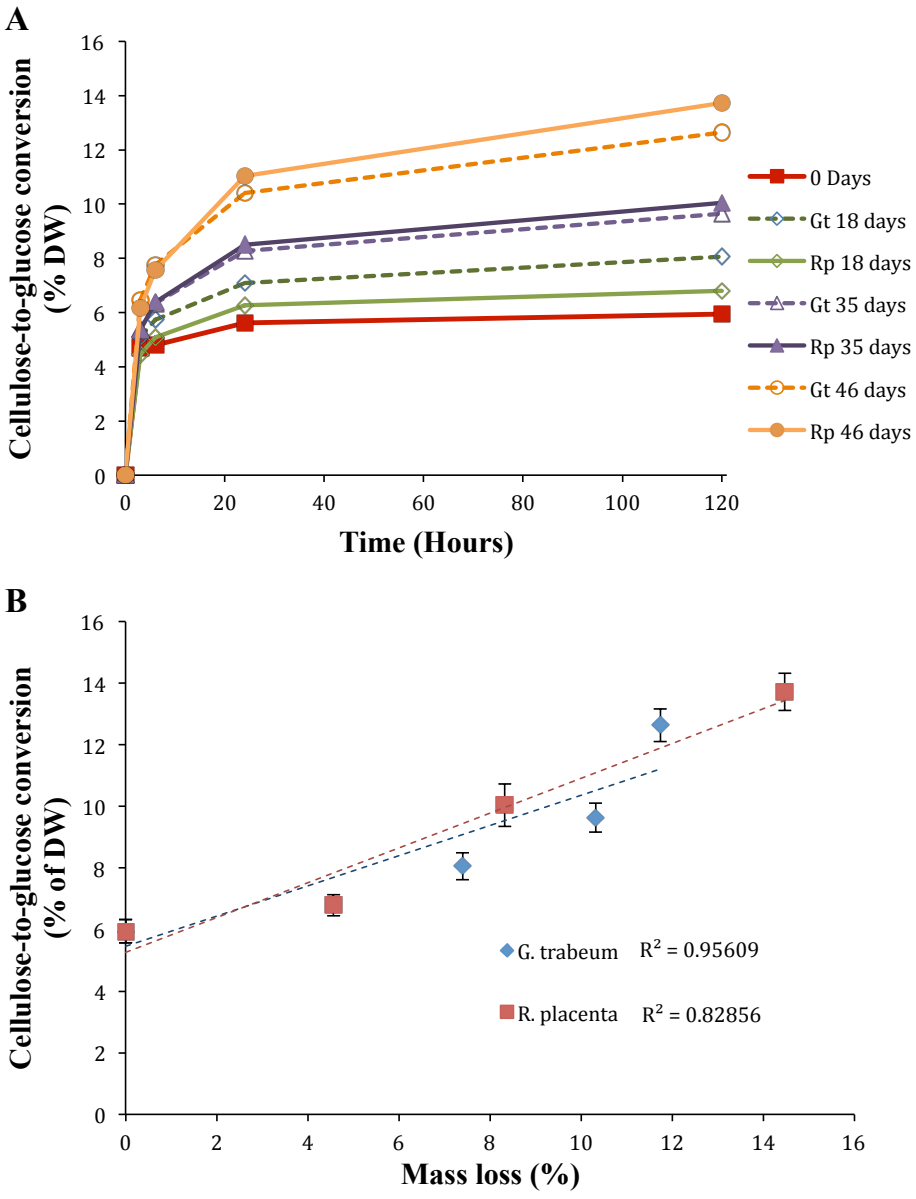

Fig. 2 Enzymatic saccharification of brown-rotted Norway spruce with Cellic CTec2. Norway spruce samples that had been degraded by *G. trabeum* (Gt) and *R. placenta* (Rp) (from Figure 1) were treated with Cellic CTec2 (3% (w/w) enzyme solution per dry substrate) at 50 °C. Panel (A) shows the glucose release over time; panel (B) shows the correlation between glucose release and mass loss. Experiments were carried out in triplicate; the error bars represent standard deviations.

Figure 2 shows that the fungal treatments led to increased glucose release during subsequent enzymatic solubilization reactions with Cellic CTec2 (Figure 2). Longer incubation times with the fungi, leading to higher mass loss, generated higher glucose yields (Figure 2A). The

highest yield was observed in the 46-day *R. placenta* samples, which gave 2.3-fold more glucose, compared to the non-treated control. Overall, there was a good correlation between the increase in glucose release relative to the control sample and the mass loss of wood samples during decay by the two fungal species (Figure 2B).

3.2 Iron-binding capacity and mild MF pre-treatment

An aim of this study was to carry out a mild CMF-type mimicking pretreatment of the wood (Modified Fenton, MF). It was hypothesized that minimizing the concentration of MF reagents is crucial for performing a brown rot-like pretreatment at conditions that are close to the natural conditions. Ideally, using iron levels equaling the iron-binding capacity of wood would leave almost no free iron in solution, allowing *in situ* generation of the short-lived radicals generated by the Fenton reaction within the wood cell wall matrix, while minimizing similar reactions outside the matrix. Since it has previously been established that ferrous iron (Fe^{2+}) binds very poorly to wood (Arantes et al. 2009), only ferric iron (Fe^{3+}) was tested. We determined the iron binding capacity of the milled Norway spruce by incubating it (2% w/v) with $FeCl_3$ (0.36 mM) in buffer solutions at pH 2.0, 3.6, 4.5 and 5.5 for 1 h. The iron concentration was measured in the liquid fractions before and after incubation to calculate iron bound to the wood. Figure 3 shows that the iron binding capacity of milled Norway spruce (0.4-0.5 mm) increased with pH, whereas increasing the buffer strength decreased the iron binding capacity. The latter phenomenon is likely due to chelation and precipitation of Fe(III) by acetate ions.

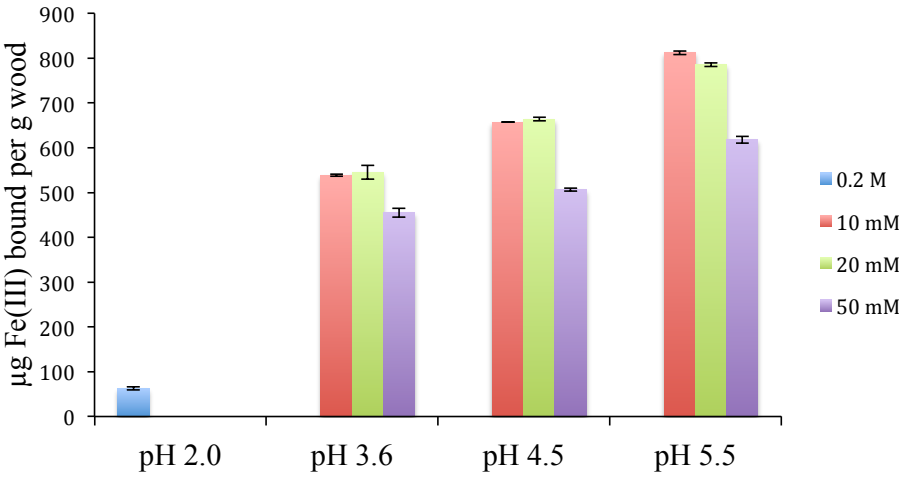

Fig. 3 The ferric iron-binding capacity of milled Norway spruce (fraction size 0.4-0.5 mm). Binding capacity was measured by incubating wood samples (2% w/v) with 0.36 mM $FeCl_3$ in buffered solutions. The iron concentration was measured in the liquid fraction before and after incubation to calculate iron bound to the wood. pH 2.0 was achieved using a 0.2 M 'HCl-KCl buffer, whereas the other reactions contained acetate buffer at three different molarities (10, 20 and 50 mM). Experiments were carried out in triplicate; the error bars represent standard deviations.

As it is well established that the generation of radicals through Fenton and Fenton-like reactions is most efficient at slightly acidic conditions (Hug and Leupin 2003), pH values close to 4.0 were used in the MF experiments. The amount of iron that was used in the subsequent MF experiments was below (0.25 mM), at (0.5 mM) and above (1 mM) the expected total binding capacity of the wood at pH 4.0 (approx. 550 µg Fe(III)/g wood at pH 3.6 in 20 mM Na-acetate; Figure 3). This iron was reduced with the biomimicking chelator/reductant 2,3-dihydroxy benzoic acid (2,3-DHBA), which was added in equimolar amounts relative to $FeCl_3$, before finally adding a 10-, 20-, or 50-fold molar excess of hydrogen peroxide. The samples were washed free of iron as described in the methods before saccharification. Released soluble sugars in the wash liquid after pretreatment were below detectable levels, corresponding with the observation that mass loss during the MF treatment was negligible.

Figure 4 shows that the MF treatment (performed with a consecutive washing step) only had minor effects on the efficiency of subsequent saccharification reactions of with Cellic CTec2 and suggests a dependency on the iron level used. It is possible that some iron is not in direct association with the wood cell wall, but in solution within wood cell wall lumens. If that

occurs, it will decrease the efficiency of the MF treatment since H_2O_2 will react with reduced iron away from the wood cell wall. Increasing iron concentration up to the calculated saturation level (0.5 mM or 558 µg Fe^{3+} per gram wood; see Fig. 3) had a positive effect on the saccharification yield which augmented from 7.3% to 9.6% (Student's t-test p=0.0305). A further increase in the iron concentration (i.e. up to twice the saturation level) had a negative impact on the saccharification yield, which could, for example, be due to reactions between hydrogen peroxide and the surplus iron that is in solution. The increase in sugar yield after MF treatment was much smaller than the increases observed following pretreatment with the two brown-rot fungal species (Fig. 2). Notably, the mass loss after the MF treatment was very low (<1%; data not shown) compared to after fungal pretreatment, suggesting that considerable removal of wood components is necessary to achieve a boost in saccharification yields.

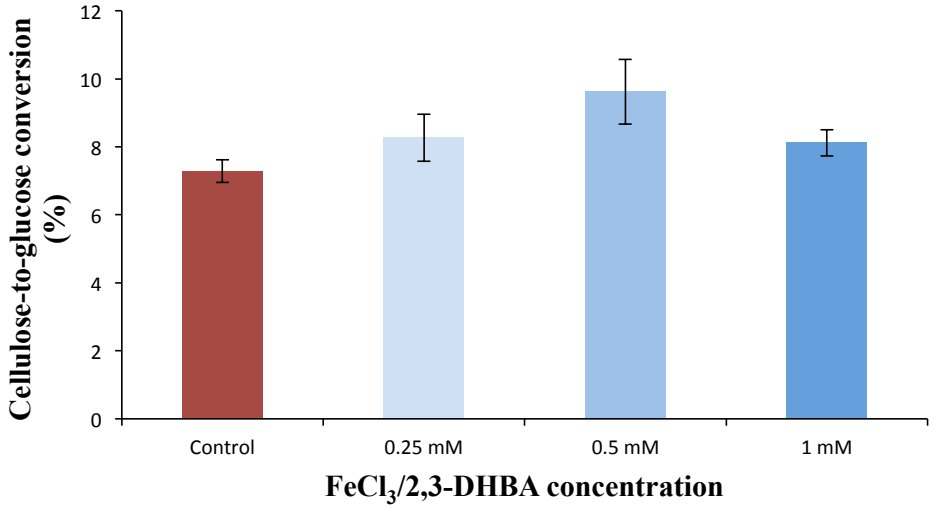

Fig. 4 Effect of mild *in situ* modified Fenton (MF) treatment on saccharification of milled Norway spruce (0.4-0.5 mm). The bars show glucose release after 96 hours after incubation with Cellic CTec2 (3% (w/w) enzyme solution per dry substrate) at 50 °C. The hydrogen peroxide concentration was 10 times that of $FeCl_3$ and 2,3-DHBA in all reactions. The MF treatments were carried out over night with shaking at room temperature, and all samples were washed before saccharification. Experiments were carried out in triplicate; the error bars represent standard deviations.

3.3 Enzymatic saccharification after Fenton-type pretreatments, without washing

In another approach, and in contrast to the experiments in the previous section, we avoided washing following the MF treatment, which is technically simpler and thus more industrially relevant and avoids loss of material that is solubilized during treatment. For comparison, both regular Fenton and MF reactions were performed on both milled Norway spruce (0.4-0.5 mm; Figure 5) and crystalline cellulose (Avicel; Figure 6). The concentrations of $FeCl_3$/2,3-DHBA and $FeSO_4$ were kept at 0.54 mM, corresponding to the iron saturation level, while the H_2O_2 concentration was 5.4 mM, 10.8 mM or 16.4 mM, equaling 10, 20, or 30 times the iron concentration, respectively. The pretreatments were performed at pH 4.5, a compromise between the slightly acidic pH needed for the pretreatment and the pH optimum of the enzyme preparation (pH 5.0), and the resulting materials were not washed. As high levels of H_2O_2 remaining from the pretreatment step could be detrimental to the enzymes, H_2O_2 concentration was measured after the pretreatment. Analysis showed values of less than 1 mg/L (30 μM) for the 1:1:10 MF reagent ratio treatments, whereas H_2O_2 concentrations of higher than 1 mg/L were measured for the 1:1:20 and 1:1:30 reactions. For the Fenton reactions, the H_2O_2 concentrations remained above 1 mg/L in all reactions after 3 h. The soluble sugars in solution after the MF treatment (but before saccharification) was below detection limits on both wood and cellulose. Subsequent saccharification reactions, performed without washing the pretreated substrate, showed that both MF and Fenton treatments had an overall negative impact on saccharification efficiency, which was stronger at higher H_2O_2 concentration levels and much more pronounced for Avicel (Figure 6) than for spruce wood (Figure 5).

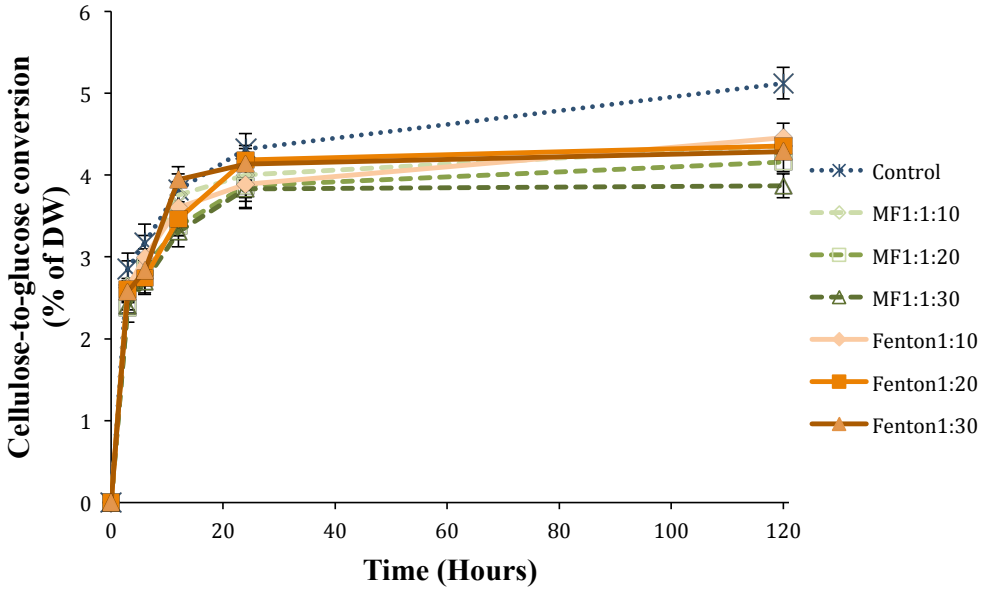

Fig. 5 Glucose release by Cellic CTec2 from milled Norway spruce subjected to MF and Fenton treatment at different H_2O_2 levels. In the pretreatment step, $FeSO_4$/$FeCl_3$ and 2,3-DHBA concentrations were 0.54 mM in all reactions; the $FeSO_4$:H_2O_2 ratios for Fenton and $FeCl_3$:2,3-DHBA:H_2O_2 ratios for MF are indicated in the legend. Saccharification was performed in the same buffer (50 mM Na-acetate buffer pH 4.5) without prior washing of the material. For the control, reagents were replaced with pure buffer. Experiments were carried out in triplicate; the error bars represent standard deviations.

Both MF and Fenton treatments had a larger negative impact on saccharification of Avicel compared with spruce wood, which is likely due to the major compositional differences between the two substrates. Notably, wood contains many redox-active components, in particular lignin, that are likely to react with H_2O_2, which could change the impact of H_2O_2 during the pretreatment step and the concentration of remaining H_2O_2 during the saccharification step. One possible side reaction during the pretreatment step is oxidation of cellulose at the C6 position (Moilanen et al. 2014), and such a modification is known to have a negative impact on saccharification. It is conceivable that this process occurs and is more prominent during pretreatment of Avicel.

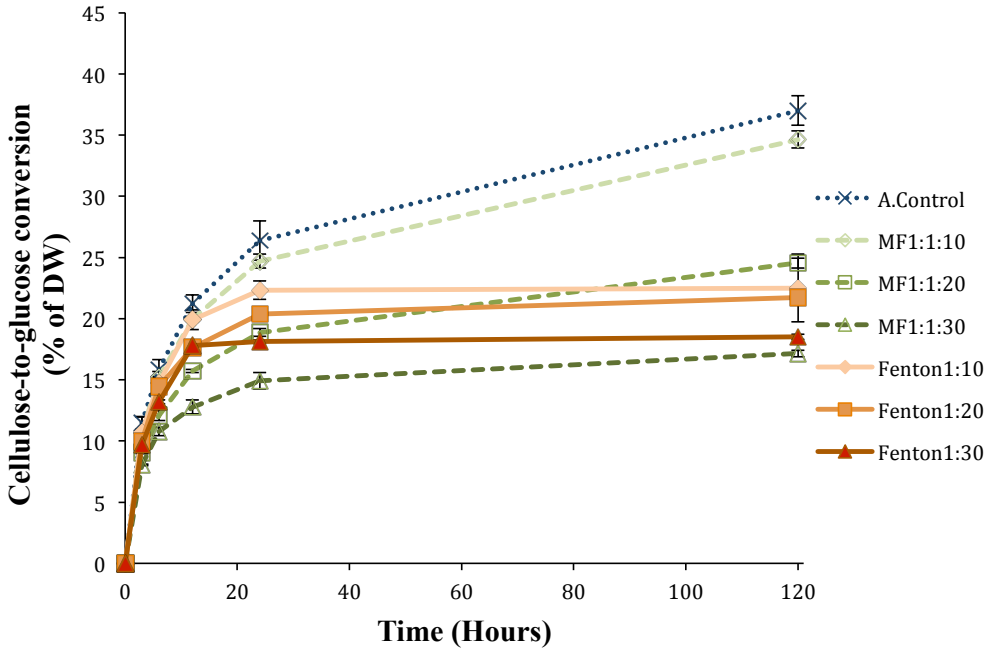

Fig. 6 Glucose release by Cellic CTec2 from Avicel subjected to various Fenton-type pretreatments at different H_2O_2 levels. In the pretreatment step, $FeSO_4$/$FeCl_3$ and 2,3-DHBA concentrations were 0.54 mM in all reactions; the $FeSO_4$:H_2O_2 ratios for Fenton and $FeCl_3$:2,3-DHBA: H_2O_2 ratios for MF are indicated in the legend. Saccharification was performed in the same buffer (50 mM Na-acetate buffer pH 4.5) without prior washing of the material. For the control, reagents were replaced with pure buffer. Experiments were carried out in triplicate; the error bars represent standard deviations.

To understand how any component or combination of components in the MF system may have inhibited/deactivated the enzymes and to assess the impact of pH on enzyme efficiency, control pretreatment reactions were set up with all combinations of reagents at pH 4.5 and 5.0, using the lowest of the three H_2O_2 concentrations, 5.4 mM (Figures 7 and 8). Of the three reagents, $FeCl_3$ had the largest negative impact on the saccharification of Avicel when used alone, lowering cellulose-to-glucose conversion from 40% to 18% at pH 4.5 (Figure 7) and from 70% to 44% at pH 5.0 (Figure 8). H_2O_2 alone only had a slight negative impact on the saccharification, both at pH 4.5 (from 40% to 37%, p=0.0176) and at pH 5.0 (67.9% to 54%). DHBA alone had no effect on the saccharification yield, regardless of the pH. Considering these observations and the low H_2O_2 levels detected at the end of the MF and Fenton pretreatments described above, it is unlikely that the saccharification yield was negatively affected by individual H_2O_2 or DHBA.

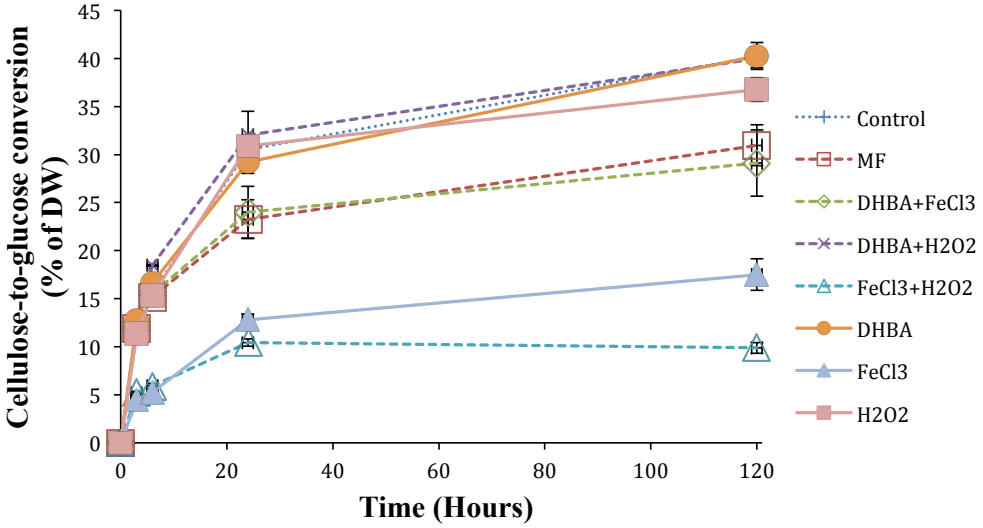

Fig. 7 Saccharification of crystalline cellulose (Avicel) that had been treated with combinations of MF reagents, at pH 4.5. Pretreatment with combinations of $FeCl_3$, 2,3-DHBA and/or H_2O_2 was at pH 4.5 for 3 h; reagent concentrations were as in Figure 6. Saccharification with Cellic CTec2 was performed at 50 °C as in Figure 6, without a prior washing step. Experiments were carried out in triplicate; the error bars represent standard deviations.

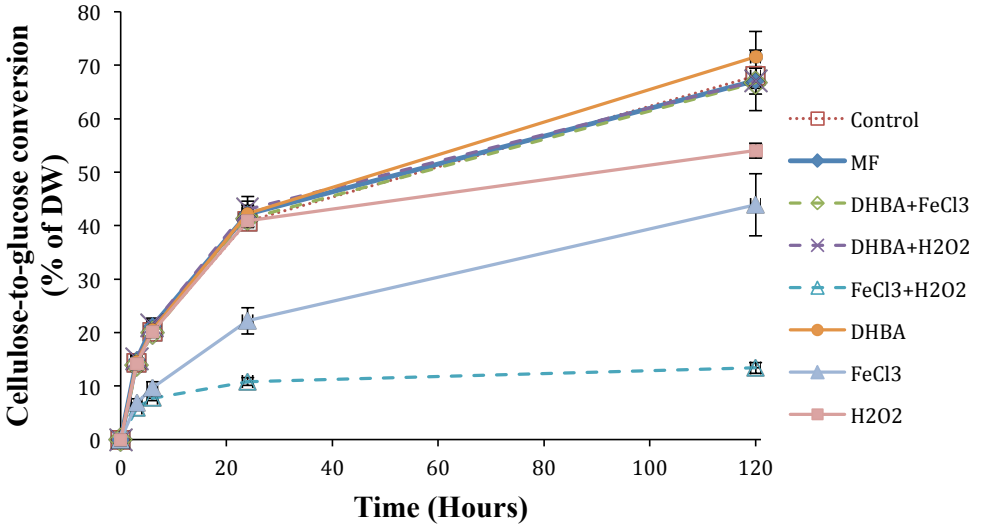

Fig. 8 Saccharification of crystalline cellulose (Avicel) that had been treated with combinations of MF reagents, at pH 5.0. Pretreatment with combinations of $FeCl_3$, 2,3-DHBA and/or H_2O_2 was performed at pH 5.0 for 3 h; reagent concentrations were as in Figure 6. Saccharification with Cellic CTec2 was performed at 50 °C as in Figure 6, without a prior washing step. Experiments were carried out in triplicate; the error bars represent standard deviations.

The overall largest negative impact of the various reagent combinations was observed with the combination of $FeCl_3$ and H_2O_2, reducing the conversion yield from 40% to 10% at pH 4.5 and from 68% to 13% at pH 5.0. Note that the apparent difference in the extent of enzyme inactivation at pH 4.5 and 5.0 is due to the fact that, according to our data (compare Figures 7 & 8), the Cellic CTec2 enzyme cocktail operates about twice as efficiently at pH 5.0 compared to pH 4.5.

DHBA counteracted the negative impact of $FeCl_3$ and H_2O_2. At pH 5.0, the full MF pretreatment and pretreatment with reagent combinations including DHBA had no impact on the saccharification yield. At pH 4.5, on the other hand, both the MF pretreatment and pretreatment with 2,3-DHBA+$FeCl_3$ decreased the saccharification yields, equally. Considering that H_2O_2 was consumed up by the end of MF treatment, this finding suggests that inhibition by DHBA and $FeCl_3$ suppressed any positive effect of the MF treatment. CMF is known to generate more reactive oxygen species at lower pH values (closer to pH 4), which could result in a higher degree of (enzyme inhibiting) cellulose oxidation at pH 4.5 as opposed to pH 5.0. It should be noted that in other research using a CMF reaction under more severe conditions (higher reagent concentrations and temperature), approximately 54% and 16% glucan digestibility was achieved using hardwood and softwood, respectively (Orejuela 2017).

The results presented in Figures 5-8 reveal some of the challenges if saccharification is to be performed after a Fenton-type of treatment without an intermediate washing step. In particular, the damaging effect of iron on the enzymes poses a problem. Other recent work has demonstrated the beneficial effect of having increased cell-wall bound iron in bioconversion of biomass by Cellic CTec2 (Yang et al. 2016). This suggests the benefit of ensuring that the iron is bound to the cell wall and removal of free iron in residual liquid fractions as in CMF treatments (Goodell et al. 2014). Figures 7 and 8 show that the overall process would likely benefit from optimizing process conditions for pretreatment and saccharification individually, which means a necessary pH adjustment after pretreatment (performed below pH 5.0, as is optimal for pretreatment) to 5.0 (which is clearly beneficial for enzyme performance).

3.4 Treatment with higher reagent levels

Since the MF pretreatment at wood fiber saturating iron levels (0.54 mM) only yielded a marginal increase in saccharification efficiency, we tested more severe pretreatments, using higher concentrations of reagents, followed by washing of the pretreated material prior to enzyme addition. In these experiments, 10 mM $FeCl_3$, an equimolar amount of 2,3-DHBA and either 200 or 300 mM H_2O_2 were added sequentially to the suspension containing 5% (w/v) wood substrate (as compared with 0.25-1.0 mM iron in the MF treatments described in the previous sections). These pretreatment reactions were performed more similar to classical single-pulse CMF reactions (Goodell et al. 2014; Goodell et al. 2017; Noriega 2016; Orejuela 2017), but omitting the commonly used drying step after washing to avoid hornification of the wood. After pretreatment and washing, all samples showed a change in color from white to yellow/orange, which could be due to oxidation of the lignin and carbohydrate components and/or to linkages formed between 2,3-DHBA and wood polymers. The concentration of released soluble sugars in the wash liquid after the more severe pretreatment was also below detectable levels and the mass loss remained below 1 w/w%.

Despite the high concentration of reagents and prolonged incubation times, these treatments had only small effects on the saccharification yields (Figure 9). For pretreatments with a reagent ratio of 1:1:20, there were no effects at all. Pretreatment with 1:1:30 reagent ratios, on the other hand, led to a small, but significant increase in the cellulose-to-glucose conversion (72 h, $p=0.032$; 96 h, $p=0.018$; 168 h, $p=0.015$). Cellic CTec2 loadings of 2% and 6% w/w were also tested, as well as higher substrate concentrations of up to 10% w/v, but yielded similar results (data not shown). Given other research with CMF reactions that demonstrate pretreatment enhancement for enzymatic action, and increase in glucan digestibility and solubilization of lignin (Noriega 2016; Orejuela 2017), our data are important in showing that the key step of soluble iron in solution appears to be critical in enhancing both mediated Fenton reactions in the wood cell wall as well as solubilization in subsequent enzymatic treatment.

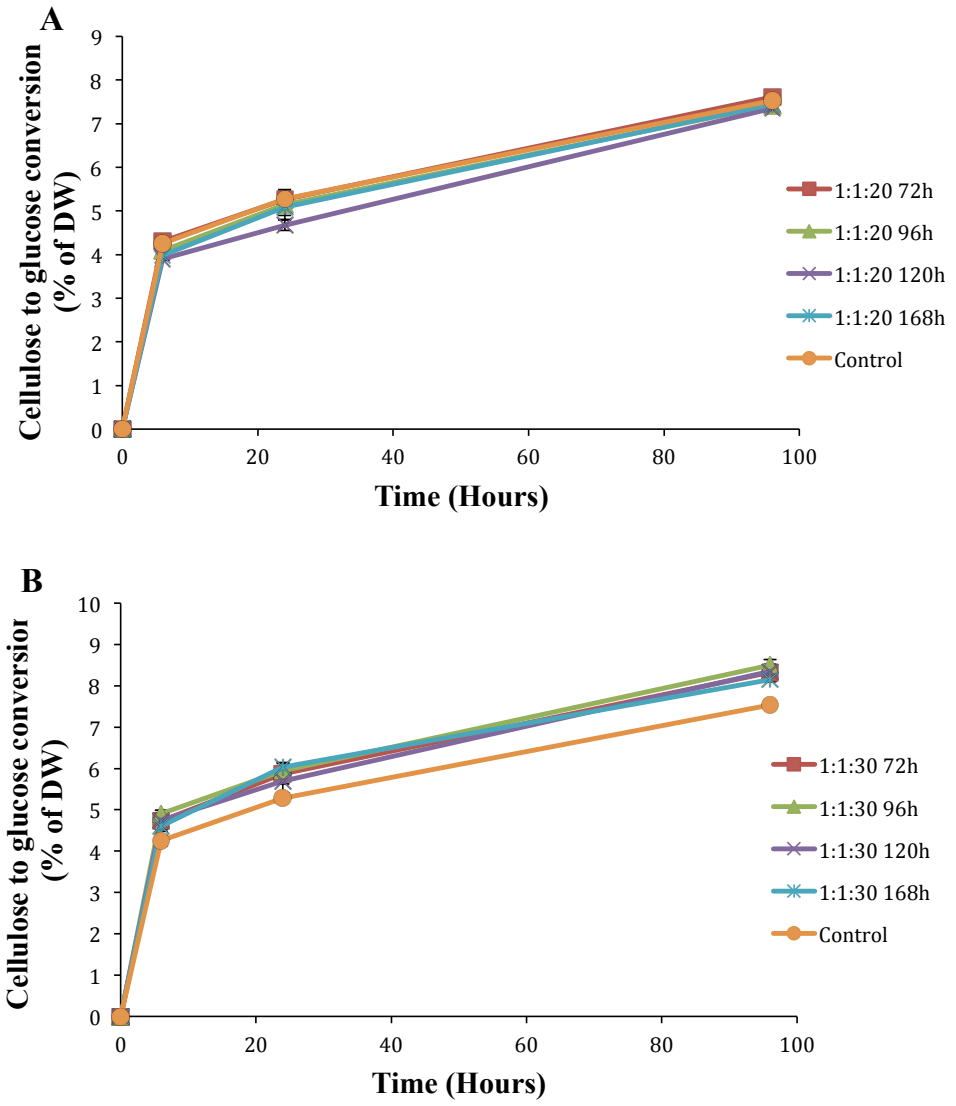

Fig. 9 Glucose release from CMF treated milled Norway spruce by Cellic CTec2. The milled wood was treated with 10 mM $FeCl_3$, 10 mM 2,3-DHBA and 200 mM (A) or 300 mM H_2O_2 (B) (meaning reagent ratios of 1:1:20 or 1:1:30), and allowed to react for 72, 96 or 168 h at room temperature. Samples were then washed with 100 mM oxalic acid and distilled water before saccharification using Cellic CTec2 (4% enzyme solution per g substrate) at 50 °C. Experiments were carried out in triplicate; the error bars represent standard deviations.

4 Concluding remarks

Previous studies on the use of Fenton chemistry in pretreatment of grasses have reported up to 3-fold increases in saccharification efficiency (Jung et al. 2015; Kato et al. 2014). There are several potential explanations as to why the pretreatments tested here did not yield similar results. Spruce wood is a different substrate than grasses and is much more recalcitrant to enzymatic hydrolysis. Cellulose-to-glucose conversion of untreated spruce using Cellic CTec2 was only 5-6%. It is worth noting that the fungal pretreatment was highly successful, even though higher mass losses than initially expected were needed to achieve these results.

The mild Fenton-inspired pretreatment developed in this study and referred to as MF, using iron concentrations close to the binding capacity of the milled wood yielded a slight increase in cellulose-to-glucose conversion (Section 3.2). However, these iron concentrations at the µg/g level in wood, appeared too low to be effective under the conditions used. It is plausible that the low reagent concentrations, as compared to classical CMF treatment, and short reaction times (3-5 h) did not open up the wood structure sufficiently for increased enzyme accessibility, hence the limited increase in saccharifiability. In a previous study, Hastrup et al. (2011) found that incubating cotton cellulose with 8 mM H_2O_2 over 16 h leads to depolymerization of cellulose due to the presence of indigenous metals in the substrate. Also in true biological pretreatment, weeks rather than hours are required to degrade the substrate and obtain an increase in saccharification. Using a continuous flow system where the CMF reagents are slowly fed into the reaction could be tested to see whether the results could be improved. Processes also need to be developed such that the pre-treated substrate is free of hydrogen peroxide and excessive amounts of iron in solution to avoid damage and inhibition of the hydrolytic enzymes. It is worth noting that our data indicate that hydrogen peroxide on its own is not that problematic. Furthermore, recent data indicate that low amounts of hydrogen peroxide sometimes may be beneficial for the efficiency of Cellic CTec2, due to a positive effect on LPMO activity (Bissaro et al. 2017).

Interestingly, recent work by Goodell et al. (2017) suggests that brown-rot fungi may not employ the CMF mechanism to open the wood for enzyme action, but rather, to solubilize wood cell wall components that then are able to diffuse to locations with better enzyme accessibility (Goodell et al. 2017). This would drastically change the way we need to think about how to use oxidative pretreatment of recalcitrant lignocellulosic materials.

The systems tested in this study are a simplification of what occurs in nature, with only three components, and key components for a successful oxidative pretreatment may thus be lacking. Brown-rot fungi have developed a system for localized nano-scale delivery of ROS that most likely requires a complex network of gene products working in concert with each other, and it might be that such a complex mechanism for high accuracy depolymerization is too complex to mimic in the laboratory or the factory. Hydrogen peroxide-generating enzymes that are in close association with the wood cell wall polymers can ensure that Fenton radicals are being generated *in situ* (i.e. in nano-scale proximity of the cell wall polymers). Therefore, they are likely to be key components in an accurate and targeted delivery of the reagents needed for sufficient non-enzymatic depolymerization.

In conclusion, while fungal pretreatment of the Norway spruce used in this study yielded a more than 2-fold higher cellulose-to-glucose conversion compared to untreated material, pretreating the same material with MF reagents, under the conditions tested, we observed limited saccharifiability most likely because the reagent concentrations were too low to open up the wood structure sufficiently during the limited treatment time. Higher reagent (and hence ROS) concentrations and removal of soluble iron during treatment are suggested to enhance the effectiveness of modified Fenton pretreatments prior to enzymatic treatment.

5 Acknowledgements

This work was financed by the Research Council of Norway 243663/E50 BioMim and the Norwegian Institute for Bioeconomy Research.

6 References

Agger, J. W., et al. (2014). Discovery of LPMO activity on hemicelluloses shows the importance of oxidative processes in plant cell wall degradation. *Proceedings of the national acadademy of sciences USA* 111(17): 6287-6292.

ARANTES, V. & GOODELL, B. 2014. Current understanding of brown-rot fungal biodegradation mechanisms: a review. *Deterioration and protection of sustainable biomaterials.* ACS Publications.

ARANTES, V., JELLISON, J. & GOODELL, B. 2012. Peculiarities of brown-rot fungi and biochemical Fenton reaction with regard to their potential as a model for bioprocessing biomass. *Applied microbiology and biotechnology,* 94**,** 323-338.

ARANTES, V., QIAN, Y., MILAGRES, A. M., JELLISON, J. & GOODELL, B. 2009. Effect of pH and oxalic acid on the reduction of Fe^{3+} by a biomimetic chelator and on Fe^{3+} desorption/adsorption onto wood: Implications for brown-rot decay. *International biodeterioration & biodegradation,* 63**,** 478-483.

BALDRIAN, P. & VALÁŠKOVÁ, V. 2008. Degradation of cellulose by basidiomycetous fungi. *FEMS microbiology reviews,* 32**,** 501-521.

BISSARO, B., RØHR, Å. K., MÜLLER, G., CHYLENSKI, P., SKAUGEN, M., FORSBERG, Z., HORN, S. J., VAAJE-KOLSTAD, G. & EIJSINK, V. G. 2017. Oxidative cleavage of polysaccharides by monocopper enzymes depends on H_2O_2. *Nature chemical biology,* 13**,** 1123.

COWLING, E. B. 1961. *Comparative biochemistry of the decay of sweetgum sapwood by white-rot and brown-rot fungi*, US Dept. of Agriculture.

CURLING, S. F., CLAUSEN, C. A. & WINANDY, J. E. 2002. Relationships between mechanical properties, weight loss, and chemical composition of wood during incipient brown-rot decay. *Forest products journal,* 52**,** 34.

EASTWOOD, D. C., FLOUDAS, D., BINDER, M., MAJCHERCZYK, A., SCHNEIDER, P., AERTS, A., ASIEGBU, F. O., BAKER, S. E., BARRY, K. & BENDIKSBY, M. 2011. The plant cell wall–decomposing machinery underlies the functional diversity of forest fungi. *Science,* 333**,** 762-765.

EVANS, C. S., GALLAGHER, I. M., ATKEY, P. T. & WOOD, D. A. 1991. Localisation of degradative enzymes in white-rot decay of lignocellulose. *Biodegradation,* 2**,** 93-106.

FLOUDAS, D., BINDER, M., RILEY, R., BARRY, K., BLANCHETTE, R. A., HENRISSAT, B., MARTÍNEZ, A. T., OTILLAR, R., SPATAFORA, J. W. & YADAV, J. S. 2012. The Paleozoic origin of enzymatic lignin decomposition reconstructed from 31 fungal genomes. *Science,* 336**,** 1715-1719.

FLOURNOY, D. S., KIRK, T. K. & HIGHLEY, T. 1991. Wood decay by brown-rot fungi: changes in pore structure and cell wall volume. *Holzforschung,* 45**,** 383-388.

GOODELL, B., NAKAMURA, M. & JELLISON, J. The Chelator Mediated Fenton System in the Brown Rot Fungi: Details of the Mechanism, and Reasons Why it has Been Ineffective as a Biomimetic Treatment in Some Biomass Applications: A Review. *In:* JERMER, J., ed. Proceedings IRG/WP, 2014 St. George, Utah. USA. IRG/WP, 8.

GOODELL, B., ZHU, Y., KIM, S., KAFLE, K., EASTWOOD, D., DANIEL, G., JELLISON, J., YOSHIDA, M., GROOM, L., PINGALI, S. V. & O'NEILL, H. 2017. Modification of the nanostructure of lignocellulose cell walls via a non-enzymatic

lignocellulose deconstruction system in brown rot wood-decay fungi. *Biotechnology for biofuels,* 10**,** 179.

GREEN, F. & HIGHLEY, T. L. 1997. Mechanism of brown-rot decay: paradigm or paradox. *International biodeterioration & biodegradation,* 39**,** 113-124.

HE, Y.-C., DING, Y., XUE, Y.-F., YANG, B., LIU, F., WANG, C., ZHU, Z.-Z., QING, Q., WU, H. & ZHU, C. 2015. Enhancement of enzymatic saccharification of corn stover with sequential Fenton pretreatment and dilute NaOH extraction. *Bioresource technology,* 193**,** 324-330.

HIMMEL, M. E., DING, S.-Y., JOHNSON, D. K., ADNEY, W. S., NIMLOS, M. R., BRADY, J. W. & FOUST, T. D. 2007. Biomass recalcitrance: engineering plants and enzymes for biofuels production. *Science,* 315**,** 804-807.

HUG, S. J. & LEUPIN, O. 2003. Iron-catalyzed oxidation of arsenic(III) by oxygen and by hydrogen peroxide: pH-dependent formation of oxidants in the Fenton reaction. *Environmental science & technology,* 37**,** 2734-2742.

JENSEN JR, K. A., RYAN, Z. C., WYMELENBERG, A. V., CULLEN, D. & HAMMEL, K. E. 2002. An NADH: quinone oxidoreductase active during biodegradation by the brown-rot basidiomycete *Gloeophyllum trabeum*. *Applied and environmental microbiology,* 68**,** 2699-2703.

JUNG, Y. H., KIM, H. K., PARK, H. M., PARK, Y.-C., PARK, K., SEO, J.-H. & KIM, K. H. 2015. Mimicking the Fenton reaction-induced wood decay by fungi for pretreatment of lignocellulose. *Bioresource technology,* 179**,** 467-472.

KATO, D. M., ELÍA, N., FLYTHE, M. & LYNN, B. C. 2014. Pretreatment of lignocellulosic biomass using Fenton chemistry. *Bioresource technology,* 162**,** 273-278.

KIRK, T. & HIGHLEY, T. 1973. Quantitative changes in structural components of conifer woods during decay by white-and brown-rot fungi. *Phytopathology,* 63**,** 1338-1342.

LEE, J.-W., KIM, H.-Y., KOO, B.-W., CHOI, D.-H., KWON, M. & CHOI, I.-G. 2008. Enzymatic saccharification of biologically pretreated *Pinus densiflora* using enzymes from brown rot fungi. *Journal of bioscience and bioengineering,* 106**,** 162-167.

LEVASSEUR, A., DRULA, E., LOMBARD, V., COUTINHO, P. M. & HENRISSAT, B. 2013. Expansion of the enzymatic repertoire of the CAZy database to integrate auxiliary redox enzymes. *Biotechnology for biofuels,* 6**,** 41.

LOMBARD, V., GOLACONDA RAMULU, H., DRULA, E., COUTINHO, P. M. & HENRISSAT, B. 2013. The carbohydrate-active enzymes database (CAZy) in 2013. *Nucleic acids research,* 42**,** D490-D495.

MARTINEZ, D., CHALLACOMBE, J., MORGENSTERN, I., HIBBETT, D., SCHMOLL, M., KUBICEK, C. P., FERREIRA, P., RUIZ-DUENAS, F. J., MARTINEZ, A. T. & KERSTEN, P. 2009. Genome, transcriptome, and secretome analysis of wood decay fungus Postia placenta supports unique mechanisms of lignocellulose conversion. *Proceedings of the national academy of sciences USA,* 106**,** 1954-1959.

MICHALSKA, K., MIAZEK, K., KRZYSTEK, L. & LEDAKOWICZ, S. 2012. Influence of pretreatment with Fenton's reagent on biogas production and methane yield from lignocellulosic biomass. *Bioresource technology,* 119**,** 72-78.

MOILANEN, U., KELLOCK, M., VÁRNAI, A., ANDBERG, M. & VIIKARI, L. 2014. Mechanisms of laccase-mediator treatments improving the enzymatic hydrolysis of pre-treated spruce. *Biotechnology for biofuels,* 7**,** 177.

NORIEGA, O. A. U. 2016. *Sistemas oxidativos e biomiméticos aplicados à hidrólise enzimática de materiais lignocelulósicos. (Oxidative-biomimetic systems applied to enzymatic hydrolysis of lignocellulosic materials).* PhD PhD, University of São Paulo. Lorena Campus, Brazil.

OGNER, G., WICKSTRØM, T., REMEDIOS, G., GJELSVIK, S., HENSEL, G. R., JACOBSEN, J. E., OLSEN, M., SKRETTING, E. & SØRLIE, B. 1999. The chemical analysis program of the Norwegian Forest Research Institute 2000. Internal report.

OREJUELA, L. M. 2017. *Lignocellulose deconstruction using glyceline and a chelator-mediated Fenton system.* PhD PhD, Virginia Polytechnic Institute and State University.

PALMQVIST, E. & HAHN-HÄGERDAL, B. 2000. Fermentation of lignocellulosic hydrolysates. II: inhibitors and mechanisms of inhibition. *Bioresource technology,* 74**,** 25-33.

PASZCZYNSKI, A., CRAWFORD, R., FUNK, D. & GOODELL, B. 1999. De Novo Synthesis of 4, 5-Dimethoxycatechol and 2, 5-Dimethoxyhydroquinone by the Brown Rot FungusGloeophyllum trabeum. *Applied and environmental microbiology,* 65**,** 674-679.

PEDERSEN, M. & MEYER, A. S. 2010. Lignocellulose pretreatment severity–relating pH to biomatrix opening. *New biotechnology,* 27**,** 739-750.

PRESLEY, G. N. & SCHILLING, J. S. 2017. Distinct growth and secretome strategies by two taxonomically-divergent brown rot fungi. *Applied and environmental microbiology***,** 83(7):e02987-16.

PROUSEK, J. 2007. Fenton chemistry in biology and medicine. *Pure and applied chemistry,* 79**,** 2325-2338.

RAY, M. J., LEAK, D. J., SPANU, P. D. & MURPHY, R. J. 2010. Brown rot fungal early stage decay mechanism as a biological pretreatment for softwood biomass in biofuel production. *Biomass and bioenergy,* 34**,** 1257-1262.

RILEY, R., SALAMOV, A. A., BROWN, D. W., NAGY, L. G., FLOUDAS, D., HELD, B. W., LEVASSEUR, A., LOMBARD, V., MORIN, E. & OTILLAR, R. 2014. Extensive sampling of basidiomycete genomes demonstrates inadequacy of the white-rot/brown-rot paradigm for wood decay fungi. *Proceedings of the national academy of sciences USA,* 111**,** 9923-9928.

SLUITER, A., HAMES, B., RUIZ, R., SCARLATA, C., SLUITER, J., TEMPLETON, D. & CROCKER, D. 2008. Determination of structural carbohydrates and lignin in biomass. *Laboratory analytical procedure,* 1617**,** 1-16.

XU, G. & GOODELL, B. 2001. Mechanisms of wood degradation by brown-rot fungi: chelator-mediated cellulose degradation and binding of iron by cellulose. *Journal of biotechnology,* 87**,** 43-57.

YANG, H., WEI, H., MA, G., ANTUNES, M. S., VOGT, S., COX, J., ZHANG, X., LIU, X., BU, L., GLEBER, S. C., CARPITA, N. C., MAKOWSKI, L., HIMMEL, M. E., TUCKER, M. P., MCCANN, M. C., MURPHY, A. S. & PEER, W. A. 2016. Cell wall targeted in planta iron accumulation enhances biomass conversion and seed iron concentration in Arabidopsis and rice. *Plant biotechnology journal,* 14**,** 1998-2009.

ZHANG, J., PRESLEY, G. N., HAMMEL, K. E., RYU, J.-S., MENKE, J. R., FIGUEROA, M., HU, D., ORR, G. & SCHILLING, J. S. 2016. Localizing gene regulation reveals a staggered wood decay mechanism for the brown rot fungus Postia placenta. *Proceedings of the national academy of sciences USA***,** 201608454.

ZHAO, X., ZHANG, L. & LIU, D. 2012. Biomass recalcitrance. Part I: the chemical compositions and physical structures affecting the enzymatic hydrolysis of lignocellulose. *Biofuels, bioproducts and biorefining,* 6**,** 465-482.

7 Appendix

Supplementary material

Table 1 Polysaccharide composition of Norway spruce. The composition of the top and the butt of a single Norway spruce tree was determined; polysaccharide content is expressed as w/w% of total dry weight.

Sample	**Cellulose (%)**	**GGM (%)**	**Xylan (%)**
Butt	38.3	18.9	4.92
Top	38.6	17.1	5.12

Table 2 Monosaccharide composition of Norway spruce. The composition of the top and the butt of a single Norway spruce tree was determined; sugars are indicated as anhydrous sugars and expressed as w/w% of total dry weight.

Sample	**Gal (%)**	**Glc (%)**	**Xyl (%)**	**Man (%)**	**Ara (%)**
Butt	1.35	42.7	4.92	13.2	1.02
Top	1.29	42.5	5.12	11.8	0.99

Table 3 The monosaccharide and lignin composition of Norway spruce decayed by *R. placenta* or *G. trabeum* for 3, 5 or 7 weeks.

Sample id	Total Ash	Structural ash	Glucan	±	Xylan	±	Galactan	±	Arabinan	±	Mannan	±	Lignin	±	Acetyl	±	Mass closure
Control	0.3	0.5	46.3	0.1	5.3	0.3	2.0	0.1	1.4	0.1	12.4	0.1	32.0	0.3	4.5	0.0	104.2
G. trabeum 3 weeks	0.3	0.1	48.8	0.1	4.4	0.0	1.4	0.2	0.4	0.1	7.4	0.1	35,7	0.3	3.7	0.2	102.1
G. trabeum 5 weeks	0.4	0.4	48.5	0.2	3.9	0.0	1.1	0.0	0.5	0.1	6.5	0.1	37,1	0.6	3.5	0.1	101.5
G. trabeum 7 weeks	0.3	0.3	49.0	0.1	3.7	0.0	1.0	0.0	0.5	0.0	5.7	0.0	38,3	0.1	3.3	0.1	101.8
R. placenta 3 weeks	0.3	0.4	46.8	0.1	5.0	0.1	1.7	0.2	0.7	0.0	9.4	0.1	34.0	0.2	4.0	0.1	101.9
R. placenta 5 weeks	0.3	0.5	47.3	0.2	4.7	0.2	1.4	0.2	0.8	0.2	7.5	0.1	35,9	0.1	3.5	0.1	101.4
R. placenta 7 weeks	0.3	0.2	47.9	0.1	4.7	0.2	1.9	0.4	0.7	0.2	6.0	0.1	38,2	0.2	3.3	0.1	103.0

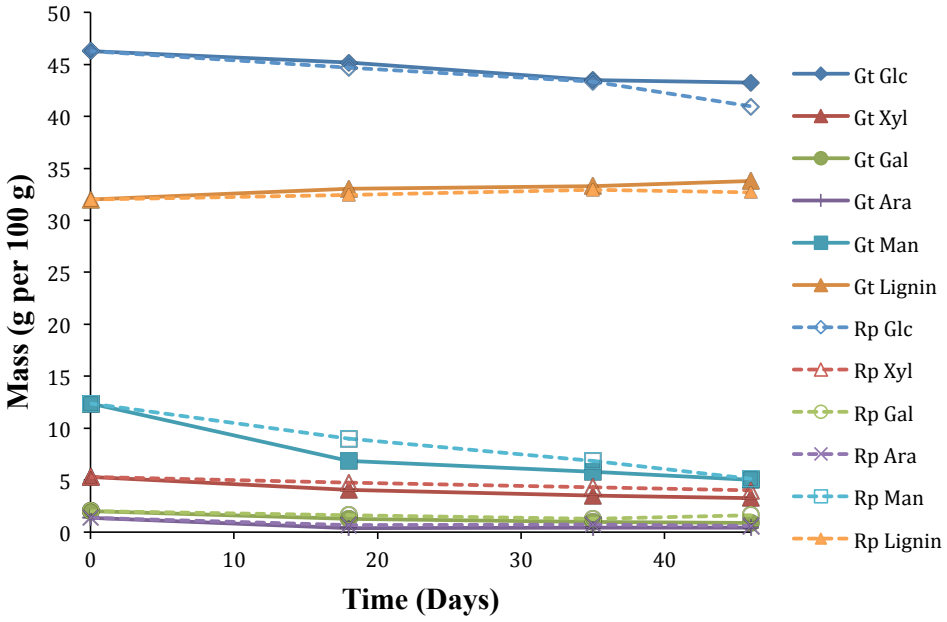

Fig. 10 Carbohydrate and lignin content of wood substrate during decay by *G. trabeum* (Gt) and *R. placenta* (Rp). Glc=Glucan, Xyl=Xylan, Gal=Galactan, Ara=Arabinan, Man=Mannan. Component mass has been calculated based on 100 g initial dry weight taking into account mass loss and composition (presented in Figure 1 and Table 3, respectively), according to the following formula: (100% Mass – Mass loss %) × Component %.

Paper II

International Biodeterioration & Biodegradation 135 (2018) 39–52

Contents lists available at ScienceDirect

International Biodeterioration & Biodegradation

journal homepage: www.elsevier.com/locate/ibiod

Acetylation of *Pinus radiata* delays hydrolytic depolymerisation by the brown-rot fungus *Rhondonia placenta*

G. Beck[a,b,*], O.A. Hegnar[a,c], C.G. Fossdal[a], G. Alfredsen[a]

[a] Norwegian Institute of Bioeconomy Research, Department of Wood Technology, PO Box 115, NO-1431, Ås, Norway
[b] Norwegian University of Life Sciences, Faculty of Environmental Sciences and Natural Resource Management, PO Box 5003, NO-1432, Ås, Norway
[c] Norwegian University of Life Sciences, Faculty of Chemistry Biotechnology & Food Science, PO Box 5003, NO-1432, Ås, Norway

ARTICLE INFO

Keywords:
Acetylated wood
brown-rot decay
Gene expression
Quantitative real-time PCR

ABSTRACT

Acetylation of wood can provide protection against wood deteriorating fungi, but the exact degradation mechanism remains unclear. The aim of this study was to determine the effect of acetylation of *Pinus radiata* wood (weight percent gain 13, 17 and 21%) on the expression of genes involved in decay by brown-rot fungus *Rhodonia placenta.* Gene expression analysis using qRT-PCR captured incipient to advanced decay stages. As expected the initiation of decay was delayed as a result the degree of acetylation. However, once decay was established, the rate of degradation in acetylated samples was similar to that of unmodified wood. This suggests a delay in decay rather than an absolute protection threshold at higher acetylation levels. In accordance with previous studies, the oxidative system of *R. placenta* was more active in wood with higher degrees of acetylation and expression of cellulose active enzymes was delayed for acetylated samples compared to untreated samples. The reason for the delay in the latter might be because of the slower diffusion rate in acetylated wood or that partially acetylated cellobiose may be less effective in triggering production of saccharification enzymes. Enzymes involved in hemicellulose and pectin degradation have previously not been focused on in studies of degradation of acetylated wood. Surprisingly, CE16 carbohydrate esterase, assumed to be involved in deacetylation of carbohydrates, was expressed significantly more in untreated samples compared to highly acetylated samples. We hypothesise that this enzyme might be regulated through a negative feedback system, where acetic acid supresses the expression. The up-regulation of two expansin genes in acetylated samples suggests that their function, to loosen the cell wall, is needed more in acetylated wood due the physical bulking of the cell wall. In this study, we demonstrate that acetylation affects the expression of specific target genes not previously reported, resulting in delayed initiation of decay. Thus, targeting these degradation mechanisms can contribute to improving wood protection systems.

1. Introduction

Wood is a renewable, natural and carbon sequestering material that requires less energy to manufacture than other nonrenewable construction materials. However, wood's biogenic origin also makes it susceptible to biological degradation. An equivalent of ten percent of the annual timber harvest of the United States is estimated to decay in service each year (Zabel and Morrell, 1992). Traditionally, wood decay has been mitigated by impregnation with biocides, but new non-toxic alternative methods are being developed. Acetylation is one such alternative preservation technique.

Rather than relying on the presence of a toxic chemical, acetylation, like other wood modification techniques, imparts decay resistance by chemically altering the wood polymers themselves (Hill, 2006). The wood is reacted with acetic anhydride which substitutes the hydrogen of hydroxyl (OH) groups on the wood polymers with an acetyl group and produces acetic acid as a byproduct (Rowell, 2005). Acetylation physically bulks the cell wall because of the larger size of the substituted moiety. It has been shown that water is excluded from the acetylated cell wall due to both direct substitution of OH groups leading to less primary sorption sites for water molecules and steric hindrance of unmodified OH groups by the bulky acetyl groups (Papadopoulos and Hill, 2003; Popescu et al., 2014; Beck et al., 2017a). In their review article, Ringman et al. (2014a) summarised several prevalent theories of how wood modification methods, such as acetylation, may impart decay resistance: (i) fungal enzymes may become ineffective due to substrate non-recognition, (ii) fungal molecules may not penetrate the modified cell wall due to micropore blocking and/or (iii) diffusion may

* Corresponding author. Norwegian Institute of Bioeconomy Research, Department of Wood Technology, PO Box 115, NO-1431, Ås, Norway.
E-mail address: greeley.beck@nibio.no (G. Beck).

https://doi.org/10.1016/j.ibiod.2018.09.003
Received 28 March 2018; Received in revised form 2 September 2018; Accepted 10 September 2018
Available online 01 October 2018

be inhibited due to low cell wall moisture content. The first theory was rejected because it would not explain hindrance of the initial non-enzymatic degradation of brown-rot fungi. The second also seems unlikely as Hill et al. (2005) demonstrated using solute exclusion that the acetylated cell wall remains accessible to probe molecules up to 4 nm in size. The last theory of diffusion inhibition was identified as the most probable.

In nature, wood is primarily decomposed by basidiomycetous fungi in two polyphyletic groups generally known as white- and brown-rot fungi. White-rot fungi are able to fully degrade cellulose, hemicelluloses and lignin, using a battery of enzymes that act upon the polysaccharides and lignin. Brown-rot fungi on the other hand remove only the polysaccharides but extensively depolymerise and modify lignin before rapidly repolymerising it (Eastwood et al., 2011; Riley et al., 2014).

The main classes of enzymes acting on cellulose in basidiomycetes are endoglucanases belonging to the GH5 and GH12 families, cellobiohydrolases belonging to families GH6 and GH7 and lytic polysaccharide monooxygenases (LPMOs) belonging to the family AA9 (as classified in the Carbohydrate-Active enZYmes database CAZy) (Floudas et al., 2012; Lombard et al., 2013). Hemicellulases play a key role in the enzyme repertoire of these fungi; some species have several dozens of genes encoding mannanases, xylanases, arabinases and glucuronidases. Working in concert with the hemicellulases are carbohydrate esterases that assist in the depolymerisation of wood cell wall polysaccharides through deacetylation. These enzymes, which are generally larger than 50 Å in diameter, are thought to be too large to penetrate the native wood cell wall, where porosity is low (Cowling, 1961, Flournoy et al., 1991). While white-rot fungal genomes generally contain a large number of genes involved in the depolymerisation of cellulose and lignin, brown-rot fungal genomes are surprisingly sparse in comparison (Floudas et al., 2012). One of the brown-rot model fungi *Rhodonia placenta* completely lacks exo-acting cellulases in families GH6 and GH7 and peroxidase genes, and only retains a few endocellulases, and LPMOs, yet is perfectly capable of depolymerising and degrading the cellulose in the wood cell wall (Martinez et al., 2009; Eastwood et al., 2011; Floudas et al., 2012; Riley et al., 2014). Interestingly, the repertoire of hemicellulose acting enzymes is not as limited as the cellulose acting enzymes, implying a particular importance of removing hemicelluloses before efficient cellulose hydrolysis by these fungi.

The apparent lack of a sufficient number of cellulase genes and the wood cell-wall porosity problem is theorised to be circumvented in brown-rot fungi by a non-enzymatic system for wood cell wall depolymerisation that uses iron, oxalic acid and iron-chelating/reducing secondary metabolites (Goodell et al., 1997; Xu and Goodell, 2001; Eastwood et al., 2011; Yelle et al., 2011). This system is referred to as the Chelator Mediated Fenton (CMF) system. It is proposed that the fungus chelates iron from the environment and produces reducing compounds as well as hydrogen peroxide, eventually leading to the generation of hydroxyl radicals through the Fenton reaction mechanism within the wood. The fungus alters its local environment by secreting large amounts of oxalic acid, lowering the pH around the hyphae to around 2 while the natural pH of the wood cell wall is approximately 5–6. These high concentrations of oxalic acid are able to chelate iron (Fe^{3+}) from iron-oxide complexes and from the wood. As a consequence of the pH and concentration gradients generated by the high concentration of oxalic acid, the iron is not reduced in the immediate environment of the fungus (Arantes et al., 2012). However, once the iron-oxalate complexes diffuses into the higher pH environment of the wood cell wall, iron-reducing compounds produced by the fungus such as 2,5-dimethoxyhydroquinone will reduce and solubilise the iron (Arantes et al., 2009). Once reduced within the wood cell wall, the iron is able to react with hydrogen peroxide, leading to generation of reactive oxygen species (ROS) (Arantes et al., 2012). It has been known for more than 50 years that strength loss precedes mass loss in brown-rot decayed wood (Cowling, 1961). This is due to oxidative depolymerisation via the CMF system, which is employed as a pre-treatment prior to secretion of the hydrolytic enzymes (Arantes et al., 2012). These two systems, the oxidative and the hydrolytic, have been shown to be spatially and temporally separated (Zhang et al., 2016).

There are several potential sources for hydrogen peroxide. The genome of *R. placenta* suggests the presence of a number of auxiliary activity enzymes that are known to generate H_2O_2. Among these are AA3 glucose-methanol-choline (GMC) oxidoreductases, AA5 copper radical oxidases and AA7 gluco-oligosaccharide oxidases, which are able to oxidise a wide variety of compounds present in wood and couple this with the reduction of molecular oxygen, leading to the generation of H_2O_2 (Floudas et al., 2012; Levasseur et al., 2013). AA6 benzoquinone reductases are most likely involved in the reduction and regeneration of catecholate and hydroquinone chelators capable of reducing iron, and are highly expressed during the early stages of brown-rot fungal decay (Jensen et al., 2002; Floudas et al., 2012). Notably, reduced catecholate compounds may also generate hydrogen peroxide under certain conditions, by reducing molecular oxygen. Brown-rot fungi produce several catecholate secondary metabolites, which can potentially penetrate the wood cell wall where they can participate in several of the steps needed for Fenton chemistry to take place (Paszczynski et al., 1999).

To the best of the authors' knowledge, all previous gene expression studies on modified wood are on *R. placenta* and only on a limited number of genes and/or a limited test period. Alfredsen et al. (2016a) compared expression of 25 selected *R. placenta* genes during eight weeks of incubation of unmodified and furfurylated Scots pine sapwood treated to a weight percent gain (WPG) of 14%. Among the findings were confirmed indications of a possible shift toward increased expression, or at least no down regulation, of genes related to oxidative metabolism and concomitant reduction of several genes related to the breakdown of holocellulose in furfurylated wood compared to unmodified wood. Ringman et al. (2014b) compared gene expression of selected genes at incipient decay stages for acetylated, DMDHEU and thermally modified *Pinus sylvestris*. They used *R. placenta* and incubation times up to 8 weeks. For the two selected genes involved in oxidative degradation of holocellulose the pattern between the genes differed, but they generally seemed to be upregulated in modified wood compared to control. The acetylated samples seemed to have a peak in alcohol oxidase expression after two weeks, while the other modifications had the highest expression after eight weeks. For the two genes tested involved in holocellulose degradation, expression levels and trends of the modified wood were similar to those of untreated wood.

Previous studies focusing on acetylated wood include Alfredsen and Pilgård (2014) and Alfredsen et al. (2016b). Alfredsen and Pilgård (2014) tested the effect of leached versus non-leached samples on gene expression of only five genes. No significant differences were found in gene expression after 28 weeks. Alfredsen et al. (2016b) studied *R. placenta* colonisation during 4, 12, 20, 28 and 36 weeks of incubation at three acetylation levels (WPG 12, 17 and 22). The number of expressed gene transcripts was limited (six genes), but the findings supported previous studies where acetylated wood seemed to have some resistance against oxidative mechanisms. This resulted in a delayed decay initiation and slower decay rate. The genes involved in oxidative depolymerisation generally had higher expression levels in acetylated wood than the control. But when comparing the treatments at the same mass loss, a significant difference was only found for two of the genes between 21 %WPG and the control. For the two genes involved in holocellulose depolymerisation, the expression levels were generally higher in the control than in acetylated wood and the highest expression levels in acetylated wood were found after 28 and 36 weeks.

The aim of the present study was determine the effect of acetylation of *Pinus radiata* wood on gene expression of decay related genes by the brown-rot fungus *Rhodonia placenta.*

2. Materials and methods

2.1. Wood material

Eight *Pinus radiata* (D. Don) sapwood boards originating from New Zealand were provided by Accsys Technologies. These boards were used to make cylindrical samples (0.6 cm diameter, 1 cm height) according to Beck et al. (2017b). The samples consisted entirely of earlywood in order to get as homogeneous samples as possible. The samples were dried at 103 °C for 18 h then cooled down in a desiccator before initial dry weights were recorded. The acetylation procedure was also performed as in the aforementioned study and the three WPG levels were achieved by reacting the wood with acetic anhydride for either 15, 150 or 1750 min. No swelling agent was used but the samples were vacuum impregnated with anhydride prior to reaction. Average WPG for the three levels of acetylation were 12.5 ± 1.0% (Ac13), 17.1 ± 0.7% (Ac17) and 21.4 ± 0.7% (Ac21). The acetylated samples were conditioned at 65% relative humidity and 20 °C for two weeks before they were sealed in plastic bags and sterilised by gamma irradiation (25 kGY) at the Norwegian Institute for Energy Technology.

2.2. Decay test

Rhodonia placenta FPRL 280 (Fr.) Niemelä, K.H. Larss. & Schigel (also widely known by the now taxonomically invalid name *Postia placenta*) was used to decay the samples. This fungus was chosen because: 1) historically it has been extensively studied as a representative brown-rot fungus (Flournoy et al., 1991; Green III et al. 1992; Winandy and Morrell, 1993; Irbe et al., 2006; Niemenmaa et al., 2008; Kim et al., 2009; Martinez et al., 2009; Yelle et al., 2011; Goodell et al., 2017); 2) *R. placenta* was one of the first brown-rot fungi to have its genome sequenced and it is of high quality and well annotated (Martinez et al., 2009); 3) it has been the focus of recent work characterising gene expression (Ringman et al., 2014b; Alfredsen et al. 2016a,b; Presley et al., 2016; Zhang et al., 2016; Zhang and Schilling, 2017). This specific strain was used because it is specified in the European decay test standard EN113 (CEN, 1997). Until recently, "Ppl" was used as the abbreviation for the protein ID of this species. This identification is kept in the current work to avoid potential misunderstanding. The fungus was first grown on 4% (w/v) malt agar and plugs of actively growing mycelia were transferred to a liquid culture containing 4% (w/v) malt. After two weeks, the liquid culture was homogenised with a tissue homogeniser (Ultra-turrax T25, IKA Werke GmbH & Co. KG, Saufen, Germany) and this mixture was then used to inoculate the samples. Petri dishes (100 × 20 mm) were filled with 20 g soil (2/3 ecological compost soil and 1/3 sandy soil) adjusted to 95% of his water holding capacity according to ENV 807 (CEN, 2001) and sterilised at 121 °C for 2 × 60 min. Sterilised plastic mesh was placed on top of the soil and the cylindrical wood samples were placed on top of this mesh with the end grain facing the mesh (8 samples per dish, four replicate plates all of the same acetylation level dedicated to each harvesting point). Each sample was individually inoculated by pipetting 300 µl of the fungal suspension on top of the sample. The samples were incubated at 22 °C and 70% relative humidity until they were harvested. The weight of the dishes (including soil and wood specimens) was monitored throughout the incubation period and when total weight dropped below 5 g less than the original weight, 5 ml deionised, sterilised water was added to the soil. Incubation times for analyses in the current study were chosen such that mass losses between the different acetylation levels would be similar at the first harvesting point. The control samples were harvested at weeks 1–4, Ac13 at weeks 2, 4 and 6, Ac17 at weeks 4, 6 and 10 and Ac21 at weeks 10, 16, 24 and 28. Three samples were provided for qRT-PCR analysis and eight samples were weighed for mass loss for each harvesting point. When the samples were harvested, the mycelia covering the surface were carefully removed with a tissue (Delicate Task Wipes, Kintech Science, UK) and then the sample mass was obtained. The eight samples measured for mass loss were then dried for 18 h at 103 °C and weighed. The samples provided for qRT-PCR were wrapped individually in aluminium foil and put directly into a container with liquid nitrogen. The samples were then stored at −80 °C.

2.3. mRNA purification and cDNA synthesis

Wood powder from frozen samples was obtained by cutting the plugs into smaller pieces with a garden shears wiped with 70% alcohol and thereafter Molecular BioProducts™ RNase AWAY™ Surface Decontaminant (Thermo Scientific, Singapore). The wood samples were immediately cooled down again in Eppendorf tubes in liquid nitrogen. Fine wood powder was produced in a Retsch 300 mill (Retsch mbH, Haan, Germany). The wood samples, the 100-mg stainless steel beads (QIAGEN, Hilden, Germany) and the containers were chilled with liquid nitrogen before grinding at maximum speed for 1.5 min. They were then cooled in liquid nitrogen again before a second round of grinding. MasterPure™ Complete DNA and RNA Purification KIT (epicentre, Madison, WI, USA) was used according to the manufacturer's instruction for plant tissue samples with the following exceptions: 1) 90 mg of wood sample; 2) 600 µl tissue and cell lysis solution; 3) incubated at 56 °C; 4) added an extra centrifugation step (12000 g, room temperature). NanoDrop™ 2000 spectrophotometer (Thermo Scientific, Singapore) was used to quantify RNA in each sample. To convert RNA to cDNA TaqMan Reverse Transcription Reagent KIT (Thermo Scientific, Singapore) was used according to the manufacturer's instructions. Total reaction volume was 50 µl. 300 ng RNA were reacted with oligo $d(T)_{16}$ primer in RNase free water (Qiagene, Hilden, Germany). The solution was incubated two cycles in the PCR machine (GeneAmp® PCR System 9700, Applied Biosystems, Foster City, CA, USA) at 65 °C/5 min and 4 °C/2 min. The PCR machine was paused and the master mix added. The next three cycles included 37 °C/30 min, 95 °C/5 min and 4 °C/indefinite time. In addition to the test samples, two samples without RNA were added as controls and used for each primer pair. After the cDNA synthesis, 50 µl RNase free water (Qiagene, Hilden, Germany) was added to the samples and mixed well.

2.4. Quantitative real-time PCR

The qRT-PCR specific primers used to determine the transcript levels of selected genes were designed with a target T_m of 60 °C and to yield a 150 base pair product. qRT-PCR was performed using ViiA 7 by Life technologies (Applied Biosystems, Foster City, CA, USA). The master mix included for each sample: 5 µl Fast SYBR®Green Master Mix (Thermo Scientific, Singapore), 0.06 µl 10 µM forward primer, 0.06 µl 10 µM reverse primer, 2.88 µl RNase free water (Qiagene, Hilden, Germany) and 2 µl test sample (total volume 10 µl). The qRT-PCR run included the following stages: Hold stage with initial ramp rate 2.63 °C/s, then 95.0 °C for 20 s. PCR stage with 40 cycles of initial ramp rate 2.63 °C/s, 95.0 °C, ramp rate of 2.42 °C followed by 60.0 °C for 20 s. The melt curve stage had an initial ramp rate of 2.63 °C/s then 95.0 °C for 15 s, ramp rate of 2.42 °C/s 60.0° for one second, then 0.05 °C/s. Two constitutive housekeeping genes, β-tubulin - βt (Ppl113871) and α-tubulin - αt (Ppl123093) were used as a baseline for gene expression. The target genes (Tg) and the endogenous controls in this study are listed in Table 1. Protein ID's are according to *Postia placenta* MAD 698-R v1.0 genome, The Joint Genome Institute (https://genome.jgi.doe.gov/pages/search-for-genes.jsf?organism=Pospl1). Threshold cycle values (C_t) obtained here were used to quantify gene expression. Software used to export the C_t values was QuantStudioTM Real-Time PCR System (Applied Biosystems by Thermo Fiches Scientific, Foster City, CA, USA).

2.5. Quantification of gene expression

C_t-values of βt, αt and Tg were used to quantify gene expression according to Eq. (1):

Table 1
qRT-PCR primers: gene (abbreviation), JGI protein id for *Rhodonia placenta*, function, forward and reverse primer.

Gene (abbreviation)	Protein id	Function	Forward primer/reverse primer
1: Genes involved in oxidative depolymerisation			
1.1: Oxalate synthesis and oxalate decomposition			
Glyoxylate dehydrogenase (GlyD)	121561	Involved in oxalate synthesis	CGGAGCTGGACCTTTGTTAC/GCGCGAAGGCAAATCTAATA
Oxaloacetate acetylhydrolase (OahA)	112832	Involved in oxalate synthesis	AAGGCGTTCTTCGAGGTCAT/AAAGCAGCAACCCGAGAAG
Oxalate decarboxylase (OxaD)	43912	Involved in oxalate decomposition	GAACCTATAACTACGAGGCAAGC/ CCAGGAATACCAGAGGCTCA
1.2: Redox enzymes			
AA3 GMC oxidoreductase (AOx1)	44331	Involved in oxidative depolymerisation Possible H_2O_2 source	GGAGGTACAGACGGACGAAC/AGAGTCGACGACACCGTTCT
AA3 GMC oxidoreductases (AOx2)	129158	Most likely involved in oxidative depolymerisation Possible H_2O_2 source	TACTCGACGGCCCTCACTAT/CCGCTTGAGACTGAACACTG
AA3 GMC oxidoreductase (AOx3)	118723	Involved in oxidative depolymerisation Likely source of H_2O_2	ACACCAAGGAGGACGACGAG/GACGAGCAAGGCAGACGAGTA
Copper radical oxidase (Cro1)	56703	Involved in oxidative depolymerisation Likely source of H_2O_2	CGGCGATGTTTCGGACGTTAT/CCGCCATTCCAATAGTAGAGC
Copper radical oxidase (Cro2)	104114	Involved in oxidative depolymerisation Likely source of H_2O_2	CGCAGACGATGGAGGTGGTC/GTGACACCGCACCGTTACCA
Benzoquinone reductases (BqR)	12517	Involved in oxidative depolymerisation Possibly involved in reduction of chelator/ reductants	CGTACAAAGAACGCCCTCTC/GTGGCCGTACATGGAGTAGA
2: Hydrolytic enzymes involved in polysaccharide depolymerisation and LPMO			
2.1: Cellulose degradation			
GH5 Endoglucanase (Cel5a)	115648	Major endocellulase	TTCTGTCCATGACACCGTACA/TCCTCTTGGTGTAGGTCCGTA
GH5 Endoglucanase (Cel5b)	103675	Major endocellulase	CTCGCATACGTGCAATCG/GGAGTAGGGCGTCACAGAGA
GH12 Glucoside hydrolase (Cel12a)	121191	Endoglucanase active on cellulose and/or xyloglucan	TCAACGTCGAGAGCTTCAG/GACGAAGAGCTAAGGACACCA
GH3 Betaglucosidase (bGlu)	128500	Hydrolyses cellobiose, releasing glucose	AGGCACAAGCCAAGTCGTCA/CTTGGCAATCGTGAAAGTGGT
AA9 Lytic polysaccharide monooxygenases (LPMO)	126811	Polysaccharide depolymerisation via oxidative cleavage of glycosidic bonds	GCCAGATATCACGGTCACCT/TCGTAGATGTCGGGAACGTA
2.2: Hemicellulose and pectin degradation			
GH5 Endomannanase (Man5a)	121831	Involved in glucomannan depolymerisation, highly expressed	GCTGACTGGCACCGACTACC/CCCACGAACGCATCCAAATAG
GH10 Endoxylanase (Xyl10a)	113670	Involved in xylose depolymerisation	CTTCGGCTCTGCTACGGACAA/ACCATACGCAGTTGTGTCCTCT
GH10b Endoxylanase (Xyl10b)	105534	Involved in xylose depolymerisation	TCGGAGCCTGAGCCATTTGT/TGCTGCGGTGTAATTGTTGG
GH3 Beta xylosidase (bXyl)	51213	Hemicellulose depolymerisation	GTGCGTTTCCCGACTGTGC/GCGGTGTTGCCGGTATTGT
Carbohydrate esterase (CE16a)	125801	Deacetylation of carbohydrates	ACACCGTGCACAACATCCT/CGTGCTCCAAGTCTGATGAT
GH28 Polygalacturonase (Gal28a)	111730	Involved in pectin depolymerisation	CCGGCAATACAATTTCTGGCA/GTTCCGGGAGTACCGTCATT
3: Expansins			
Expansin (Exp1)	126976	Most likely involved in increasing enzyme accessibility	TGTCGGAATGAGCGGTCT/ATGCATGAACCGCCTTTGT
Expansin (Exp2)	128179	Most likely involved in increasing enzyme accessibility	AATGTGACTTGGGCCATTGT/AATACCGTGCAAGCGTCAGT
4: Housekeeping			
α-tubulin (αt)	123093	Major component of the eukaryotic cytoskeleton	GGAGTCGCCTTGACCACAA/TGCCCTCACCAACGTACCA
β-tubulin (βt)	113871	Major component of the eukaryotic cytoskeleton	CAGGATCTTGTCGCCGAGTAC/CCTCATACTCGCCCTCCTCTT

$$Expression\ level = 10^4 \times 2^{C_t\beta t - C_t Tg} \quad (1)$$

This gives an arbitrary baseline expression of β-tubulin and α-tubulin of 10^4. As an internal control, the expression of βt and αt were compared using the same equation, showing a stable expression, with αt being expressed at approximately 80% relative to βt. Only data for βt was included in this paper.

2.6. Statistical analysis

All statistics were performed in JMP (Version Pro 13, SAS Institute Inc., Cary, NC, USA). Significance of differences in expression levels of each gene were calculated with Tukey's honest significant difference (HSD) test. A probability of ≤ 0.05 was the statistical type-I error level. Differences were compared between harvesting points within treatment, between the first harvesting points among treatments and between overall expressions of all harvesting points among treatments.

3. Results

3.1. Mass loss and wood moisture content

The mass losses for the acetylated samples are calculated relative to the post-acetylation dry mass and are thus lower compared to unmodified samples due to the added mass from the acetylation (Thybring, 2017). Mass loss could also be calculated relative to unmodified wood mass, but we cannot rule out that the fungus may degrade the modification agent along with the wood polymers. Acetyl groups are already present in substantial amounts in unmodified hemicelluloses (Rowell, 2005) and *R. placenta* possesses several enzymes with acetyl esterase activity capable of removing these groups (Zhang et al., 2016). Therefore, it is expected that the fungus would, at least partly, degrade the modification chemical with the same biochemistry it uses in unmodified wood and, consequently, fungal growth represented by mass loss is best determined in acetylated samples relative to the modified dry mass.

Mass loss was delayed as a result of acetylation and the initial lag phase increased with the degree of acetylation (Fig. 1). Significant mass loss was first detected after 2 weeks for control samples, 4 weeks for Ac13 samples, 6 weeks for Ac17 and 16 weeks for Ac21 samples. High standard deviations are most likely due to the small size of the test samples and the heterogeneity of the wood. It is important to note that once decay is established, the rate of degradation in acetylated samples is similar to that of unmodified wood. Particularly noteworthy is the high level of degradation achieved in the highly acetylated samples.

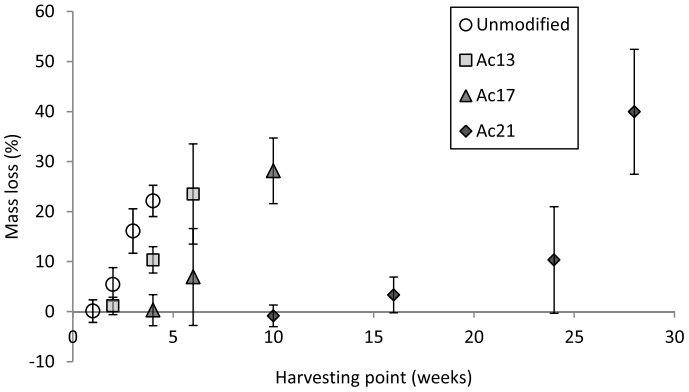

Fig. 1. Mass loss in percent for *Pinus radiata* (unmodified) and acetylated samples with WPG 13 (Ac13), WPG17 (Ac17) and WPG 21 (Ac21) at different harvesting points (weeks).

The wood moisture content after the last harvesting point was calculated relative to initial dry mass prior to decay, in order to correct for the mass lost during degradation (Thybring, 2017). These harvest moisture contents were as follows: control 58.3 ± 8.5% after 4 weeks, Ac13 38.7 ± 9.7% after 6 weeks, Ac17 26.3 ± 2.2% after 10 weeks, Ac21 31.0 ± 6% after 28 weeks. Significantly lower values for acetylated samples compared to controls (Tukey's HSD, $p < 0.05$) indicate the reduced water capacity of the acetylated cell wall.

3.2. Relative gene expression

The mean expression level (n = 3) of all selected genes were divided into five groups related to function and summed within each group (Fig. 2). The total summed expression level of the selected genes was lower in all initial harvesting points for the controls and for the three different acetylation levels when compared to later harvesting points. In the control samples at week 1, oxalic acid metabolism and oxidative genes constituted almost 60% of the relative expression. Hemicellulase expression was also relatively high, while the expression of the cellulolytic enzymes remained low. At the first harvesting point for the Ac13 samples, the relative expression of the oxalic acid synthesis genes was lower than the control, while the oxidative genes were at a similar level. The first harvesting point for the Ac17 and Ac21 samples were, on the other hand, dominated by oxidative genes. From 2 to 4 weeks a major up-regulation of the cellulases and hemicellulases was observed, with the relative expression of cellulases increasing over time in the control samples. A similar pattern was also observed in the acetylated samples. Interestingly, the relative expression of the oxidative genes remained high in the Ac21 samples even after 16 weeks when there was significant mass loss, and the relative expression of cellulases did not increase significantly until 24 weeks. Expansin expression was relatively higher in all initial harvesting points for all treatment levels and then showed a relative decrease in expression over time. In the more heavily acetylated samples Ac17 and Ac21, the relative expression of the two selected expansins was higher than in the control and the Ac13 samples.

3.3. Genes involved in oxidative depolymerisation

3.3.1. Oxalate synthesis and oxalate decomposition

Fig. 3 illustrates the two genes presumed to be involved in oxalic acid synthesis in *R. placenta* – glyoxylate dehydrogenase (GlyD Ppl121561) and oxaloacetate dehydrogenase (OahA Ppl112832) and one involved in oxalic acid degradation – oxalate decarboxylate (OxaD Ppl43912). No significant trends were observed in the expression levels of GlyD and OahA, except for a significant up-regulation for Ac17 w4 compared to w10.

The expression levels of OxaD were very low and should be interpreted with caution. Among the harvesting points within treatment, both Ac17 and Ac21 showed significant up-regulation for this gene at later harvesting points compared to early ones.

3.3.2. Redox enzymes

Fig. 4 illustrates six genes assumed to be involved in processes of oxidative brown-rot decay, including three GMC oxidoreductases (AOx1 Ppl44331, AOx2 Ppl129158 and AOx3 Ppl118723), two copper radical oxidases (Cro1 Ppl56703, Cro2 Ppl104114) and a benzoquinone reductase (BqR Ppl12517).

In unmodified samples no significant up-regulation was observed during early decay for any of the GMC oxidoreductases or copper radical oxidases. The only significant difference between harvesting points for unmodified samples was an up-regulation during late decay (w4 vs. w1 and w2) for AOx2. Interestingly, the GMC oxidoreductases and copper radical oxidases did not show a co-regulated expression pattern. BqR showed no significant difference between harvesting points.

Several of the genes involved in oxidative chemistry showed different expression patterns for acetylated samples compared to controls. AOx2 is significantly up-regulated in acetylated samples compared to unmodified samples when comparing the treatments at the initial decay harvesting point and when all harvesting points are pooled. Moreover, pooled harvesting point expression of AOx3 was significantly higher in Ac17 and Ac21 compared to controls and initial decay expression of Cro1 in Ac21 was significantly up-regulated compared to other treatments.

3.4. Hydrolytic enzymes involved in polysaccharide depolymerisation and LPMO

3.4.1. Cellulose degradation

Fig. 5 illustrates selected cellulose degrading enzymes. Expression levels of the three endocellulases (Cel5a Ppl115648, Cel5b Ppl103675 and Cel12a Ppl121191) and the betaglucosidase (bGlu Ppl128500) were delayed, with close to no transcription at the first harvesting points in both unmodified and acetylated samples. For Cel5a and Cel5b, expression at the initial harvesting point was significantly lower than later harvesting points for controls and acetylated samples (except Cel5b Ac21). Cel12a also showed significantly lower expression at the first harvesting point for Ac13 and Ac17 and bGlu expression was significantly lower at earlier incubation times for unmodified and Ac13 samples. Expression of these cellulose active enzymes was delayed for

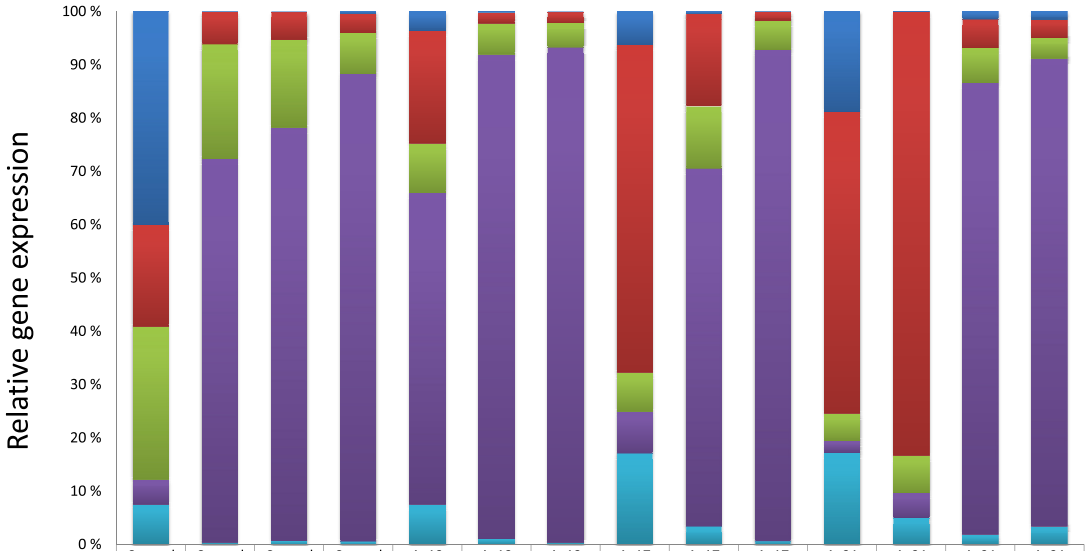

	Control week 1	Control week 2	Control week 3	Control week 4	Ac13 week2	Ac13 week 4	Ac13 week 6	Ac17 week4	Ac17 week6	Ac17 week10	Ac21 week 10	Ac21 week 16	Ac21 week 24	Ac21 week 28
Oxalate synthesis	12904	283	711	2088	8211	1828	1953	5336	1414	582	8067	278	5813	5777
Oxidative	6148	26524	31552	25405	48208	23136	33559	52467	65676	17568	24357	290476	20403	12939
Hemicellulolytic	9259	92267	101997	53603	21045	65948	77126	6159	44178	58905	2173	24286	25537	14324
Cellulolytic	1511	310489	479679	606412	133266	1028376	1535878	6824	253281	983356	975	16648	328117	331314
Expansins	2437	1898	4131	3677	16974	11953	6635	14502	12313	6507	7399	17185	7154	12846

Fig. 2. Relative expression of 22 R. *placenta* genes during decay of unmodified and acetylated (13, 17 and 21% WPG) *Pinus radiata* earlywood. The units given are arbitrary gene expression units, in relation to the constitutive beta-tubulin gene with an expression level of 10^4. Note that the sum total expression level varies between harvesting points and treatment levels.

acetylated samples compared to controls. For Ac21, expression levels of Cel5a, Cel5b, Cel12a and the LPMO were still negligible at 10 weeks of decay.

Generally, the *R. placenta* cellulose active enzymes showed lower levels of expression at higher levels of acetylation. Overall expression levels of pooled harvesting points for Cel5a and Cel12a were significantly reduced for Ac21 compared to Ac13 and bGlu was significantly reduced for Ac21 compared to both Ac13 and controls.

We were only able to detect expression of a single LPMO (Ppl126811). Unlike the other cellulose active enzymes which showed a tendency for down-regulation in acetylated samples, no significant differences were found in LPMO expression levels between treatments (Fig. 5). Within treatment, there was a significant up-regulation at the second harvesting point compared to the first harvesting point for Control, Ac17 and Ac21 samples. In control samples, this expression pattern correlates well with the expression of Cel5a and lags slightly behind that of bGlu.

3.4.2. Hemicellulose and pectin degradation

Fig. 6 illustrates expression of hemicellulose and pectin active enzymes. Expression levels of Man5a (Ppl121831) and the two endoxylanases (Xyl10a Ppl113670, Xyl10b Ppl105534) showed a similar trend within the control samples where the first harvesting point was down-regulated when compared to later harvesting points. This expression pattern for control samples is similar to Cel5a and Cel5b (Fig. 5) but relative expression levels are higher in the hemicellulases, particularly at the first harvesting point. CE16a (Ppl125801) expression in control samples followed the same pattern as Man5a, Xyl10a and Xyl10b showing a significant down-regulation at the first harvesting point compared to later harvesting points. There were no significant changes in expression levels of bXyl (Ppl51213) for control samples throughout degradation, but values tended to be higher at later harvesting points. Expression levels of Gal28a (Ppl111730) were up-regulated during the first harvesting point compared to later harvesting points for control samples.

The effect of acetylation on the level of hemicellulose and pectin active enzyme transcripts was variable. Both overall expression and expression level at the first harvesting point were up-regulated in control samples compared to all acetylated samples for Man5a, but no significant differences were observed for Xyl10a and Xyl10b. Comparison of expression levels of Gal28a at the first harvesting point showed significant up-regulation in control samples compared to all acetylated samples. Overall CE16a expression levels were significantly higher in control samples compared to Ac21.

3.5. Expansins

Fig. 7 illustrates the two selected genes predicted to encode expansins (Exp1 Ppl126976 and Exp2 Ppl128179). The expression of the two expansins was highly variable and no general trends were observed in unmodified samples at the various stages of decay. Overall expression levels of pooled harvesting points for Exp1 were up-regulated in Ac13 compared to the other treatments and for Exp2 they were up-regulated in all acetylated samples compared to control samples.

4. Discussion

4.1. Mass loss and wood moisture content

Much of the literature on decay of acetylated wood claims that

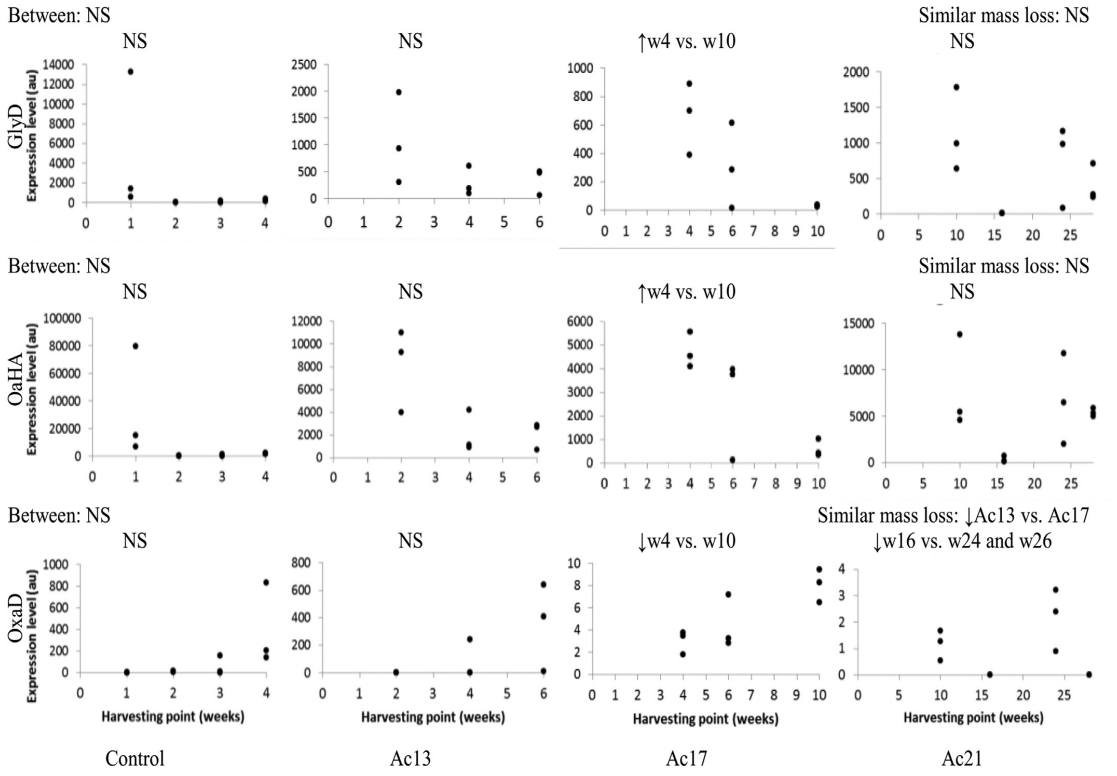

Fig. 3. Oxalate synthesis (glyoxylate dehydrogenase, GlyD Ppl125161, oxaloacetate dehydrogenase OahA, Ppl112832) and oxalate decomposition (oxalate decarboxylase OxaD Ppl43912) at different harvesting points (weeks). Tukey's HSD comparisons are provided between treatments (top row left), between treatments at the first harvesting point (top row right), and within treatments (second row).

acetylation of around 20% WPG infers complete resistance to fungal degradation (Goldstein et al., 1961; Peterson and Thomas, 1978; Kumar and Agarwal, 1983; Takahashi et al., 1989; Beckers et al., 1994; Papadopoulos and Hill, 2002; Mohebby, 2003; Hill et al., 2006). However, as suggested by Hill (2006), this protection threshold may only be present due to the insufficient timeframe of the standard decay experiments employed. Studies using longer decay periods (> 250 days) have shown low but observable mass loss (< 5%) for 20% WPG acetylated wood decayed with *R. placenta*, which indicates that decay is not fully inhibited by the modification but rather delayed (Alfredsen et al., 2016b; Ringman et al., 2017). The results of this study confirm this delay for brown-rot degradation in acetylated wood. However, the mass losses obtained for highly acetylated samples reported here are much higher than those of the aforementioned studies which used even longer decay periods (Fig. 1). The smaller wood sample dimensions used in the current study provide a possible explanation for the much higher mass losses reported. The higher surface area to volume ratio of smaller samples may facilitate diffusion of water into the wood cell walls and thus promote fungal degradation.

The acetylated cell wall has reduced water capacity compared to the native wood cell wall (Papadopoulos and Hill, 2003; Popescu et al., 2014; Passarini et al., 2017; Beck et al., 2017b). Lower wood moisture contents after the last harvesting point for more highly acetylated samples indicate this reduced water capacity.

4.2. Relative gene expression

For the unmodified wood samples at the first harvesting point, the relatively high hemicellulase expression indicates that the fungus most likely was in a transitional phase from oxidative degradation to hydrolytic depolymerisation, while the expression of the cellulolytic enzymes remained relatively low (Fig. 2). Up-regulation of hemicellulases prior to cellulases in control samples is in agreement with previous observations that hemicelluloses are selectively removed prior to cellulose in brown-rot decayed wood (Winandy and Morrell, 1993; Irbe et al., 2006). This trend was also observed in the acetylated samples.

The oxidative genes were highly represented at the first harvesting point for the Ac17 and Ac21 samples which may suggest that the fungus was still in the oxidative pre-treatment stage of decay. For the Ac21 samples, reduction in the relative expression levels of oxidative genes did not occur until week 24. Here it is important to note that the major contributor to this relative high expression in these particular samples was AOx3 (93% of the expression in the oxidative category). This GMC oxidoreductase shows a high degree of similarity to known methanol oxidases (Waterham et al., 1997). We hypothesise that acetylation leads to an increased need for oxidative depolymerisation, and that this oxidative attack more severely demethoxylates lignin, generating methanol. AOx3 would then oxidise and detoxify the methanol, generating H_2O_2 as a by-product (Filley et al., 2002; Niemenmaa et al., 2008).

Expansin expression was relatively higher in the Ac17 and Ac21 samples at the first harvesting point in comparison to Ac13 and control samples. A possible explanation for this is an increased need for

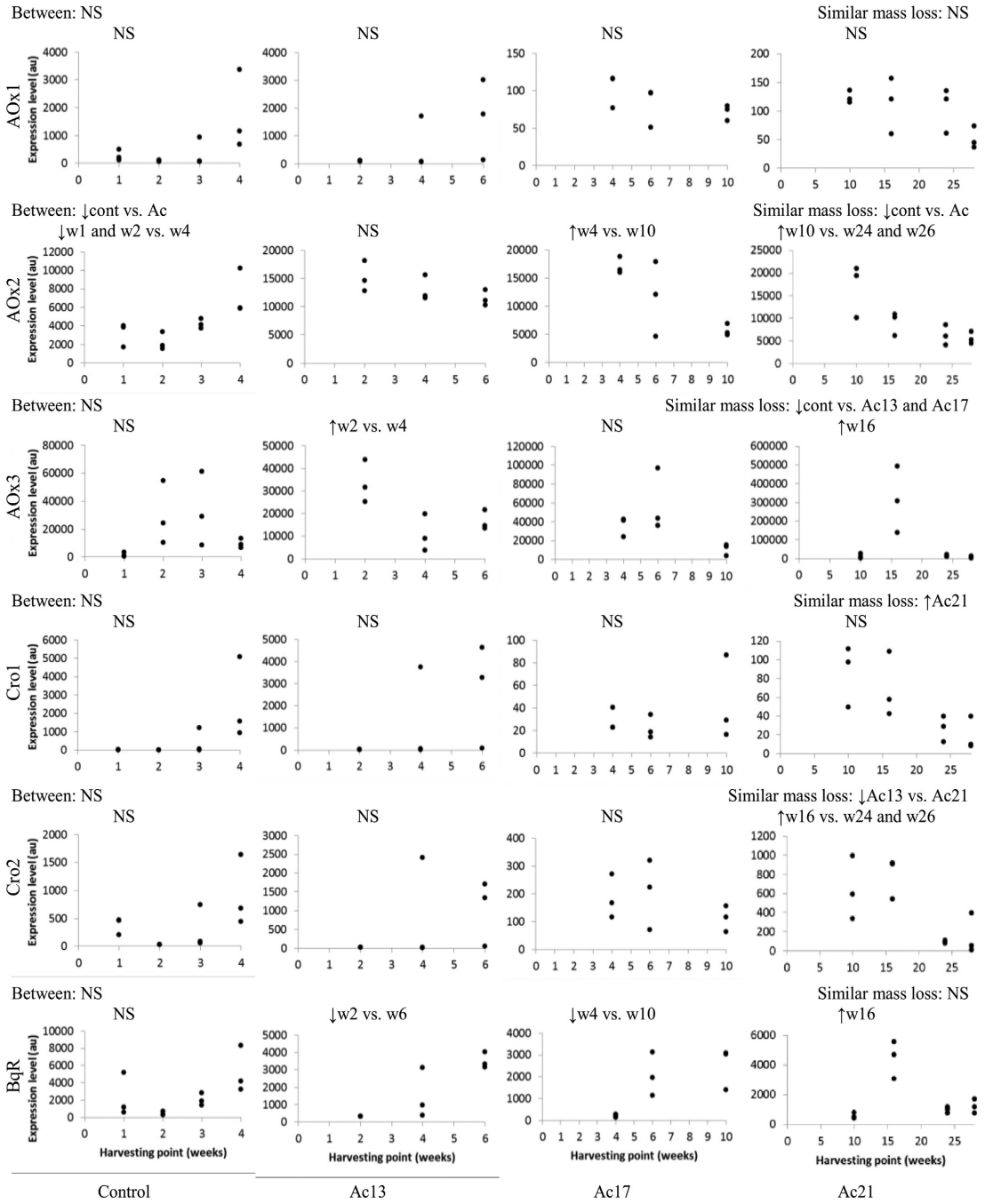

Fig. 4. Redox enzymes at different harvesting points (weeks). Tukey's HSD comparisons are provided between treatments (top row left), between treatments at the first harvesting point (top row right), and within treatments (second row).

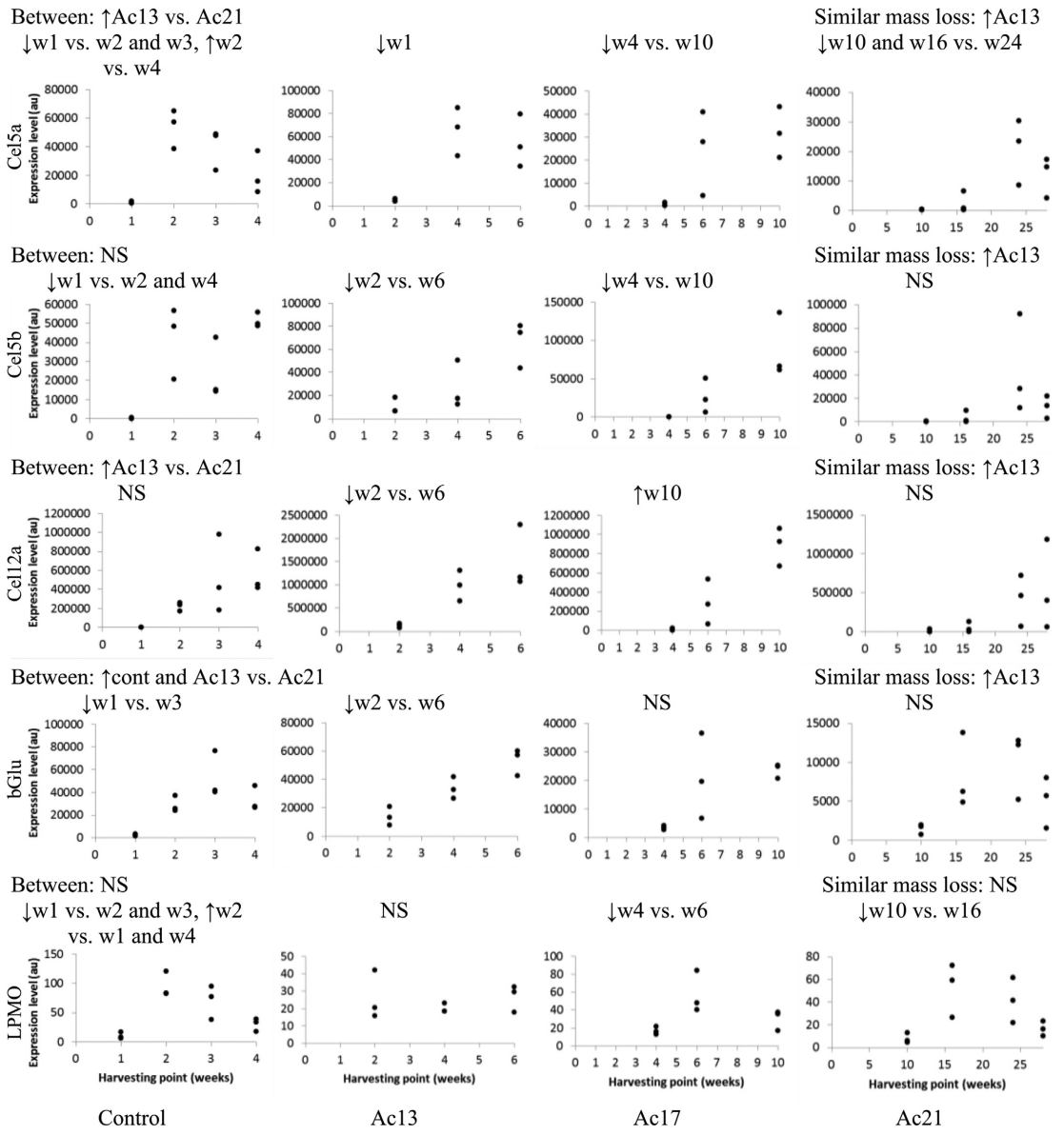

Fig. 5. Cellulose degrading enzymes at different harvesting points (weeks). Tukey's HSD comparisons are provided between treatments (top row left), between treatments at the first harvesting point (top row right), and within treatments (second row).

opening of the wood cell-wall structure due to the increased bulking caused by acetylation.

4.3. Genes involved in oxidative depolymerisation

4.3.1. Oxalate synthesis and oxalate decomposition

Brown-rot fungi are known to secrete organic acids, including oxalic acid. Calcium oxalate crystals have been found in furfurylated wood (Alfredsen et al., 2016a), thermally modified and acetylated wood (Pilgård et al., 2017). Oxalic acid is, according to Arantes and Goodell (2014), assumed to play an important role as an iron chelator and a phase transfer agent in the CMF system. The selected genes have previously been shown to be regulated spatially during decay by *P. placenta* MAD-698, with the GlyD and OahA being up-regulated at the hyphal front and OxaD up-regulated in older parts of the hyphae (Zhang et al., 2016). Alfredsen et al. (2016a,b) studied five genes involved in oxalic acid metabolism after 2–8 weeks of incubation and found no statistically significant changes in gene expression during *R. placenta* decay in *P. sylvestris* sapwood. The lack of statistical trends in that study and the results presented here for up-regulation of genes involved in oxalic acid

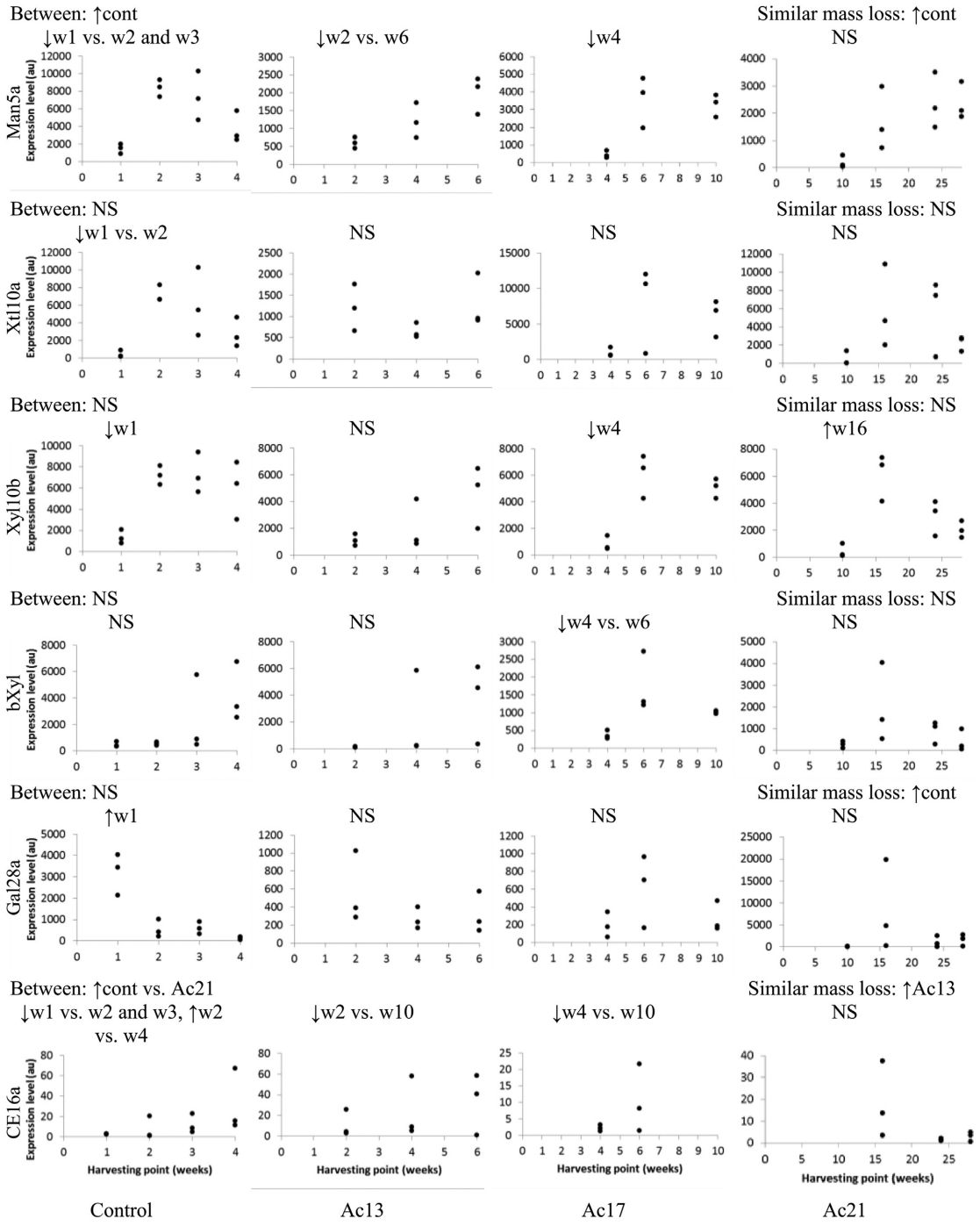

Fig. 6. Hemicellulose and pectin degrading enzymes at different harvesting pints (weeks). Tukey's HSD comparisons are provided between treatments (top row left), between treatments at the first harvesting point (top row right), and within treatments (second row).

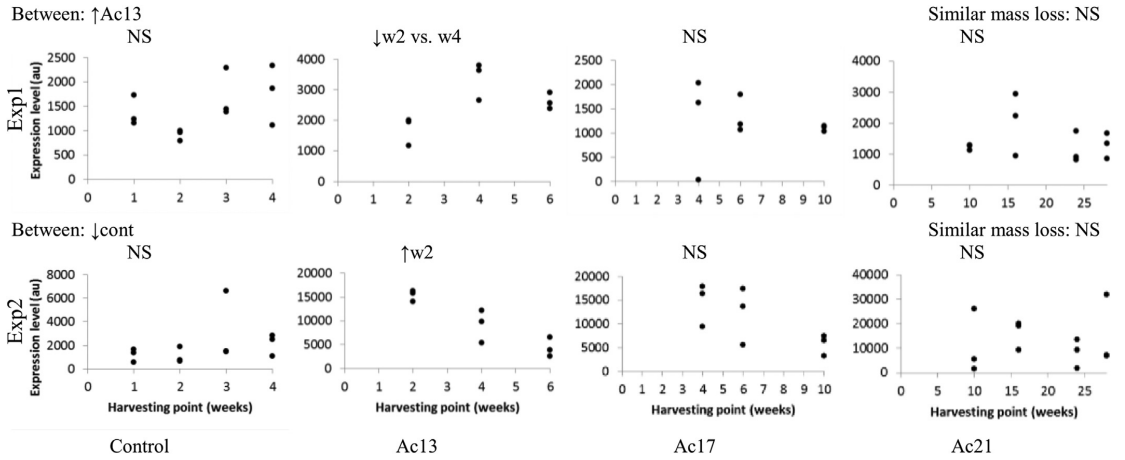

Fig. 7. Expansin enzymes at different harvesting pints (weeks). Tukey's HSD comparisons are provided between treatments (top row left), between treatments at the first harvesting point (top row right), and within treatments (second row).

synthesis (GlyD and OahA) during the early decay stage (except Ac17, Fig. 3) may be because the harvesting points selected did not capture the early peak of expression. Zhang et al. (2016) showed that after only 48 h of growth, *R. placenta* has already begun the transition from oxidative pre-treatment to enzymatic polysaccharide hydrolysis. This suggests that the shortest incubation time of the present study (1 week) may not capture this oxidative behaviour. Later expression of OxaD agrees with the results of Zhang et al. (2016) and affirms the role of this enzyme in oxalic acid decomposition.

4.3.2. Redox enzymes

GMC oxidoreductases (CAZy family AA3) are a family of flavoenzymes that oxidise aliphatic alcohols, aryl alcohols and mono- and disaccharides. This oxidation is coupled with the reduction of a variety of electron acceptors, including O_2 (resulting in the formation of H_2O_2), quinones or other enzymes (such as LPMOs) (Sützl et al., 2018). Copper radical oxidases (CAZy family AA5) are known to be a major constituent of the secretome of several brown rot fungi (Kersten and Cullen, 2014). They oxidise a variety of substrates, with the concurrent production of H_2O_2 via the reduction of O_2. Benzoquinone reductases (CAZy family AA6) are intracellular enzymes that protect the fungus from toxic compounds, but have also been suggested to contribute to a non-enzymatic depolymerisation of wood cell wall components by mediating the regeneration/reduction of catecholate iron chelators (Jensen et al., 2002).

It has been suggested that the role of GMC oxidoreductases and copper radical oxidases during brown-rot decay is to generate H_2O_2 which reacts with ferrous iron in the CMF system during initial oxidative degradation (Arantes and Goodell, 2014). In unmodified samples no significant up-regulation was observed in this study during early decay for any of the five members analysed in these two families (Fig. 4). Zhang and Schilling (2017) found gradual up-regulation of AOx3 and Cro1 in *R. placenta* incubated on spruce media for 70 h and Zhang et al. (2016) reported up-regulation of the same genes at the hyphal front compared to older parts of the hyphae for *R. placenta* grown on solid spruce wood. As mentioned previously, the first harvesting point used in this study may have failed to capture the early oxidation behaviour. Alfredsen et al. (2016b) and Ringman et al. (2014b) were also unable to find any significant differences in *R. placenta* degraded Scots pine sapwood between 2 week and 8 week harvesting points for AOx3.

The lack of co-regulation of the enzymes in the GMC oxidoreductase and copper radical oxidase families suggests different roles for the individual enzymes within the same families. H_2O_2 is known to be damaging to enzymes, and the current paradigm suggests that the oxidative and the hydrolytic systems need to be spatially separated. Up-regulation of AOx2 during later decay stages may suggest that this particular enzyme does not produce H_2O_2, but instead detoxifies and reduces quinone derived compounds, potentially serving as Fe^{3+} reductants, thereby regenerating them in a similar manner to benzoquinone reductases (Jensen et al., 2002; Cohen et al., 2004; Arantes and Goodell, 2014). It is important to note here that even though several of the genes chosen here have a proposed function, they are not as well characterised and understood as those involved in hydrolytic depolymerisation.

Higher expression levels of redox enzymes in samples with higher degrees of acetylation suggest that the oxidative system of *R. placenta* is more active in acetylated wood. This is in accordance with previous work which has shown up-regulation of redox enzymes in both acetylated (Alfredsen and Pilgård, 2014; Alfredsen et al., 2016b) and chemically modified wood (Alfredsen and Fossdal, 2009; Ringman et al., 2014b; Alfredsen et al., 2016a). The reduced water capacity of the acetylated cell wall (Papadopoulos and Hill, 2003; Popescu et al., 2014; Passarini et al., 2017; Beck et al., 2017b) will reduce the rate of diffusion into it and may hinder the oxidative system. Since it appears that the transition from oxidative degradation to enzymatic hydrolysis is triggered by the presence of degradation products like cellobiose (Zhang and Schilling, 2017) which must diffuse out of the cell wall (Goodell et al., 2017), the slower diffusion rate in acetylated wood may delay the signal to switch between the two systems.

4.4. Hydrolytic enzymes involved in polysaccharide depolymerisation and LPMO

4.4.1. Cellulose degradation

The two endoglucanases, Cel5a and Cel5b, cause chain breaks in amorphous cellulose. In addition, we chose one endoglucanase, Cel12a, in CAZy family GH12 that, based on sequence similarity, is most likely an endocellulase. The *R. placenta* genome contains no known processive cellulases (cellobiohydrolases), and it is not well understood how the depolymerisation of cellulose to cellobiose by *R. placenta* occurs. One possibility is that its endocellulases can hydrolyse soluble short chain cellulose oligomers that have been generated via the oxidative mechanism. Betaglucosidases (CAZY family GH3) are enzymes that release

glucose from the non-reducing end of disaccharides and oligosaccharides and play a key role in all wood decaying organisms, as they catalyse the final glucose producing step. We chose one cellobiose active betaglucosidase, bGlu, and one xylobiose active betaglucosidase, bXyl (see next section), from family GH3 that are known to be highly expressed by *R. placenta* (Zhang et al., 2016).

Higher expression levels during later decay for the cellulose degradating enzymes observed in this study (Fig. 5) agrees with the theory that enzymatic saccharification is segregated from the potentially damaging CMF system (Arantes et al., 2012; Zhang et al., 2016).

Higher levels of acetylation resulted in lower levels of expression for the cellulose active enzymes. Zhang and Schilling (2017) showed that the transcription of these cellulase genes is induced by the presence of cellobiose. In highly acetylated samples, mass loss includes not only the degraded wood polysaccharides capable of producing cellobiose, but also the added mass of the acetyl groups. This may contribute to lower cellobiose concentration at equivalent levels of mass loss for more highly acetylated samples. Additionally, some of the cellobiose produced via oxidative degradation in acetylated samples may remain partially acetylated. This acetylated cellobiose may be less effective in triggering production of saccharification enzymes.

The delayed expression of cellulolytic enzymes and concurrent delayed mass loss in highly acetylated samples raises the question of what nutrient source the fungus is utilising during this period of apparent inactivity. Some nutrition may be available to the fungus from the soil in the Petri dish. Brown rot fungi have been shown to translocate calcium and magnesium from forest soils into woody debris (Smith et al., 2007; Schilling and Bissonnette, 2008). It seems the fungus is able to sustain the oxidative system in highly acetylated wood with only the limited amount of nutrition available to it in the soil.

LPMOs are a class of oxidative enzymes that are known to cause chain breaks in crystalline and amorphous regions of both cellulose and hemicelluloses. Eukaryotic LPMOs are placed in CAZy auxiliary activity families 9, 11, 13 and 14, with AA9s showing activity on both cellulose and hemicelluloses. The *R. placenta* genome contains two AA9s (Martinez et al., 2009; Zhang et al., 2016), but we were only able to detect expression of a single one (Ppl126811). Although the expression level is several orders of magnitude lower than the classical cellulases, AA9s are known to play a major role as catalysts of efficient cellulose depolymerisation (Hemsworth et al., 2015). No significant differences were found between treatments for expression levels of the LPMO assessed here. This suggests that LPMO expression may not be regulated by the same mechanism as the other enzymes, or that the expression levels were too low to detect any significant differences. Whether cellobiose, which induces the expression of Cel5a, Cel5b, Cel12a and bGlu (Zhang and Schilling, 2017), also controls LPMO expression is not known. LPMOs, like other cellulolytic enzymes, are sensitive to H_2O_2 and will be deactivated in the presence of high ROS concentrations. Thus, they also need to be separated from the oxidative system.

In control samples, the LPMO expression levels correlate with those of Cel5a and lag slightly behind those of bGlu. Coordinated expression of the LPMO with Cel5a affirms the auxiliary role of the LPMO. Betaglucosidase, which showed highest expression levels after three weeks in the control samples, reflects a high production of soluble cellulose oligomers at this stage.

4.4.2. Hemicellulose and pectin degradation

In addition to the limited set of cellulases, the *R. placenta* genome also contains a suite of hemicellulases that attack and depolymerise a wide variety of polysaccharides, including xylans, mannans and other glucans. In this study, we assessed one endomannanase in CAZy family GH5 (Man5a), two endoxylanases in CAZy family GH10 (Xyl10a and Xyl10b) and one betaxylosidase in CAZy family GH3 (bXyl). Enzymes capable of deacetylating polysaccharides were of particular interest for this study. We selected several carbohydrate esterases, but were only able to detect expression of one in CAZy family CE16 (CE16a). Esterases in family CE16 are polysaccharide esterases known to deacetylate xylans and glucans (Li et al., 2008; Zhang et al., 2011). The *R. placenta* genome does not contain any carbohydrate esterases in the well characterised families CE1 and CE2 (Martinez et al., 2009).

For control samples, Man5a, Xyl10a, Xyl10b and CE16a were down-regulated at the first harvesting point and showed coordinated up-regulation at later harvest points (Fig. 6). This coordinated expression indicates the synergistic role of CE16a in deacetylating the hemicelluloses to facilitate their hydrolysis by the hemicellulase enzymes.

Based on previously published work by Zhang et al. (2016), we selected a polygalacturonase in CAZy family GH28 that is highly expressed during decay (Gal28a). Brown-rot fungi have been shown to rapidly degrade pectin during incipient decay because it is a readily available carbohydrate and its removal from pit membranes allows the fungus to further colonise the wood (Tschernitz and Sachs, 1975, Green III et al., 1996). With its high galacturonic acid content, pectin is highly vulnerable to hydrolysis by Gal28a. Thus, the up-regulation of this gene during early decay gives access to an important carbon source when the other carbohydrates remain inaccessible.

Comparing acetylated samples to control samples, both overall expression and expression level at the first harvesting point were up-regulated in all acetylated samples compared to controls for Man5a, while no significant differences were observed for Xyl10a and Xyl10b. Zhang and Schilling (2017) showed Man5a was strongly up-regulated in the presence of cellobiose compared to no carbon source controls, while Xyl10a expression was unaffected by cellobiose and Xyl10b expression was only significantly up-regulated by cellobiose during the first 24 h of incubation. The effect of acetylation on cellobiose concentration discussed previously in section 4.4.1 may explain the significant down-regulation of Man5a in acetylated samples.

Pectin may be degraded by the sustained high temperature used during the acetylation reaction. Thus, less available pectin in acetylated samples may explain the lower expression levels of Gal28a compared to controls. As mentioned above, pectin might serve as an important initial carbon source, thus if some is removed during treatment this will further inhibit initial fungal growth.

The fact that overall expression levels of CE16a were significantly higher in control samples than in Ac21 samples was surprising. With higher acetylation levels one might expect up-regulation of enzymes capable of deacetylating wood polysaccharides. It was hypothesised that these enzymes would be part of the machinery involved in deacetylating the wood polymers facilitating hemicellulase and cellulase degradation. Deacetylation of the wood polymers is necessary for the cellulase and hemicellulase enzymes to function most efficiently, and a negative impact of cellulose acetylation has been reported (Pan et al., 2006). However, Ringman et al. (2015) showed that cellulase enzymes are still capable of degradating acetylated substrates, and it has even been suggested that under certain conditions acetylation will actually improve saccharification of the cellulose polymer (Olaru et al., 2011). Furthermore, deacetylation may still occur in acetylated wood but it may happen during initial oxidative degradation. We hypothesise that CE16a is regulated through a negative feedback system, where acetic acid, potentially produced via deacetylation during oxidative degradation, supresses CE16a expression.

4.5. Expansins

Expansins are enigmatic proteins with no known catalytic activity involved in cell wall loosening that synergistically increase the depolymerisation of wood cell wall components when acting in concert with cellulases and hemicellulases. They are believed to increase enzyme access by loosening plant cell-wall interactions (Rose and Bennett, 1999; Baker et al., 2000; Arantes and Saddler, 2010). The significantly higher expression levels observed for the two expansin genes (Fig. 7) and the higher relative expression for the expansin group (Fig. 2) compared to control samples suggest the fungus may up-regulate

expression of these enzymes to cope with the lower cell wall nanoporsity in acetylated wood (Hill et al., 2005).

5. Conclusion

As previously reported, the expression of oxidative genes of *R. placenta* was upregulated in wood with higher degrees of acetylation and the expression of cellulose active genes was delayed for acetylated samples compared to untreated samples. The delay observed for cellulose active enzymes could be due to the slower diffusion rate in acetylated wood or that acetylated cellobiose is less effective in triggering production of the saccharification enzymes. The gene expression analysis revealed differential expression of selected genes not previously reported. We demonstrate specific upregulation of expansins believed to be involved in creating access to acetylated wood cell wall components. The studied carbohydrate esterase appeared to be under the influence of a negative feedback system.

Declarations of interest

None.

Acknowledgments

Sigrun Kolstad and Inger Heldal are acknowledged for molecular analyses. This project was financed by NIBIO (PhD scholarship project no. 335006) and The Research Council of Norway 243663/E50 BioMim.

References

Alfredsen, G., Fossdal, C.G., 2009. *Postia placenta* Gene Expression of Oxidative and Carbohydrate Metabolism Related Genes during Growth in Furfurylated Wood. IRG/WP 09-10701. The International Research Group on Wood Protection, Stockholm, Sweden.

Alfredsen, G., Pilgård, A., 2014. *Postia placenta* decay of acetic anhydride modified wood – effect of leaching. Wood Mater. Sci. Eng. 9 (3), 162–169.

Alfredsen, G., Fossdal, C.G., Nagy, N.E., Jellison, J., Goodell, B., 2016a. Furfurylated wood - impact on *Postia placenta* gene expression and oxalate crystal formation. Holzforchung 70 (10), 947–962.

Alfredsen, G., Pilgård, A., Fossdal, C.G., 2016b. Characterisation of *Postia placenta* colonisation during 36 weeks in acetylated southern yellow pine sapwood at three acetylation levels including genomic DNA and gene expression quantification of the fungus. Holzforschung 70 (11), 1055–1065.

Arantes, V., Goodell, B., 2014. Current understanding of brown-rot fungal biodegradation mechanisms: a review. In: Deterioration and Protection of Sustainable Biomaterials, vol 1158. American Chemical Society, pp. 3–21.

Arantes, V., Jellison, J., Goodell, B., 2012. Peculiarities of brown-rot fungi and biochemical Fenton reaction with regard to their potential as a model for bioprocessing biomass. Appl. Microbiol. Biotechnol. 94 (2), 323–338.

Arantes, V., Qian, Y., Milagres, A.M., Jellison, J., Goodell, B., 2009. Effect of pH and oxalic acid on the reduction of Fe 3+ by a biomimetic chelator and on Fe 3+ desorption/adsorption onto wood: implications for brown-rot decay. Int. Biodeterior. Biodegrad. 63 (4), 478–483.

Arantes, V., Saddler, J.N., 2010. Access to cellulose limits the efficiency of enzymatic hydrolysis: the role of amorphogenesis. Biotechnol. Biofuels 3 (1), 4.

Baker, J.O., King, M.R., Adney, W.S., Decker, S.R., Vinzant, T.B., Lantz, S.E., Nieves, R.E., Thomas, S.R., Li, L.-C., Cosgrove, D.J., Himmel, M.E., 2000. Investigation of the cell-wall loosening protein expansin as a possible additive in the enzymatic saccharification of lignocellulosic biomass. In: Finkelstein, M., Davidson, B.H. (Eds.), Twenty-first Symposium on Biotechnology for Fuels and Chemicals. Applied Biochemistry and Biotechnology. Humana Press, Totowa, NJ, USA, pp. 217–223.

Beck, G., Strohbusch, S., Larnøy, E., Militz, H., Hill, C.A.S., 2017a. Accessibility of hydroxyl groups in anhydride modified wood as measured by deuterium exchange and saponification. Holzforschung 72 (1), 17–23.

Beck, G., Thybring, E.E., Thygesen, L.G., Hill, C.A.S., 2017b. Characterisation of moisture in acetylated and propionylated radiata pine using low-field nuclear magnetic resonance (LFNMR) relaxometry. Holzforschung 72 (3), 225–233.

Beckers, E.P.J., Militz, H., Stevens, M., 1994. Resistance of Wood to Basidiomycetes, Soft Rot and Blue Stain. IRG/WP 94-40021. The International Research Group on Wood Protection, Stockholm, Sweden.

CEN, 1997. EN113. Wood Preservatives - Test Method for Determining the Protective Effectiveness against Wood Destroying Basidiomycetes. Determination of the Toxic Values. CEN (European committee for standardization), Brussels.

CEN, 2001. ENV807. Wood Preservatives - Determination of the Effectiveness against Soft Rotting Micro-fungi and Other Soil Inhabiting Micro-organisms. CEN (European committee for standardization), Brussels.

Cowling, E.B., 1961. Comparative Biochemistry of the Decay of Sweetgum Sapwood by White-rot and Brown-rot Fungi. No. 1258. US Dept. of Agriculture., Washington, USA.

Cohen, R., Suzuki, M.R., Hammel, K.E., 2004. Differential stress-induced regulation of two quinone reductases in the brown rot basidiomycete *Gloeophyllum trabeum*. Appl. Environ. Microbiol. 70 (1), 324–331.

Eastwood, D.C., Floudas, D., Binder, M., Majcherczyk, A., Schneider, P., Aerts, A., Asiegbu, F.O., Baker, S.E., Barry, K., Bendiksby, M., Blumentritt, M., Coutinho, P.M., Cullen, D., de Vries, R.P., Gathman, l., Goodell, B., Henrissat, B., Ihrmark, K., Kauserud, H., Kohler, A., LaButti, K., Lapidus, A., Lavin, J.L., Lee, Y.-H., Lindquist, E., Lilly, W., Lucas, S., Morin, E., Murat, C., Oguiza, J.A., Park, J., Pisabarro, A.G., Riley, R., Rosling, A., Salamov, A., Schmidt, O., Schmutz, J., Skrede, I., Stenlid, J., Wiebenga, A., Xie, X., Kües, U., Hibbett, D.S., Hoffmeister, D., Högberg, N., Martin, F., Grigoriev, I.V., Watkinson, S.C., 2011. The plant cell wall–decomposing machinery underlies the functional diversity of forest fungi. Science 333 (6043), 762–765.

Filley, T.R., Cody, G.D., Goodell, B., Jellison, J., Noser, C., Ostrofsky, A., 2002. Lignin demethylation and polysaccharide decomposition in spruce sapwood degraded by brown rot fungi. Org. Geochem. 33 (2), 111–124.

Flournoy, D.S., Kirk, T.K., Highley, T., 1991. Wood decay by brown-rot fungi: changes in pore structure and cell wall volume. Holzforschung 45 (5), 383–388.

Floudas, D., Binder, M., Riley, R., Barry, K., Blanchette, R.A., Henrissat, B., Martínez, A.T., Otillar, R., Spatafora, J.W., Yadav, J.S., Aerts, A., Benoit, I., Boyd, A., Carlson, A., Copeland, A., Coutinho, P.M., de Vries, R.P., Ferreira, P., Findley, K., Foster, B., Gaskell, J., Glotzer, D., Górecki, P., Heitman, J., Hesse, C., Hori, C., Igarashi, K., Jurgens, J.A., Kallen, N., Kersten, P., Kohler, A., Kües, U., Kumar, T.K., Kuo, A., LaButti, K., Larrondo, L.F., Lindquist, E., Ling, A., Lombard, V., Lucas, S., Lundell, T., Martin, R., McLaughlin, D.J., Morgenstern, I., Morin, E., Murat, C., Nagy, L.G., Nolan, M., Ohm, R.A., Patyshakuliyeva, A., Rokas, A., Ruiz-Dueñas, F.J., Sabat, G., Salamov, A., Samejima, M., Schmutz, J., Slot, J.C., St John, F., Stenlid, J., Sun, H., Sun, S., Syed, K., Tsang, A., Wiebenga, A., Young, D., Pisabarro, A., Eastwood, D.C., Martin, F., Cullen, D., Grigoriev, I.V., Hibbett, D.S., 2012. The Paleozoic origin of enzymatic lignin decomposition reconstructed from 31 fungal genomes. Science 336 (6089), 1715–1759.

Goldstein, I.S., Jeroski, E.B., Lund, A.E., Nielson, J.F., Weaver, J.W., 1961. Acetylation of wood in lumber thickness. For. Prod. J. 11, 363–370.

Goodell, B., Jellison, J., Liu, J., Daniel, G., Paszczynski, A., Fekete, F., Krishnamurthy, S., Jun, L., Xu, G., 1997. Low molecular weight chelators and phenolic compounds isolated from wood decay fungi and their role in the fungal biodegradation of wood. J. Biotechnol. 53, 133–162.

Goodell, B., Zhu, Y., Kim, S., Kafle, K., Eastwood, D., Daniel, G., Jellison, J., Yoshida, M., Groom, L., Pingali, S.V., O'Neill, H., 2017. Modification of the nanostructure of lignocellulose cell walls via a non-enzymatic lignocellulose deconstruction system in brown rot wood-decay fungi. Biotechnol. Biofuels 10, 179.

Green III, F., Clausen, C.A., Larsen, M.J., Highley, T.L., 1992. Immuno-scanning electron microscopic localization of extracellular wood-degrading enzymes within the fibrillar sheath of the brown-rot fungus Postia placenta. Can. J. Microbiol. 38 (9), 898–904.

Green III, F., Kuster, T.A., Highley, T.L., 1996. Pectin degradation during colonization of wood by brown-rot fungi. Recent Res. Dev. Plant Pathol. 1, 83–93.

Hemsworth, G.R., Johnston, E.M., Davies, G.J., Walton, P.H., 2015. Lytic polysaccharide monooxygenases in biomass conversion. Trends Biotechnol. 33 (12), 747–761.

Hill, C.A.S., 2006. Wood Modification: Chemical, Thermal and Other Processes. John Wiley & Sons.

Hill, C.A.S., Forster, S.C., Farahani, M.R.M., Hale, M.D.C., Ormondroyd, G.A., Williams, G.R., 2005. An investigation of cell wall micropore blocking as a possible mechanism for the decay resistance of anhydride modified wood. Int. Biodeterior. Biodegrad. 55 (1), 69–76.

Hill, C.A.S., Hale, M.D., Ormondroyd, G.A., Kwon, J.H., Forster, S.C., 2006. Decay resistance of anhydride-modified Corsican pine sapwood exposed to the brown-rot fungus *Coniophora puteana*. Holzforschung 60, 625–629.

Irbe, I., Andersons, B., Chirkova, J., Kallavus, U., Andersone, I., Faix, O., 2006. On the changes of pinewood (*Pinus sylvestris* L.) Chemical composition and ultrastructure during the attack by brown-rot fungi *Postia placenta* and *Coniophora puteana*. Int. Biodeterior. Biodegrad. 57 (2), 99–106.

Jensen Jr., K.A., Ryan, Z.C., Wymelenberg, A.V., Cullen, D., Hammel, K.E., 2002. An NADH: quinone oxidoreductase active during biodegradation by the brown-rot basidiomycete *Gloeophyllum trabeum*. Appl. Environ. Microbiol. 68 (6), 2699–2703.

Kersten, P., Cullen, D., 2014. Copper radical oxidases and related extracellular oxidoreductases of wood-decay Agaricomycetes. Fungal Genet. Biol. 72, 124–130.

Kim, Y.S., Goodell, B., Jellison, J., 2009. Immuno-electron microscopic localization of extracellular metabolites in spruce wood decayed by brown-rot fungus *Postia placenta*. Holzforschung 45 (5), 389–393.

Kumar, S., Agarwal, S.C., 1983. Biological Degradation Resistance of Wood Acetylated with Thioacetic Acid. IRG/WP 83-3223. The International Research Group on Wood Protection, Stockholm, Sweden.

Levasseur, A., Drula, E., Lombard, V., Coutinho, P.M., Henrissat, B., 2013. Expansion of the enzymatic repertoire of the CAZy database to integrate auxiliary redox enzymes. Biotechnol. Biofuels 6 (1), 41.

Li, X.L., Skory, C.D., Cotta, M.A., Puchart, V., Biely, P., 2008. Novel family of carbohydrate esterases, based on identification of the Hypocrea jecorina acetyl esterase gene. Appl. Environ. Microbiol. 74 (24), 7482–7489.

Lombard, V., Golaconda, Ramulu, H., Drula, E., Coutinho, P.M., Henrissat, B., 2013. The carbohydrate-active enzymes database (CAZy) in 2013. Nucleic Acids Res. 42 (1), 490–495.

Martinez, D., Challacombea, J., Morgensternc, I., Hibbettc, D., Schmolld, M., Kubicekd,

C.P., Ferreirae, P., Ruiz-Duenase, F.J., Martineze, A.T., Kerstenf, P., Hammelf, K.E., Vanden Wymelenberg, A., Gaskellf, J., Lindquisth, E., Sabati, G., BonDuranti, S.S., Larrondoj, L.F., Canessaj, P., Vicunaj, R., Yadavk, J., Doddapanenik, H., Subramaniank, V., Pisabarrol, A.G., Lavínl, J.L., Oguizal, J.A., Masterm, E., Henrissatn, B., Coutinhon, P.M., Harriso, P., Magnusonp, J.K., Bakerp, S.E., Brunop, K., Kenealyq, W., Hoegger, P.J., Kuesr, U., Ramaiyao, P., Lucash, S., Salamovh, A., Shapiroh, H., Tuh, H., Cheeb, C.L., Misraa, M., Xiea, G., Tetero, S., Yavero, D., Jamess, T., Mokrejst, M., Pospisekt, M., Grigorievh, I.V., Brettina, T., Rokhsarh, D., Berkao, R., Cullenf, D., 2009. Genome, transcriptome, and secretome analysis of wood decay fungus *Postia placenta* supports unique mechanisms of lignocellulose conversion. Proc. Natl. Acad. Sci. Unit. States Am. 106 (6), 1954–1959.

Mohebby, B., 2003. Biologicial Attack of Acetylated Wood. PhD Thesis. Institute of Wood Biology and Wood Technology. Georg-August-Universität Göttingen. Göttingen, Germany.

Niemenmaa, O., Uusi-Rauva, A., Hatakka, A., 2008. Demethoxylation of [O 14 CH 3]-labelled lignin model compounds by the brown-rot fungi *Gloeophyllum trabeum* and *Poria (Postia) placenta*. Biodegradation 19 (4), 555.

Olaru, N., Olaru, L., Vasile, C., Ander, P., 2011. Surface modified cellulose obtained by acetylation without solvents of bleached and unbleached kraft pulps. Polimery 56.

Pan, X., Gilkes, N., Saddler, J.N., 2006. Effect of acetyl groups on enzymatic hydrolysis of cellulosic substrates. Holzforschung 60 (4), 398–401.

Papadopoulos, A.N., Hill, C.A.S., 2002. The biological effectiveness of wood modified with linear chain carboxylic acid anhydrides against *Coniophora puteana*. Holz Als Roh-und Werkstoff 60, 329–332.

Papadopoulos, A.N., Hill, C.A.S., 2003. The sorption of water vapour by anhydride modified softwood. Wood Sci. Technol. 37 (3–4), 221–231.

Passarini, L., Zelinka, S.L., Glass, S.V., Hunt, C.G., 2017. Effect of weight percent gain and experimental method on fiber saturation point of acetylated wood determined by differential scanning calorimetry. Wood Sci. Technol. 51 (6), 1291–1305.

Paszczynski, A., Crawford, R., Funk, D., Goodell, B., 1999. De Novo synthesis of 4, 5-Dimethoxycatechol and 2, 5-dimethoxyhydroquinone by the Brown rot fungus *Gloeophyllum trabeum*. Appl. Environ. Microbiol. 65 (2), 674–679.

Peterson, M.D., Thomas, R.J., 1978. Protection of wood from decay fungi by acetylation – an ultrastructural and chemical study. Wood Fiber Sci. 10, 149–163.

Pilgård, A., Schmöllerl, B., Risse, M., Fossdal, C.G., Alfredsen, G., 2017. Profiling postia placenta colonization in modified wood – Microscopy, DNA quantification and gene expression. In: 13th Annual Meeting of the Northern European Network for Wood Science and Engineering (WSE 2017). September 28-29. University of Copenhagen, Denmark 6 pp.

Popescu, C.M., Hill, C.A.S., Curling, S., Ormondroyd, G., Xie, Y., 2014. The water vapour sorption behaviour of acetylated birch wood: how acetylation affects the sorption isotherm and accessible hydroxyl content. J. Mater. Sci. 49 (5), 2362–2371.

Presley, G.N., Zhang, J., Schilling, J.S., 2016. A genomics-informed study of oxalate and cellulase regulation by brown rot wood-degrading fungi. Fungal Genet. Biol. 12, 64–70.

Riley, R., Salamov, A.A., Brown, D.W., Nagy, L.G., Floudas, D., Held, B.W., Levasseur, A., Lombard, V., Morin, E., Otillar, R., Lindquist, E.A., Sun, H., LaButti, K.M., Schmutz, J., Jabbour, D., Luo, H., Baker, S.E., Pisabarro, A.G., Walton, J.D., Blanchette, R.A., Henrissat, B., Martin, F., Cullen, D., Hibbett, D.S., Grigoriev, I.V., 2014. Extensive sampling of basidiomycete genomes demonstrates inadequacy of the white-rot/brown-rot paradigm for wood decay fungi. Proc. Natl. Acad. Sci. Unit. States Am. 111 (27), 9923–9928.

Ringman, R., Pilgård, A., Brischke, C., Richter, K., 2014a. Mode of action of brown rot decay resistance in modified wood: a review. Holzforschung 68, 239–246.

Ringman, R., Pilgård, A., Brischke, C., Windeisen, E., Richter, K., 2017. Incipient brown rot decay in modified wood: patterns of mass loss, structural integrity, moisture and acetyl content in high resolution. Int. Wood Prod. J. 8 (3), 172–182.

Ringman, R., Pilård, A., Richter, K., 2014b. Effect of wood modification on gene expression during incipient *Postia placenta* decay. Int. Biodeterior. Biodegrad. 86, 86–91.

Ringman, R., Pilgård, A., Richter, K., 2015. In vitro oxidative and enzymatic degradation of modified wood. Int. Wood Prod. J. 6 (1), 36–39.

Rose, J.K., Bennett, A.B., 1999. Cooperative disassembly of the cellulose–xyloglucan network of plant cell walls: parallels between cell expansion and fruit ripening. Trends Plant Sci. 4 (5), 176–183.

Rowell, R.M., 2005. Handbook of Wood Chemistry and Wood Composites. CRC Press.

Sützl, L., Laurent, C.V., Abrera, A.T., Schütz, G., Ludwig, R., Haltrich, D., 2018. Multiplicity of enzymatic functions in the CAZy AA3 family. Appl. Microbiol. Biotechnol. 102 (6), 2477–2492.

Smith, K.T., Shortle, W.C., Jellison, J., Connolly, J., Schilling, J., 2007. Concentrations of Ca and Mg in early stages of sapwood decay in red spruce, eastern hemlock, red maple, and paper birch. Can. J. For. Res. 37 (5), 957–965.

Schilling, J.S., Bissonnette, K.M., 2008. Iron and calcium translocation from pure gypsum and iron-amended gypsum by two brown rot fungi and a white rot fungus. Holzforschung 62 (6), 752–758.

Takahashi, M., Imamura, Y., Tanahashi, M., 1989. Effect of Acetylation on Decay Resistance of Wood against Brown-rot, White-rot and Soft-rot Fungi. IRG/WP 89-3540. International Research Group on Wood Protection, Stockholm, Sweden.

Tschernitz, J.L., Sachs, I.B., 1975. Observations on microfibril organization of Douglas-fir bordered pit-pair membranes by scanning electron microscopy. Wood Fiber Sci. 6 (4), 332–340.

Thybring, E.E., 2017. Water relations in untreated and modified wood under brown-rot and white-rot decay. Int. Biodeterior. Biodegrad. 118, 134–142.

Waterham, H.R., Russell, K.A., De Vries, Y., Cregg, J.M., 1997. Peroxisomal targeting, import, and assembly of alcohol oxidase in *Pichia pastoris*. J. Cell Biol. 139 (6), 1419–1431.

Winandy, J.E., Morrell, J.J., 1993. Relationship between incipient decay, strength, and chemical composition of Douglas-fir heartwood. Wood Fiber Sci. 25 (3), 278–288.

Xu, G., Goodell, B., 2001. Mechanisms of wood degradation by brown-rot fungi: chelator-mediated cellulose degradation and binding of iron by cellulose. J. Biotechnol. 87 (1), 43–57.

Yelle, D.J., Wei, D., Ralph, J., Hammel, K.E., 2011. Multidimensional NMR analysis reveals truncated lignin structures in wood decayed by the brown rot basidiomycete *Postia placenta*. Environ. Microbiol. 13, 1091–1100.

Zabel, R.A., Morrell, J.J., 1992. Wood Microbiology: Decay and its Prevention. Academic Press.

Zhang, J., Presley, G.N., Hammel, K.E., Ryu, J.S., Menke, J.R., Figueroa, M., Hu, D., Orr, G., Schilling, J.S., 2016. Localizing gene regulation reveals a staggered wood decay mechanism for the brown rot fungus *Postia placenta*. Proc. Natl. Acad. Sci. Unit. States Am. 113 (39), 10968–10973.

Zhang, J., Schilling, J.S., 2017. Role of carbon source in the shift from oxidative to hydrolytic wood decomposition by *Postia placenta*. Fungal Genet. Biol. 106, 1–8.

Zhang, J., Siika-aho, M., Tenkanen, M., Viikari, L., 2011. The role of acetyl xylan esterase in the solubilization of xylan and enzymatic hydrolysis of wheat straw and giant reed. Biotechnol. Biofuels 4 (1), 60.

Paper III

Characterization of a lytic polysaccharide monooxygenase from *Gloeophyllum trabeum* shows a pH-dependent relationship between catalytic activity and hydrogen peroxide production

Olav A. Hegnar[1,2], Dejan M. Petrovic[2], Bastien Bissaro [2], Gry Alfredsen[1], Anikó Várnai[2], Vincent G.H. Eijsink[2,#]

Norwegian Institute for Bioeconomy Research, Department of Wood Technology, PO Box 115, 1431 Ås, Norway. [1]

Norwegian University of Life Sciences, Faculty of Chemistry, Biotechnology and Food Science, Chr. Magnus Falsens vei 1, 1432 Ås, Norway [2]

[#]To whom correspondence should be addressed: Prof. Vincent G. H. Eijsink, vincent.eijsink@nmbu.no

Running title: pH dependent catalysis by a fungal LPMO

Keywords: Lytic polysaccharide monooxygenases, LPMO, lignocellulose, brown-rot fungi, wood decay, hydrogen peroxide.

Abstract

Lytic polysaccharide monooxygenases (LPMOs) are copper-dependent enzymes that perform oxidative cleavage of recalcitrant polysaccharides. We have purified and characterized a recombinant family AA9 LPMO from *Gloeophyllum trabeum*, *Gt*LPMO9B, which is active on both cellulose and xyloglucan. Activity of the enzyme was tested in the presence of three different reductants: ascorbic acid, gallic acid and 2,3-dihydroxybenzoic acid (2,3-DHBA). When using standard aerobic conditions typically used in LPMO experiments, the former two reductants could drive LPMO catalysis whereas 2,3-DHBA could not. In agreement with the recent discovery that H_2O_2 can drive LPMO catalysis, we show that gradual addition of H_2O_2 allowed LPMO activity at very low, sub-stoichiometric (relative to products formed) reductant concentrations. Most importantly, we found that while 2,3-DHBA is not capable of driving the LPMO reaction under standard aerobic conditions, it can do so in the presence of externally added H_2O_2. At alkaline pH, 2,3-DHBA is able to drive the LPMO reaction without externally added H_2O_2 and this ability overlaps entirely with endogenous generation of H_2O_2 by *Gt*LPMO9B-catalyzed oxidation of 2,3-DHBA. These findings support the notion that H_2O_2 is a co-substrate of LPMOs, and provide insight into how LPMO reactions depend on, and may be controlled by, the choice of pH and reductant.

Importance

Lytic polysaccharide monooxygenases promote enzymatic depolymerization of lignocellulosic materials by microorganisms, due to their ability to oxidatively cleave recalcitrant polysaccharides. The properties of these copper-dependent enzymes are currently of high scientific and industrial interest. We describe a previously uncharacterized fungal LPMO and show how reductants, which are needed to prime the LPMO by reducing Cu(II) to Cu(I) and for supplying electrons during catalysis, affect enzyme efficiency and stability. The results support claims that H_2O_2 is a natural co-substrate for LPMOs by demonstrating that when using certain reductants, catalysis can only be driven by H_2O_2 and not by O_2. Furthermore, we show how auto-inactivation resulting from endogenous generation of H_2O_2 in the LPMO-reductant system may be prevented. Finally, we identified a reductant that leads to enzyme activation without any endogenous H_2O_2 generation, allowing for improved control of LPMO reactivity and providing a valuable tool for future LPMO research.

Introduction

Lignocellulosic biomass is the most abundant biogenic material on earth. In nature, microorganisms that degrade lignocellulose utilize a plethora of different enzymes that attack the various components of the plant cell wall (lignin, cellulose and hemicelluloses). Among these are traditional hydrolytic cellulases and hemicellulases (1), as well as oxidoreductases with a wide range of functions (2). Crucial among these oxidoreductases are enzymes called lytic polysaccharide monooxygenases (LPMOs), whose beneficial effect on biomass degradation was first described in 2005 for chitin (3), and subsequently for cellulose (4). The genomes of lignocellulose degrading organisms often encode multiple LPMOs. These enzymes are found in all three domains of life, and are classified in the Carbohydrate-Active Enzymes (CAZy) database (5) in the Auxiliary Activity (AA) families 9, 10, 11, 13, 14 and 15. LPMOs are mono-copper oxidases that cause chain breaks in crystalline and amorphous polysaccharides, such as cellulose, hemicelluloses, chitin, and starch (6, 7, 8, 9). Cellulose-active fungal LPMOs form family AA9. Depending on the organism, the number of LPMO genes in fungi can range from a few to dozens (10, 11).

Gloeophyllum trabeum is a model wood-degrading basidiomycete that causes brown-rot by the selective removal of the cell wall polysaccharides without the mineralization of lignin (12). Brown-rot fungi form a polyphyletic group, characterized not by their shared ancestry but the type of decay they cause (13). Comparatively limited in their number of lignocellulose active enzymes to other decay organisms such as white-rot fungi, they are hypothesized to use a Fenton-like mechanism involving iron, oxalic acid and phenolic secondary metabolites to generate reactive oxygen species (ROS) that depolymerize wood cell wall polysaccharides (12, 14-16). These mechanisms are well known from *G. trabeum*, which secretes oxalic acid to chelate transition metals and to maintain a low pH in its surroundings (12, 14, 15). While the genome of *G. trabeum* encodes a relatively limited

number of traditional hydrolytic cellulase and hemicellulase genes (nine GH3s, five GH5s, three GH10s, and two GH12s, one GH74, and five GH43s) compared to white-rot fungi, it encodes a considerable number of AA-family enzymes, including six LPMOs (four AA9s and two AA14s), 24 GMC oxidoreductases (AA3) and 2 copper radical oxidases (AA5) (10). GMC oxidoreductases are flavoenzymes that oxidize various sugars and alcohols with the concomitant reduction of either O_2 (to H_2O_2) or quinones/phenoxy radicals (to phenols) or other compounds (17).

The role of H_2O_2 in wood degrading fungi has traditionally been attributed to oxidative depolymerization of plant cell-wall lignin by lignolytic peroxidases, and polysaccharides via non-enzymatic generation of reactive oxygen species (ROS). Recent developments regarding the oxidative mechanisms of LPMOs, however, have shed new light on the potential role of H_2O_2 during enzymatic depolymerization of cell-wall polysaccharides (2, 18). Since their identification as oxidative enzymes, LPMOs were thought to use molecular oxygen as co-substrate (19, 20), hence the name monooxygenase (Fig. 1). The suggested mechanism for the monooxygenase reaction entails a one-electron reduction of Cu(II) to Cu(I), followed by the binding of O_2 and formation of a superoxide intermediate (Cu(II)-O-O$^{\bullet}$) (21). A second electron and two protons are then required to complete the catalytic cycle, via different possible routes (6, 22), leading to incorporation of a hydroxyl group at the C_1 or C_4 in the scissile glycosidic bond, which is followed by spontaneous bond cleavage (20). This mechanism has recently been challenged by Bissaro et al. 2017 (18), who suggested that H_2O_2 is the natural co-substrate of LPMOs (Fig. 1). In this scenario a one-electron "priming" reduction of the active site Cu(II) to Cu(I), is followed by a reaction with H_2O_2 that leads to hydrogen abstraction and subsequent hydroxylation of the substrate via different possible routes (18). Subsequent experimental (23-25) and computational studies (26, 27) support

H_2O_2-driven LPMO catalysis, but the nature of the natural co-substrate, O_2 or H_2O_2, remains under debate.

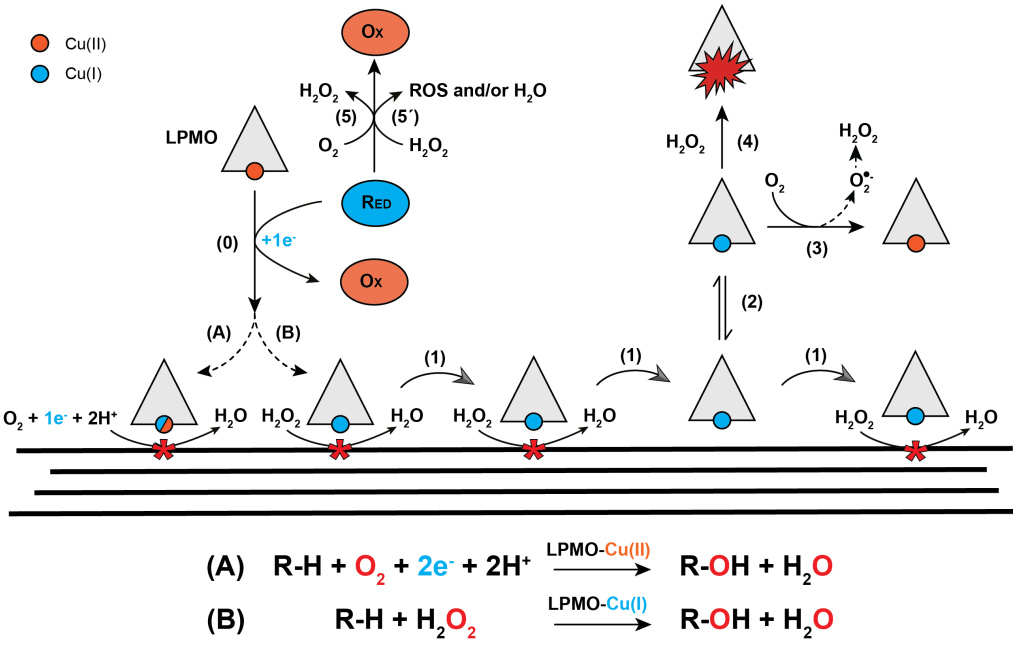

Figure 1. Overview of LPMO reactions. (0) Cu(II) in the LPMO is reduced to Cu(I) by the reductant (e.g. AscA or 2,3-DHBA) via a single-electron reduction. Reduced LPMO then performs oxidative cleavage of the cellulose substrate through one of two suggested mechanisms: **(A)** the reduced LPMO uses O_2 directly and requires two protons and a second electron to complete the hydroxylation of a carbon in the scissile glycosidic bond, or **(B)**, the reduced LPMO uses H_2O_2. Several scenarios have been proposed for reaction A, including scenarios where the copper stays reduced in between reactions (this uncertainty is indicated by the mixed blue/red colour of the copper); in any case, each catalytic cycle requires two externally delivered electrons as shown in the reaction scheme below the drawing. For reaction B the copper stays in the Cu(I) state and the enzyme will go through multiple catalytic cycles without a need for additional delivery of electrons. **(2,3)** Non-substrate-bound, reduced LPMO will generate H_2O_2 through reduction of O_2, via superoxide formed by the reaction of the reduced copper with O_2. H_2O_2 production may occur through the release of superoxide from the LPMO, followed by reduction or dismutation in solution, or via delivery of a second electron and two protons to the LPMO-superoxide complex, with subsequent release of H_2O_2. **(4)** Reaction of a reduced LPMO with H_2O_2 in solution, i.e. in the absence of substrate, will lead to formation of reactive oxygen species that can damage and inactivate the LPMO. **(5)** Reductants can reduce O_2 to H_2O_2, and **(5')** may also be oxidized by H_2O_2, generating reactive oxygen species (ROS) and/or water. The processes denoted by 5 and 5' may be affected by the presence of transition metals in the solution. See the main text for references and further details.

No matter their true mechanism, it is clear that LPMOs need to be reduced to become active. The source of the necessary reducing power *in vivo* is not known, but it is well established that LPMOs are promiscuous when it comes to interacting with reductants *in vitro* (28, 29). Several AA3 enzymes (28, 30), including well-known CDHs (31, 32) and an AA12 pyranose dehydrogenase (33) are able to drive LPMO action. In addition to enzymatic electron donors, phenolics (29, 34) and lignin-derived compounds (35) can also drive LPMO reactions. While CDH sometimes is considered a "natural" reductant for LPMOs, several brown-rot fungi, including *G. trabeum*, lack genes that encode CDH but have several genes encoding other AA3 family enzymes (e.g. aryl alcohol oxidases) that may reduce LPMOs (28, 30) and that are expressed during growth on lignocellulosic biomass (36). Of note, several AA3 enzymes produce H_2O_2 and may fuel H_2O_2-driven LPMO catalysis (2).

The observed promiscuity of LPMOs when it comes to reductants can likely be attributed in part to the open structure of the LPMO active site, where the copper is directly exposed on the flat catalytic surface of the enzyme. Previous studies have reported the redox potential of LPMO-Cu(II)/LPMO-Cu(I) to be 155-326 mV (most are >240 mV), while that of soluble copper is approximately 160 mV (Cu(II)/Cu(I)) (30).

Reactions in the presence of reductant and absence of substrate have shown that LPMOs can act as oxidases, reducing O_2 to produce H_2O_2 (37). There are two potential pathways for the observed generation of H_2O_2. In one scenario, single-electron reduction of molecular oxygen in the LPMO active site is followed by the release of superoxide that will then undergo spontaneous disproportionation or react with a reductant. The other possible mechanism involves H_2O_2 production in the active site of the enzyme, meaning that the first single electron reduction of molecular oxygen is followed by delivery of an additional electron and two protons to reduce copper-bound superoxide to H_2O_2. There is some disagreement in the literature as to why H_2O_2 production is not observed in reactions containing an LPMO

150 substrate. Some argue that the oxidase reaction is suppressed by the formation of a productive
151 enzyme-substrate complex and that substrate cleavage is a monooxygenase reaction (25),
152 whereas others argue that, even in the presence of substrate, non substrate-bound LPMOs
153 generate H_2O_2, which is not observed because substrate-bound LPMOs use the H_2O_2 in
154 carrying out a peroxygenase reaction (2, 18). Of note, the role of the interaction of the LPMO
155 with the reductant varies quite considerably between these two scenarios.

156 We have studied the properties of a not previously characterized LPMO from the brown-rot
157 fungus *G. trabeum*, *Gt*LPMO9B, focusing on the effects of reductant, pH and H_2O_2 on
158 catalytic activity. We demonstrate how the activity of *Gt*LPMO9B is modulated by different
159 reductants, reductant concentrations and supply of H_2O_2. Importantly, these studies revealed
160 that a reductant not previously used in LPMO activity studies, 2,3-dihydroxybenzoic acid
161 (2,3-DHBA), is capable of activating the LPMO for H_2O_2-driven catalysis but, in contrast to
162 e.g. ascorbic acid, cannot drive the LPMO reaction on its own. This interesting observation
163 provides a useful tool for further LPMO studies and lends support to the proposal that H_2O_2 is
164 a natural co-substrate of LPMOs.

Results and discussion

Enzyme production

Recombinant *Gt*LPMO9B was successfully produced in *Pichia pastoris* and the purified enzyme revealing an approximate mass of 50 kDa when analyzed by SDS-PAGE. Sequence analysis of secreted *Gt*LPMO9B shows a predicted mass of 24.5 kDa, indicating significant post-translational modification (glycosylation) of the recombinant protein. *Gt*LPMO9B carries two putative *N*-glycosylation sites (Asn138 and Asn217) and five putative *O*-glycosylation sites (Thr26, Ser99, Ser100, Ser139, and Ser192), as determined by the NetNGlyc 1.0 (38) and NetOGlyc 4.0 (39) Servers of the Technical University of Denmark. *Gt*LPMO9B is a single domain AA9 LPMO and the closest characterized relative is *Gt*LPMO9A-2 from *G. trabeum* (76.6% sequence identity), and the second closest relative with a known structure (PDB: 4EIS) is *Nc*LPMO9M from *Neurospora crassa* (54.8% identity).

A structural model of *Gt*LPMO9B built with PHYRE2 (40) showed the presence of a typical catalytic copper site comprising two conserved histidines (His1 and His86) and a tyrosine (Tyr175) in the proximal axial coordination position (Figure S1). The potential glycosylation sites are not located on the catalytic surface in the enzyme model; the closest residues, Asn138 and Ser139, are more than 10 Å away from the His-brace. Still, since glycosylation was considerable, we cannot exclude that the attached glycans interact with the catalytic surface.

Substrate and reductant specificity

The activity of *Gt*LPMO9B was tested on a wide range of substrates, including phosphoric acid swollen cellulose (PASC), soluble cello-oligosaccharides (Glc_5 and Glc_6), konjac

189 glucomannan, lichenan from Iceland moss, birchwood xylan, galactomannan, wheat
190 arabinoxylan, barley beta-glucan, ivory nut mannan, and xyloglucan from tamarind seed
191 using ascorbic acid (AscA) as reducing agent. Product analysis by HPAEC-PAD revealed
192 reductant-dependent product formation for cellulose and xyloglucan only (Fig. 2). Fig. 2A
193 shows that *Gt*LPMO9B produces both C_1- and C_4-oxidized cello-oligosaccharides from
194 PASC, which implies that also native and double oxidized oligomers are prominent (41). Of
195 the *G. trabeum* LPMO9s, *Gt*LPMO9B shares 76.6% identity with the AA9 domain of
196 *Gt*LPMO9A-2 (characterized by Kojima et al. 2016). Both enzymes are C_1/C_4-oxidizing
197 LPMOs and have activity on cellulose and xyloglucan (Fig. 2; (42)). *Gt*LPMO9A-2 has broad
198 specificity and is able to cleave the xyloglucan backbone regardless of substitution pattern of
199 glucosyl residues. Of note, in a previous study, *Gt*LPMO9B was shown to increase the
200 activity of the *G. trabeum* endoglucanase *Gt*Cel5B and xylanase *Gt*Xyl10G on pretreated oak
201 and kenaf (a hemp type) (43), but in this study the activity of the LPMO alone was not
202 analyzed.

203 Analysis of product formation after incubating *Gt*LPMO9B with PASC for 24 h in the
204 presence of 1 mM of various reducing agents at pH 6.5 showed C_1- and C_4-oxidized product
205 levels similar to those obtained with AscA for gallic acid, pyrogallol, caffeic acid, catechol
206 and hydroquinone, all of which are di-hydroxy or tri-hydroxy aromatic compounds (results
207 not shown; note that these were end-point measurements; kinetic data for selected reductants
208 are discussed below). Monohydroxy coniferyl alcohol, a natural lignin precursor, gave low
209 product yields, with peak intensities >15 times lower than with AscA, whereas no product
210 formation was observed in reactions with 2,3-dihydroxybenzoic acid, 3,5-dihydroxybenzoic
211 acid, vanillic acid, guaiacol, veratryl alcohol, 2,4-hexadiene-1-ol and 4-hydroxybenzoic acid
212 under these standard conditions.

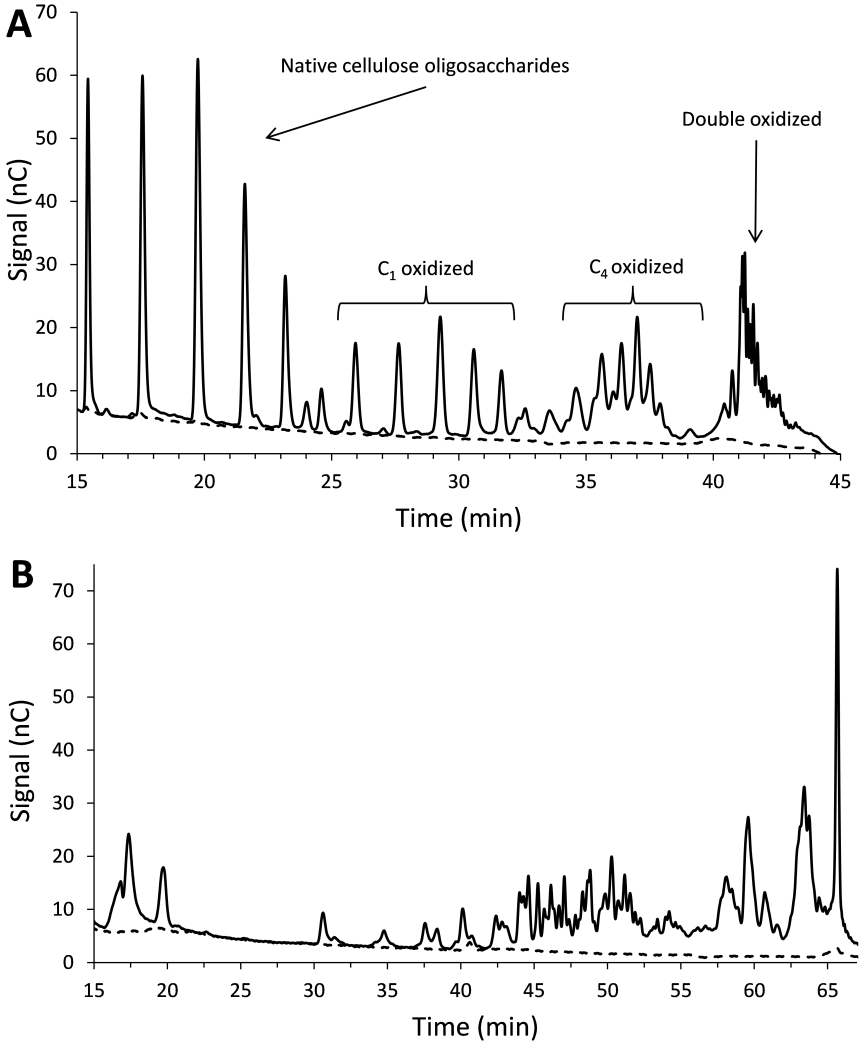

Figure 2. Products generated by *Gt*LPMO9B. (A) HPAEC-PAD chromatogram showing soluble native and oxidized cello-oligosaccharides released from PASC. The peaks were annotated based on Isaksen et al. 2014 (47); double-oxidized oligomers elute at 40 – 43 minutes. (**B**) HPAEC-PAD chromatogram showing soluble native and oxidized xyloglucan-oligomers released from tamarind xyloglucan (TXG). Reactions contained 0.2% (w/v) PASC or TXG, 1 µM *Gt*LPMO9B and 1 mM AscA (solid line) or no AscA (dashed line) and were incubated in 50 mM BisTris-HCl buffer (pH 6.5) for 24 h at 45 °C.

Activity with ascorbic acid (AscA)

The activity of *Gt*LPMO9B with AscA as the reducing agent was tested under aerobic conditions either using mM range concentrations of the reductant only, or using multiple additions of reductant and H_2O_2, at μM concentrations. The multiple additions strategy was used to keep the maximum concentrations of H_2O_2 low, since high concentrations may lead to autocatalytic inactivation of the LPMO (18). Solublized oligomeric products were treated with *Tr*Cel7A from *Trichoderma reesei* to generate a mixture containing only C_1-oxidized cellobiose (cellobionic acid or GlcGlcA) and C_4-oxidized cellobiose (Glc4gemGlc) as oxidized products. The amounts of these two oxidized disaccharides were quantified by HPAEC-PAD using in-house prepared standards and summed up to determine total product formation by the LPMO. The ratio of C1- to C4-oxidized products was constant in all experiments carried out at standard pH.

Fig. 3A shows that in the initial linear phase of reactions with 1 mM AscA at pH 6.5, i.e. conditions that are generally used in LPMO research, 1 μM of *Gt*LPMO9B produced approximately 0.88 μM oxidized products per minute and the reaction stopped after about 120 min. Increasing the concentration of AscA to 5 mM increased initial rate (1.18 μM min^{-1}) but product formation leveled off already after 60 min, meaning that the product final yield was reduced.

Notably, the final yield of oxidized products in both reactions with mM concentrations of AscA remained far below the theoretical yield, which would at least 250 μM of product if molecular oxygen was limiting or 1 mM and 5 mM, respectively, if AscA was limiting. This is commonly observed for *in vitro* LPMO reactions. Some oxidations will be overlooked because the oxidized sites remain on the insoluble substrate (44). While this fraction may be as high as 50% in some cases (44, 45), it cannot explain why the total yield in the reaction

247 with 5 mM AscA is only 60 µM. A more likely explanation is that the LPMOs become
248 inactivated during the reaction due to oxidative damage in their active sites (18, 25, 46).

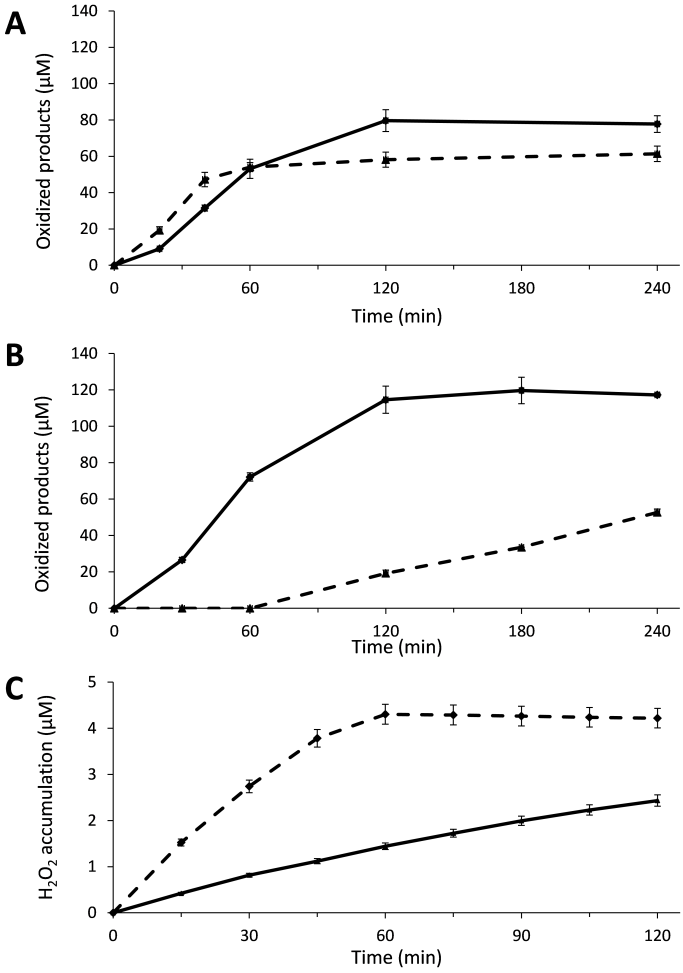

249

250 **Figure 3. Cellulose-degradation and H_2O_2-generation by *Gt*LPMO9B with ascorbic acid (AscA)**
251 **as reductant**. Reactions contained 0.2% (**A**) or 0.5% (**B**) (w/v) PASC and 1 µM *Gt*LPMO9B, in 50
252 mM BisTris-HCl buffer pH 6.5 and were incubated at 45 °C and 1000 rpm. LPMOs were activated by
253 adding (**A)** 1 mM (solid line) or 5 mM (dashed line) AscA only at time zero, or (**B)** 15 µM AscA and
254 50 µM H_2O_2 (solid line) or 15 µM AscA only (dashed line) (and replacing the volume of H_2O_2 with
255 water) every 15 minutes starting at time zero. Control reactions with only H_2O_2 added (no AscA) did
256 not produce detectable amounts of oxidized products. Solubilized oxidized products were quantified
257 as C_1- (cellobionic acid), and C_4-oxidized (Glc4gemGlc) dimers using HPAEC-PAD, and the sum of
258 both products was calculated. (**C)** H_2O_2 accumulation in a reaction with 1 µM *Gt*LPMO9B and 30 µM
259 AscA without PASC (dashed line) and in a control reaction containing 1 µM $CuSO_4$ instead of the
260 LPMO (solid line); reactions without AscA did not show H_2O_2 accumulation. Error bars show
261 standard deviations (n=3, independent experiments).

In the presence of O_2 and AscA and in the absence of substrate, LPMOs produce H_2O_2 (37, 47), and it has been claimed that H_2O_2 production by non-substrate-bound reduced enzyme contributes to driving LPMO reactions under commonly used conditions (18). It has further been shown that accumulation of H_2O_2 and/or poor substrate binding correlate with LPMO inactivation (18, 24, 46). Fig. 3C shows that *Gt*LPMO9B incubated under aerobic conditions with AscA indeed produces H_2O_2 in the absence of substrate.

Fig. 3B shows that *Gt*LPMO9B activity may be driven by stepwise addition of H_2O_2 and low amounts of AscA. At AscA concentrations (15 μM per addition) that, alone, gave low LPMO activity, the reaction with added H_2O_2 showed a rate similar to that obtained in the reaction with 5 mM AscA. Similarly to standard reactions with mM amounts of AscA, the reactions with added H_2O_2 showed enzyme inactivation. As shown in Müller et al., 2018 (48) and also below, in the section on 2,3-DHBA as a reductant, such inactivation can be overcome by lowering the H_2O_2 concentrations.

Activity with gallic acid (GA)

Of the other tested reductants, gallic acid (GA) was considered the most interesting one, because it is known to react more slowly with O_2 (28) and could thus perhaps lead to more controlled reactions, with less inactivation. Indeed, in contrast to reactions with AscA, in reactions with GA, product formation continued after 4 hours (Fig. 4A). In accordance with the presumed slower generation of reactive species by GA, and in contrast with what was observed with AscA (Fig 3A), increasing the concentration of GA increased both the reaction rate and the final yield after 24 hours (Fig. 4A). Fig. 4C shows that H_2O_2 accumulation in the absence of substrate was lower for GA compared to AscA (both at 30 μM concentration; the H_2O_2 production rates were 0.29 $\mu M \cdot h^{-1}$ and 4.8 $\mu M \cdot h^{-1}$, respectively).

To investigate whether this could be attributed to H_2O_2 scavenging by GA, we incubated 30 μM reductant (AscA, GA or 2,3-DHBA) with 30 μM H_2O_2 for 1 hour (pH 6.5 at room temperature) (Fig. S2). This revealed that while AscA and 2,3-DHBA removed 54% and 31% of H_2O_2 respectively, GA removed 94%. We interpret these observations to indicate that GA is protecting the LPMO from excessive H_2O_2 generated in the reaction with PASC (Fig. 4A), explaining the prolonged longevity of the enzyme in the reaction. Notably, this finding highlights that the Amplex Red assay should be used with caution to determine absolute H_2O_2 production by LPMOs (37) in the presence of reductants. Reductants may react with H_2O_2, which will mask H_2O_2 production by LPMOs, and thus the values obtained in the Amplex Red assay reflect the total accumulation and not production. These observations underpin the impact of the choice of reductant on the activity and longevity of LPMOs.

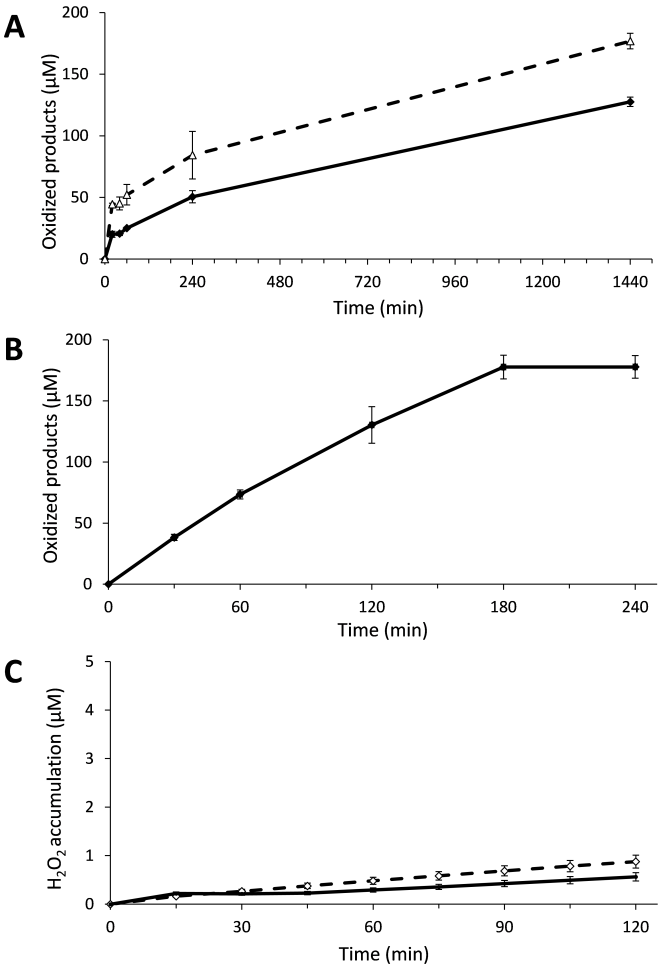

299

300 **Figure 4. Activity of *Gt*LPMO9B with gallic acid (GA) as reductant**. The reaction mixtures of
301 panels **A** and **B** were incubated at 45°C, 1000 rpm, and contained 1 µM enzyme, 50 mM BisTris
302 buffer pH 6.5, 0.2% (**A**) or 0.5% (**B**) PASC (w/v), and (**A)** 1mM (solid line) GA or 5mM (dashed
303 line) GA added only at time zero, or (**B)** with repetitive addition of 15 µM GA, and 50 µM H_2O_2,
304 every 15 minutes, starting at time zero. Solubilized oxidized products were quantified as C_1-
305 (cellobionic acid), and C_4-oxidized (Glc4gemGlc) dimers using HPAEC-PAD, and the sum of the two
306 was calculated. Note the difference in time scale between panels **A** (24 hours) and **B** (240 minutes).
307 Panel (**C)** shows H_2O_2 accumulation in a reaction with 1 µM *Gt*LPMO9B and 30 µM GA without
308 PASC (dashed line) and in a control reaction containing 1 µM $CuSO_4$ instead of the LPMO (solid);
309 reactions without GA did not show H_2O_2 accumulation. Error bars show standard deviations (n=3,
310 independent experiments).
311

312 Interestingly, replacing 15 µM AscA with 15 µM GA in reactions with multiple additions of
313 reductant and H_2O_2 (Fig. 4B), revealed much less difference between the reductants.

Compared to reactions with mM amounts of GA, this H_2O_2-based set-up gave faster kinetics, and the progress curves with GA that were quite similar to those obtained with AscA under the same conditions. The observation that GA and AscA gave similar results when applied at low concentrations in reactions with added H_2O_2 indicated that difference in reductant performance in standard O_2-driven reactions is not due to differences in the ability to carry out the first "priming" reduction of the LPMO, but rather to a difference in the ability to promote generation and accumulation of H_2O_2 in the reaction mixture.

Activity with 2,3-dihydroxybenzoic acid (2,3-DHBA) and hydrogen peroxide

Considering the observation that GA was equally effective as AscA in reactions with added H_2O_2, we then tested whether something similar might apply to the reductants that were not able to drive LPMO reactions under standard (aerobic, no added H_2O_2) conditions. Of three reductants tested, 2,3-DHBA, 3,5-DHBA and vanillic acid, one, 2,3-DHBA, indeed led to the formation of oxidized products in reactions with added H_2O_2 at pH 6.5 (Fig. 5). This experiment shows that 2,3-DHBA was able to prime *Gt*LPMO9B, but was unable to drive LPMO reaction without the added H_2O_2. Accordingly, under the conditions used, H_2O_2 production in a reaction without substrate at pH 6.5 was not detected (Fig. 6; discussed in detail below). This finding supports the notion that LPMO activity requires H_2O_2, which can either be generated in the reaction, as in standard reactions with AscA, or which needs to be added, as in reactions with 2,3-DHBA.

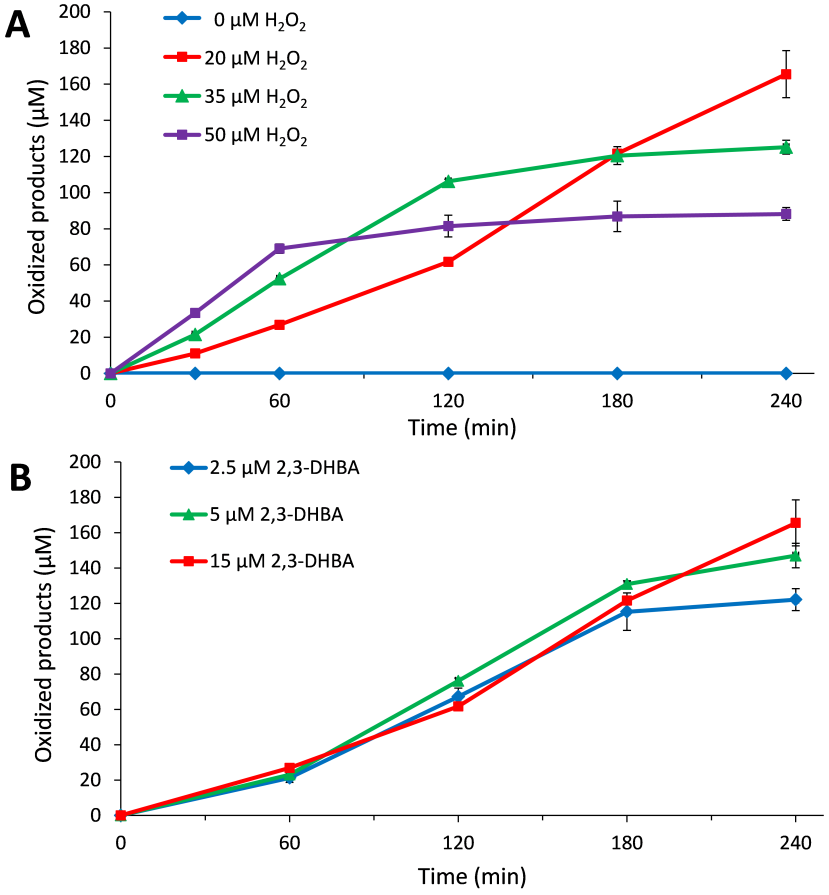

334

335 **Figure 5. Activity of *Gt*LPMO9B with gradual addition of 2,3-dihydroxybenzoic acid (2,3-**
336 **DHBA) and H_2O_2.** The reaction mixtures were incubated at 45°C, 1000 rpm and contained 1 µM
337 enzyme, 50 mM BisTris buffer pH 6.5, 0.5% (w/v) PASC and were subjected to repetitive additions,
338 every 15 minutes, starting at time zero of (**A**) 15 µM 2,3-DHBA and either 0, 20, 35 or 50 µM H_2O_2
339 (indicated in the figure) or (**B**) 20 µM H_2O_2 and either 2.5, 5 or 15 µM 2,3-DHBA. Solubilized
340 oxidized products were quantified as C_1- (cellobionic acid) and C_4-oxidized (Glc4gemGlc) dimers
341 using HPAEC-PAD and the sum of the two was calculated. Error bars show standard deviations (n=3,
342 independent experiments).
343

344 Experiments with varying amounts of added H_2O_2 showed that higher amounts led to faster
345 initial enzyme rates and faster inactivation (Fig. 5A). Estimated initial reaction rates were
346 0.52 µM·min^{-1}, 0.88 µM·min^{-1}, and 1.30 µM·min^{-1}, in reactions supplied with 20, 35 and 50
347 µM H_2O_2 every 15 minutes, respectively. Enzyme inactivation, which is likely due to

accumulation of H_2O_2 in solution, became visible after 60 min in the reaction with 50 μM H_2O_2, after 120 min in the reaction with 35 μM H_2O_2, and not at all (within the 240 min sampling period) in the reaction with 20 μM H_2O_2. In agreement with recent studies describing how LPMO activity may be controlled and maintained during cellulose saccharification by controlled addition of H_2O_2 (48), the present results show that keeping the H_2O_2 concentration at an appropriate, low concentration is essential for LPMO performance.

Fig. 5B shows that, within the tested range of 2.5 – 15 μM, in reactions with 20 μM H_2O_2, the reductant (2,3-DHBA) concentration had a relatively modest effect on LPMO performance, including the initial rate of the reaction. When using 5 or 2.5 μM 2,3-DHBA combined with 20 μM H_2O_2 feeds, 147 and 122 μM soluble oxidized products were detected after 240 min, i.e. 1.8- and 3.1-fold more than the total amount of added reductant (80 and 40 μM, resulting from 16 additions of 5 μM or 2.5 μM each, respectively). This confirms the notion that only non-stoichiometric amounts of reductant (with respect to amounts of oxidized products) are required when the LPMO is fueled with H_2O_2. After 240 minutes the cumulative H_2O_2 concentration would be 320 μM, which would imply that in the most stable reaction depicted in Fig. 5A (15 μM 2,3-DHBA, 20 μM H_2O_2 curve), giving a product yield after 240 minutes of 165 μM, 51.5% of the H_2O_2 has been converted to soluble oxidized cello-oligomers. Of note, only soluble oxidized sites were measured, whereas existing data (44, 49) indicate that in the early phases of LPMO reactions a considerable fraction of oxidized sites may remain in the insoluble fraction. Thus, the actual level of incorporation of H_2O_2 into oxidized sites will be higher than 51.5%, and the present data are compatible with an expected 1:1 stoichiometry between the amount of added H_2O_2 and the amount of generated oxidized sites.

The effect of pH on the LPMO–AscA/2,3-DHBA systems

As the redox potential of 2,3-DHBA is strongly affected by pH (50), we tested the activity of *Gt*LPMO9B (1 μM) with either 1 mM AscA or 2,3-DHBA at pH 6.0, 6.5 (the pH used in the experiments described above), 7.0, 8.0 and 9.0 on 0.5% PASC, in the presence of O_2 only for 24 hours. The reactions were evaluated based on C_1-oxidized products only as C_4-oxidized products are unstable at alkaline pH (41). AscA was able to drive *Gt*LPMO9B action in the full pH range of 6.0-9.0. On the other hand, while 2,3-DHBA was not able to drive the LPMO reaction at pH 6.5 in the absence of H_2O_2 (Fig. 5A, 6A), it was able to do so at pH 8.0 and 9.0 (Fig. 6A). Importantly, Fig. 6B shows that the pH-dependency of LPMO activity (Fig. 6A) correlates with the pH-dependency of the ability of the *Gt*LPMO9B/2,3-DHBA system to generate H_2O_2: production of H_2O_2 was detected at pH 8.0 and 9.0, but not at pH 6.0 and 7.0. Of note, the same type of pH-dependency applies to control reactions with $CuSO_4$ (Fig. 6B), albeit with lower H_2O_2 production rates compared to reactions containing the LPMO.

Since the redox potential of 2,3-DHBA becomes less positive with increasing pH (50), possibly as a result of deprotonation of a phenolic hydroxyl group (50), it is conceivable that increased pH leads to an increased ability to generate H_2O_2, by LPMO-dependent or LPMO-independent reduction of O_2 (Fig. 1). Fig. 6B shows that accumulation of H_2O_2 is much higher in reactions containing the LPMO and 2,3-DHBA, compared to control reactions lacking the enzyme. Thus, by far most of the H_2O_2 generated in the LPMO-containing reactions is generated by the LPMO, and not by enzyme-independent processes, i.e. direct oxidation of 2,3-DHBA, possibly catalyzed by free copper in solution. Apparently, at pH 6-7, neither LPMO-dependent nor LPMO-independent H_2O_2 generation is sufficient to drive the reaction. However, at this pH 2,3-DHBA does reduce the LPMO, allowing H_2O_2-driven catalysis.

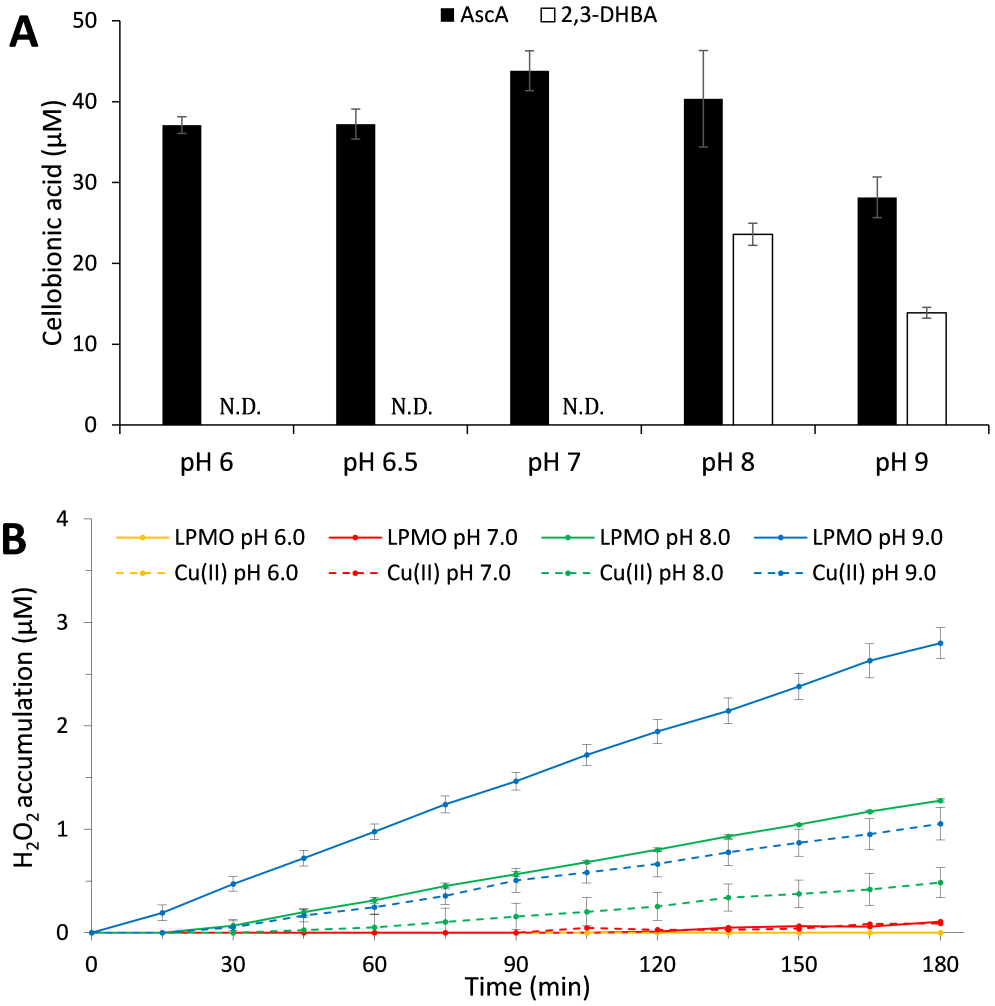

Figure 6. pH dependency of LPMO activity (A) Product formation in reaction mixtures containing 1 µM *Gt*LPMO9B on 0.5% (w/v) PASC and 1 mM AscA or 2,3-DHBA as reductants at pH 6.0-9.0 after incubation for 24 h at 45 °C. Only cellobionic acid (C_1-oxidized dimers) was analyzed due to instability of C_4 oxidized dimers (Glc4gemGlc) at alkaline pH. N.D. indicates "not detected". **(B)** H_2O_2 accumulation in reaction mixtures containing 1 µM *Gt*LPMO9B and 30 µM 2,3-DHBA at pH 6.0-9.0, and in control reactions containing 1 µM Cu(II) ($CuSO_4$) instead of the LPMO. At each tested pH, H_2O_2 accumulation in reactions containing the reductant only (not shown) was similar to, but slightly lower than H_2O_2 accumulation in the control reactions with ($CuSO_4$). Note that this experiment, which was primarily done to show the effect of pH on the ability of 2,3-DHBA to drive LPMO reactions, only shows end points and that, thus, differences in initial rates and enzyme inactivation are not visible in panel **A**. Error bars show standard deviations (n=3, independent experiments).

Concluding remarks

In this study, we analyzed the properties of the second of in total four predicted family AA9 LPMOs encoded by the genome of *Gloeophyllum trabeum*, *Gt*LPMO9B. The substrate specificity of this single domain LPMO is similar to that of the previously characterized *Gt*LPMO9A-2 (42).

The interplay of LPMOs with reducing compounds, reactive oxygen species and other redox enzymes is of great current interest (2, 28, 29). We therefore used *Gt*LPMO9B to study some of these issues, which led to the discovery of a reductant, 2,3-DHBA, which had remarkable effects on LPMO catalytic activity.

The present data indicate that, at pH 6.5, 2,3-DHBA reduces Cu(II) to Cu(I) via a single electron reduction and that this reduced copper center, in what is now a "primed" LPMO, reacts with externally supplied H_2O_2 to perform catalytic cleavage of the cellulose substrate. The absence of LPMO activity in the absence of externally supplied H_2O_2 correlates with the lack of H_2O_2 generation by the 2,3-DHBA – LPMO redox system. It is remarkable that H_2O_2 production was not detected at pH 6 or 7, since a reduced LPMO [Cu(I)] will react with molecular oxygen to generate superoxide (21) and since redox potentials suggest that a reductant that is capable of reducing the LPMO (E_o = + 155-326 mV) would also be capable of reducing superoxide to H_2O_2 (E_o = + 890 mV; (50)). One explanation could be that the superoxide remains bound to the now oxidized copper ion [Cu(II)], which would strongly affect its redox potential.

We would argue that the present results support the notion that H_2O_2 is the natural substrate for LPMOs (18), but it must be noted that the option that LPMOs can use molecular oxygen directly cannot be dismissed (25, 52). Interestingly, no matter the true nature of the oxygen co-substrate, the present data show that *Gt*LPMO9B, at pH 6-7 with 2,3-DHBA acting as

electron donor, is not able to reduce this co-substrate to a species powerful enough to carry out hydrogen abstraction from the polysaccharide substrate. Use of 2,3-DHBA enables good control of LPMO activity and we expect that this reductant will be useful in future LPMO studies. Preliminary studies with 2,3-DHBA and another LPMO, C4-oxidizing *Nc*LPMO9C from *Neurospora crassa*, gave results similar to those described above (Fig. S3). It is worth noting that, in contrast to e.g. AscA, use of 2,3-DHBA may allow reducing the LPMO without creating conditions that lead to enzyme inactivation, and this can be done under aerobic conditions.

Materials and methods

Cloning and expression of *Gt*LPMO9B

The gene encoding *Gt*LPMO9B (UniProt ID: S7RK00) including its native signal sequence was codon optimized for *Pichia pastoris* (GenScript, NJ, USA). The synthetic gene was inserted into the pPink-GAP vector, which was then transformed into *P. pastoris* PichiaPink™ Strain 4 cells (Invitrogen, CA, USA), as described earlier (53). Transformants were screened for protein production in BMGY medium (containing 1% (v/v) glycerol).

The best-producing transformant was grown in 25 ml BGMY medium (containing 1% (v/v) glycerol), overnight in a 100-ml shake flask at 29 °C and 200 rpm. The culture was then used to inoculate 500 ml BGMY medium (containing 1% (v/v) glycerol) in a 2-l baffled shake flask. The culture was incubated at 29 °C and 200 rpm for 48 hours. After 24 hours of incubation the medium was re-supplemented with 1% (v/v) glycerol. After 48 hours the culture was centrifuged at 4 °C and 10,000 *g* for 10 minutes, to remove the cells. The supernatant was filtered through a 0.2-µm polyethersulfone membrane (Millipore, MA, USA), dialyzed against 50 mM Bis-Tris buffer (pH 6.5), and concentrated to 100 ml with a

460 VivaFlow 50 tangential crossflow concentrator (MWCO 10 kDa, Sartorius Stedim Biotech,
461 Germany).

462

463 **Purification of recombinant protein**

464 The recombinant *Gt*LPMO9B protein was purified in a two-step protocol using hydrophobic
465 interaction chromatography (HIC) followed by size exclusion chromatography (SEC), as
466 described earlier (54). Purified *Gt*LPMO9B was copper saturated by incubating the enzyme
467 with an excess of $Cu(II)SO_4$ (at ~3:1 molar ratio of copper:enzyme) for 30 min at room
468 temperature as described previously (55). The Cu(II) loaded sample of *Gt*LPMO9B was
469 buffer exchanged to 50 mM Bis-Tris buffer (pH 6.5), using Amicon Ultra centrifugal filters
470 (MWCO 3kDa, Merck Millipore, Burlington, MA, USA). The resulting protein solution was
471 filtered through a sterile 0.22 μm Millex®-GV filter (Merck Millipore, Burlington, MA,
472 USA) and stored at 4 °C. Protein concentrations were determined by measuring absorbance at
473 280 nm in a spectrophotometer, calculating the concentration based on the extinction
474 coefficient (ε=55,475 $M^{-1} \cdot cm^{-1}$; calculated using ProtParam (56)).

475

476 **Screening of substrates and reductants**

477 Activity of *Gt*LPMO9B was tested on the following substrates: phosphoric acid swollen
478 cellulose (PASC), prepared from Avicel as described before (57), konjac glucomannan,
479 galactomannan, ivory nut mannan, xyloglucan from tamarind seed, lichenan from Iceland
480 moss, wheat arabinoxylan and barley beta-glucan, all purchased from Megazyme (Bray,
481 Ireland), and birchwood xylan, obtained from Sigma-Aldrich (St. Louis, MO, USA).
482 Substrate specificity was tested by setting up reaction mixtures (100 μl) containing 0.2%
483 (w/v) substrate, 1 μM *Gt*LPMO9B, and 1 mM ascorbic acid (AscA) in 50 mM BisTris buffer

pH 6.5. The samples were incubated in an Eppendorf ThermoMixer C (Eppendorf, Hamburg, Germany) at 45 °C and 1000 rpm for 24 hours. Control reactions were performed in the absence of ascorbic acid. Reactions were stopped by separating the soluble fractions from the insoluble substrates by filtration using a 96-well filter plate (Millipore) operated with a vacuum manifold.

Activity assays with PASC, using the conditions described above, were also done with the following alternative reducing agents: gallic acid, pyrogallol, caffeic acid, catechol and hydroquinone coniferyl alcohol, 2,3-dihydroxybenzoic acid, 3,5-dihydroxybenzoic acid, vanillic acid, guaiacol, veratryl alcohol, 2,4-hexadien-1-ol and 4-hydroxybenzoic acid. All reducing agents were purchased from Sigma-Aldrich.

_Gt_LPMO9B activity on PASC: time series and quantification of oxidized products

Reaction mixtures (600 µL) contained 1 µM *Gt*LPMO9B, 0.2% (w/v) PASC and 1 mM reductant in 50 mM BisTris pH 6.5. The reactions were incubated in an Eppendorf ThermoMixer C (Eppendorf, Hamburg, Germany) at 45 °C and 1000 rpm. At various time points (20, 40, 60, 120 and 240 min), 100 µL samples were taken and boiled for 5 minutes. For gallic acid, a final sample was taken after 24 hours. Separation of soluble and insoluble material was achieved by centrifugation at 11,000 g for 10 min. The soluble fractions (25 µL) were mixed with 24 µL of 150 mM sodium-acetate buffer (pH 4.5) and 1 µL *Tr*Cel7A from *Trichoderma reesei* (~1 µM) and incubated for 24 hours at 37 °C. The treatment with *Tr*Cel7A converts soluble oxidized cello-oligomers to cellobionic acid (C_1 oxidized) and Glc4gemGlc (C_4 oxidized). Soluble fractions treated in this way were subsequently analyzed using high-performance anion exchange chromatography with pulsed amperometric detection (HPAEC-PAD). The amount of released oxidized products was quantified using the following standards: 4-hydroxy-β-D-xylo-Hex*p*-(1→4)-β-D-Glcp (Glc4gemGlc), prepared as

described previously (58) and cellobionic acid, prepared by treating cellobiose with cellobiose dehydrogenase from *Myriococcum thermophilum* (*Mt*CDH) (59). All experiments were performed in triplicate.

The effect of pH on *Gt*LPMO9B activity

*Gt*LPMO9B (1 μM) was incubated with 0.5% (w/v) PASC in 50 mM buffer solution with 1 mM reductant in a final volume of 100 μL. For the reaction mixtures with pH 6.0, 6.5 or 7.0, 50 mM BisTris-HCl was used as the buffering agent, while 50 mM Tris-HCl was used for the reaction mixtures with pH 8.0 or 9.0. The samples were incubated in an Eppendorf ThermoMixer at 45 °C and 1000 rpm for 24 hours. The reactions were stopped by boiling for 5 minutes. Samples were hydrolyzed with *Tr*Cel7A as previously described, and oxidized product quantified as cellobionic acid. All reactions were performed in triplicate.

H_2O_2 as co-substrate

In reactions added H_2O_2, 1 μM *Gt*LPMO9B was mixed with 0.5% (w/v) PASC in 50 mM BisTris buffer (pH 6.5), and various initial concentrations of reductant and H_2O_2, 2.5 and 20, 5 and 35, or 15 and 50 μM, respectively, were added. *Gt*LPMO9B was pre-mixed with PASC in the buffer (588 μL), after which we added first 6 μL of freshly prepared reductant solutions with concentrations of 0.25, 0.5 or 1.5 mM reductant, followed by addition of 6 μL of a freshly prepared 2, 3.5 or 5 mM H_2O_2 stock solution. Reductant and H_2O_2, in that same order, were subsequently added to the reaction mixtures, every 15 minutes for a total period of 240 minutes. Added volumes were adapted to the changes in total reaction volume that were due to previous additions and sampling, so that the added amounts corresponded to final concentrations identical to the concentrations at t = 0. Reactions were stopped by boiling and

frozen (-20 °C) prior to further analysis. The amount of released oxidized products was quantified as described above. In control experiments either H_2O_2 or reductant was replaced with water. All reactions were performed aerobically and in triplicate.

H_2O_2 production in the absence of substrate at different pH

The production of H_2O_2 by *Gt*LPMO9B at different pH in the absence of substrate was monitored using an assay with Amplex Red and horseradish peroxidase (HRP), both purchased from Sigma-Aldrich (St. Louis, USA), after (37). In brief, 100 µl reactions were prepared in 96 well micro titer plates containing 1 µM *Gt*LPMO9B, 5U horseradish peroxidase, 50 µM Amplex Red and 30 µM reductant in the appropriate buffer. The reactions were initiated by addition of the reductant followed by real-time measurement of absorbance at 540 nm for 120 min in a Thermo Scientific Multiscan FC microplate reader at room temperature. For pH 6.0, 6.5 and 7.0, 50 mM BisTris buffer was used, while at pH 8.0 and 9.0, 50 mM Tris buffer was used. In control reactions 1 µM *Gt*LPMO9B was replaced by either 1 µM $CuSO_4$ or water. Standard curves for quantification of H_2O_2 were made in the concentration range of 0.5-20 µM, at the pHs used in the experiment. All reactions were performed in triplicate.

H_2O_2 scavenging by reductants

Reductants (AscA, GA and 2,3-DHBA) were incubated with H_2O_2 at a 1:1 molar ration (30 µM) in 50 mM BisTris pH 6.5 buffer solution for 60 minutes at room temperature. In the control reaction, reductant was replaced with water. H_2O_2 concentrations were determined by a single time point measurement of (maximal) conversion of Amplex Red (50 µM starting

concentration) to resorufin by 5U HRP using a Multiscan FC microplate reader (540 nm). H_2O_2 quantification was achieved using a standard curve covering the range of 1-30 μM.

Detection of oxidized products

Oxidized products were analyzed using high-performance anion exchange chromatography with pulsed amperometric detection (HPAEC-PAD). HPAEC was performed on a Dionex ICS5000 system, equipped with a CarboPac PA1 analytical column (2×250 mm) and a CarboPac PA1 guard column (2×50 mm), using a 50-minute gradient for cellulosic (60) A), and a 75-minute gradient (61) for hemicellulosic substrates. Chromatograms were recorded and analyzed using Chromeleon 7.0 software (Thermo Fisher Scientific, Waltham, MA, USA).

Acknowledgements

This work was financed by the Research Council of Norway 243663/E50 BioMim and the Norwegian Institute for Bioeconomy Research. The authors gratefully thank Dr. Piotr Chylenski for insightful comments and suggestions.

Abbreviations

2,3-DHBA, 2,3-dihydroxybenzoic acid; AA, auxiliary activity; AscA, ascorbic acid; CAZyme, Carbohydrate active enzyme; CDH, cellobiose dehydrogenase; GA, gallic acid; GH, glycoside hydrolase; HPAEC-PAD, high-performance anion exchange chromatography with pulsed amperometric detection; LPMO, lytic polysaccharide monooxygenase; PASC, phosphoric acid swollen cellulose; ROS, reactive oxygen species; TXG, tamarin xyloglucan.

Appendices

Supplemental information is included in Figures S1 - S3.

References

1. Cragg SM, Beckham GT, Bruce NC, Bugg TDH, Distel DL, Dupree P, Etxabe AG, Goodell BS, Jellison J, McGeehan JE, McQueen-Mason SJ, Schnorr K, Walton PH, Watts JEM, Zimmer M, (2015). Lignocellulose degradation mechanisms across the Tree of Life. Curr Opin Chem Biol, 29, 108-119.

2. Bissaro B, Várnai A, Røhr ÅK, Eijsink VGH. 2018. Oxidoreductases and reactive oxygen species in conversion of lignocellulosic biomass. Microbiol Mol Biol Rev 82:e00029-18.

3. Vaaje-Kolstad G, Horn SJ, van Aalten DM, Synstad B, Eijsink VGH. 2005. The non-catalytic chitin-binding protein CBP21 from *Serratia marcescens* is essential for chitin degradation. J Biol Chem 280(31):28492-28497

4. Forsberg Z, Vaaje-Kolstad G, Westereng B, Bunæs AC, Stenstrøm Y, Mackenzie A, Sørlie M, Horn SJ,Eijsink VGH. 2011. Cleavage of cellulose by a CBM33 protein. Protein Sci, 20**,** 1479-1483.

5. Lombard V, Golaconda Ramulu H, Drula E, Coutinho PM, Henrissat B. 2013. The carbohydrate-active enzymes database (CAZy) in 2013. Nucleic Acids Res 42:D490-D495.

6. Beeson WT, Vu VV, Span EA, Phillips CM, Marletta MA. 2015. Cellulose degradation by polysaccharide monooxygenases. Annu Rev Biochem 84:923-946.

7. Couturier M, Ladevèze S, Sulzenbacher G, Ciano K, Fanuel M, Moreau C, Villares A, Cathala B, Chaspoul F, Frandsen KE. 2018. Lytic xylan oxidases from wood-decay fungi unlock biomass degradation. Nat Chem Biol*,* 14(3)**,** 306-310.

603 8. Vaaje-Kolstad G, Westereng B, Horn SJ, Liu Z, Zhai H, Sørlie M, Eijsink VGH.
604 2010. An oxidative enzyme boosting the enzymatic conversion of recalcitrant
605 polysaccharides. Science, 330, 219-222.
606 9. Leggio LL, Simmons TJ, Poulsen J-CN, Frandsen KE, Hemsworth GR, Stringer MA,
607 Von Freiesleben P, Tovborg M, Johansen KS, De Maria L. 2015. Structure and
608 boosting activity of a starch-degrading lytic polysaccharide monooxygenase. Nat
609 Commun 6:5961.
610 10. Floudas D, Binder M, Riley R, Barry K, Blanchette RA, Henrissat B, Martínez AT,
611 Otillar R, Spatafora JW, Yadav JS. 2012. The Paleozoic origin of enzymatic lignin
612 decomposition reconstructed from 31 fungal genomes. Science 336:1715-1719.
613 11. Zhao Z, Liu H, Wang C, Xu J-R. 2013. Comparative analysis of fungal genomes
614 reveals different plant cell wall degrading capacity in fungi. BMC Genomics 14:274.
615 12. Kerem Z, Jensen KA, Hammel KE. 1999. Biodegradative mechanism of the brown rot
616 basidiomycete *Gloeophyllum trabeum*: evidence for an extracellular hydroquinone-
617 driven fenton reaction. FEBS lett 446:49-54.
618 13. Riley R, Salamov AA, Brown DW, Nagy LG, Floudas D, Held BW, Levasseur A,
619 Lombard V, Morin E, Otillar R. 2014. Extensive sampling of basidiomycete genomes
620 demonstrates inadequacy of the white-rot/brown-rot paradigm for wood decay fungi.
621 Proc Natl Acad Sci U S A 111:9923-9928.
622 14. Jensen KA, Houtman CJ, Ryan ZC, Hammel KE. 2001. Pathways for extracellular
623 Fenton chemistry in the brown rot basidiomycete *Gloeophyllum trabeum*. Appl
624 Environ Microbiol 67:2705-2711.
625 15. Jellison J, Chandhoke V, Goodell B, Fekete FA. 1991. The isolation and
626 immunolocalization of iron-binding compounds produced by *Gloeophyllum trabeum*.
627 Appl Microbiol Biotechnol 35:805-809.

16. Xu G, Goodell B. 2001. Mechanisms of wood degradation by brown-rot fungi: chelator-mediated cellulose degradation and binding of iron by cellulose. J Biotechnol 87:43-57.

17. Cavener DR. 1992. GMC oxidoreductases: a newly defined family of homologous proteins with diverse catalytic activities. J Mol Biol 223:811-814.

18. Bissaro B, Røhr ÅK, Müller G, Chylenski P, Skaugen M, Forsberg Z, Horn SJ, Vaaje-Kolstad G, Eijsink VGH. 2017. Oxidative cleavage of polysaccharides by monocopper enzymes depends on H_2O_2. Nat Chem Biol 13:1123.

19. Vaaje-Kolstad G, Westereng B, Horn SJ, Liu Z, Zhai H, Sørlie M, Eijsink VGH. 2010. An oxidative enzyme boosting the enzymatic conversion of recalcitrant polysaccharides. Science 330:219-222.

20. Beeson WT, Phillips CM, Cate JH, Marletta MA. 2012. Oxidative cleavage of cellulose by fungal copper-dependent polysaccharide monooxygenases. J Am Chem Soc 134:890-892.

21. Kjaergaard CH, Qayyum MF, Wong SD, Xu F, Hemsworth GR, Walton DJ, Young NA, Davies GJ, Walton PH, Johansen KS. 2014. Spectroscopic and computational insight into the activation of O_2 by the mononuclear Cu center in polysaccharide monooxygenases. Proc Natl Acad Sci U S A: 111(24):8797-8802.

22. Walton PH, Davies GJ. 2016. On the catalytic mechanisms of lytic polysaccharide monooxygenases. Curr Opin Chem Biol 31:195-207.

23. Petrovic DM, Bissaro B, Chylenski P, Skaugen M, Sørlie M, Jensen MS, Aachmann FL, Courtade G, Várnai A, Eijsink VGH. 2018. Methylation of the N-terminal histidine protects a lytic polysaccharide monooxygenase from auto-oxidative inactivation. Protein Sci, 27:1636-1650.

24. Kuusk S, Bissaro B, Kuusk P, Forsberg Z, Eijsink VGH, Sørlie M, Väljamäe P. 2018. Kinetics of H_2O_2-driven degradation of chitin by a bacterial lytic polysaccharide monooxygenase. J Biol Chem 293:523-531.

25. Hangasky JA, Iavarone AT, Marletta MA. 2018. Reactivity of O2 versus H_2O_2 with polysaccharide monooxygenases. Proc Natl Acad Sci U S A 115:4915-4920.

26. Wang B, Johnston EM, Li P, Shaik S, Davies GJ, Walton PH, Rovira C. 2018. QM/MM studies into the H_2O_2-dependent activity of lytic polysaccharide monooxygenases: Evidence for the formation of a caged hydroxyl radical intermediate. ACS Catal 8:1346-1351.

27. Hedegård ED, Ryde U. 2018. Molecular mechanism of lytic polysaccharide monooxygenases. Chem Sci 9:3866-3880.

28. Kracher D, Scheiblbrandner S, Felice AK, Breslmayr E, Preims M, Ludwicka K, Haltrich D, Eijsink VGH, Ludwig R. 2016. Extracellular electron transfer systems fuel cellulose oxidative degradation. Science 352:1098-1101.

29. Frommhagen M, Westphal AH, Van Berkel WJ, Kabel MA. 2018. Distinct substrate specificities and electron-donating systems of fungal lytic polysaccharide monooxygenases. Front Microbiol 9:1080.

30. Garajova S, Mathieu Y, Beccia MR, Bennati-Granier C, Biaso F, Fanuel M, Ropartz D, Guigliarelli B, Record E, Rogniaux H. 2016. Single-domain flavoenzymes trigger lytic polysaccharide monooxygenases for oxidative degradation of cellulose. Sci Rep 6:28276.

31. Phillips CM, Beeson IV WT, Cate JH, Marletta MA. 2011. Cellobiose dehydrogenase and a copper-dependent polysaccharide monooxygenase potentiate cellulose degradation by *Neurospora crassa*. ACS Chem Biol 6:1399-1406.

32. Langston JA, Shaghasi T, Abbate E, Xu F, Vlasenko E, Sweeney MD. 2011. Oxidoreductive cellulose depolymerization by the enzymes cellobiose dehydrogenase and glycoside hydrolase 61. Appl Environ Microbiol 77(19):7007-7015.

33. Várnai A, Umezawa K, Yoshida M, Eijsink VGH. 2018. The pyrroloquinoline-quinone dependent pyranose dehydrogenase from *Coprinopsis cinerea* (CcPDH) drives lytic polysaccharide monooxygenase (LPMO) action. Appl Environ Microbiol. pii: AEM.00156-18..

34. Frommhagen M, Koetsier MJ, Westphal AH, Visser J, Hinz SW, Vincken J-P, Berkel WJ, Kabel MA, Gruppen H. 2016. Lytic polysaccharide monooxygenases from *Myceliophthora thermophila* C1 differ in substrate preference and reducing agent specificity. Biotechnol Biofuels 9:186.

35. Westereng B, Cannella D, Agger JW, Jørgensen H, Andersen ML, Eijsink VGH, Felby C. 2015. Enzymatic cellulose oxidation is linked to lignin by long-range electron transfer. Sci Rep 5:18561.

36. Zhang J, Presley GN, Hammel KE, Ryu, JS, Menke JR, Figueroa M, Hu D, Orr G, Schilling JS. 2016. Localizing gene regulation reveals a staggered wood decay mechanism for the brown rot fungus *Postia placenta*. Proc Natl Acad Sci U S A, 113**:**10968-10973.

37. Kittl R, Kracher D, Burgstaller D, Haltrich D, Ludwig R. 2012. Production of four *Neurospora crassa* lytic polysaccharide monooxygenases in *Pichia pastoris* monitored by a fluorimetric assay. Biotechnol Biofuels 5:79.

38. Gupta R, Brunak S. 2001. Prediction of glycosylation across the human proteome and the correlation to protein function, p 310-322, Biocomputing 2002. World Scientific.

39. Steentoft C, Vakhrushev SY, Joshi HJ, Kong Y, Vester-Christensen MB, Katrine T, Schjoldager B, Lavrsen K, Dabelsteen S, Pedersen NB. 2013. Precision mapping of

the human *O*-GalNAc glycoproteome through SimpleCell technology. EMBO J 32:1478-1488.

40. Kelley LA, Mezulis S, Yates CM, Wass MN, Sternberg MJ. 2015. The Phyre2 web portal for protein modeling, prediction and analysis. Nat Protoc 10:845.

41. Westereng B, Arntzen MØ, Aachmann FL, Várnai A, Eijsink VGH, Agger JW. 2016. Simultaneous analysis of C1 and C4 oxidized oligosaccharides, the products of lytic polysaccharide monooxygenases acting on cellulose. J Chromatogr A 1445:46-54.

42. Kojima Y, Várnai A, Ishida T, Sunagawa N, Petrovic DM, Igarashi K, Jellison J, Goodell B, Alfredsen G, Westereng B. 2016. Characterization of an LPMO from the brown-rot fungus *Gloeophyllum trabeum* with broad xyloglucan specificity, and its action on cellulose-xyloglucan complexes. Appl Environ Microbiol 82(22):6557-6572.

43. Jung S, Song Y, Kim HM, Bae H-J. 2015. Enhanced lignocellulosic biomass hydrolysis by oxidative lytic polysaccharide monooxygenases (LPMOs) GH61 from *Gloeophyllum trabeum*. Enzyme Microb Technol 77:38-45.

44. Loose JS, Forsberg Z, Kracher D, Scheiblbrandner S, Ludwig R, Eijsink VGH, Vaaje-Kolstad G. 2016. Activation of bacterial lytic polysaccharide monooxygenases with cellobiose dehydrogenase. Prot Sci 25:2175-2186.

45. Courtade G, Forsberg Z, Heggset EB, Eijsink VGH, Aachmann FL. 2018. The carbohydrate-binding module and linker of a modular lytic polysaccharide monooxygenase promote localized cellulose oxidation. J Biol Chem 293:13006-13015.

46. Loose JS, Arntzen MØ, Bissaro B, Ludwig R, Eijsink VGH, Vaaje-Kolstad G. 2018. Multipoint precision binding of substrate protects lytic polysaccharide

monooxygenases from self-destructive off-pathway processes. Biochemistry 57:4114-4124.

47. Isaksen T, Westereng B, Aachmann FL, Agger JW, Kracher D, Kittl R, Ludwig R, Haltrich D, Eijsink VGH, Horn SJ. 2014. A C4-oxidizing lytic polysaccharide monooxygenase cleaving both cellulose and cello-oligosaccharides. J Biol Chem 289:2632-2642.

48. Müller G, Chylenski P, Bissaro B, Eijsink VGH, Horn SJ. 2018. The impact of hydrogen peroxide supply on LPMO activity and overall saccharification efficiency of a commercial cellulase cocktail. Biotechnol Biofuels 11:209.

49. Forsberg Z, Bissaro B, Gullesen J, Dalhus B, Vaaje-Kolstad G, Eijsink VGH. 2018. Structural determinants of bacterial lytic polysaccharide monooxygenase functionality. J Biol Chem 293:1397-1412.

50. Liu R, Goodell B, Jellison J, Amirbahman A. 2005. Electrochemical study of 2, 3-dihydroxybenzoic acid and its interaction with Cu (II) and H_2O_2 in aqueous solutions: implications for wood decay. Environ Sci Technol 39:175-180.

51. Wood PM. 1988. The potential diagram for oxygen at pH 7. Biochem J 253:287-289.

52. Simmons TJ, Frandsen KE, Ciano L, Tryfona T, Lenfant N, Poulsen J, Wilson LF, Tandrup T, Tovborg M, Schnorr K. 2017. Structural and electronic determinants of lytic polysaccharide monooxygenase reactivity on polysaccharide substrates. Nat Commun 8:1064.

53. Várnai A, Tang C, Bengtsson O, Atterton A, Mathiesen G, Eijsink VGH. 2014. Expression of endoglucanases in *Pichia pastoris* under control of the GAP promoter. Microb Cell Fact 13:57.

748 54. Nekiunaite L, Petrović DM, Westereng B, Vaaje-Kolstad G, Hachem MA, Várnai A,
749 Eijsink VGH. 2016. *Fg*LPMO9A from *Fusarium graminearum* cleaves xyloglucan
750 independently of the backbone substitution pattern. FEBS Lett 590:3346-3356.
751 55. Loose JS, Forsberg Z, Fraaije MW, Eijsink VGH, Vaaje-Kolstad G. 2014. A rapid
752 quantitative activity assay shows that the Vibrio cholerae colonization factor GbpA is
753 an active lytic polysaccharide monooxygenase. FEBS Lett 588:3435-3440.
754 56. Gasteiger E, Hoogland C, Gattiker A, Wilkins MR, Appel RD, Bairoch A. 2005.
755 Protein identification and analysis tools on the ExPASy server, p 571-607, The
756 Proteomics Protocols Handbook. Springer.
757 57. Wood TM. 1988. Preparation of crystalline, amorphous, and dyed cellulase substrates.
758 Methods Enzymol 160:19-25.
759 58. Müller G, Várnai A, Johansen KS, Eijsink VGH, Horn SJ. 2015. Harnessing the
760 potential of LPMO-containing cellulase cocktails poses new demands on processing
761 conditions. Biotech Biofuels 8:187.
762 59. Zámocký M, Schümann C, Sygmund C, O'Callaghan J, Dobson AD, Ludwig R,
763 Haltrich D, Peterbauer CK. 2008. Cloning, sequence analysis and heterologous
764 expression in *Pichia pastoris* of a gene encoding a thermostable cellobiose
765 dehydrogenase from *Myriococcum thermophilum*. Protein Expr Purif 59:258-265.
766 60. Westereng B, Agger JW, Horn SJ, Vaaje-Kolstad G, Aachmann FL, Stenstrøm YH,
767 Eijsink VGH. 2013. Efficient separation of oxidized cello-oligosaccharides generated
768 by cellulose degrading lytic polysaccharide monooxygenases. J Chromatogr A
769 1271:144-152.
770 61. Agger JW, Isaksen T, Várnai A, Vidal-Melgosa S, Willats WG, Ludwig R, Horn SJ,
771 Eijsink VGH, Westereng B. 2014. Discovery of LPMO activity on hemicelluloses

772 shows the importance of oxidative processes in plant cell wall degradation. Proc Natl
773 Acad Sci USA 111(17):6287-6292.

774

Supplementary material

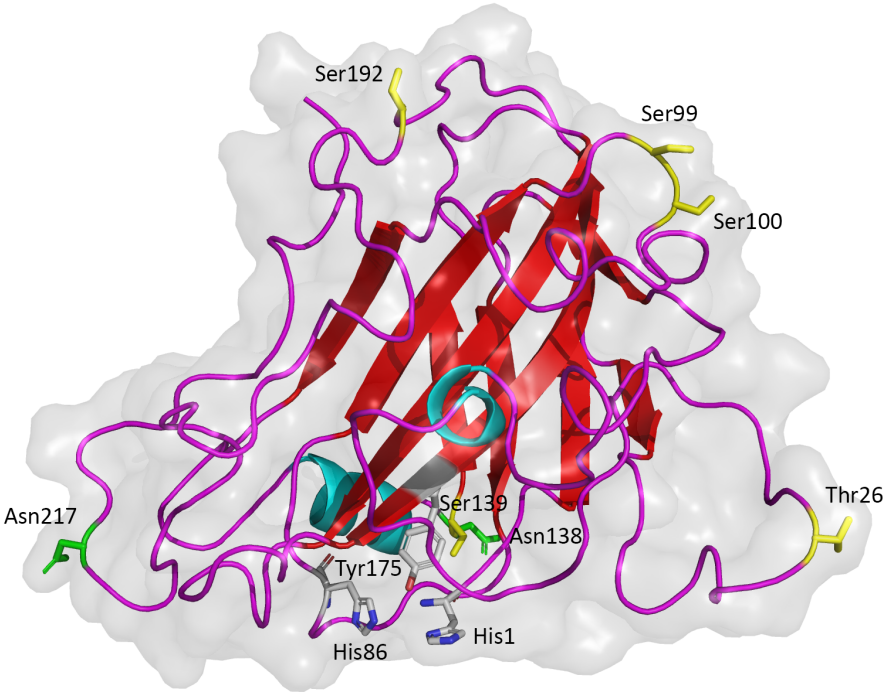

Figure S1. Structural model of *Gt*LPMO9B. Beta-strands, helices and loops are coloured red, blue and magenta, respectively**.** The side chains of the copper coordinating histidines (His1 and His86) and of Tyr175 in the proximal axial coordination sphere are shown as grey sticks. Putative *N*-glycosylation sites (Asn138, Asn217) are shown as green sticks, and putative *O*-glycosylation sites (Thr26, Ser99, Ser100, Ser139, and Ser192) are shown as yellow sticks. The model was built with PHYRE2, using *Nc*LPMO9M (PDB: 4EIS) as template.

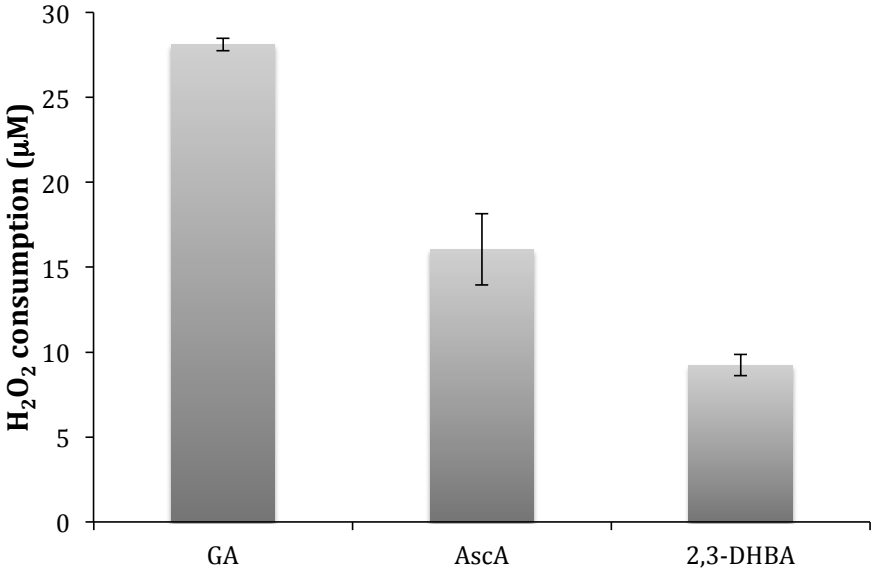

784

785 **Figure S2. H_2O_2 scavenging by gallic acid (GA), ascorbic acid (AscA) and 2,3-dihydroxybenzoic**
786 **acid (2,3-DHBA).** Reductants were incubated with H_2O_2 at a 1:1 molar ratio (30 µM) in 50 mM
787 BisTris pH 6.5 for 1 h. H_2O_2 concentrations were determined using the AmplexRed-HRP assay by
788 adding 50 µM AmplexRed and 5U HRP and measuring absorbance at 540 nm after 60 minutes of
789 incubation at room temperature. A control with only H_2O_2 (water replacing reductant) was used to
790 correct for spontaneous H_2O_2 dismutation. The data show that 94%, 54% and 31% H_2O_2 was
791 consumed by GA, AscA and 2,3-DHBA respectively.

792

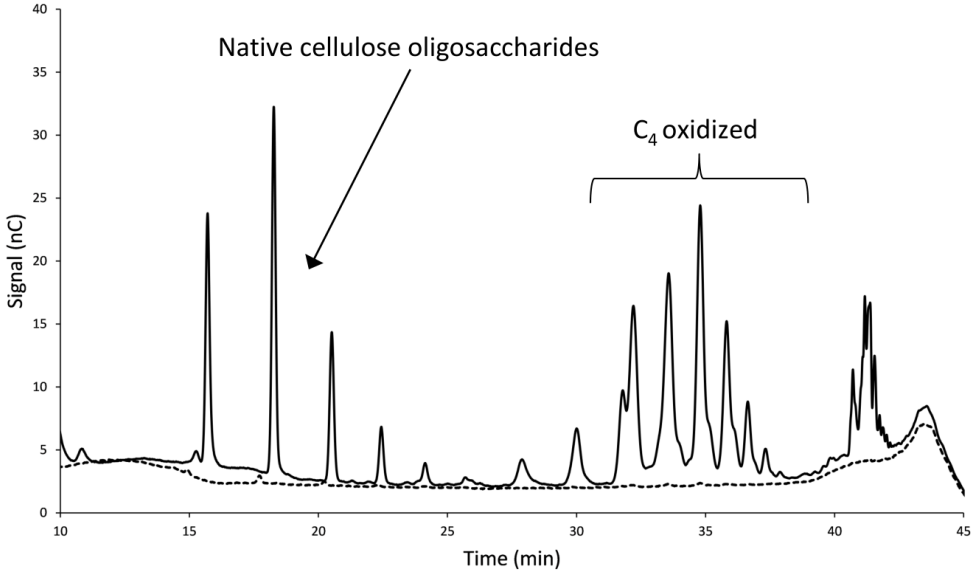

Figure S3. Activity of the C_4 oxidizing *Nc*LPMO9C with gradual addition of 2,3-dihydroxybenzoic acid (2,3-DHBA) and H_2O_2. HPAEC-PAD chromatograms showing soluble native and C4-oxidized cello-oligosaccharides released from PASC. The peaks were annotated based on Isaksen et al. 2014 (47). The reaction mixtures were incubated at 45°C, 1000 rpm and contained 1 µM enzyme, 50 mM BisTris buffer pH 6.5, 0.5% (w/v) PASC and were subjected to repetitive additions, every 15 minutes, starting at time zero of 15 µM 2,3-DHBA and 20 µM H_2O_2 (solid line) or 15 µM 2,3-DHBA and water (same volume as for H_2O_2; dotted line) for a total of 240 minutes. The graphs show products formed after 240 minutes and demonstrate that 2,3-DHBA alone cannot drive the LPMO reaction, but can prime the LPMO to carry out H_2O_2-driven catalysis.

ISBN: 978-82-575-1579-9
ISSN: 1894-6402

Norwegian University
of Life Sciences

Postboks 5003
NO-1432 Ås, Norway
+47 67 23 00 00
www.nmbu.no

101708 / ANDVORDGRAFISK.NO